

# Quantum Optics

## Notes

*Mingda Li*

# Contents

本课程主讲第1、2、3、4、5、6、8、9、17章节

考核：四学分、闭卷、考试没有>10min做不出来的题

Preface	xix
<b>1/ Quantum theory of radiation</b>	1
1.1 Quantization of the free electromagnetic field	2
1.1.1 Mode expansion of the field	3
1.1.2 Quantization	4
1.1.3 Commutation relations between electric and magnetic field components	7
1.2 Fock or number states	9
1.3 Lamb shift	13
1.4 Quantum beats	16
1.5 What is light? – The photon concept	20
1.5.1 Vacuum fluctuations and the photon concept	20
1.5.2 Vacuum fluctuations	22
1.5.3 Quantum beats, the quantum eraser, Bell's theorem, and more	24
1.5.4 ‘Wave function for photons’	24
1.A Equivalence between a many-particle Bose gas and a set of quantized harmonic oscillators	35
<i>Problems</i>	40
<i>References and bibliography</i>	43
<b>2/ Coherent and squeezed states of the radiation field</b>	46
2.1 Radiation from a classical current	48
2.2 The coherent state as an eigenstate of the annihilation operator and as a displaced harmonic oscillator state	50
2.3 What is so coherent about coherent states?	51
2.4 Some properties of coherent states	54
2.5 Squeezed state physics	56

这一部分没讲

---

2.6 Squeezed states and the uncertainty relation	60
2.7 The squeeze operator and the squeezed coherent states	63
2.7.1 Quadrature variance	65
2.8 Multi-mode squeezing	66
<i>Problems</i>	67
<i>References and bibliography</i>	70
<b>3/ Quantum distribution theory and partially coherent radiation</b>	72
3.1 Coherent state representation	73
3.1.1 Definition of the coherent state representation	75
3.1.2 Examples of the coherent state representation	77
3.2 <i>Q</i> -representation	79
3.3 The Wigner–Weyl distribution	81
3.4 Generalized representation of the density operator and connection between the <i>P</i> -, <i>Q</i> -, and <i>W</i> -distributions	83
3.5 <i>Q</i> -representation for a squeezed coherent state	86
3.A Verifying equations (3.1.12a, 3.1.12b)	90
3.B <i>c</i> -number function correspondence for the Wigner–Weyl distribution	92
<i>Problems</i>	94
<i>References and bibliography</i>	96
<b>4/ Field–field and photon–photon interferometry</b>	97
4.1 The interferometer as a cosmic probe	98
4.1.1 Michelson interferometer and general relativity	98
4.1.2 The Sagnac ring interferometer	101
4.1.3 Proposed ring laser test of metric gravitation theories	106
4.1.4 The Michelson stellar interferometer	108
4.1.5 Hanbury-Brown–Twiss interferometer	110
4.2 Photon detection and quantum coherence functions	111
4.3 First-order coherence and Young-type double-source experiments	115
4.3.1 Young’s double-slit experiment	115
4.3.2 Young’s experiment with light from two atoms	119
4.4 Second-order coherence	120
4.4.1 The physics behind the Hanbury-Brown–Twiss effect	121
4.4.2 Detection and measurement of squeezed states via homodyne detection	125
4.4.3 Interference of two photons	131
4.4.4 Photon antibunching, Poissonian, and sub-Poissonian light	134
4.5 Photon counting and photon statistics	137

这一部分采用Elements  
那本的Chap 13

4.A	Classical and quantum descriptions of two-source interference	139
4.B	Calculation of the second-order correlation function	140
	<i>Problems</i>	141
	<i>References and bibliography</i>	143
<b>5✓</b>	<b>Atom–field interaction – semiclassical theory</b>	145
5.1	Atom–field interaction Hamiltonian	146
5.1.1	Local gauge (phase) invariance and minimal-coupling Hamiltonian	146
5.1.2	Dipole approximation and $\mathbf{r} \cdot \mathbf{E}$ Hamiltonian	148
5.1.3	$\mathbf{p} \cdot \mathbf{A}$ Hamiltonian	149
5.2	Interaction of a single two-level atom with a single-mode field	151
5.2.1	Probability amplitude method	151
5.2.2	Interaction picture	155
5.2.3	Beyond the rotating-wave approximation	158
5.3	Density matrix for a two-level atom	160
5.3.1	Equation of motion for the density matrix	161
5.3.2	Two-level atom	162
5.3.3	Inclusion of elastic collisions between atoms	163
5.4	Maxwell–Schrödinger equations	164
5.4.1	Population matrix and its equation of motion	165
5.4.2	Maxwell's equations for slowly varying field functions	166
5.5	Semiclassical laser theory	168
5.5.1	Basic principle	169
5.5.2	Lamb's semiclassical theory	169
<b>未讲 →</b>	5.6 A physical picture of stimulated emission and absorption	173
	5.7 Time delay spectroscopy	174
5.A	Equivalence of the $\mathbf{r} \cdot \mathbf{E}$ and the $\mathbf{p} \cdot \mathbf{A}$ interaction Hamiltonians	178
5.A.1	Form-invariant physical quantities	178
5.A.2	Transition probabilities in a two-level atom	180
5.B	Vector model of the density matrix	183
5.C	Quasimode laser physics based on the modes of the universe	185
	<i>Problems</i>	187
	<i>References and bibliography</i>	190
<b>6✓</b>	<b>Atom–field interaction – quantum theory</b>	193
6.1	Atom–field interaction Hamiltonian	194

了解即可

未讲

6✓

---

6.2	Interaction of a single two-level atom with a single-mode field	196
6.2.1	Probability amplitude method	197
6.2.2	Heisenberg operator method	202
6.2.3	Unitary time-evolution operator method	204
6.3	Weisskopf–Wigner theory of spontaneous emission between two atomic levels	206
6.4	Two-photon cascades	210 ← 了解即可
6.5	Excitation probabilities for single and double photo-excitation events	213
	<i>Problems</i>	215
	<i>References and bibliography</i>	217

7

7	Lasing without inversion and other effects of atomic coherence and interference	220
---	---------------------------------------------------------------------------------	-----

7.1	The Hanle effect	221
7.2	Coherent trapping – dark states	222
7.3	Electromagnetically induced transparency	225
7.4	Lasing without inversion	230
7.4.1	The LWI concept	230
7.4.2	The laser physics approach to LWI: simple treatment	232
7.4.3	LWI analysis	233
7.5	Refractive index enhancement via quantum coherence	236
7.6	Coherent trapping, lasing without inversion, and electromagnetically induced transparency via an exact solution to a simple model	241

	<i>Problems</i>	244
	<i>References and bibliography</i>	245

8

8	Quantum theory of damping – density operator and wave function approach	248 ← 薛定谔绘景下的耗散
---	-------------------------------------------------------------------------	-----------------

8.1	General reservoir theory	249
8.2	Atomic decay by thermal and squeezed vacuum reservoirs	250
8.2.1	Thermal reservoir	251
8.2.2	Squeezed vacuum reservoir	253
8.3	Field damping	255
* 8.4	Fokker–Planck equation	256
* 8.5	The ‘quantum jump’ approach to damping	260
8.5.1	Conditional density matrices and the null measurement	261
8.5.2	The wave function Monte Carlo approach to damping	263

海森堡绘景下的涨落耗散 → 9/

<i>Problems</i>	267
<i>References and bibliography</i>	269
<b>9 Quantum theory of damping – Heisenberg–Langevin approach</b>	271
9.1 Simple treatment of damping via oscillator reservoir: Markovian white noise	272
9.2 Extended treatment of damping via atom and oscillator reservoirs: non-Markovian colored noise	276
9.2.1 An atomic reservoir approach	276
9.2.2 A generalized treatment of the oscillator reservoir problem	278
9.3 Equations of motion for the field correlation functions	281
9.4 Fluctuation–dissipation theorem and the Einstein relation	283
9.5 Atom in a damped cavity	284
<i>Problems</i>	289
<i>References and bibliography</i>	290
<b>10 Resonance fluorescence</b>	291
10.1 Electric field operator for spontaneous emission from a single atom	292
10.2 An introduction to the resonance fluorescence spectrum	293
10.2.1 Weak driving field limit	293
10.2.2 The strong field limit: sidebands appear	295
10.2.3 The widths of the three peaks in the very strong field limit	296
10.3 Theory of a spectrum analyzer	298
10.4 From single-time to two-time averages: the Onsager–Lax regression theorem	300
10.5 The complete resonance fluorescence spectrum	302
10.5.1 Weak field limit	305
10.5.2 Strong field limit	305
10.6 Photon antibunching	307
10.7 Resonance fluorescence from a driven $V$ system	309
10.A Electric field operator in the far-zone approximation	311
10.B The equations of motion for and exact solution of the density matrix in a dressed-state basis	316
10.B.1 Deriving the equation of motion in the dressed-state basis	316
10.B.2 Solving the equations of motion	317

---

<b>17 Atom optics</b>	487
17.1 Mechanical effects of light	488
17.1.1 Atomic deflection	488
17.1.2 Laser cooling	489
17.1.3 Atomic diffraction	490
17.1.4 Semiclassical gradient force	493
17.2 Atomic interferometry	494
17.2.1 Atomic Mach–Zehnder interferometer	494
17.2.2 Atomic gyroscope	496
17.3 Quantum noise in an atomic interferometer	498
17.4 Limits to laser cooling	499
17.4.1 Recoil limit	499
17.4.2 Velocity selective coherent population trapping	501
<i>Problems</i>	503
<i>References and bibliography</i>	504
<b>18 The EPR paradox, hidden variables, and Bell's theorem</b>	507
18.1 The EPR ‘paradox’	508
18.2 Bell's inequality	513
18.3 Quantum calculation of the correlations in Bell's theorem	515
18.4 Hidden variables from a quantum optical perspective	520
18.5 Bell's theorem without inequalities: Greenberger–Horne–Zeilinger (GHZ) equality	529
18.6 Quantum cryptography	531
18.6.1 Bennett–Brassard protocol	531
18.6.2 Quantum cryptography based on Bell's theorem	532
18.A Quantum distribution function for a single spin-up particle	533
18.B Quantum distribution function for two particles	534
<i>Problems</i>	536
<i>References and bibliography</i>	539
<b>19 Quantum nondemolition measurements</b>	541
19.1 Conditions for QND measurements	542
19.2 QND measurement of the photon number via the optical Kerr effect	543
19.3 QND measurement of the photon number by dispersive atom–field coupling	547
19.4 QND measurements in optical parametric processes	554
<i>Problems</i>	558
<i>References and bibliography</i>	560

---

# Quantum theory of radiation

---

Light occupies a special position in our attempts to understand nature both classically and quantum mechanically. We recall that Newton, who made so many fundamental contributions to optics, championed a particle description of light and was not favorably disposed to the wave picture of light. However, the beautiful unification of electricity and magnetism achieved by Maxwell clearly showed that light was properly understood as the wave-like undulations of electric and magnetic fields propagating through space.

The central role of light in marking the frontiers of physics continues on into the twentieth century with the ultraviolet catastrophe associated with black-body radiation on the one hand and the photoelectric effect on the other. Indeed, it was here that the era of quantum mechanics was initiated with Planck's introduction of the quantum of action that was necessary to explain the black-body radiation spectrum. The extension of these ideas led Einstein to explain the photoelectric effect, and to introduce the photon concept.

It was, however, left to Dirac\* to combine the wave- and particle-like aspects of light so that the radiation field is capable of explaining all interference phenomena and yet shows the excitation of a specific atom located along a wave front absorbing one photon of energy. In this chapter, following Dirac, we associate each mode of the radiation field with a quantized simple harmonic oscillator, this is the essence of the quantum theory of radiation. An interesting consequence of the quantization of radiation is the fluctuations associated with the zero-

\* The pioneering papers on the quantum theory of radiation by Dirac [1927] and Fermi [1932] should be read by every student of the subject. Excellent modern treatments are to be found in the textbooks by: Loudon, *The Quantum Theory of Light* [1973], Cohen-Tannoudji, Dupont-Roc, and Grynberg, *Atom-Photon Interactions* [1992], Weinberg, *Theory of Quantum Fields* [1995], and Pike and Sarkar, *Quantum Theory of Radiation* [1995].

point energy or the so-called vacuum fluctuations. These fluctuations have no classical analog and are responsible for many interesting phenomena in quantum optics. As is discussed at length in Chapters 5 and 7, a semiclassical theory of atom–field interaction in which only the atom is quantized and the field is treated classically, can explain many of the phenomena which we observe in modern optics. The quantization of the radiation field is, however, needed to explain effects such as spontaneous emission, the Lamb shift, the laser linewidth, the Casimir effect, and the full photon statistics of the laser. In fact, each of these physical effects can be understood from the point of view of vacuum fluctuations perturbing the atoms, e.g., spontaneous emission is often said to be the result of ‘stimulating’ the atom by vacuum fluctuations. However, as compelling as these reasons are for quantizing the radiation field, there are other strong reasons and logical arguments for quantizing the radiation field.

For example, the problem of quantum beat phenomena provides us with a simple example in which the results of self-consistent fully quantized calculation differ qualitatively from those obtained via a semiclassical theory with or without vacuum fluctuations. Another experiment wherein a quantized theory of radiation is required for the proper interpretation of the observed results is two-photon interferometry and the production of entangled states associated with such a configuration. This is discussed in detail in Chapter 21. Further support that the electromagnetic field is quantized is provided by the experimental observations of nonclassical states of the radiation field, e.g., squeezed states, sub-Poissonian photon statistics, and photon antibunching.

Following this brief motivation for the quantum theory of radiation, we now turn to the quantization of the free electromagnetic field.

## 1.1 Quantization of the free electromagnetic field

With the objective of quantizing the electromagnetic field in free space, it is convenient to begin with the classical description of the field based on Maxwell’s equations. These equations relate the electric and magnetic field vectors **E** and **H**, respectively, together with the displacement and inductive vectors **D** and **B**, respectively, and have the form (in mks units):

$$\nabla \times \mathbf{H} = \frac{\partial \mathbf{D}}{\partial t}, \quad (1.1.1a)$$

$$\nabla \times \mathbf{E} = -\frac{\partial \mathbf{B}}{\partial t}, \quad (1.1.1b)$$

$$\nabla \cdot \mathbf{B} = 0, \quad (1.1.1c)$$

$$\nabla \cdot \mathbf{D} = 0, \quad (1.1.1d)$$

with the constitutive relations

$$\mathbf{B} = \mu_0 \mathbf{H}, \quad (1.1.2)$$

$$\mathbf{D} = \epsilon_0 \mathbf{E}. \quad (1.1.3)$$

Here  $\epsilon_0$  and  $\mu_0$  are the free space permittivity and permeability, respectively, and  $\mu_0 \epsilon_0 = c^{-2}$  where  $c$  is the speed of light in vacuum.

It follows, on taking the curl of Eq. (1.1.1b) and using Eqs. (1.1.1a), (1.1.1d), (1.1.2), and (1.1.3), that  $\mathbf{E}(\mathbf{r}, t)$  satisfies the wave equation

$$\nabla^2 \mathbf{E} - \frac{1}{c^2} \frac{\partial^2 \mathbf{E}}{\partial t^2} = 0. \quad (1.1.4)$$

In deriving Eq. (1.1.4) we also used  $\nabla \times (\nabla \times \mathbf{E}) = \nabla(\nabla \cdot \mathbf{E}) - \nabla^2 \mathbf{E}$ .

### 1.1.1 Mode expansion of the field

We first consider the electric field to have the spatial dependence appropriate for a cavity resonator of length  $L$  (Fig. 1.1). We take the electric field to be linearly polarized in the  $x$ -direction and expand in the normal modes of the cavity

$$E_x(z, t) = \sum_j A_j q_j(t) \sin(k_j z), \quad (1.1.5)$$

where  $q_j$  is the normal mode amplitude with the dimension of a length,  $k_j = j\pi/L$ , with  $j = 1, 2, 3, \dots$ , and

$$A_j = \left( \frac{2v_j^2 m_j}{V \epsilon_0} \right)^{1/2}, \quad (1.1.6)$$

with  $v_j = j\pi c/L$  being the cavity eigenfrequency,  $V = LA$  ( $A$  is the transverse area of the optical resonator) is the volume of the resonator and  $m_j$  is a constant with the dimension of mass. The constant  $m_j$  has been included only to establish the analogy between the dynamical problem of a single mode of the electromagnetic field and that of the simple harmonic oscillator. The equivalent mechanical oscillator will have a mass  $m_j$ , and a Cartesian coordinate  $q_j$ . The nonvanishing component of the magnetic field  $H_y$  in the cavity\* is obtained from Eq. (1.1.5):

\* In the present treatment of field quantization in vacuum we are focussing on the electric  $\mathbf{E}(\mathbf{r}, t)$  and magnetic  $\mathbf{H}(\mathbf{r}, t)$  fields. In a material medium it is preferable to work with  $\mathbf{D}(\mathbf{r}, t)$  and  $\mathbf{B}(\mathbf{r}, t)$ ; see Bialynicki-Birula and Bialynicka-Birula [1976].

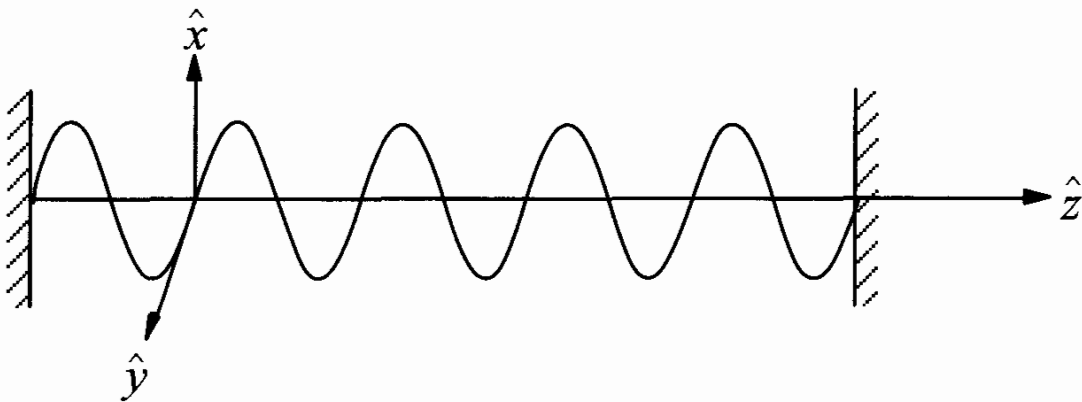


Fig. 1.1  
Electromagnetic field of frequency  $\nu$  inside a cavity. The field is assumed to be transverse with the electric field polarized in the  $x$ -direction.

$$H_y = \sum_j A_j \left( \frac{\dot{q}_j \epsilon_0}{k_j} \right) \cos(k_j z). \quad (1.1.7)$$

The classical Hamiltonian for the field is

$$\mathcal{H} = \frac{1}{2} \int_V d\tau (\epsilon_0 E_x^2 + \mu_0 H_y^2), \quad (1.1.8)$$

where the integration is over the volume of the cavity. It follows, on substituting from Eqs. (1.1.5) and (1.1.7) for  $E_x$  and  $H_y$ , respectively, in Eq. (1.1.8), that

$$\begin{aligned} \mathcal{H} &= \frac{1}{2} \sum_j (m_j v_j^2 q_j^2 + m_j \dot{q}_j^2) , \quad \text{直接代入即可, 其中用到 } \int d\tau \cos(k_j z) \cos(k_j z) = C \delta_{jj} \\ &= \frac{1}{2} \sum_j \left( m_j v_j^2 q_j^2 + \frac{p_j^2}{m_j} \right), \end{aligned} \quad (1.1.9)$$

where  $p_j = m_j \dot{q}_j$  is the canonical momentum of the  $j$ th mode. Equation (1.1.9) expresses the Hamiltonian of the radiation field as a sum of independent oscillator energies. Each mode of the field is therefore dynamically equivalent to a mechanical harmonic oscillator.

### 1.1.2 Quantization (本章里在 Heisenberg 表象下)

The present dynamical problem can be quantized by identifying  $q_j$  and  $p_j$  as operators which obey the commutation relations

$$[q_j, p_{j'}] = i\hbar \delta_{jj'}, \quad (1.1.10a)$$

$$[q_j, q_{j'}] = [p_j, p_{j'}] = 0. \quad (1.1.10b)$$

It is convenient to make a canonical transformation to operators  $a_j$  and  $a_j^\dagger$ :

$$a_j e^{-iv_j t} = \frac{1}{\sqrt{2m_j \hbar v_j}} (m_j v_j q_j + i p_j), \quad (1.1.11a)$$

$$a_j^\dagger e^{iv_j t} = \frac{1}{\sqrt{2m_j \hbar v_j}} (m_j v_j q_j - i p_j). \quad (1.1.11b)$$

In terms of  $a_j$  and  $a_j^\dagger$ , the Hamiltonian (1.1.9) becomes

$$\mathcal{H} = \hbar \sum_j v_j \left( a_j^\dagger a_j + \frac{1}{2} \right). \quad (1.1.12)$$

The commutation relations between  $a_j$  and  $a_{j'}^\dagger$  follow from those between  $q_j$  and  $p_j$ :

$$[a_j, a_{j'}^\dagger] = \delta_{jj'}, \quad (1.1.13)$$

$$[a_j, a_{j'}] = [a_{j'}^\dagger, a_{j'}^\dagger] = 0. \quad (1.1.14)$$

The operators  $a_j$  and  $a_j^\dagger$  are referred to as the annihilation and the creation operators, respectively. The reason for these names will become clear in the next section. In terms of  $a_j$  and  $a_j^\dagger$ , the electric and magnetic fields (Eqs. (1.1.5) and (1.1.7)) take the form

$$E_x(z, t) = \sum_j \mathcal{E}_j (a_j e^{-iv_j t} + a_j^\dagger e^{iv_j t}) \sin k_j z, \quad (1.1.15)$$

$$H_y(z, t) = -i\epsilon_0 c \sum_j \mathcal{E}_j (a_j e^{-iv_j t} - a_j^\dagger e^{iv_j t}) \cos k_j z, \quad (1.1.16)$$

where the quantity

$$\mathcal{E}_j = \left( \frac{\hbar v_j}{\epsilon_0 V} \right)^{1/2} \quad (1.1.17)$$

has the dimensions of an electric field.

So far we have considered the quantization of the radiation field in a finite one-dimensional cavity. We can now quantize the field in unbounded free space as follows.

We consider the field in a large but finite cubic cavity of side  $L$ . Here we regard the *cavity* merely as a region of space with no specific boundaries. We consider the running-wave solutions instead of the standing-wave solutions considered above and impose periodic boundary conditions.

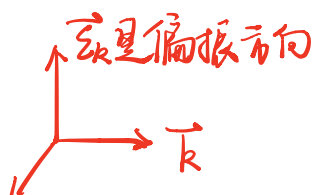
The classical electric and magnetic fields can be expanded in terms of the plane waves

$$\mathbf{E}(\mathbf{r}, t) = \sum_{\mathbf{k}} \hat{\epsilon}_{\mathbf{k}} \mathcal{E}_{\mathbf{k}} \alpha_{\mathbf{k}} e^{-iv_k t + i\mathbf{k} \cdot \mathbf{r}} + \text{c.c.}, \quad (1.1.18)$$

$$\mathbf{H}(\mathbf{r}, t) = \frac{1}{\mu_0} \sum_{\mathbf{k}} \frac{\mathbf{k} \times \hat{\epsilon}_{\mathbf{k}}}{v_k} \mathcal{E}_{\mathbf{k}} \alpha_{\mathbf{k}} e^{-iv_k t + i\mathbf{k} \cdot \mathbf{r}} + \text{c.c.}, \quad (1.1.19)$$

where the summation is taken over an infinite discrete set of values of the wave vector  $\mathbf{k} \equiv (k_x, k_y, k_z)$ ,  $\hat{\epsilon}_{\mathbf{k}}$  is a unit polarization vector,  $\alpha_{\mathbf{k}}$  is a dimensionless amplitude and

腔电场向量波



$$\mathcal{E}_k = \left( \frac{\hbar v_k}{2\epsilon_0 V} \right)^{1/2}. \quad (1.1.20)$$

In Eqs. (1.1.18) and (1.1.19) c.c. stands for complex conjugate. The periodic boundary conditions require that

$$k_x = \frac{2\pi n_x}{L}, \quad k_y = \frac{2\pi n_y}{L}, \quad k_z = \frac{2\pi n_z}{L}, \quad (1.1.21)$$

where  $n_x, n_y, n_z$  are integers ( $0, \pm 1, \pm 2, \dots$ ). A set of numbers  $(n_x, n_y, n_z)$  defines a mode of the electromagnetic field. Equation (1.1.1d) requires that

$$\mathbf{k} \cdot \hat{\mathbf{e}}_k = 0, \quad (1.1.22)$$

i.e., the fields are purely transverse. There are, therefore, two independent polarization directions of  $\hat{\mathbf{e}}_k$  for each  $\mathbf{k}$ .

The change from a discrete distribution of modes to a continuous distribution can be made by replacing the sum in Eqs. (1.1.18) and (1.1.19) by an integral:

$$\sum_{\mathbf{k}} \rightarrow 2 \left( \frac{L}{2\pi} \right)^3 \int d^3 k, \quad (1.1.23)$$

where the factor 2 accounts for two possible states of polarization.

In many problems, we shall be interested in the density of modes between the frequencies  $v$  and  $v + dv$ . This can be obtained by transforming from the rectangular components  $(k_x, k_y, k_z)$  to the polar coordinates  $(k \sin \theta \cos \phi, k \sin \theta \sin \phi, k \cos \theta)$ , so that the volume element in  $\mathbf{k}$  space is

$$d^3 k = k^2 dk \sin \theta d\theta d\phi = \frac{v^2}{c^3} dv \sin \theta d\theta d\phi. \quad (1.1.24)$$

The total number of modes in volume  $L^3$  in the range between  $v$  and  $v + dv$  is given by

$$dN = 2 \left( \frac{L}{2\pi} \right)^3 \frac{v^2 dv}{c^3} \int_0^\pi d\theta \sin \theta \int_0^{2\pi} d\phi = \frac{L^3 v^2}{\pi^2 c^3} dv. \quad (1.1.25)$$

Therefore the number of modes with frequencies in the range  $v$  to  $v + dv$  is

$$D(v)dv = \frac{L^3 v^2}{\pi^2 c^3} dv, \quad (1.1.26)$$

where  $D(v)$  is called the mode density.

$\sum_{\mathbf{k}} \rightarrow \int$  連續分布

模密度表达式

As before, the radiation field is quantized by identifying  $\alpha_{\mathbf{k}}$  and  $\alpha_{\mathbf{k}}^*$  with the harmonic oscillator operators  $a_{\mathbf{k}}$  and  $a_{\mathbf{k}}^\dagger$ , respectively, which satisfy the commutation relation  $[a_{\mathbf{k}}, a_{\mathbf{k}}^\dagger] = 1$ . The quantized electric and magnetic fields take the form

$$\mathbf{E}(\mathbf{r}, t) = \sum_{\mathbf{k}} \hat{\epsilon}_{\mathbf{k}} \mathcal{E}_{\mathbf{k}} a_{\mathbf{k}} e^{-iv_k t + i\mathbf{k} \cdot \mathbf{r}} + \text{H.c.}, \quad (1.1.27)$$

$$\mathbf{H}(\mathbf{r}, t) = \frac{1}{\mu_0} \sum_{\mathbf{k}} \frac{\mathbf{k} \times \hat{\epsilon}_{\mathbf{k}}}{v_k} \mathcal{E}_{\mathbf{k}} a_{\mathbf{k}} e^{-iv_k t + i\mathbf{k} \cdot \mathbf{r}} + \text{H.c.}, \quad (1.1.28)$$

where H.c. stands for Hermitian conjugate. Usually the positive and negative frequency parts of these field operators are written separately. For example, the electric field operator  $\mathbf{E}(\mathbf{r}, t)$  is written as

$$\mathbf{E}(\mathbf{r}, t) = \mathbf{E}^{(+)}(\mathbf{r}, t) + \mathbf{E}^{(-)}(\mathbf{r}, t), \quad (1.1.29)$$

where

$$\mathbf{E}^{(+)}(\mathbf{r}, t) = \sum_{\mathbf{k}} \hat{\epsilon}_{\mathbf{k}} \mathcal{E}_{\mathbf{k}} a_{\mathbf{k}} e^{-iv_k t + i\mathbf{k} \cdot \mathbf{r}}, \quad (1.1.30)$$

$$\mathbf{E}^{(-)}(\mathbf{r}, t) = \sum_{\mathbf{k}} \hat{\epsilon}_{\mathbf{k}} \mathcal{E}_{\mathbf{k}} a_{\mathbf{k}}^\dagger e^{iv_k t - i\mathbf{k} \cdot \mathbf{r}}. \quad (1.1.31)$$

Here  $\mathbf{E}^{(+)}(\mathbf{r}, t)$  contains only the annihilation operators and its adjoint  $\mathbf{E}^{(-)}(\mathbf{r}, t)$  contains only the creation operators.

### 1.1.3 Commutation relations between electric and magnetic field components

An important consequence of imposing the quantum conditions (1.1.13) and (1.1.14) is that as the electric and magnetic field strengths do not commute they are thus not measurable simultaneously. In order to show this we rewrite the quantized mode expansions (1.1.27) and (1.1.28) for  $\mathbf{E}(\mathbf{r}, t)$  and  $\mathbf{H}(\mathbf{r}, t)$ , respectively by including explicitly the two states of polarization denoted by the symbol  $\lambda$ :

$$\mathbf{E}(\mathbf{r}, t) = \sum_{\mathbf{k}, \lambda} \hat{\epsilon}_{\mathbf{k}}^{(\lambda)} \mathcal{E}_{\mathbf{k}, \lambda} a_{\mathbf{k}, \lambda} e^{-iv_k t + i\mathbf{k} \cdot \mathbf{r}} + \text{H.c.}, \quad (1.1.32)$$

$$\mathbf{H}(\mathbf{r}, t) = \frac{1}{\mu_0} \sum_{\mathbf{k}, \lambda} \frac{\mathbf{k} \times \hat{\epsilon}_{\mathbf{k}}^{(\lambda)}}{v_k} \mathcal{E}_{\mathbf{k}, \lambda} a_{\mathbf{k}, \lambda} e^{-iv_k t + i\mathbf{k} \cdot \mathbf{r}} + \text{H.c.} \quad (1.1.33)$$

The corresponding commutation relations between the operators  $a_{\mathbf{k}, \lambda}$  and  $a_{\mathbf{k}', \lambda}'$  are

$$\begin{aligned} [a_{\mathbf{k}, \lambda}, a_{\mathbf{k}', \lambda'}] &= [a_{\mathbf{k}, \lambda}^\dagger, a_{\mathbf{k}', \lambda'}^\dagger] = 0, \\ [a_{\mathbf{k}, \lambda}, a_{\mathbf{k}', \lambda'}^\dagger] &= \delta_{\mathbf{k}\mathbf{k}'} \delta_{\lambda\lambda'}. \end{aligned} \quad (1.1.34)$$

It then follows that the equal time commutator between the field components is given by

$$[E_x(\mathbf{r}, t), H_y(\mathbf{r}', t)] = \frac{\hbar c^2}{2V} \sum_{\mathbf{k}, \lambda} \epsilon_{\mathbf{k}x}^{(\lambda)} \left[ \epsilon_{\mathbf{k}x}^{(\lambda)} k_z - \epsilon_{\mathbf{k}z}^{(\lambda)} k_x \right] \times \left[ e^{i\mathbf{k}\cdot(\mathbf{r}-\mathbf{r}')} - e^{-i\mathbf{k}\cdot(\mathbf{r}-\mathbf{r}')} \right], \quad (1.1.35)$$

where  $\epsilon_{\mathbf{k}i}^{(\lambda)}$  ( $i = x, y, z$ ) is the  $i$ th component of  $\hat{\epsilon}_{\mathbf{k}}^{(\lambda)}$ . We proceed by using the operator identity of Problem 1.9 to write

$$\hat{\epsilon}_{\mathbf{k}}^{(1)} \hat{\epsilon}_{\mathbf{k}}^{(1)} + \hat{\epsilon}_{\mathbf{k}}^{(2)} \hat{\epsilon}_{\mathbf{k}}^{(2)} + \frac{\mathbf{k}\mathbf{k}}{k^2} = \mathbf{1}, \quad \text{---> 约简关系} \quad (1.1.36)$$

where  $\hat{\epsilon}_{\mathbf{k}}^{(1)} \hat{\epsilon}_{\mathbf{k}}^{(1)}$ ,  $\hat{\epsilon}_{\mathbf{k}}^{(2)} \hat{\epsilon}_{\mathbf{k}}^{(2)}$ , and  $\mathbf{k}\mathbf{k}$  denote dyadic products. One can verify that taking the inner product of (1.1.36) with the Cartesian unit vector  $\hat{\mathbf{e}}_i$  from the left and  $\hat{\mathbf{e}}_j$  from the right yields

$$\epsilon_{\mathbf{k}i}^{(1)} \epsilon_{\mathbf{k}j}^{(1)} + \epsilon_{\mathbf{k}i}^{(2)} \epsilon_{\mathbf{k}j}^{(2)} = \delta_{ij} - \frac{k_i k_j}{k^2}. \quad (1.1.37)$$

The summation over the polarization states in Eq. (1.1.35) can now be carried out using (1.1.37). The resulting expression for the commutator is

$$[E_x(\mathbf{r}, t), H_y(\mathbf{r}', t)] = \frac{\hbar c^2}{2V} \sum_{\mathbf{k}} k_z \left[ e^{i\mathbf{k}\cdot(\mathbf{r}-\mathbf{r}')} - e^{-i\mathbf{k}\cdot(\mathbf{r}-\mathbf{r}')} \right]. \quad (1.1.38)$$

We now replace the summation by an integral via

$$\sum_{\mathbf{k}} \rightarrow \frac{V}{(2\pi)^3} \int d^3k. \quad (1.1.39)$$

The factor of 2 has not been included as was done in Eq. (1.1.23) because, in the present case, we have summed over two polarization states explicitly. We obtain

$$[E_x(\mathbf{r}, t), H_y(\mathbf{r}', t)] = -i\hbar c^2 \frac{\partial}{\partial z} \delta^{(3)}(\mathbf{r} - \mathbf{r}'). \quad (1.1.40)$$

In general

$$[E_j(\mathbf{r}, t), H_j(\mathbf{r}', t)] = 0 \quad (j = x, y, z), \quad \text{平行分量 (对称, 可同时测量)} \quad (1.1.41)$$

$$[E_j(\mathbf{r}, t), H_k(\mathbf{r}', t)] = -i\hbar c^2 \frac{\partial}{\partial \ell} \delta^{(3)}(\mathbf{r} - \mathbf{r}'), \quad \text{正交分量 (不对称, 不可同时测量)} \quad (1.1.42)$$

where  $j$ ,  $k$ , and  $\ell$  form a cyclic permutation of  $x$ ,  $y$ , and  $z$ .

We, therefore, conclude that the parallel components of  $\mathbf{E}$  and  $\mathbf{H}$  may be measured simultaneously whereas the perpendicular components cannot.

## 1.2 Fock or number states

In this section we first restrict ourselves to a single mode of the field of frequency  $\nu$  having creation and annihilation operators  $a^\dagger$  and  $a$ , respectively. Let  $|n\rangle$  be the energy eigenstate corresponding to the energy eigenvalue  $E_n$ , i.e.,

$$\mathcal{H}|n\rangle = \hbar\nu \left( a^\dagger a + \frac{1}{2} \right) |n\rangle = E_n |n\rangle. \quad (1.2.1)$$

If we apply the operator  $a$  from the left, we obtain after using the commutation relation  $[a, a^\dagger] = 1$  and some rearrangement

$$\mathcal{H}a|n\rangle = (E_n - \hbar\nu)a|n\rangle. \quad (1.2.2)$$

This means that the state

$$|n-1\rangle = \frac{a}{\alpha_n} |n\rangle, \quad (1.2.3)$$

is also an energy eigenstate but with the reduced eigenvalue

$$E_{n-1} = E_n - \hbar\nu. \quad (1.2.4)$$

In Eq. (1.2.3),  $\alpha_n$  is a constant which will be determined from the normalization condition

$$\langle n-1|n-1\rangle = 1. \quad (1.2.5)$$

If we repeat this procedure  $n$  times we move down the energy ladder in steps of  $\hbar\nu$  until we obtain

$$\mathcal{H}a|0\rangle = (E_0 - \hbar\nu)a|0\rangle. \quad (1.2.6)$$

Here  $E_0$  is the ground state energy such that  $(E_0 - \hbar\nu)$  would correspond to an energy eigenvalue smaller than  $E_0$ . Since we do not allow energies lower than  $E_0$  for the oscillator, we must conclude

$$a|0\rangle = 0. \quad (1.2.7)$$

The state  $|0\rangle$  is referred to as the vacuum state. Using this relation we can find the value of  $E_0$  from the eigenvalue equation

$$\mathcal{H}|0\rangle = \frac{1}{2}\hbar\nu|0\rangle = E_0|0\rangle. \quad (1.2.8)$$

This gives

$$E_0 = \frac{1}{2}\hbar\nu. \quad (1.2.9)$$

It then follows from Eq. (1.2.4) that

$$E_n = \left( n + \frac{1}{2} \right) \hbar v. \quad (1.2.10)$$

From Eq. (1.2.1), we obtain

$$a^\dagger a |n\rangle = n |n\rangle, \quad (1.2.11)$$

i.e., the energy eigenstate  $|n\rangle$  is also an eigenstate of the ‘number’ operator

$$n = a^\dagger a. \quad (1.2.12)$$

The normalization constant  $\alpha_n$  in Eq. (1.2.3) can now be determined.

$$\langle n-1|n-1\rangle = \frac{1}{|\alpha_n|^2} \langle n|a^\dagger a|n\rangle = \frac{n}{|\alpha_n|^2} \langle n|n\rangle = \frac{n}{|\alpha_n|^2} = 1. \quad (1.2.13)$$

If we take the phase of the normalization constant  $\alpha_n$  to be zero then  $\alpha_n = \sqrt{n}$ . Equation (1.2.3) then becomes

$$a|n\rangle = \sqrt{n}|n-1\rangle. \quad (1.2.14)$$

We can proceed along the same lines with the operator  $a^\dagger$ . The resulting equation is

$$a^\dagger|n\rangle = \sqrt{n+1}|n+1\rangle. \quad (1.2.15)$$

A repeated use of this equation gives

$$|n\rangle = \frac{(a^\dagger)^n}{\sqrt{n!}} |0\rangle. \quad (1.2.16)$$

It is useful to interpret the energy eigenvalues (1.2.10) as corresponding to the presence of  $n$  quanta or *photons* of energy  $\hbar v$ . The eigenstates  $|n\rangle$  are called Fock states or photon number states. They form a complete set of states, i.e.,

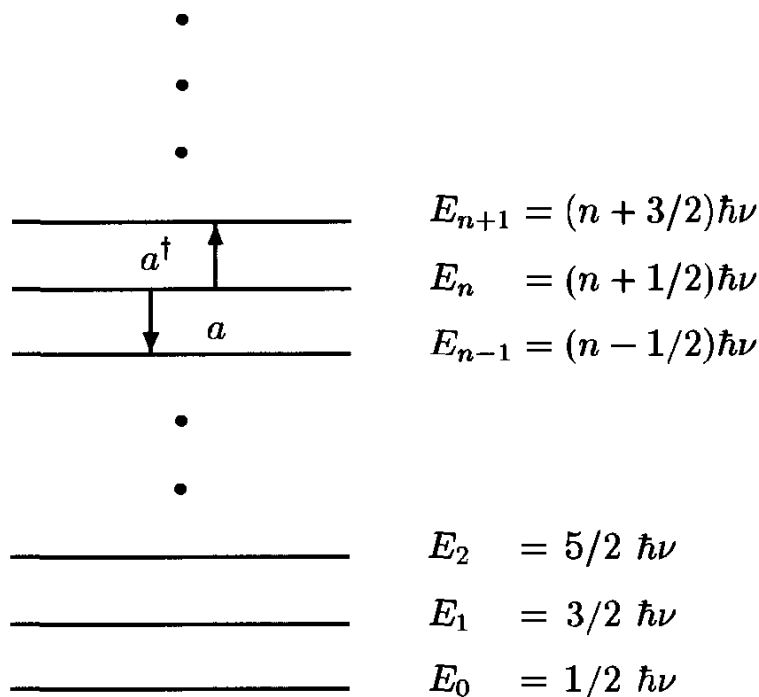
$$\sum_{n=0}^{\infty} |n\rangle \langle n| = 1. \quad (1.2.17)$$

The energy eigenvalues are discrete, in contrast to classical electromagnetic theory where energy can have any value. The energy expectation value can however take on any value, for the state vector is, in general, an arbitrary superposition of energy eigenstates, i.e.,

$$|\psi\rangle = \sum_n c_n |n\rangle \quad (1.2.18)$$

Fig. 1.2

Energy levels for the quantum mechanical harmonic oscillators associated with the electromagnetic field. The creation operator  $a^\dagger$  adds a quantum of energy  $\hbar\nu$ , whereas the destruction operator  $a$  subtracts the same amount of energy.



where  $c_n$  are complex coefficients. The residual energy  $\hbar\nu/2$  corresponding to  $E_0$  is called the zero-point energy. In Fig. 1.2, the energy levels for the quantum mechanical oscillations associated with the electromagnetic field are given.

An important property of the number state  $|n\rangle$  is that the corresponding expectation value of the single-mode linearly polarized field operator

$$E(\mathbf{r}, t) = \mathcal{E}ae^{-i\omega t + ik\cdot\mathbf{r}} + \text{H.c.} \quad (1.2.19)$$

vanishes, i.e.,

$$\langle n | E | n \rangle = 0. \quad (1.2.20)$$

However, the expectation value of the intensity operator  $E^2$  is given by

$$\langle n | E^2 | n \rangle = 2|\mathcal{E}|^2 \left( n + \frac{1}{2} \right), \quad (1.2.21)$$

i.e., there are fluctuations in the field about its zero ensemble average. It is interesting to note that there are nonzero fluctuations even for a *vacuum* state  $|0\rangle$ . These vacuum fluctuations are responsible for many interesting phenomena in quantum optics as discussed earlier. For example, it may be considered that they *stimulate* an excited atom to emit spontaneously. They also account for the Lamb shift of  $2P_{1/2} \rightarrow 2S_{1/2}$  energy levels of atomic hydrogen. In particular in Section 1.3,

we shall see how the vacuum fluctuations of the electromagnetic field are responsible for the Lamb shift.

The operators  $a$  and  $a^\dagger$  annihilate and create photons, respectively, for, as seen in Eqs. (1.2.14) and (1.2.15), they change a state with  $n$  photons into one with  $n - 1$  or  $n + 1$  photons. The operators  $a$  and  $a^\dagger$  are therefore referred to as annihilation (or destruction) and creation operators, respectively. These operators are not themselves Hermitian ( $a \neq a^\dagger$ ) and do not represent observable quantities such as the electric and magnetic field amplitudes. However, some combinations of the operators are Hermitian such as  $a_1 = (a + a^\dagger)/2$  and  $a_2 = (a - a^\dagger)/2i$ .

So far we have considered a single-mode field and have found that, in general, the wave function can be written as a linear superposition of photon number states  $|n\rangle$ . We now extend this formalism to deal with multi-mode fields.

We can rewrite the Hamiltonian  $\mathcal{H}$  in Eq. (1.1.12) as

$$\mathcal{H} = \sum_{\mathbf{k}} \mathcal{H}_{\mathbf{k}} \quad (1.2.22)$$

where

$$\mathcal{H}_{\mathbf{k}} = \hbar v_k \left( a_{\mathbf{k}}^\dagger a_{\mathbf{k}} + \frac{1}{2} \right). \quad (1.2.23)$$

The energy eigenstate  $|n_{\mathbf{k}}\rangle$  of  $\mathcal{H}_{\mathbf{k}}$  is defined in a manner similar to the single-mode field via the energy eigenvalue equation

$$\mathcal{H}_{\mathbf{k}} |n_{\mathbf{k}}\rangle = \hbar v_k \left( n_{\mathbf{k}} + \frac{1}{2} \right) |n_{\mathbf{k}}\rangle. \quad (1.2.24)$$

The general eigenstate of  $\mathcal{H}$  can therefore have  $n_{\mathbf{k}_1}$  photons in the first mode,  $n_{\mathbf{k}_2}$  in the second,  $n_{\mathbf{k}_\ell}$  in the  $\ell$ th and so forth, and can be written as  $|n_{\mathbf{k}_1}\rangle|n_{\mathbf{k}_2}\rangle\dots|n_{\mathbf{k}_\ell}\rangle\dots$  or more conveniently

$$|n_{\mathbf{k}_1}, n_{\mathbf{k}_2}, \dots, n_{\mathbf{k}_\ell}, \dots\rangle \equiv |\{\mathbf{n}_{\mathbf{k}}\}\rangle. \quad (1.2.25)$$

The annihilation and creation operators  $a_{\mathbf{k}_\ell}$  and  $a_{\mathbf{k}_\ell}^\dagger$  lower and raise the  $\ell$ th entry alone, i.e.,

$$a_{\mathbf{k}_\ell} |n_{\mathbf{k}_1}, n_{\mathbf{k}_2}, \dots, n_{\mathbf{k}_\ell}, \dots\rangle = \sqrt{n_{\mathbf{k}_\ell}} |n_{\mathbf{k}_1}, n_{\mathbf{k}_2}, \dots, n_{\mathbf{k}_\ell} - 1, \dots\rangle, \quad (1.2.26)$$

$$a_{\mathbf{k}_\ell}^\dagger |n_{\mathbf{k}_1}, n_{\mathbf{k}_2}, \dots, n_{\mathbf{k}_\ell}, \dots\rangle = \sqrt{n_{\mathbf{k}_\ell} + 1} |n_{\mathbf{k}_1}, n_{\mathbf{k}_2}, \dots, n_{\mathbf{k}_\ell} + 1, \dots\rangle. \quad (1.2.27)$$

The general state vector for the field is a linear superposition of these eigenstates:

$$\begin{aligned} |\psi\rangle &= \sum_{n_{\mathbf{k}_1}} \sum_{n_{\mathbf{k}_2}} \dots \sum_{n_{\mathbf{k}_\ell}} \dots c_{n_{\mathbf{k}_1}, n_{\mathbf{k}_2}, \dots, n_{\mathbf{k}_\ell}, \dots} |n_{\mathbf{k}_1}, n_{\mathbf{k}_2}, \dots, n_{\mathbf{k}_\ell}, \dots\rangle \\ &\equiv \sum_{\{\mathbf{n}_{\mathbf{k}}\}} c_{\{\mathbf{n}_{\mathbf{k}}\}} |\{\mathbf{n}_{\mathbf{k}}\}\rangle. \end{aligned} \quad (1.2.28)$$

多模光场态

This is a more general superposition than

~~$$|\psi\rangle = |\psi_{k_1}\rangle|\psi_{k_2}\rangle\dots|\psi_{k_r}\rangle\dots,$$~~
X
(1.2.29)

where  $|\psi_{k_i}\rangle$  are state vectors for individual modes. Equation (1.2.28) includes state vectors of the type (1.2.29) as well as more general states having correlations between the field modes which can result from interaction of the various field modes with a common system.

### 1.3 Lamb shift

The precision observation of the Lamb shift, between the  $2S_{1/2}$  and  $2P_{1/2}$  levels in hydrogen, was in a real sense the stimulus for modern quantum electrodynamics (QED). According to Dirac theory, the  $2S_{1/2}$  and  $2P_{1/2}$  levels should have equal energies. However, radiative corrections due to the interaction between the atomic electron and the vacuum, shift the  $2S_{1/2}$  level higher in energy by around 1057 MHz relative to the  $2P_{1/2}$  level.

Early attempts to calculate such ‘vacuum induced’ radiative corrections were frustrated in that they predicted infinite level shifts. However, the beautiful measurement of Lamb and Rutherford provided the stimulus for renormalization theory which has been so successful in handling these divergences.

On the occasion of Lamb’s sixty-fifth birthday, Freeman Dyson\* wrote:

Your work on the hydrogen fine structure led directly to the wave of progress in quantum electrodynamics on which I took a ride to fame and fortune. You did the hard, tedious, exploratory work. Once you had started the wave rolling, the ride for us theorists was easy. And after we had zoomed ashore with our fine, fancy formalisms, you still stayed with your stubborn experiment. For many years thereafter you were at work, carefully coaxing the hydrogen atom to give us the accurate numbers which provided the solid foundations for all our speculations...

Those years, when the Lamb shift was the central theme of physics, were golden years for all the physicists of my generation. You were the first to see that that tiny shift, so elusive and hard to measure, would clarify in a fundamental way our thinking about particles and fields.

\* Dyson [1978].

Shortly after the experimental results were announced, Bethe produced a simple nonrelativistic calculation which was in good qualitative agreement with theory, by using the suggestion of Kramers, Schwinger, and Weisskopf for ‘subtracting off’ infinities. This was extended to a full relativistic theory in quantitative agreement with experiments by Kroll and Lamb, and French and Weisskopf; and was the harbinger of modern QED as developed by Schwinger, Feynman, and Dyson.

The excellent agreement between the full quantum theory of radiation and matter, and experiment, e.g., the Lamb shift, provides strong support for the quantization of the radiation field. However, a detailed calculation of the Lamb shift would take us too far from mainstream quantum optics. Therefore, we will present here a heuristic derivation of the electromagnetic level shift following Welton.

The effect of the fluctuations in the electric and magnetic fields associated with the vacuum is a perturbation of the electron in a hydrogen atom from the standard orbits of the Coulomb potential  $-e^2/4\pi\epsilon_0 r$  due to the proton; so the electron radius  $r \rightarrow r + \delta r$ , where  $\delta r$  is the fluctuation in the position of the electron due to the fluctuating fields. The change in potential energy, and thus the associated level shift, is given by

$$\begin{aligned}\Delta V &= V(\mathbf{r} + \delta\mathbf{r}) - V(\mathbf{r}) \\ &= \delta\mathbf{r} \cdot \nabla V + \frac{1}{2}(\delta\mathbf{r} \cdot \nabla)^2 V(\mathbf{r}) + \dots\end{aligned}\quad (1.3.1)$$

Since the fluctuations are isotropic,  $\langle \delta\mathbf{r} \rangle_{\text{vac}} = 0$ , the first term can be neglected. Moreover,

$$\langle (\delta\mathbf{r} \cdot \nabla)^2 \rangle_{\text{vac}} = \frac{1}{3} \langle (\delta\mathbf{r})^2 \rangle_{\text{vac}} \nabla^2, \quad (1.3.2)$$

again due to the isotropy of the fluctuations. We therefore obtain

$$\langle \Delta V \rangle = \frac{1}{6} \langle (\delta\mathbf{r})^2 \rangle_{\text{vac}} \left\langle \nabla^2 \left( \frac{-e^2}{4\pi\epsilon_0 r} \right) \right\rangle_{\text{at}}, \quad (1.3.3)$$

where  $\langle \dots \rangle_{\text{at}}$  represents the quantum average with respect to the atomic states.

For the  $2S$  state of hydrogen

$$\begin{aligned}\left\langle \nabla^2 \left( \frac{-e^2}{4\pi\epsilon_0 r} \right) \right\rangle_{\text{at}} &= \frac{-e^2}{4\pi\epsilon_0} \int d\mathbf{r} \psi_{2S}^*(\mathbf{r}) \nabla^2 \left( \frac{1}{r} \right) \psi_{2S}(\mathbf{r}) \\ &= \frac{e^2}{\epsilon_0} |\psi_{2S}(0)|^2 \\ &= \frac{e^2}{8\pi\epsilon_0 a_0^3},\end{aligned}\quad (1.3.4)$$

$$\begin{aligned}&\langle \delta\mathbf{r}^2 \rangle_{\text{vac}} = \langle (\delta x)^2 + (\delta y)^2 + (\delta z)^2 \rangle \\ &\text{由于 } \delta x, \delta y, \delta z \text{ 互不相关, } \langle \delta x \delta y \rangle = \langle \delta y \delta z \rangle = \langle \delta z \delta x \rangle = 0, \text{ 故只取第一项} \\ &= \langle (\delta x)^2 \rangle + \langle (\delta y)^2 \rangle + \langle (\delta z)^2 \rangle \\ &\text{而又由各向同性, } \langle (\delta x)^2 \rangle = \langle (\delta y)^2 \rangle = \langle (\delta z)^2 \rangle = \frac{\langle (\delta x)^2 + (\delta y)^2 + (\delta z)^2 \rangle}{3} = \frac{4\pi r^2}{3} \\ &= \frac{1}{3} \langle \delta\mathbf{r}^2 \rangle \quad (\text{由 } \delta\mathbf{r}^2 = (\delta x)^2 + (\delta y)^2 + (\delta z)^2) \\ &= \frac{1}{3} \langle \delta\mathbf{r}^2 \rangle \cdot \frac{1}{r^2}\end{aligned}$$

where  $a_0 = 4\pi\epsilon_0\hbar^2/me^2$  ( $m$  is the mass of the electron) is the Bohr radius and we use

$$\nabla^2 \left( \frac{1}{r} \right) = -4\pi\delta(\mathbf{r}), \quad (1.3.5)$$

and

$$\psi_{2s}(0) = \frac{1}{(8\pi a_0^3)^{1/2}}. \quad (1.3.6)$$

For  $P$ -states, the nonrelativistic wave function vanishes at the origin and hence so does the energy shift.

Next we consider the contribution  $\langle (\delta\mathbf{r})^2 \rangle_{\text{vac}}$  due to the vacuum fluctuations in Eq. (1.3.3). The classical equation of motion for the electron displacement  $(\delta r)_\mathbf{k}$  induced by a single mode of the field of wave vector  $\mathbf{k}$  and frequency  $\nu$  is

$$m \frac{d^2}{dt^2} (\delta r)_\mathbf{k} = -e E_\mathbf{k}. \quad (1.3.7)$$

决定于  $k$  的下界

This is valid if the field frequency  $\nu$  is greater than the frequency  $\nu_0$  in the Bohr orbit, i.e., if  $\nu > \pi c/a_0$ . For the field oscillating at frequency  $\nu$ ,

$$\delta r(t) \cong \delta r(0)e^{-i\nu t} + \text{c.c.} \quad (1.3.8)$$

We thus have

$$(\delta r)_\mathbf{k} \cong \frac{e}{mc^2 k^2} E_\mathbf{k}, \quad (1.3.9)$$

where, from Eq. (1.1.27),

$$E_\mathbf{k} = \mathcal{E}_\mathbf{k} (a_\mathbf{k} e^{-i\nu t + i\mathbf{k}\cdot\mathbf{r}} + \text{H.c.}) \quad (1.3.10)$$

After summing over all modes, we obtain

$$\begin{aligned} \langle (\delta\mathbf{r})^2 \rangle_{\text{vac}} &= \sum_{\mathbf{k}} \left( \frac{e}{mc^2 k^2} \right)^2 \langle 0 | (E_\mathbf{k})^2 | 0 \rangle \\ &= \sum_{\mathbf{k}} \left( \frac{e}{mc^2 k^2} \right)^2 \left( \frac{\hbar ck}{2\epsilon_0 V} \right), \end{aligned} \quad (1.3.11)$$

where we have made the substitution  $\mathcal{E}_\mathbf{k} = (\hbar ck/2\epsilon_0 V)^{1/2}$ . For the continuous mode distribution, the summation in Eq. (1.3.11) is changed to an integral (Eq. (1.1.23)). We then obtain after carrying out the angular integrations

$$\begin{aligned} \langle (\delta\mathbf{r})^2 \rangle_{\text{vac}} &= 2 \frac{V}{(2\pi)^3} 4\pi \int dk k^2 \left( \frac{e}{mc^2 k^2} \right)^2 \left( \frac{\hbar ck}{2\epsilon_0 V} \right) \\ &= \frac{1}{2\epsilon_0 \pi^2} \left( \frac{e^2}{\hbar c} \right) \left( \frac{\hbar}{mc} \right)^2 \int \frac{dk}{k}. \end{aligned} \quad (1.3.12)$$

This gives a divergent result. However as noted before, the present method is only valid for  $v > \pi c/a_0$ , or equivalently  $k > \pi/a_0$ . It is also valid only for wavelengths longer than the Compton wavelength, i.e.,  $k < mc/\hbar$ , because of magnetic effects on the motion which begin when  $v/c = p/mc = \hbar k/mc \lesssim 1$ . The present method is invalid if the electron is relativistic. We can therefore choose the lower and upper limits for the integral in Eq. (1.3.12) to be  $\pi/a_0$  and  $mc/\hbar$ , respectively. We then obtain

$$\langle(\delta\mathbf{r})^2\rangle_{\text{vac}} \approx \frac{1}{2\epsilon_0\pi^2} \left(\frac{e^2}{\hbar c}\right) \left(\frac{\hbar}{mc}\right)^2 \ln\left(\frac{4\epsilon_0\hbar c}{e^2}\right). \quad (1.3.13)$$

On substituting Eqs. (1.3.4) and (1.3.13) into Eq. (1.3.3), we obtain the following expression for the Lamb shift

$$\langle\Delta V\rangle = \frac{4}{3} \frac{e^2}{4\pi\epsilon_0} \frac{e^2}{4\pi\epsilon_0\hbar c} \left(\frac{\hbar}{mc}\right)^2 \frac{1}{8\pi a_0^3} \ln\left(\frac{4\epsilon_0\hbar c}{e^2}\right). \quad (1.3.14)$$

$\approx 0.512 \text{ GHz}$

This shift is about 1 GHz in good agreement with the observed shift, considering the crude approximations made in the calculation.

Finally, we note the exciting developments in Lamb shift physics made possible by modern quantum optical techniques, namely the measurement of the radiation shift of the  $1S$  state via precise measurements of the two-photon  $1S-2S$  transition first performed by Hänsch and co-workers.

## 1.4 Quantum beats (stochastic ED是错的，因为引入了真空涨落，没引入光场量子化) Δ型原子双线干涉，V型有。

Over the past decades several alternative theories to quantum electrodynamics (QED) have been proposed. One such theory is based on stochastic electrodynamics. In this theory, matter is treated quantum mechanically while radiation is described according to Maxwell's equations, to which one adds *vacuum fluctuations*. In this picture, it would seem that almost all quantum phenomena, such as spontaneous emission, Lamb shift, and the laser linewidth, can be understood in a semiquantitative fashion.

Quantum beat\* phenomena however provide us with a simple example of a case in which the results of a self-consistent fully quantized calculation differ substantially from those obtained via a semiclassical theory (SCT) even when augmented by the notion of vacuum fluctuations. This is a good example of a problem which cannot be explained, let alone calculated, by semiclassical-type arguments.

\* Svanberg [1991].

## Problems

- 1.1** The radiation field in an empty cubic cavity of side  $L$  satisfies the wave equation

$$\nabla^2 \mathbf{A} - \frac{1}{c^2} \frac{\partial^2 \mathbf{A}}{\partial t^2} = 0,$$

together with the Coulomb gauge condition  $\nabla \cdot \mathbf{A} = 0$ . Show that the solution that satisfies the boundary conditions has components

$$A_x(\mathbf{r}, t) = A_x(t) \cos(k_x x) \sin(k_y y) \sin(k_z z),$$

$$A_y(\mathbf{r}, t) = A_y(t) \sin(k_x x) \cos(k_y y) \sin(k_z z),$$

$$A_z(\mathbf{r}, t) = A_z(t) \sin(k_x x) \sin(k_y y) \cos(k_z z),$$

where  $\mathbf{A}(t)$  is independent of position and the wave vector  $\mathbf{k}$  has components given by Eq. (1.1.21). Hence show that the integers  $n_x, n_y, n_z$  in Eq. (1.1.21) are restricted in that only one of them can be zero at a time.

- 1.2** If  $A$  and  $B$  are two noncommuting operators that satisfy the conditions

$$[[A, B], A] = [[A, B], B] = 0,$$

then show that

$$\begin{aligned} e^{A+B} &= e^{-\frac{1}{2}[A,B]} e^A e^B, \\ &= e^{+\frac{1}{2}[A,B]} e^B e^A. \end{aligned}$$

This is a special case of the so-called Baker–Hausdorff theorem of group theory.

- 1.3** If  $A$  and  $B$  are two noncommuting operators and  $\alpha$  is a parameter, then show that

$$e^{-\alpha A} B e^{\alpha A} = B - \alpha [A, B] + \frac{\alpha^2}{2!} [A, [A, B]] + \dots$$

- 1.4** If  $f(a, a^\dagger)$  is a function which can be expanded in a power series of  $a$  and  $a^\dagger$ , then show that

$$(a) [a, f(a, a^\dagger)] = \frac{\partial f}{\partial a^\dagger},$$

$$(b) [a^\dagger, f(a, a^\dagger)] = -\frac{\partial f}{\partial a},$$

$$(c) e^{-\alpha a^\dagger a} f(a, a^\dagger) e^{\alpha a^\dagger a} = f(a e^\alpha, a^\dagger e^{-\alpha}),$$

where  $\alpha$  is a parameter.

**1.5** Show that

$$[a, e^{-\alpha a^\dagger a}] = (e^{-\alpha} - 1)e^{-\alpha a^\dagger a}a,$$

$$[a^\dagger, e^{-\alpha a^\dagger a}] = (e^{\alpha} - 1)e^{-\alpha a^\dagger a}a^\dagger,$$

where  $\alpha$  is a parameter.

**1.6** Show that the free-field Hamiltonian

$$\mathcal{H} = \hbar v \left( a^\dagger a + \frac{1}{2} \right)$$

can be written in terms of the number states as

$$\mathcal{H} = \sum_n E_n |n\rangle \langle n|,$$

and hence

$$e^{i\mathcal{H}t/\hbar} = \sum_n e^{iE_nt/\hbar} |n\rangle \langle n|.$$

**1.7** Show that Maxwell's equations in free space may be written in the form of Eqs. (1.5.27a) and (1.5.27b) by first showing that

$$\frac{1}{c} \frac{\partial \tilde{\mathbf{E}}}{\partial t} = \nabla \times \tilde{\mathbf{H}}, \quad \nabla \cdot \tilde{\mathbf{E}} = 0,$$

$$-\frac{1}{c} \frac{\partial \tilde{\mathbf{H}}}{\partial t} = \nabla \times \tilde{\mathbf{E}}, \quad \nabla \cdot \tilde{\mathbf{H}} = 0,$$

where  $\tilde{\mathbf{E}} = \sqrt{\epsilon_0} \mathbf{E}$  and  $\tilde{\mathbf{H}} = \sqrt{\mu_0} \mathbf{H}$ . Then prove that

$$\mathbf{s} \cdot \nabla \mathbf{V} = \nabla \times \mathbf{V},$$

$$s_x = \begin{bmatrix} 0 & 0 & 0 \\ 0 & 0 & -1 \\ 0 & 1 & 0 \end{bmatrix}, \quad s_y = \begin{bmatrix} 0 & 0 & 1 \\ 0 & 0 & 0 \\ -1 & 0 & 0 \end{bmatrix},$$

$$s_z = \begin{bmatrix} 0 & -1 & 0 \\ 1 & 0 & 0 \\ 0 & 0 & 0 \end{bmatrix},$$

where  $\mathbf{s}$  and  $\mathbf{V}$  on the left-hand side are regarded as  $1 \times 3$  column vectors. Use this identity to obtain Eqs. (1.5.27a) and (1.5.27b).

- 1.8** Derive the current density (1.5.32) by writing the equations of motion for  $\varphi_\gamma$  and  $\chi_\gamma$  in the form

$$\begin{aligned}\dot{\varphi}_\gamma &= c\mathbf{s} \cdot \nabla \chi_\gamma, \\ \dot{\chi}_\gamma &= -c\mathbf{s} \cdot \nabla \varphi_\gamma, \quad \dot{\varphi}_\gamma^\dagger = c\nabla \chi_\gamma^\dagger \cdot \mathbf{s}^\dagger, \\ \dot{\chi}_\gamma^\dagger &= -c\nabla \varphi_\gamma^\dagger \cdot \mathbf{s}^\dagger,\end{aligned}$$

and noting that  $\mathbf{s}^\dagger = -\mathbf{s}$ .

- 1.9** Verify that  $\sum_i \hat{\mathbf{e}}_i \hat{\mathbf{e}}_i = \mathbf{1}$  by taking the dot product with any vector  $\mathbf{v}$ . Thus if  $\hat{\mathbf{e}}_1 = \hat{\epsilon}_{\mathbf{k}}^{(1)}$ ,  $\hat{\mathbf{e}}_2 = \hat{\epsilon}_{\mathbf{k}}^{(2)}$ , and  $\hat{\mathbf{e}}_3 = \mathbf{k}/k$  we have equation (1.1.36). It is also possible to prove (1.1.37) by letting  $k, \theta, \phi$  be the polar coordinates of the wave vector  $\mathbf{k}$ , so that

$$\mathbf{k} \equiv k(\sin \theta \cos \phi, \sin \theta \sin \phi, \cos \theta).$$

The two transverse polarization vectors can then be represented by

$$\begin{aligned}\hat{\epsilon}_{\mathbf{k}}^{(1)} &\equiv (\sin \phi, -\cos \phi, 0), \\ \hat{\epsilon}_{\mathbf{k}}^{(2)} &\equiv (\cos \theta \cos \phi, \cos \theta \sin \phi, -\sin \theta),\end{aligned}$$

and it can be verified that

$$\epsilon_{\mathbf{k}i}^{(1)} \epsilon_{\mathbf{k}j}^{(1)} + \epsilon_{\mathbf{k}i}^{(2)} \epsilon_{\mathbf{k}j}^{(2)} = \delta_{ij} - \frac{k_i k_j}{k^2},$$

where  $i, j$  represent the Cartesian components. Demonstrate this by direct substitution.

# 一、算符代数的諸公式

## 1. 常用公式

$$\left\{ \begin{array}{l} [A, B^n] = n[A, B]B^{n-1} \quad \text{if } [B, [A, B]] = 0 \\ [A^n, B] = nA^{n-1}[A, B] \quad \text{if } [A, [A, B]] = 0 \\ \frac{d}{dx} e^{\lambda A} = \lambda e^{\lambda A} \\ [A, e^{\lambda B}] = \lambda C e^{\lambda B} \quad \text{where } C = [A, B] \quad \text{if } [C, A] = [C, B] = 0 \\ e^{\lambda(A+B)} = e^{\lambda A} e^{\lambda B} e^{-\frac{\lambda^2}{2}[A, B]} \quad \text{where } C = [A, B] \quad \text{if } [C, A] = [C, B] = 0 \end{array} \right.$$

$$\left\{ \begin{array}{l} e^{xa} a^+ e^{-xa} = a^+ + x \\ e^{xa^+} a e^{-xa^+} = a + x \end{array} \right.$$

$$\left\{ \begin{array}{l} e^{x\alpha} a^- e^{-x\alpha} = a e^x \\ e^{x\alpha^-} a^+ e^{-x\alpha^-} = a^+ e^x \end{array} \right.$$

$$\left\{ \begin{array}{l} e^{xa} f(a, a^+) e^{-xa} = f(a, a^+ + x) \\ e^{xa^+} f(a, a^+) e^{-xa^+} = f(a + x, a^+) \end{array} \right.$$

$$e^{x\alpha} f(a, a^-) e^{-x\alpha} = f(a e^x, a^- e^x)$$

2. 如果  $f(a, a^+)$  可以表示为  $a, a^+$  的多项式，即

$$[a, f(a, a^+)] = \frac{\partial f}{\partial a^+} \quad [a^+, f(a, a^+)] = \frac{\partial f}{\partial a}$$

证明：记  $[a, (a^+)^n] = n(a^+)^{n-1}$

$$f(a, a^+) = \sum_{m,n} f_{mn} a^m (a^+)^n$$

$$\frac{\partial f}{\partial a^+} = \sum f_{mn} a^m n(a^+)^{n-1} = \sum f_{mn} a^m [a, (a^+)^n]$$

$$= a \sum f_{mn} a^m (a^+)^{n-1} - \sum f_{mn} a^m (a^+)^n a$$

$$= [a, f(a, a^+)]$$

$$\text{证二: } \frac{\partial f}{\partial a^+} = \lim_{\delta \rightarrow 0} \frac{f(a, a^+ + \delta) - f(a, a^+)}{\delta} = \frac{e^{\delta a} f(a, a^+) e^{-\delta a} - f(a, a^+)}{\delta}$$

$$= \frac{(1+\delta a) f(a, a^\dagger) (1-\delta a) - f(a, a^\dagger)}{\delta} = [a, f(a, a^\dagger)]$$

二、熵最大原理  $\Rightarrow$  热力学第一定律

$$S(\rho) = -k \text{Tr}(\rho \ln \rho) \quad S = -k \sum_i p_i \ln p_i$$

$$\text{Tr}(\rho) = 1 \quad \langle E \rangle = \text{Tr}(\rho \hat{H}) \quad \text{能量}$$

熵最大条件

$$\left\{ \begin{array}{l} (1) \delta S = 0, \text{Tr}(1 + \ln \rho) \delta \rho = 0 \\ (2) \text{Tr}(S) = 0 \quad (\text{约束条件}) \\ (3) \text{Tr}(\hat{H} \delta \rho) = 0 \end{array} \right.$$

$$\Downarrow \text{拉格朗日乘子法} \quad \lambda(2) + \beta(3) = 0$$

$$\text{Tr}(1 + \ln \rho + \lambda + \beta \hat{H}) \delta \rho = 0$$

$$\Rightarrow \rho = e^{-(\lambda + \beta \hat{H})} e^{-\beta \hat{H}}$$

$$\text{又因} \text{Tr}(\rho) = 1$$

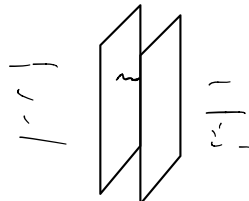
$$\Rightarrow \rho = \frac{e^{-\beta \hat{H}}}{\text{Tr}(e^{-\beta \hat{H}})} \quad \text{经典对应} \quad \beta = \frac{1}{kT}$$

$$\Rightarrow \rho = \frac{\exp(-\hat{A}/kT)}{\sum_n \langle n | \exp(-\hat{n}h\nu/kT) | n \rangle} = (1 - e^{-\hbar h\nu/kT}) e^{-\hat{A}/kT}$$

三、Casimir 效应

外若种核式

内泡核



$$\langle \hat{E}^2 \rangle = \langle 0 | \hat{E}^2 | 0 \rangle \neq 0, \quad \langle \hat{E} \rangle = 0 \quad \text{电场强度}$$

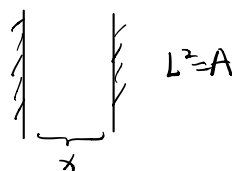
外辐射压 > 内辐射压，引力

$$\Rightarrow F \sim \frac{A}{d^4}$$

$$P \sim -\frac{\pi^2}{240} \frac{\hbar c}{d^4} \quad \text{例 } A=1\text{cm}^2, d=1\mu\text{m} \approx, F=10^{-7}\text{N}$$

$$d=10\text{nm}, \quad P=1\text{大气压}$$

近似计算



$$U = \int \frac{1}{2} \hbar \omega_k p(k) dk = \int_0^{+\infty} \frac{1}{2} \hbar k c \frac{2V}{(2\pi)^3} 4\pi k^2 dk$$

$$k \left\{ \begin{array}{l} \text{下限} \\ \text{上限} \end{array} \right. \quad k_1 \sim \frac{2x}{2x} \sim \frac{x}{x} \quad \text{限制} \leq k \leq x \\ k_2 \sim \frac{1}{a_0} \quad \text{高斯波波长}$$

$$\Rightarrow U = A \frac{\hbar c}{2\pi^2} \int_{\frac{x}{x}}^{\frac{1}{a_0}} x k^3 dk = \frac{A \hbar c}{2\pi^2} \left( \frac{x}{4a_0^4} - \frac{x^4}{4x^3} \right)$$

$$\text{压强 } P = \frac{1}{A} \frac{du}{dx} \propto \frac{1}{x^4} \sim \frac{-\hbar c x^2}{8x^4}$$

#### 四、Unruh 效应 W.G. Unruh

振动频率  $\propto A$  真空场  
 加速度  $\propto B$  热光场 (产生加速度)

# Coherent and squeezed states of the radiation field

Following the development of the quantum theory of radiation and with the advent of the laser, the states of the field that most nearly describe a classical electromagnetic field were widely studied. In order to realize such ‘classical’ states, we will consider the field generated by a classical monochromatic current, and find that the quantum state thus generated has many interesting properties and deserves to be called a *coherent state*.<sup>\*</sup> An important consequence of the quantization of the radiation field is the associated uncertainty relation for the conjugate field variables. It therefore appears reasonable to propose that the wave function which corresponds most closely to the classical field must have *minimum* uncertainty for all times subject to the appropriate simple harmonic potential.

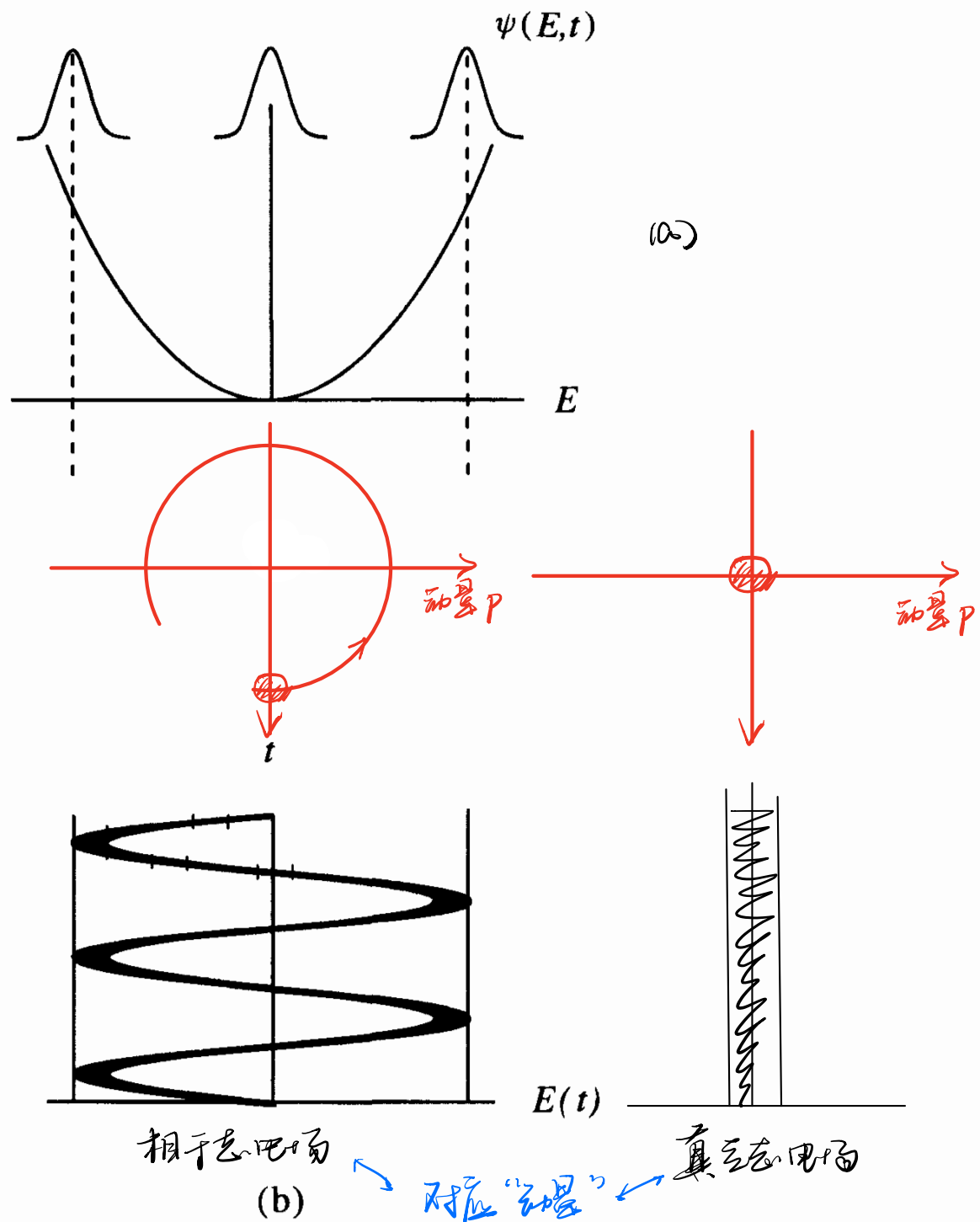
In this chapter we show that a displaced simple harmonic oscillator ground state wave function satisfies this property and the wave packet oscillates sinusoidally in the oscillator potential without changing shape as shown in Fig. 2.1. This *coherent* wave packet always has *minimum uncertainty*, and resembles the classical field as nearly as quantum mechanics permits. The corresponding state vector is the *coherent state*  $|\alpha\rangle$ , which is the eigenstate of the positive frequency part of the electric field operator, or, equivalently, the eigenstate of the destruction operator of the field.

Classically an electromagnetic field consists of waves with well-defined amplitude and phase. Such is not the case when we treat the field quantum mechanically. There are fluctuations associated with both the amplitude and phase of the field. An electromagnetic field in a number state  $|n\rangle$  has a well-defined amplitude but completely

\* The coherent state concept was introduced by Schrödinger [1926]. For an excellent treatment of the subject see the Les Houches lectures of Glauber [1965].

Fig. 2.1

(a) Minimum-uncertainty wave packet at different times in a harmonic oscillator potential.  
 (b) Corresponding electric field.



uncertain phase, whereas a field in a coherent state has equal amount of uncertainties in the two variables. Equivalently, we can describe the field in terms of the two conjugate quadrature components. The uncertainties in the two conjugate variables satisfy the Heisenberg uncertainty principle such that the product of the uncertainties in the two variables is equal to or greater than half the magnitude of the expectation value of the commutator of the variables (see Eq. (2.6.2) below). A field in a coherent state is a minimum-uncertainty state with equal uncertainties in the two quadrature components.

After developing the coherent states of the radiation field, we turn

to the so-called *squeezed states*. In principle, it is possible to generate states in which fluctuations are reduced below the symmetric quantum limit in one quadrature component. This is accomplished at the expense of enhanced fluctuations in the canonically conjugate quadrature, such that the Heisenberg uncertainty principle is not violated. Such states of the radiation field are called *squeezed states*. A quadrature of electromagnetic field with reduced fluctuations below the standard quantum limit, has attractive applications in optical communication, photon detection techniques, gravitational wave detection, and noise-free amplification. In this chapter, we physically motivate and present the definition and properties of the squeezed states, with special reference to the so-called *squeezed coherent states*. These states result from applying the ‘squeeze operator’ to the coherent state.

## 2.1 Radiation from a classical current (相干态的产生)

In this section, we define the coherent state and show that the radiation emitted by a classical current distribution is such a state. By *classical* we mean that the current can be described by a prescribed vector  $\mathbf{J}(\mathbf{r}, t)$  which is not an operator. We consider coupling of this current to the vector potential operator (cf. Eq. (1.1.27) and Section 5.1)

$$\underline{\mathbf{A}}(\mathbf{r}, t) = -i \sum_{\mathbf{k}} \frac{1}{v_k} \hat{\epsilon}_{\mathbf{k}} \mathcal{E}_{\mathbf{k}} a_{\mathbf{k}} e^{-iv_k t + i\mathbf{k} \cdot \mathbf{r}} + \text{H.c.} \quad (2.1.1)$$

~~算符~~

The Hamiltonian that describes the interaction between the field and the current is then given by

$$\underline{\mathcal{V}(t)} = \int \mathbf{J}(\mathbf{r}, t) \cdot \mathbf{A}(\mathbf{r}, t) d^3 r \quad H_0 = \hbar \omega (\hat{a}^\dagger \hat{a} + \frac{1}{2}) \quad (2.1.2)$$

~~Schrödinger 方程~~

and the state vector  $|\psi(t)\rangle$  for the combined system obeys the interaction picture Schrödinger equation

$$\frac{d}{dt} |\psi(t)\rangle = -\frac{i}{\hbar} \underline{\mathcal{V}} |\psi(t)\rangle. \quad \underline{\mathcal{V}_I} = e^{-i \frac{H_0}{\hbar} t} \underline{\mathcal{V}} e^{i \frac{H_0}{\hbar} t} \quad (2.1.3)$$

~~Interaction term~~

The vector function  $\mathbf{J}(\mathbf{r}, t)$  commutes with itself at different times, but the operator  $\mathbf{A}(\mathbf{r}, t)$  does not. Hence the interaction energy  $\mathcal{V}(t)$  does not either, and ordinarily the Schrödinger equation cannot be integrated as

$$|\psi(t)\rangle = \exp \left[ -\frac{i}{\hbar} \int_0^t dt' \underline{\mathcal{V}}(t') \right] |\psi(0)\rangle. \quad (2.1.4)$$

However, the various commutators introduced in obtaining the correct integration yield (2.1.4) multiplied by an overall phase factor which we discard. With (2.1.1) and (2.1.2), the exponential in (2.1.4) becomes

$$\exp \left[ -\frac{i}{\hbar} \int_0^t dt' \mathcal{V}(t') \right] = \prod_{\mathbf{k}} \exp(\alpha_{\mathbf{k}} a_{\mathbf{k}}^\dagger - \alpha_{\mathbf{k}}^* a_{\mathbf{k}}), \quad (2.1.5)$$

where the complex time-dependent amplitude  $\alpha_{\mathbf{k}}$  is

$$\alpha_{\mathbf{k}} = \frac{1}{\hbar v_k} \mathcal{E}_{\mathbf{k}} \int_0^t dt' \int d\mathbf{r} \hat{\epsilon}_{\mathbf{k}} \cdot \mathbf{J}_v(\mathbf{r}, t) e^{iv_k t' - i\mathbf{k} \cdot \mathbf{r}}. \quad (2.1.6)$$

In Eq. (2.1.6) the dipole current  $\mathbf{J}_v(\mathbf{r}, t)$  is given the subscript  $v$  to denote the fact that it is a monochromatic dipole oscillating at frequency  $v = ck$ . We choose the initial state  $|\psi(0)\rangle$  to be the vacuum  $|0\rangle$ , and the state vector (2.1.4) then becomes

$$|\psi(t)\rangle = \prod_{\mathbf{k}} \exp(\alpha_{\mathbf{k}} a_{\mathbf{k}}^\dagger - \alpha_{\mathbf{k}}^* a_{\mathbf{k}}) |0\rangle_{\mathbf{k}}. \quad (2.1.7)$$

This state of the radiation field is called a coherent state and is denoted as  $|\{\alpha_{\mathbf{k}}\}\rangle$ . It is apparent that the multi-mode coherent state in Eq. (2.1.7) can be expressed as a product of single-mode coherent states  $|\alpha_{\mathbf{k}}\rangle$ :

$$|\{\alpha_{\mathbf{k}}\}\rangle = \prod_{\mathbf{k}} |\alpha_{\mathbf{k}}\rangle, \quad (2.1.8)$$

where

$$|\alpha_{\mathbf{k}}\rangle = \exp(\alpha_{\mathbf{k}} a_{\mathbf{k}}^\dagger - \alpha_{\mathbf{k}}^* a_{\mathbf{k}}) |0\rangle_{\mathbf{k}}. \quad (2.1.9)$$

In the remainder of this chapter, we shall be mostly concerned with a single-mode coherent state. We shall therefore remove the index  $\mathbf{k}$  from our definition in Eq. (2.1.9) and write

$$|\alpha\rangle = \exp(\alpha a^\dagger - \alpha^* a) |0\rangle. \quad (2.1.10)$$

In the following, we present alternative approaches to the coherent state.

## 2.2 The coherent state as an eigenstate of the annihilation operator and as a displaced harmonic oscillator state

Expression (2.1.10) was obtained by defining the coherent state of the radiation field  $|\alpha\rangle$  as a state of the field which is generated by a classically oscillating current distribution. The same expression for  $|\alpha\rangle$  can be obtained by defining it as an eigenstate of the annihilation operator  $a$  with an eigenvalue  $\alpha$ , i.e.,

$$a|\alpha\rangle = \alpha|\alpha\rangle. \quad (2.2.1)$$

An expression of  $|\alpha\rangle$  in terms of the number state  $|n\rangle$  is given by

$$|\alpha\rangle = e^{-|\alpha|^2/2} \sum_{n=0}^{\infty} \frac{\alpha^n}{\sqrt{n!}} |n\rangle, \quad (2.2.2)$$

and since  $|n\rangle = [(a^\dagger)^n / \sqrt{n!}]|0\rangle$  this can be written as

$$|\alpha\rangle = e^{\alpha a^\dagger} |0\rangle e^{-|\alpha|^2/2}. \quad (2.2.3)$$

Next we note that since  $\exp(-\alpha^* a)|0\rangle = |0\rangle$ , Eq. (2.2.3) can be rewritten as

$$|\alpha\rangle = D(\alpha)|0\rangle, \quad (2.2.4)$$

where

$$D(\alpha) = e^{-|\alpha|^2/2} e^{\alpha a^\dagger} e^{-\alpha^* a}. \quad (2.2.5)$$

Now, in view of the Baker–Hausdorff formula, if  $A$  and  $B$  are any two operators such that

$$[[A, B], A] = [[A, B], B] = 0, \quad (2.2.6)$$

then

$$e^{A+B} = e^{-[A,B]/2} e^A e^B. \quad (2.2.7)$$

If we write  $A = \alpha a^\dagger$ ,  $B = -\alpha^* a$ , it follows that

$$D(\alpha) = e^{\alpha a^\dagger - \alpha^* a}, \quad (2.2.8)$$

in agreement with Eq. (2.1.10). Another equivalent antinormal form of  $D(\alpha)$  is

$$D(\alpha) = e^{|\alpha|^2/2} e^{-\alpha^* a} e^{\alpha a^\dagger}. \quad (2.2.9)$$

The operator  $D(\alpha)$  is a unitary operator, i.e.,

$$D^\dagger(\alpha) = D(-\alpha) = [D(\alpha)]^{-1}. \quad (2.2.10)$$

It acts as a displacement operator upon the amplitudes  $a$  and  $a^\dagger$ , i.e.,

$$D^{-1}(\alpha)aD(\alpha) = a + \alpha, \quad (2.2.11)$$

$$D^{-1}(\alpha)a^\dagger D(\alpha) = a^\dagger + \alpha^*. \quad (2.2.12)$$

The displacement property can be proved by writing

$$D^{-1}(\alpha)aD(\alpha) = e^{\alpha^*a}e^{-\alpha a^\dagger}ae^{\alpha a^\dagger}e^{-\alpha^*a}, \quad (2.2.13)$$

where we have used the form (2.2.9) for  $D^{-1}(\alpha)$  and the form (2.2.5) for  $D(\alpha)$ . For any operators  $A$  and  $B$

$$e^{-\alpha A}Be^{\alpha A} = B - \alpha[A, B] + \frac{\alpha^2}{2!}[A, [A, B]] + \dots \quad (2.2.14)$$

For  $A = a^\dagger, B = a$ , this becomes

$$e^{-\alpha a^\dagger}ae^{\alpha a^\dagger} = a + \alpha. \quad (2.2.15)$$

Use of this result in Eq. (2.2.13) gives the displacement property (2.2.11) for  $D(\alpha)$ . The displacement property (2.2.12) can be proved in a similar way.

According to Eq. (2.2.4), a coherent state is obtained by applying the displacement operator on the vacuum state. The coherent state is therefore the displaced form of the harmonic oscillator ground state.

## 2.3 What is so coherent about coherent states?

To answer this question it is instructive to consider the coordinate representation of the oscillator number state  $|n\rangle$ . The coordinate representation of  $|n\rangle$  is given by

$$\phi_n(q) = \langle q|n\rangle. \quad (2.3.1)$$

It follows from Eqs. (1.1.11) that

$$a = \frac{1}{\sqrt{2\hbar\nu}} \left( vq + \hbar \frac{\partial}{\partial q} \right), \quad a^\dagger = \frac{1}{\sqrt{2\hbar\nu}} \left( vq - \hbar \frac{\partial}{\partial q} \right), \quad (2.3.2)$$

where we have used  $p = -i\hbar\partial/\partial q$ . Equation (1.2.7) then leads to

$$\left( vq + \hbar \frac{\partial}{\partial q} \right) \phi_0(q) = 0. \quad (2.3.3)$$

A normalized solution of this equation is

$$\phi_0(q) = \left( \frac{v}{\pi\hbar} \right)^{1/4} \exp \left( -\frac{vq^2}{2\hbar} \right). \quad (2.3.4)$$

Higher order eigenfunctions in the coordinate representation can be obtained from Eqs. (1.2.16), (2.3.1), and (2.3.2):

$$\begin{aligned}\phi_n(q) &= \frac{(a^\dagger)^n}{\sqrt{n!}} \phi_0(q) = \frac{1}{\sqrt{n!}} \frac{1}{(2\hbar\nu)^{n/2}} \left( \nu q - \hbar \frac{\partial}{\partial q} \right)^n \phi_0(q) \\ &= \frac{1}{(2^n n!)^{1/2}} H_n \left( \sqrt{\frac{\nu}{\hbar}} q \right) \phi_0(q),\end{aligned}\quad (2.3.5)$$

where  $H_n$  are the Hermite polynomials. These are the well-known eigenfunctions of the harmonic oscillator. It can be verified that these wave functions satisfy the orthonormality condition

$$\int_{-\infty}^{\infty} \phi_n^*(q) \phi_m(q) dq = \delta_{nm}. \quad (2.3.6)$$

It follows from the definition of the harmonic oscillator wave functions  $\phi_n(q)$  that

$$\langle q \rangle = \int_{-\infty}^{\infty} \phi_n^*(q) q \phi_n(q) dq = 0. \quad (2.3.7)$$

Similarly

$$\langle p \rangle = 0, \quad (2.3.8)$$

$$\langle p^2 \rangle = \hbar\nu \left( n + \frac{1}{2} \right), \quad (2.3.9)$$

$$\langle q^2 \rangle = \frac{\hbar}{\nu} \left( n + \frac{1}{2} \right). \quad (2.3.10)$$

The uncertainties in the generalized momentum and coordinate variables are therefore given by

$$\begin{aligned}(\Delta p)^2 &= \langle p^2 \rangle - \langle p \rangle^2 \\ &= \hbar\nu \left( n + \frac{1}{2} \right),\end{aligned}\quad (2.3.11)$$

$$(\Delta q)^2 = \frac{\hbar}{\nu} \left( n + \frac{1}{2} \right). \quad (2.3.12)$$

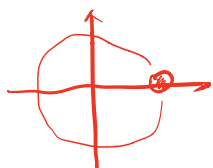
The uncertainty product is

$$\Delta p \Delta q = \left( n + \frac{1}{2} \right) \hbar. \quad (2.3.13)$$

This has minimum possible value of  $\hbar/2$  for the ground state wave function  $\phi_0(q)$ .

It is of special interest to find a wave packet which maintains the same variance  $\Delta q$  while undergoing simple harmonic motion. Such a wave function would correspond most closely to a classical field. In order to investigate this possibility we assume that, at time  $t = 0$ , the wave function  $\psi(q, t)$  is of the form (2.3.4) of the minimum-uncertainty wave packet except that it is displaced in the positive  $q$  direction by an amount  $q_0$ . We then have

$$\psi(q, 0) = \left(\frac{v}{\pi\hbar}\right)^{1/4} \exp\left[-\frac{v}{2\hbar}(q - q_0)^2\right]. \quad (2.3.14)$$



The time evolution of this wave packet is derived in Problem 2.3, where it is shown that the initial packet given by Eq. (2.3.14) implies that the probability density later in time is

$$\rightarrow |\psi(q, t)|^2 = \left(\frac{v}{\pi\hbar}\right)^{1/2} \exp\left[-\frac{v}{\hbar}(q - q_0 \cos vt)^2\right]. \quad (2.3.15)$$

*同演化方程*

$$|\alpha(t)\rangle = |\alpha e^{-i\omega t}\rangle$$

而  $q_0$  正相干

$$\text{从 } q_0 \rightarrow q_0 e^{-i\omega t}$$

指数取模  $\rightarrow$  ~~holosc~~  $vt = \pi/2$

We note that the wave packet (2.3.14) oscillates back and forth in a simple harmonic oscillator potential without changing its shape, i.e., it sticks together or *coheres*. This is to be contrasted with the wave packet which is a delta function at  $t = 0$ , goes to a plane wave at  $vt = \pi/2$ , and is again a delta function at  $vt = \pi$ , see Section 2.5 for more details. Although the delta function packet returns to its original shape at the end of a period, it has a variance which is a strong function of time, i.e., it does not *cohere*.

The packet  $\psi$  has the minimum-uncertainty product allowed by quantum mechanics, namely  $\Delta p \Delta q = \hbar/2$ . These states therefore provide the closest quantum mechanical analog to a free classical single-mode field.

The minimum-uncertainty wave packet (2.3.14) which *coheres* in a simple harmonic oscillator potential is given by (Problem 2.4)

$$\psi(q, 0) = e^{-|\alpha|^2/2} \sum_{n=0}^{\infty} \frac{\alpha^n}{\sqrt{n!}} \langle q | n \rangle, \quad (2.3.16)$$

with  $\alpha = (v/2\hbar)^{1/2} q_0$ , where we use  $\phi(q) = \langle q | n \rangle$ . The state  $|\alpha\rangle$  associated with  $\psi(q, 0)$  therefore has an expansion in number states identical to that for a coherent state, as given by Eq. (2.2.2). The minimum-uncertainty wave packet  $\psi(q, 0)$  is therefore the coordinate representation of the coherent state.

## 2.4 Some properties of coherent states

In this section, we list some important properties of the coherent states of the radiation field.

(a) The mean number of photons in the coherent state  $|\alpha\rangle$  is given by

$$\langle\alpha|a^\dagger a|\alpha\rangle = |\alpha|^2. \quad (2.4.1)$$

平均光子数  $|\alpha|^2$

The probability of finding  $n$  photons in  $|\alpha\rangle$  is given by a Poisson distribution, i.e.,

$$p(n) = \langle n|\alpha\rangle\langle\alpha|n\rangle = \frac{|\alpha|^{2n}e^{-|\alpha|^2}}{n!} = \frac{\langle n\rangle^n e^{-\langle n\rangle}}{n!}. \quad (2.4.2)$$

泊松分布

$$e^{-\lambda} \frac{\lambda^n}{n!} = e^{-|\alpha|^2} \frac{|\alpha|^{2n}}{n!}$$

where  $\langle n\rangle = |\alpha|^2$ . As we shall see in Chapter 11, the photon distribution for the laser approaches this distribution for sufficiently high excitations. In Fig. 2.2 we have plotted  $p(n)$  versus  $n$  for different values of  $|\alpha|^2$ . It is seen that, for  $|\alpha|^2 \leq 1$ ,  $p(n)$  is maximum at  $n = 0$ , whereas, for  $|\alpha|^2 > 1$ ,  $p(n)$  has a peak at  $n = |\alpha|^2$ .

(b) As discussed earlier, the coherent state is a minimum-uncertainty state so that

$$\Delta p \Delta q = \frac{\hbar}{2}. \quad \left. \begin{array}{l} q = \sqrt{\frac{\hbar}{2m\omega}}(a + a^\dagger) \\ p = \frac{a - a^\dagger}{i}\sqrt{\frac{\hbar m\omega}{2}} \end{array} \right\} \quad \text{q很大时, } \frac{\Delta q}{q} \rightarrow 0, \text{ 经典近似} \quad (2.4.3)$$

(c) The set of all coherent states  $|\alpha\rangle$  is a complete set. To show this, we first consider the integral identity (with  $\alpha = |\alpha|e^{i\theta}$ )

$$\int (\alpha^*)^n \alpha^m e^{-|\alpha|^2} d^2\alpha = \int_0^\infty |\alpha|^{n+m+1} e^{-|\alpha|^2} d|\alpha| \int_0^{2\pi} e^{i(m-n)\theta} d\theta \quad \text{复数二维} = \pi n! \delta_{nm}, \quad (2.4.4)$$

in which the integration is carried out over the entire area of the complex plane. With the help of this identity it follows, on using the expansion (2.2.2) for the coherent states, that

$$\int |\alpha\rangle\langle\alpha| d^2\alpha = \pi \sum_n |n\rangle\langle n|. \quad \text{不正交} \rightarrow \text{超完备} \quad (2.4.5)$$

注：重定义成高阶量级会  
解决不完备，但这样不完  
不归一了。

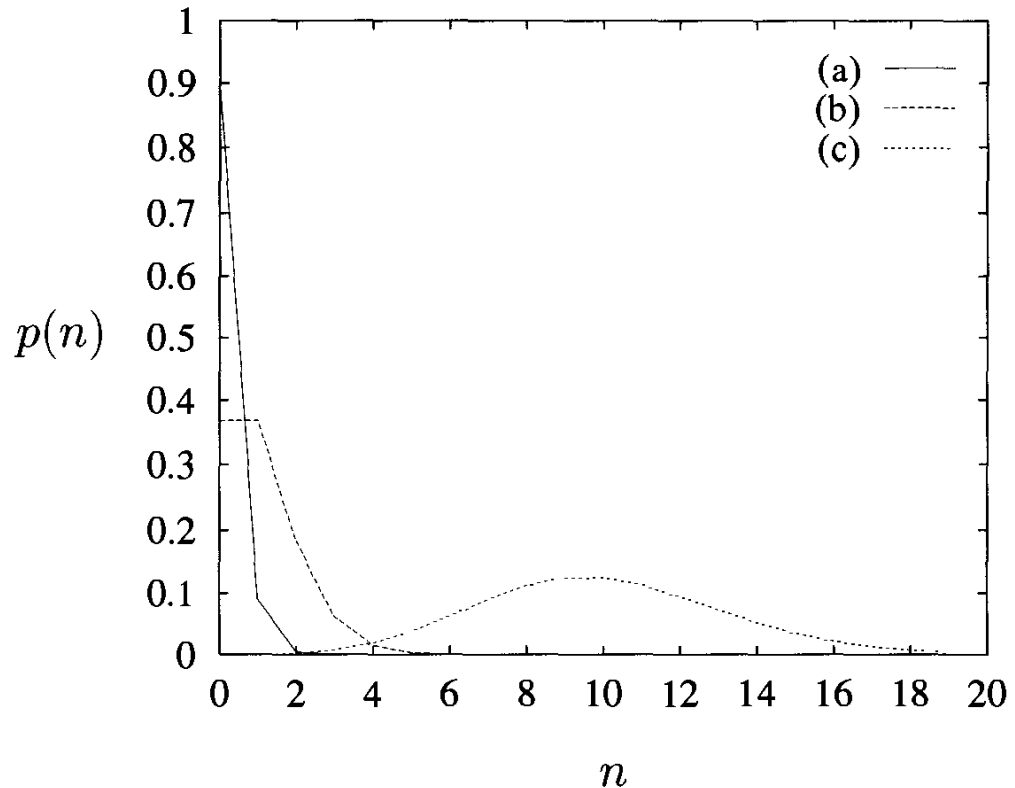
Since the Fock states  $|n\rangle$  form a complete orthonormal set, the sum over  $n$  is simply the unit operator. We thus have

$$\frac{1}{\pi} \int |\alpha\rangle\langle\alpha| d^2\alpha = 1, \quad (2.4.6)$$

which is the completeness relation for the coherent states.

Fig. 2.2

The photon distribution  $p(n)$  for a coherent state with  
 (a)  $|\alpha|^2 = 0.1$ ,  
 (b)  $|\alpha|^2 = 1$ , and  
 (c)  $|\alpha|^2 = 10$ .



因为  $\alpha$  非正交  
 (d) Two coherent states corresponding to different eigenstates  $\alpha$  and  $\alpha'$  are not orthogonal, i.e.,

$$\langle \alpha | \alpha' \rangle = \exp \left( -\frac{1}{2} |\alpha|^2 + \alpha' \alpha^* - \frac{1}{2} |\alpha'|^2 \right), \quad (2.4.7)$$

反而是正交

and

$$|\langle \alpha | \alpha' \rangle|^2 = \exp(-|\alpha - \alpha'|^2). \quad \text{但有向不正交} \quad (2.4.8)$$

Here we see that, if the magnitude of  $\alpha - \alpha'$  is much greater than unity, the states  $|\alpha\rangle$  and  $|\alpha'\rangle$  are nearly orthogonal to one another. The degree to which these wave functions overlap determines the size of the inner product  $\langle \alpha | \alpha' \rangle$ . A consequence of Eq. (2.4.7) is the fact that any coherent state can be expanded in terms of the other states:

$$\begin{aligned} |\alpha\rangle &= \frac{1}{\pi} \int d^2 \alpha' |\alpha'\rangle \langle \alpha' | \alpha \rangle \\ &= \frac{1}{\pi} \int d^2 \alpha' |\alpha'\rangle \exp \left( -\frac{1}{2} |\alpha|^2 + \alpha'^* \alpha - \frac{1}{2} |\alpha'|^2 \right). \end{aligned} \quad (2.4.9)$$

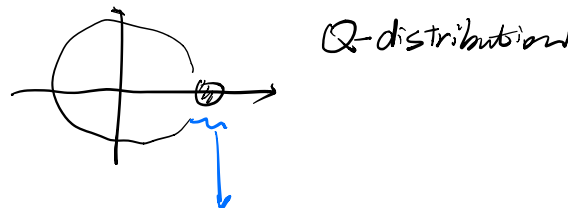
This indicates that the coherent states are overcomplete.

# 相干态的角位移

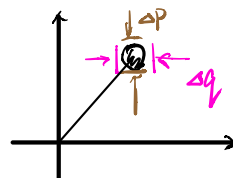
$$i\hbar \frac{\partial}{\partial t} |n\rangle = \hat{H} |n\rangle \quad \hat{H} = \hbar \omega (a^\dagger a + \frac{1}{2})$$

$$\begin{aligned} |\alpha(t)\rangle &= \exp(-i\frac{\hbar}{\hbar}\omega t) |\alpha\rangle \\ &= \exp(-i(\hat{a}^\dagger a + \frac{1}{2})\omega t) |\alpha\rangle \\ &= \exp(-i\frac{\hbar\omega t}{2}) \equiv \exp(-i\hbar\omega t) \frac{\alpha^n |n\rangle}{\sqrt{n!}} e^{-\frac{|\alpha|^2}{2}} \\ &= \underbrace{\exp(-i\frac{\hbar\omega t}{2})}_{\text{产生一个相移}} |\alpha e^{-i\hbar\omega t}\rangle \end{aligned}$$

$\frac{1}{2}\hbar\omega$  产生一个相移，一般不考虑。

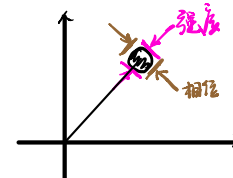


$\Delta p$  和  $\Delta q$  的不确定度



$$\Delta p \Delta q = \frac{\hbar}{2}$$

此不确定度关系



$$\Delta E \Delta t = \Delta(\hbar\omega a) \Delta\left(\frac{\theta}{\theta}\right) = \frac{\hbar}{2}$$

$$\Rightarrow \Delta(a^\dagger a) \cdot \Delta\theta = \frac{1}{2}$$

① 若是  $|n\rangle$  纯，则  $\Delta\theta$  完全不确定

干涉  $\langle 1 | k \rangle$  由于相位混乱，无所谓

$$\begin{array}{cccccc} 1 & 1 & 0 & 0 & 0 & 1 \\ 0 & 0 & 1 & 1 & 1 & 0 \end{array}$$

## 2.5 Squeezed state physics

Natural philosophy, the union of experimental and theoretical science, abounds with wonderful examples of the fruitful interplay between experimental and theoretical thought. The ‘ultraviolet catastrophe’ observed in black-body radiation led Planck to introduce the notion of the quantum. These considerations led Einstein to the concept of ‘stimulated emission’ which was the key to understanding the differences between the radiation distributions of Planck and Wien. Stimulated emission is, of course, the basis for the laser which ushered in the modern era of quantum optics.

Squeezed states of the radiation field provide another, near term, example of the rich interplay between experiment and theory. By itself, the squeezing of states of the field is of limited interest. For example, the number state consisting of  $n$  photons clearly exists, but how to make it and who cares if we do?

One answer to the ‘who cares?’ question comes from the search for gravitational radiation. As is further discussed in Chapter 4, the acceleration of distant matter, e.g., the explosion of a supernova, leads to tiny forces on laboratory instruments. For example, an oscillating gravity wave can drive a mechanical oscillator which thus serves as a gravity wave detector.

But the amplitudes of oscillation generated by many sources of gravitational radiation are anticipated to be much smaller than the width of the ground state wave function. This prompted people to think about squeezing the ground state wave function (zero-point noise) of quantum mechanical oscillators.

That such ‘squeezing’ is possible in principle is made clear by considering the elementary quantum mechanics of the simple harmonic oscillator (SHO). As is depicted in Fig. 2.3, a wave packet which is sharply peaked (i.e., squeezed) initially will spread out and return to its initial state periodically. A little review of the SHO time evolution makes this clear.\* Recall that the wave function at time  $t$  is related to that at  $t = 0$  by the expression

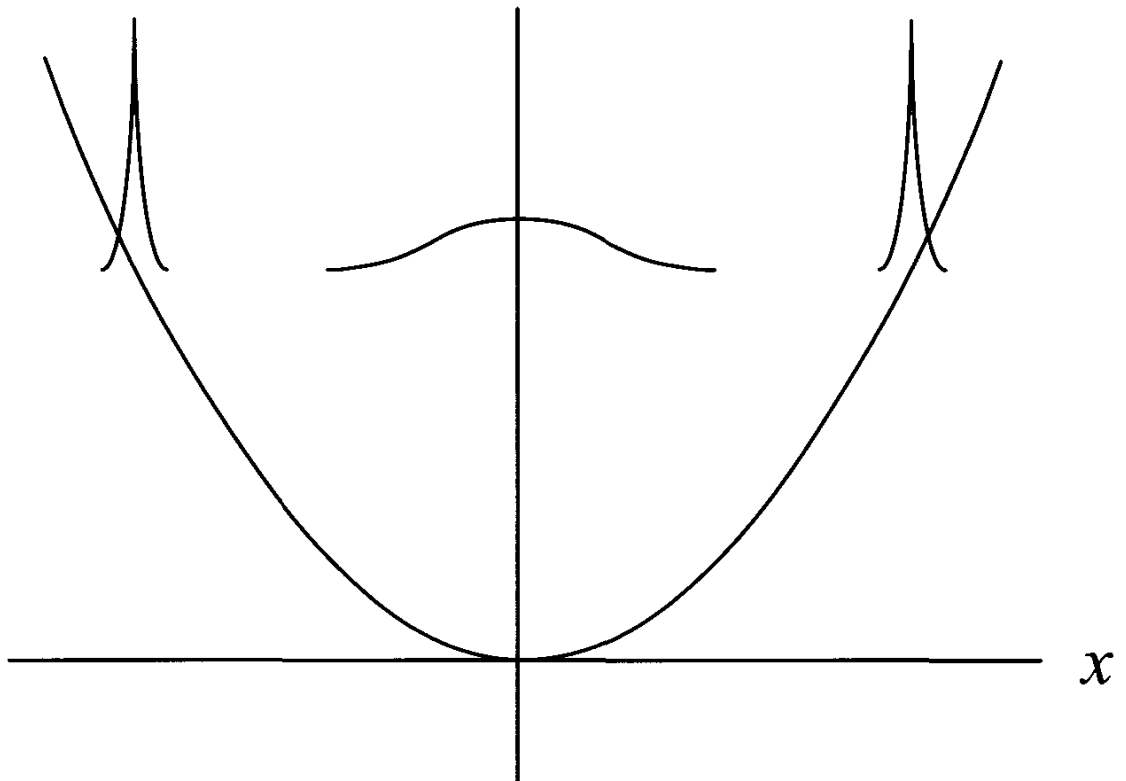
$$\psi(x, t) = \int dx' G(x, x', t) \psi(x', 0), \quad (2.5.1)$$

where the well known SHO propagator, as given in quantum mechanics texts, is

$$G(x, x', t) = \sqrt{\frac{mv}{2\pi\hbar|\sin vt|}} \exp\left\{\frac{imv}{2\hbar\sin vt} [(x^2 + x'^2) \cos vt - 2xx']\right\}, \quad (2.5.2)$$

\* See, for example, Sargent, Scully, and Lamb, *Laser Physics* [1974] Appendix H.

**Fig. 2.3**  
Evolution of a  
squeezed state of a  
simple harmonic  
oscillator.



with  $m$  and  $v$  being the mass and frequency of the oscillator.

Now if we begin at  $t = 0$  with a  $\delta$ -function wave packet  $\psi(x', 0) = \delta(x' - x_0)$  then at a time  $t = \pi/2v$  later the wave function will be a plane wave; that is, our squeezed state evolves as

$$\psi(x, t = 0) = \delta(x - x_0), \quad (2.5.3a)$$

$$\psi(x, t = \pi/2v) = \sqrt{\frac{mv}{2\pi\hbar}} \exp\left[i\left(\frac{mvx_0}{\hbar}\right)x\right], \quad (2.5.3b)$$

$$\psi(x, t = \pi/v) = \delta(x + x_0). \quad (2.5.3c)$$

Thus, from Fig. 2.3 and Eqs. (2.5.3), we see that if we start with a sharp or squeezed state we will return to a sharp state every half period. In this sense we have the possibility of a kind of ‘stroboscopic’ measurement, in which we look at our oscillator at  $t = 0, \pi/v, 2\pi/v, \dots$ , so that we are not limited by the width of the ground state wave function.

Having motivated and illustrated squeezed states, let us proceed to a better understanding of these states by considering a *gedanken* experiment illustrating how we might prepare such states. To this end, let us return briefly to the question of how we might prepare a coherent state.

In classical mechanics we can excite a SHO into motion by, e.g., stretching the spring of Fig. 2.4 to a new equilibrium position and releasing it to produce oscillation. In quantum mechanics a similar procedure can be followed but we must be more specific about how

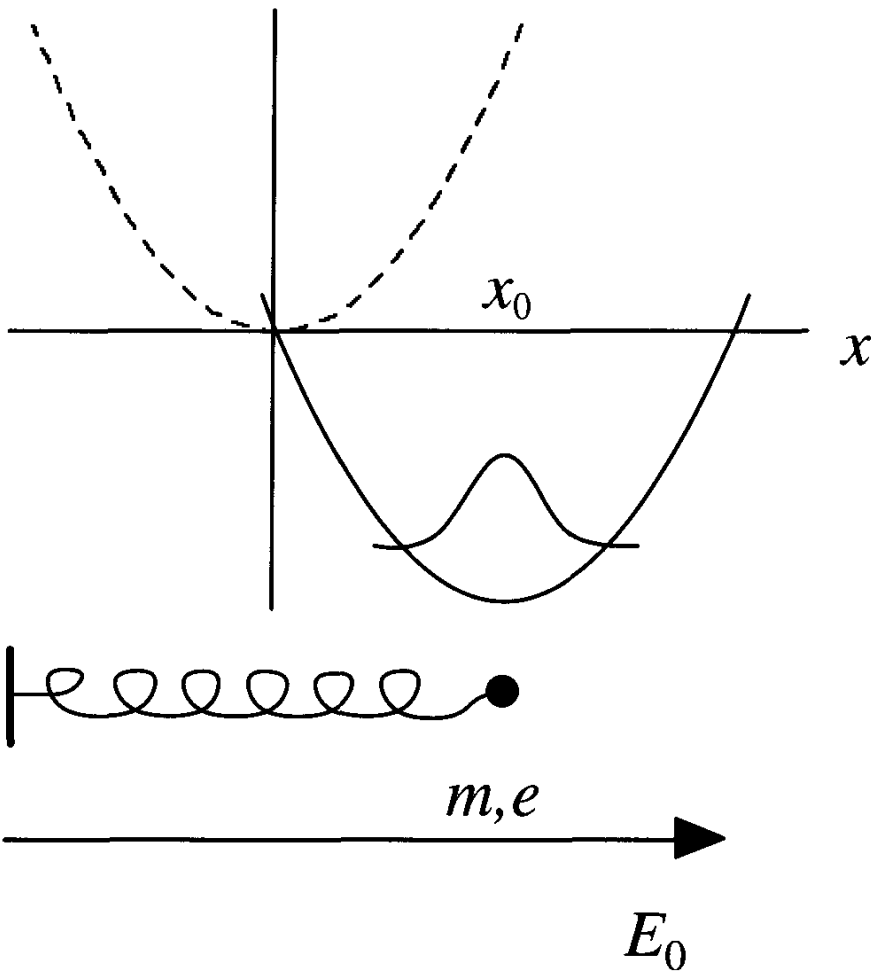


Fig. 2.4  
Dashed potential applies for a spring-type SHO and causes a particle of mass  $m$  and charge  $e$  to oscillate about  $x = 0$ . Applying a dc electric field stretches the spring to a new equilibrium position  $x_0$  about which the point charge particle now oscillates.

we prepare the initial state of the SHO. Let us envision a SHO characterized by mass  $m$  and charge  $e$  in a field  $E_0$ , as in Fig. 2.4; then the Hamiltonian is

$$\mathcal{H} = \frac{p^2}{2m} + \frac{1}{2}kx^2 - eE_0x, \quad (2.5.4a)$$

which we may write as

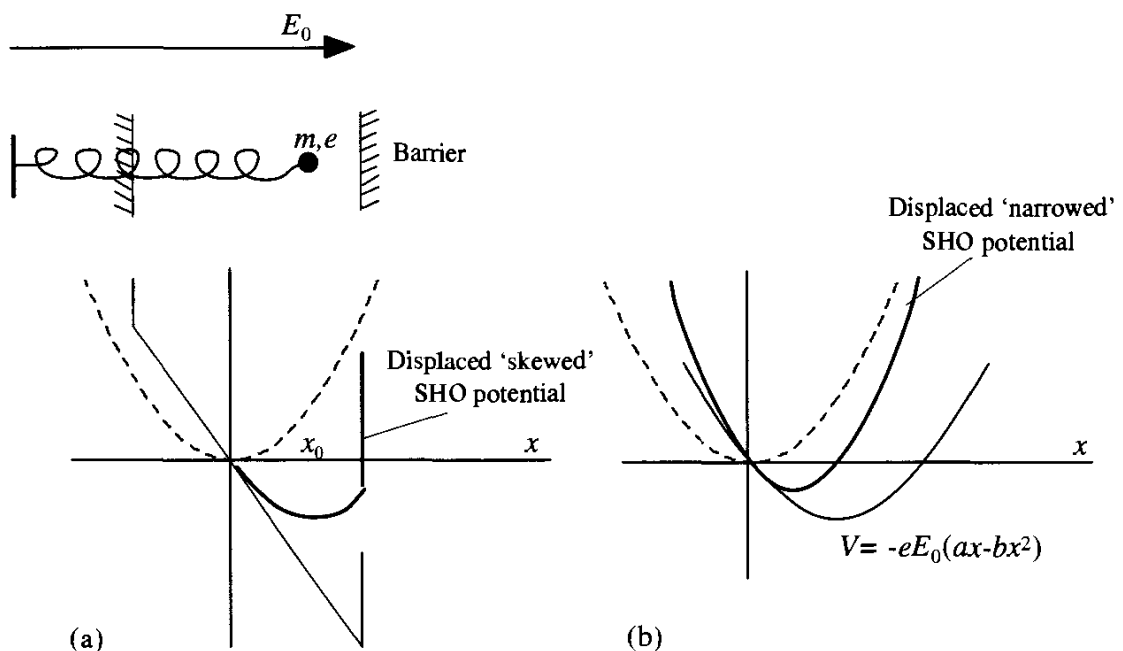
$$\mathcal{H} = \frac{p^2}{2m} + \frac{1}{2}k \left( x - \frac{eE_0}{k} \right)^2 - \frac{1}{2}k \left( \frac{eE_0}{k} \right)^2. \quad (2.5.4b)$$

We have in (2.5.4b) the well-known fact that applying a linear potential to a SHO just shifts its equilibrium point. Clearly the same solutions obtain. We have thus prepared a displaced ground state as in Fig. 2.4. And upon turning off the dc field, i.e., setting  $E_0 = 0$ , we will have a coherent state  $|\alpha\rangle$  which oscillates without changing its shape.

It is to be noted that applying the dc field to the SHO is mathematically equivalent to applying the displacement operator (2.2.8) to the state  $|0\rangle$ . This is summarized in Fig. 2.4.

Fig. 2.5

- (a) The SHO potential is first displaced by a dc electric field and then ‘skewed’ by barriers which limit the charge oscillation to a finite region.
- (b) The SHO potential is displaced and ‘narrowed’ by a quadratic displacement potential.



Next, let us consider how we might prepare a squeezed state. Suppose we again apply a dc field but this time with a ‘wall’ which limits the SHO to a finite region as in Fig. 2.5(a).

In such a case, it would be expected that the wave packet would be deformed or ‘squeezed’ when it is pushed against the barrier. Similarly the quadratic displacement potential of Fig. 2.5(b) would be expected to produce a squeezed wave packet. To see that this is indeed the case, consider the Hamiltonian for the SHO in the presence of the quadratic potential

$$\mathcal{H} = \frac{p^2}{2m} + \frac{1}{2}kx^2 - eE_0(ax - bx^2), \quad (2.5.5a)$$

where the  $ax$  term will displace the oscillator and the  $bx^2$  is added in order to give us a barrier to ‘squeeze the packet against’. We rewrite (2.5.5a) as

$$\mathcal{H} = \frac{p^2}{2m} + \frac{1}{2}(k + 2ebE_0)x^2 - eaE_0x. \quad (2.5.5b)$$

From Eq. (2.5.5b) it is clear that we again have a displaced ground state, but this time with the larger effective spring constant  $k' = k + 2ebE_0$ . This, of course, means that we have a *squeezed* displaced wave packet as depicted in Fig. 2.6. This is the desired result.

In conclusion we note that, just as it is the creation operator part of the linear displacement potential which is most important in preparing a coherent state; we shall find that it is the two-photon  $a^{\dagger 2}$  and  $a^2$  contributions, contained within the  $bx^2$  term in Eqs. (2.5.5), that are most important in preparing a squeezed coherent state.

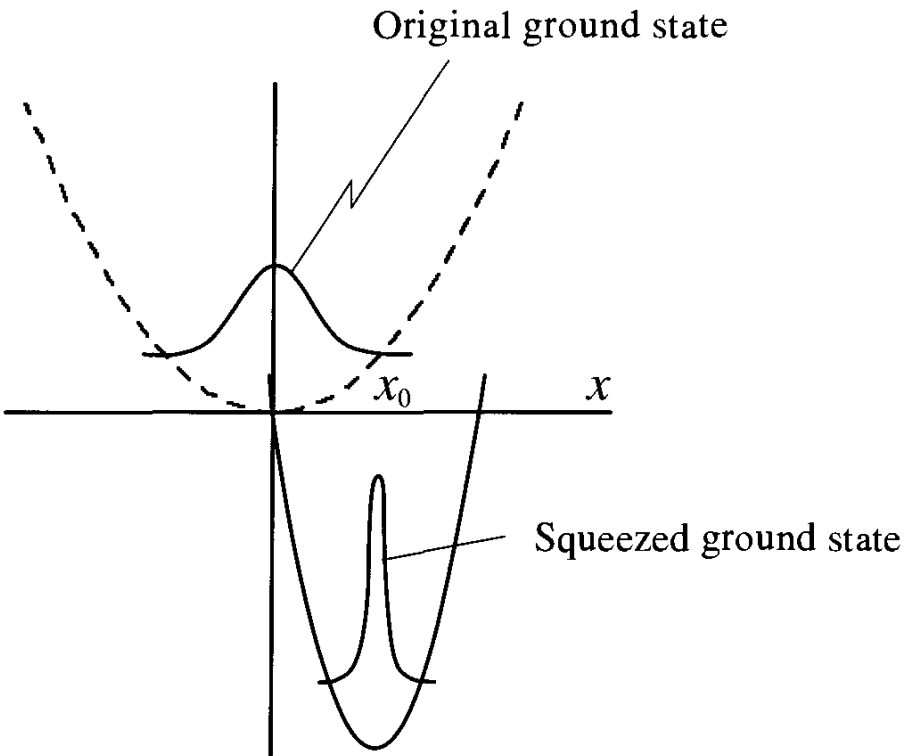


Fig. 2.6  
The displaced  
'narrowed' SHO  
potential squeezes  
the wave packet.

## 2.6 Squeezed states and the uncertainty relation

Having motivated the study and nature of squeezed states, let us consider what other properties we might expect from them. Consider two Hermitian operators  $A$  and  $B$  which satisfy the commutation relation

$$[A, B] = iC. \quad (2.6.1)$$

According to the Heisenberg uncertainty relation, the product of the uncertainties in determining the expectation values of two variables  $A$  and  $B$  is given by

$$\Delta A \Delta B \geq \frac{1}{2} |\langle C \rangle|. \quad (2.6.2)$$

A state of the system is called a squeezed state if the uncertainty in one of the observables (say  $A$ ) satisfies the relation

$$(\Delta A)^2 < \frac{1}{2} |\langle C \rangle|. \quad (2.6.3)$$

If, in addition to the condition (2.6.3), the variances satisfy the minimum-uncertainty relation, i.e.,

$$\Delta A \Delta B = \frac{1}{2} |\langle C \rangle|, \quad (2.6.4)$$

then the state is called an ideal squeezed state.

In a squeezed state, therefore, the quantum fluctuations in one variable are reduced below their value in a symmetric minimum-uncertainty state ( $(\Delta A)^2 = (\Delta B)^2 = |\langle C \rangle|/2$ ) at the expense of the corresponding increased fluctuations in the conjugate variable such that the uncertainty relation is not violated.

As an illustration, we consider a quantized single-mode electric field of frequency  $\nu$ :

$$\mathbf{E}(t) = \mathcal{E}\hat{\epsilon}(ae^{-i\nu t} + a^\dagger e^{i\nu t}), \quad (2.6.5)$$

where  $a$  and  $a^\dagger$  obey the commutation relation

$$[a, a^\dagger] = 1. \quad (2.6.6)$$

We introduce the Hermitian amplitude operators

$$X_1 = \frac{1}{2}(a + a^\dagger), \quad (2.6.7)$$

$$X_2 = \frac{1}{2i}(a - a^\dagger). \quad (2.6.8)$$

It is, of course, clear that  $X_1$  and  $X_2$  are essentially dimensionless position and momentum operators

$$x = \frac{\sqrt{2\hbar/m\nu}}{2}(a + a^\dagger),$$

$$p = \frac{\sqrt{2m\hbar\nu}}{2i}(a - a^\dagger).$$

It follows from the commutation relation (2.6.6) that  $X_1$  and  $X_2$  satisfy

$$[X_1, X_2] = \frac{i}{2}. \quad (2.6.9)$$

In terms of these operators, Eq. (2.6.5) can be rewritten as

$$\mathbf{E}(t) = 2\mathcal{E}\hat{\epsilon}(X_1 \cos \nu t + X_2 \sin \nu t). \quad (2.6.10)$$

The Hermitian operators  $X_1$  and  $X_2$  are now readily seen to be the amplitudes of the two quadratures of the field having a phase difference  $\pi/2$ . From Eq. (2.6.9), the uncertainty relation for the two amplitudes is

$$\Delta X_1 \Delta X_2 \geq \frac{1}{4}. \quad (2.6.11)$$

A squeezed state of the radiation field is obtained if

$$(\Delta X_i)^2 < \frac{1}{4} \quad (i = 1 \text{ or } 2). \quad (2.6.12)$$

An ideal squeezed state is obtained if in addition to Eq. (2.6.12), the relation

$$\Delta X_1 \Delta X_2 = \frac{1}{4} \quad (2.6.13)$$

also holds.

In the next section we will consider the two-photon coherent state which is an example of an ideal squeezed state. Here we mention that the coherent state  $|\alpha\rangle$  and the Fock state  $|n\rangle$  are not squeezed states. It follows from Eq. (2.6.7) that, in a coherent state,

$$\begin{aligned} (\Delta X_1)^2 &= \langle \alpha | X_1^2 | \alpha \rangle - (\langle \alpha | X_1 | \alpha \rangle)^2 \\ &= \frac{1}{4} \langle \alpha | [a^2 + aa^\dagger + a^\dagger a + (a^\dagger)^2] | \alpha \rangle - \frac{1}{4} [\langle \alpha | (a + a^\dagger) | \alpha \rangle]^2 \\ &= \frac{1}{4}. \end{aligned} \quad (2.6.14)$$

Similarly

$$(\Delta X_2)^2 = \frac{1}{4}. \quad (2.6.15)$$

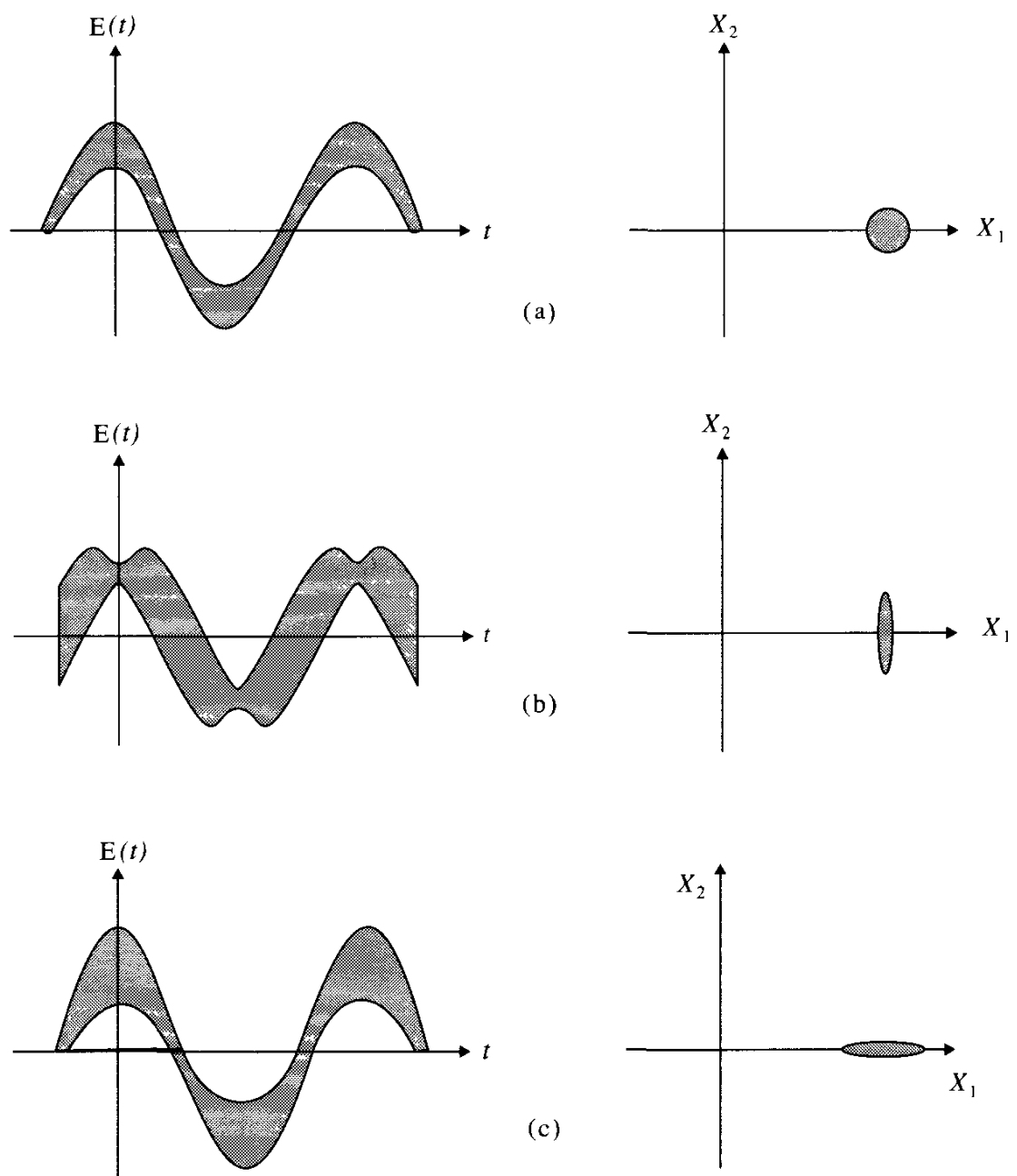
In a similar manner, in a Fock state,

$$\begin{aligned} (\Delta X_1)^2 &= \langle n | X_1^2 | n \rangle - (\langle n | X_1 | n \rangle)^2, \\ &= \frac{1}{4}(2n+1), \end{aligned} \quad (2.6.16)$$

$$(\Delta X_2)^2 = \frac{1}{4}(2n+1). \quad (2.6.17)$$

In Fig. 2.7 error contours of the uncertainties in  $X_1$  and  $X_2$ , along with the corresponding graphs of the electric field versus time are shown for a coherent state, a squeezed state with reduced noise in  $X_1$ , and a squeezed state with reduced noise in  $X_2$ . Each point in the error contour for various states corresponds to a wave with a certain amplitude and a certain phase. A summation of all such waves in the error contours thus leads to the uncertainties of the electric field represented by the shaded region. A coherent state (Fig. 2.7(a)), having identical uncertainties in both  $X_1$  and  $X_2$ , has a constant value for the variance of the electric field. A squeezed state with reduced noise in  $X_1$  (Fig. 2.7(b)) has reduced uncertainty in the amplitude at the expense of large uncertainty in the phase of the electric field whereas the situation is reversed for a squeezed state with reduced noise in  $X_2$  (Fig. 2.7(c)).

**Fig. 2.7**  
 Error contours and the corresponding graphs of electric field versus time for (a) a coherent state, (b) a squeezed state with reduced noise in  $X_1$ , and (c) a squeezed state with reduced noise in  $X_2$ .  
 (From C. Caves,  
*Phys. Rev. D* **23**, 1693  
 (1981).)



## 2.7 The squeeze operator and the squeezed coherent states

In Section 2.5 we found that quadratic terms in  $x$ , i.e., terms of the form  $(a + a^\dagger)^2$ , were important in the preparation of squeezed states. With that thought in mind, we are naturally motivated to consider degenerate parametric processes in connection with the generation of such states of the radiation field. In fact, much of squeezed state physics is nicely illustrated by the degenerate parametric process, as discussed in Chapter 16. The associated two-photon Hamiltonian can be written as

$$\mathcal{H} = i\hbar (ga^{\dagger 2} - g^*a^2), \quad (2.7.1)$$

where  $g$  is a coupling constant. Hence the state of the field generated by this expression is

$$|\psi(t)\rangle = e^{(ga^{\dagger 2} - g^* a^2)t} |0\rangle \quad (2.7.2)$$

and this leads us to define the unitary squeeze operator

$$S(\xi) = \exp\left(\frac{1}{2}\xi^* a^2 - \frac{1}{2}\xi a^{\dagger 2}\right), \quad (2.7.3)$$

$S^\dagger S = SS^\dagger = I$

where  $\xi = r \exp(i\theta)$  is an arbitrary complex number. It is easy to see that

$\downarrow$  正频率  $\downarrow$  负频率

$$S^\dagger(\xi) = S^{-1}(\xi) = S(-\xi). \quad (2.7.4)$$

A straightforward application of the formula

$$\underbrace{e^A B e^{-A}}_{\text{leads to the following useful unitary transformation properties of the squeeze operator}} = B + [A, B] + \frac{1}{2!} [A, [A, B]] + \dots, \quad (2.7.5)$$

leads to the following useful unitary transformation properties of the squeeze operator

$$S^\dagger(\xi) a S(\xi) = a \cosh r - a^\dagger e^{i\theta} \sinh r, \quad (2.7.6)$$

$$S^\dagger(\xi) a^\dagger S(\xi) = a^\dagger \cosh r - a e^{-i\theta} \sinh r. \quad (2.7.7)$$

If we define a rotated complex amplitude at an angle  $\theta/2$

$$\underbrace{Y_1 + iY_2}_{\alpha} = (\underbrace{X_1 + iX_2}_{a}) e^{-i\theta/2}, \quad \Rightarrow (2.7.14) \quad (2.7.8)$$

it follows from Eq. (2.7.6) that

$$S^\dagger(\xi)(Y_1 + iY_2)S(\xi) = Y_1 e^{-r} + iY_2 e^r. \quad (2.7.9)$$

A squeezed coherent state  $|\alpha, \xi\rangle$  is obtained by first acting with the displacement operator  $D(\alpha)$  on the vacuum followed by the squeeze operator  $S(\xi)$ , i.e.,

$$|\alpha, \xi\rangle = S(\xi)D(\alpha)|0\rangle, \quad (2.7.10)$$

with  $\alpha = |\alpha| \exp(i\varphi)$ . As discussed earlier, whereas a coherent state is generated by linear terms in  $a$  and  $a^\dagger$  in the exponent, the squeezed coherent state requires quadratic terms.

In the following we discuss some properties of the squeezed coherent state since it is a canonical example of a squeezed state.

### 2.7.1 Quadrature variance

The operator expectation values of the state  $|\alpha, \xi\rangle$  can be determined from the definition (2.7.10) by making use of the transformation properties of the displacement and squeezing operators (Eq. (2.7.3)). It then follows that

$$\begin{aligned}\langle a \rangle &= \langle \alpha, \xi | a | \alpha, \xi \rangle \\ &= \langle 0 | D^\dagger(\alpha) S^\dagger(\xi) a S(\xi) D(\alpha) | 0 \rangle \\ &= \langle \alpha | (a \cosh r - a^\dagger e^{i\theta} \sinh r) | \alpha \rangle \\ &= \alpha \cosh r - \alpha^* e^{i\theta} \sinh r,\end{aligned}\tag{2.7.11}$$

$$\begin{aligned}\langle a^2 \rangle &= \langle (a^\dagger)^2 \rangle^* \\ &= \langle 0 | D^\dagger(\alpha) S^\dagger(\xi) a^2 S(\xi) D(\alpha) | 0 \rangle \\ &= \langle \alpha | S^\dagger(\xi) a S(\xi) S^\dagger(\xi) a S(\xi) | \alpha \rangle \\ &= \alpha^2 \cosh^2 r + (\alpha^*)^2 e^{2i\theta} \sinh^2 r - 2|\alpha|^2 e^{i\theta} \sinh r \cosh r \\ &\quad - e^{i\theta} \cosh r \sinh r,\end{aligned}\tag{2.7.12}$$

$$\begin{aligned}\langle a^\dagger a \rangle &= |\alpha|^2 (\cosh^2 r + \sinh^2 r) - (\alpha^*)^2 e^{i\theta} \sinh r \cosh r \\ &\quad - \alpha^2 e^{-i\theta} \sinh r \cosh r + \sinh^2 r.\end{aligned}\tag{2.7.13}$$

The variances of the rotated amplitudes  $Y_1$  and  $Y_2$  can be determined from these expectation values. On substituting for  $X_1$  and  $X_2$  from Eqs. (2.6.7) and (2.6.8) into Eq. (2.7.8) we obtain

$$\text{若 } \theta = 0, \text{ 则 } Y_1 = X_1, Y_2 = X_2 \Rightarrow Y_1 + iY_2 = a \exp(-i\theta/2), \tag{2.7.14}$$

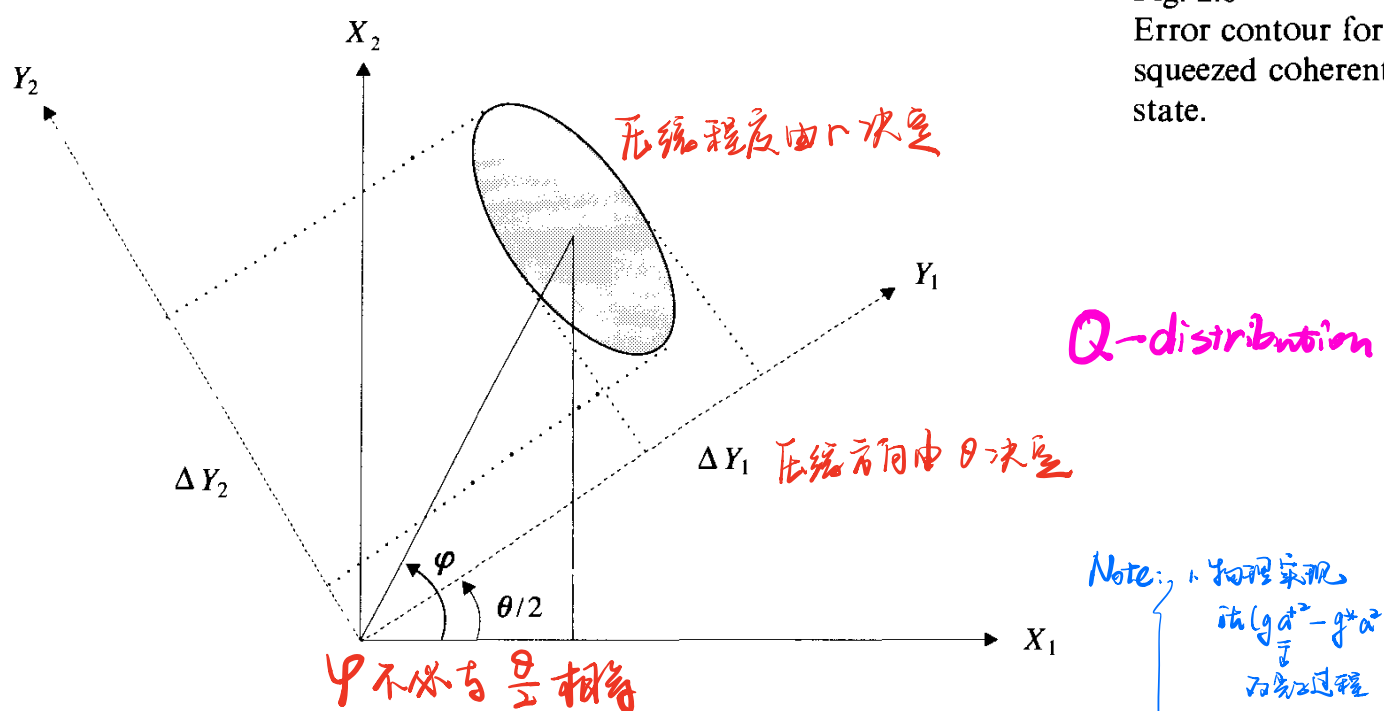
so that

$$\begin{aligned}(\Delta Y_1)^2 &= \langle Y_1^2 \rangle - \langle Y_1 \rangle^2 \\ &= \frac{1}{4} \langle (ae^{-i\theta/2} + a^\dagger e^{i\theta/2})^2 \rangle - \frac{1}{4} (\langle ae^{-i\theta/2} + a^\dagger e^{i\theta/2} \rangle)^2 \\ &= \frac{1}{4} \langle a^2 e^{-i\theta} + a^{\dagger 2} e^{i\theta} + aa^\dagger + a^\dagger a \rangle \\ &\quad - \frac{1}{4} (\langle ae^{-i\theta/2} + a^\dagger e^{i\theta/2} \rangle)^2 = \frac{1}{4} e^{-2r},\end{aligned}\tag{2.7.15}$$

$$(\Delta Y_2)^2 = \frac{1}{4} e^{2r}, \tag{2.7.16}$$

$$\Delta Y_1 \Delta Y_2 = \frac{1}{4}. \text{ 请想方设法去} \tag{2.7.17}$$

A squeezed coherent state is therefore an ideal squeezed state. As shown in Fig. 2.8, in the complex amplitude plane the coherent state error circle is *squeezed* into an *error ellipse* of the same area. The principal axes of the ellipse lie along  $Y_1$  and  $Y_2$  rotated at an angle  $\theta/2$  from  $X_1$  and  $X_2$ , respectively. The degree of squeezing is determined by  $r = |\xi|$  which is therefore called the squeeze parameter.



## 2.8 Multi-mode squeezing

The single-mode two-photon coherent state can be generalized to a multi-mode squeezed state by using a generator which incorporates the product of annihilation (and creation) operators for correlated pairs of modes symmetrically placed around a mode of frequency, say,  $\nu$ . First, we discuss the simple case of two-mode squeezing and then generalize it to the multi-mode case. The two-mode squeezed state is obtained by the action of the unitary operator

$$S(\xi) = e^{\xi^* a_{\nu+\nu'} a_{\nu-\nu'} - \xi a_{\nu+\nu'}^\dagger a_{\nu-\nu'}^\dagger}, \quad \text{双模} \quad (2.8.1)$$

on the two-mode vacuum.

To show that the operators spanning the two modes exhibit squeezing, we define collective creation and destruction operators

$$b^\dagger = \frac{1}{\sqrt{2}} [a_{\nu+\nu'}^\dagger + e^{i\delta} a_{\nu-\nu'}^\dagger], \quad \left. \begin{array}{l} \text{定义集体算符} \\ \text{正交} \end{array} \right\} \quad (2.8.2)$$

$$b = \frac{1}{\sqrt{2}} [a_{\nu+\nu'} + e^{-i\delta} a_{\nu-\nu'}]. \quad (2.8.3)$$

The in-phase and in-quadrature components are given by

$$b_1 = \frac{1}{2}(b + b^\dagger), \quad \begin{array}{c} \text{同相} \\ \text{正交} \end{array} \quad (2.8.4)$$

$$b_2 = \frac{1}{2i}(b - b^\dagger). \quad \sim \text{类似 } X_1, Y_1 \quad (2.8.5)$$

The corresponding uncertainty relation is

$$\Delta b_1 \Delta b_2 \geq \frac{1}{4}. \quad (2.8.6)$$

The variances in the two components in the two-mode squeezed vacuum are

$$\begin{aligned} (\Delta b_1)^2 &= \langle b_1^2 \rangle - \langle b_1 \rangle^2 = \langle 0 | S(\omega) b_1 S(\omega) | 0 \rangle \\ &= \frac{1}{4} \left[ \exp(-2r) \cos^2 \left( \frac{\delta}{2} - \frac{\theta}{2} \right) + \exp(2r) \sin^2 \left( \frac{\delta}{2} - \frac{\theta}{2} \right) \right], \end{aligned} \quad (2.8.7)$$

$$\begin{aligned} (\Delta b_2)^2 &= \frac{1}{4} \left[ \exp(2r) \cos^2 \left( \frac{\delta}{2} - \frac{\theta}{2} \right) + \exp(-2r) \sin^2 \left( \frac{\delta}{2} - \frac{\theta}{2} \right) \right]. \end{aligned} \quad (2.8.8)$$

For the particular choices of the phase  $\delta - \theta = 0$  and  $\pi$ , it is an ideal squeezed state with reduced fluctuations in  $b_1$  and  $b_2$ , respectively.

In a similar manner, a large number of modes of the vacuum can be squeezed. The multi-mode squeeze operator is defined as

$$S[\xi(v)] = \int \frac{dv'}{2\pi} \exp \left[ \xi^*(v') a_{v+v'} a_{v-v'} - \xi(v') a_{v+v'}^\dagger a_{v-v'}^\dagger \right]. \quad (2.8.9)$$

Here the integration is over the positive half-band of frequencies and  $\xi(v) = r(v) \exp[i\theta(v)]$ . A multi-mode squeezed coherent state is obtained, as in definition (2.7.10), by first displacing the vacuum and then squeezing it through a multi-mode displacement operator

$$|\alpha(v), \xi(v)\rangle \equiv S[\xi(v)] D[\alpha(v)] |\tilde{0}\rangle, \quad (2.8.10)$$

where  $|\tilde{0}\rangle$  is a multi-mode vacuum state.

## Problems

**2.1** Show that

$$a^\dagger |\alpha\rangle\langle\alpha| = \left( \alpha^* + \frac{\partial}{\partial\alpha} \right) |\alpha\rangle\langle\alpha|,$$

and

$$|\alpha\rangle\langle\alpha| a = \left( \alpha + \frac{\partial}{\partial\alpha^*} \right) |\alpha\rangle\langle\alpha|.$$

**2.2** Show that the expectation value of the displacement operator  $D(\alpha)$  for a thermal field is given by

$$\langle D(\alpha) \rangle = \exp \left[ -|\alpha|^2 \left( \langle n \rangle + \frac{1}{2} \right) \right],$$

where  $\langle n \rangle$  is the mean number of photons in the field.

压缩方向  $\theta$   
观察方向  $\delta$   
 $\Rightarrow$   $\downarrow$

双模：  
一对-态和  
 $(\gamma+\delta\gamma, \gamma-\delta\gamma)$   
单模：  
一对-态和  
 $(\gamma, \gamma)$

- 2.3** The time evolution of the wave packet (2.3.14) is determined by the Schrödinger equation for the harmonic oscillator

$$i\hbar \frac{\partial \psi}{\partial t} = \left( -\frac{\hbar^2}{2} \frac{\partial^2}{\partial q^2} + \frac{v^2 q^2}{2} \right) \psi.$$

A general solution of this equation can be given in terms of the stationary wave functions

$$\psi(q, t) = \sum_{n=0}^{\infty} a_n \phi_n(q) e^{-iE_n t/\hbar},$$

where  $E_n = (n+1/2)\hbar v$  and  $a_n$  are arbitrary coefficients. Using the orthonormality conditions on the wave functions  $\phi_n(q)$ , find  $a_n$  and hence prove Eq. (2.3.15).

- 2.4** Derive Eq. (2.3.16).

- 2.5** An alternate definition of a squeezed coherent state is

$$|\alpha, \xi\rangle = D(\alpha)S(\xi)|0\rangle,$$

where  $\xi = r \exp(i\theta)$ . Show that the variances in the quadrature components  $Y_1$  and  $Y_2$ , such that

$$Y_1 + iY_2 = ae^{-i\theta/2},$$

are given by

$$\begin{aligned} (\Delta Y_1)^2 &= \frac{1}{4}e^{-2r}, \\ (\Delta Y_2)^2 &= \frac{1}{4}e^{2r}. \end{aligned}$$

- 2.6** Consider a two-mode squeezed state defined by

$$|\alpha_1, \alpha_2, \xi\rangle = D_1(\alpha_1)D_2(\alpha_2)S_{12}(\xi)|0\rangle,$$

where

$$D_i(\alpha_i) = \exp(\alpha_i a_i^\dagger - \alpha_i^* a_i) \quad (i = 1, 2),$$

is the coherent displacement operator for the two modes described by destruction and creation operators  $a_i$  and  $a_i^\dagger$ , respectively,

$$S_{12}(\xi) = \exp(\xi^* a_1 a_2 + \xi a_1^\dagger a_2^\dagger)$$

is the two-mode squeeze operator, and  $|0\rangle$  is the two-mode vacuum state. Show that there is no squeezing in the two individual modes. (Hint: see S. M. Barnett and P. L. Knight, *J. Opt. Soc. Am. B* **2**, 467 (1985).)

- 2.7** A state is said to be squeezed in the  $N$ th order if  $\langle(\Delta X_i)^N\rangle$  ( $i = 1$  or  $2$ ) is lower than its corresponding coherent state value. Here

$$X_1 = \frac{1}{2}(a + a^\dagger),$$

$$X_2 = \frac{1}{2i}(a - a^\dagger).$$

Show that the condition of the  $N$ th-order squeezing is

$$q^N < 0,$$

where

$$q^N = (\Delta X_i)^N - \left(\frac{1}{4}\right)^{N-2} (N-1)!!$$

(Hint: see C. K. Hong and L. Mandel, *Phys. Rev. Lett.* **54**, 323 (1985).)

- 2.8** Consider the Hermitian operators corresponding to the real and imaginary parts of the square of the complex amplitude of the field

$$X_1 = \frac{1}{2}(a^2 + a^{\dagger 2}),$$

$$X_2 = \frac{1}{2i}(a^2 - a^{\dagger 2}).$$

Show that the squeezing condition is

$$\langle\Delta X_i^2\rangle < \langle a^\dagger a \rangle + \frac{1}{2} \quad (i = 1 \text{ or } 2).$$

This type of squeezing is called amplitude-squared squeezing. Show that the amplitude-squared squeezing is a nonclassical effect. (Hint: see M. Hillery, *Phys. Rev. A* **36**, 3796 (1987).)

# Chapter 3 Quasi-Probability Distribution

本章不照 Scully 书，而用 P. Meystre 书第十三章 § 13.6.

## 13.6 Quasi-Probability Distributions

In many problems, it is useful to describe the state of the field in terms of coherent states, rather than with photon number states. This presents some surprises and difficulties since as discussed in Sect. 3.4, the coherent states are not orthogonal and are overcomplete. On the other hand, as we shall see this overcompleteness allows us to obtain a useful diagonal expansion of the density operator in terms of complex matrix elements  $P(\alpha)$ . This representation can be interpreted as a quasi-probability distribution function, whose dynamics can under appropriate conditions be expressed in the form of a Fokker-Planck equation. One such example is given in Sect. 15.2. A number of further quasi-probability distribution descriptions of the electromagnetic field can be introduced, including the Wigner function  $W(\alpha)$  and the  $Q$ -function  $Q(\alpha)$ . These various representations, which are called *quasi-probability* functions, as they are not positive-definite, find applications in the evaluation of correlation functions of the electromagnetic field.

The  $P(\alpha)$  representation is defined in terms of the expansion of the field density operator  $\rho$  in coherent states as

$$\rho = \int d^2\alpha P(\alpha) |\alpha\rangle\langle\alpha| . \quad (13.80)$$

Here,  $d^2\alpha = d\operatorname{Re}(\alpha) d\operatorname{Im}(\alpha)$ . In terms of  $P(\alpha)$ , the expectation value of an operator  $\hat{A}$  is given by

$$\begin{aligned} \langle \hat{A} \rangle &= \operatorname{Tr}(\rho \hat{A}) = \sum_n \langle n | \int d^2\alpha P(\alpha) |\alpha\rangle\langle\alpha| \hat{A} |n\rangle \\ &= \int d^2\alpha P(\alpha) \sum_n \langle \alpha | \hat{A} | n \rangle \langle n | \alpha \rangle \\ &= \int d^2\alpha P(\alpha) \langle \alpha | \hat{A} | \alpha \rangle = \int d^2\alpha P(\alpha) A(\alpha) , \end{aligned} \quad (13.81)$$

where  $A(\alpha) = \langle \alpha | \hat{A} | \alpha \rangle$ . This leads to simple calculations involving only c-numbers, provided that the operator  $\hat{A}$  is expressed in *normal order*, that is, so that the creation operators stand to the left of the annihilation operators.

In order to compute the  $P(\alpha)$  distribution, it is often convenient to introduce the characteristic function

$$C_N(\lambda) = \operatorname{Tr}(\rho e^{\lambda a^\dagger} e^{-\lambda^* a}) , \quad (13.82)$$

where the subscript  $N$  stands for “normal order” and  $\lambda$  is a complex number. Similarly, one can also introduce antinormally ordered and symmetrically ordered characteristic functions

$$C_A(\lambda) = \text{Tr}(\rho e^{-\lambda^* a} e^{\lambda a^\dagger}), \quad (13.83)$$

and

$$C_S(\lambda) = \text{Tr}(\rho e^{\lambda a^\dagger - \lambda^* a}). \quad (13.84)$$

From the Baker-Hausdorff relation (13.56), it is easily seen that

$$\underbrace{e^{\hat{A}+\hat{B}}}_{= e^{\hat{A}} e^{\hat{B}} e^{-\frac{1}{2}[\hat{A}, \hat{B}]}} = e^{\hat{A}} e^{\hat{B}} e^{-\frac{1}{2}[\hat{A}, \hat{B}]} \quad C_N(\lambda) = C_S(\lambda) e^{|\lambda|^2/2} = C_A(\lambda) e^{|\lambda|^2}. \quad (13.85)$$

From (13.80, 13.83), one has readily that

$$\begin{aligned} C_N(\lambda) &= \sum_n \langle n | \int d^2\alpha P(\alpha) |\alpha\rangle \langle \alpha | e^{\lambda a^\dagger} e^{-\lambda^* a} |n\rangle \\ &= \sum_n \int d^2\alpha P(\alpha) \langle n | e^{-\lambda^* a} |\alpha\rangle \langle \alpha | e^{\lambda a^\dagger} |n\rangle \\ &= \int d^2\alpha P(\alpha) e^{\lambda\alpha^* - \lambda^*\alpha}. \end{aligned} \quad (13.86)$$

That is,  $C_N(\lambda)$  is the Fourier transform of  $P(\alpha)$ . Similarly, we introduce the  $Q$ -distribution  $Q(\alpha)$  and the Wigner distribution  $W(\alpha)$  via

$$\begin{aligned} C_A(\lambda) &= \frac{1}{\pi} \int d^2\alpha \langle \alpha | \rho e^{-\lambda^* a} e^{\lambda a^\dagger} | \alpha \rangle \\ &\equiv \int d^2\alpha Q(\alpha) e^{\lambda\alpha^* - \lambda^*\alpha}, \end{aligned} \quad (13.87)$$

where

$$\text{算 } Q(\alpha) = \boxed{Q(\alpha) = \frac{1}{\pi} \langle \alpha | \rho | \alpha \rangle}, \quad (13.88)$$

and

$$\begin{aligned} C_S(\lambda) &= \frac{1}{\pi} \int d^2\alpha \langle \alpha | \rho e^{\lambda a^\dagger - \lambda^* a} | \alpha \rangle \\ &\equiv \int d^2\alpha W(\alpha) e^{\lambda\alpha^* - \lambda^*\alpha}. \end{aligned} \quad (13.89)$$

The quasi-probability distributions functions  $P(\alpha)$ ,  $Q(\alpha)$  and  $W(\alpha)$  are therefore defined as the Fourier transforms of the normally ordered, antinormally ordered and symmetrically ordered characteristic functions as

$$\begin{aligned} \text{算 } P(\alpha) &= \frac{1}{\pi^2} \int d^2\lambda e^{\alpha\lambda^* - \alpha^*\lambda} C_N(\lambda), \quad \text{算 } C_N(\lambda) = \text{Tr}(\rho e^{\lambda a^\dagger} e^{-\lambda a}) \\ Q(\alpha) &= \frac{1}{\pi^2} \int d^2\lambda e^{\alpha\lambda^* - \alpha^*\lambda} C_A(\lambda), \\ \text{算 } W(\alpha) &= \frac{1}{\pi^2} \int d^2\lambda e^{\alpha\lambda^* - \alpha^*\lambda} C_S(\lambda), \quad \text{算 } C_S(\lambda) = \text{Tr}(\rho e^{\lambda a^\dagger - \lambda^* a}) \end{aligned} \quad (13.90)$$

	$P$	$Q$	$W$
Normal	↑	↑	↑
Antinormal	↑	↓	↑
Symmetric	↑	↑	↑
$C(\lambda)$	↑	↓	↑

Problem 13.11 shows how these relations permit us to express the Wigner distribution and  $Q$ -function in terms of the  $P$  distribution as

$$W(\alpha) = \frac{2}{\pi} \int d^2\beta P(\beta) \exp(-2|\beta - \alpha|^2) \quad (13.91)$$

and

$$Q(\alpha) = \frac{1}{\pi} \int d^2\beta P(\beta) \exp(-|\beta - \alpha|^2). \quad (13.92)$$

This shows that both the  $Q$ -function and the Wigner distribution are convolutions of Gaussians with the  $P$ -function. Note, however, that the  $Q$ -function is convoluted with a Gaussian of width  $\sqrt{2}$  times larger than that for the Wigner function. As a consequence, the  $Q$ -function is positive-definite, as can be seen directly from its definition, (13.88), while  $P(\alpha)$  and  $W(\alpha)$  are not. In particular, Prob. 13.4 shows an example where the  $P$ -representation becomes highly singular.

As an illustration of a  $P(\alpha)$  distribution, we consider the situation of the thermal field described by the density operator (13.38). The corresponding  $P(\alpha)$  is best obtained by considering first the  $Q(\alpha)$  distribution

$$\begin{aligned} Q(\alpha) &= (1 - e^{-x}) \sum_n e^{-nx} \langle \alpha | n \rangle \langle n | \alpha \rangle \\ &= (1 - e^{-x}) \exp[-\alpha|^2(1 - e^{-x})], \end{aligned} \quad (13.93)$$

where  $x = \hbar\Omega/k_B T$ . Inverting (13.44) for the average photon number  $\bar{n}$ , we find  $1 - e^{-x} = 1/(\bar{n} + 1)$ , which gives

$$Q(\alpha) = \frac{1}{\bar{n} + 1} \exp[-|\alpha|^2/(\bar{n} + 1)]. \quad (13.94)$$

From this result, we can readily obtain  $P(\alpha)$  since from a 2-dimensional Fourier transform of (13.92) we have

$$\mathcal{F}[Q(\alpha)] = \mathcal{F}[P(\alpha)] \mathcal{F}[\exp -|\alpha|^2]$$

and hence

$$P(\beta) = \mathcal{F}^{-1} \frac{\mathcal{F}[Q(\alpha)]}{\mathcal{F}[\exp(-|\alpha|^2)]}.$$

This gives, after carrying out the integrals,

$$P(\alpha) = \frac{1}{\pi \bar{n}} \exp[-|\alpha|^2/\bar{n}]. \quad (13.95)$$

It is interesting to note that in the classical limit of large mean photon numbers, the expressions for  $Q(\alpha)$  and  $P(\alpha)$  coincide. This is because in that limit, distinctions depending on the ordering of operators vanish. This point is discussed further in Glauber's Les Houches Lectures (1965), while a more

detailed discussion of quasi-probability distributions and their use in quantum optics is presented in Walls and Milburn (1994).

The probability for finding  $n$  photons is given by the photon statistics  $\rho_{nn}$  of (13.38). This exponentially decaying distribution contrasts with the Poisson distribution characteristic of a coherent state. The difference between  $Q(\alpha)$  and  $P(\alpha)$  for the two cases is even more striking, since for thermal light  $P(\alpha)$  is given by a Gaussian distribution, as we have seen, while for the coherent state  $|\alpha_0\rangle$  it is given by the  $\delta$ -function  $\delta(\alpha - \alpha_0)$ . From this and (13.91) and (13.92), we immediately find that both the Wigner and the  $Q$ -distributions for a coherent state are Gaussian.

While one might be tempted to interpret  $P(\alpha)$  as the probability of finding the field in the coherent state  $|\alpha\rangle$ , this is not correct in general, because  $P(\alpha)$  – and likewise  $W(\alpha)$  – are not positive-definite and hence cannot be interpreted as probabilities. Sometimes, fields described by a positive  $P(\alpha)$  and/or  $W(\alpha)$  are referred to as “classical fields.” This does not mean that these fields have vanishing quantum mechanical uncertainties. For example, a coherent state itself is described by a positive definite Dirac delta function, but has minimum, not vanishing, quantum mechanical uncertainties.

The description of electromagnetic fields in terms of quasi-probability distribution functions is very convenient in that it often permits to replace the quantum-mechanical description of the problem by an equivalent description in terms of c-numbers. For instance, if one is interested in computing anti-normally ordered correlation functions, one has

$$\begin{aligned} \langle a^m(a^\dagger)^n \rangle &= \int d^2\alpha \sum_n \langle n | \rho a^m |\alpha\rangle \langle \alpha | (a^\dagger)^n | n \rangle \\ &= \int d^2\alpha \alpha^m \alpha^{*n} Q(\alpha). \end{aligned} \quad (13.96)$$

Similarly, for normally ordered correlation functions

$$\begin{aligned} \langle (a^\dagger)^m a^n \rangle &= \sum_n \langle n | \int d^2\alpha P(\alpha) |\alpha\rangle \langle \alpha | (a^\dagger)^m a^n | n \rangle \\ &= \int d^2\alpha \alpha^{*m} \alpha^n P(\alpha). \end{aligned} \quad (13.97)$$

In particular, correlation functions can readily be computed from the appropriate characteristic function. From the definitions of  $C_A(\lambda)$  and  $C_N(\lambda)$  we find readily

$$\begin{aligned} \frac{\partial^{m+n} C_A(\lambda, \lambda^*)}{(\partial \lambda^*)^m (\partial \lambda)^n} &= \text{Tr}[\rho e^{-\lambda^* a} (-a)^m e^{\lambda a^\dagger} (a^\dagger)^n] \\ &= (-1)^m \langle a^m (a^\dagger)^n \rangle, \\ (\lambda = \lambda^* = 0) \end{aligned} \quad (13.98)$$

where the last equality holds for  $\lambda = \lambda^* = 0$ . Similarly,

$$\begin{aligned} \frac{\partial^{m+n} C_S(\lambda, \lambda^*)}{(\partial \lambda)^m (\partial \lambda^*)^n} &= \text{Tr}[\rho e^{\lambda a^\dagger} (a^\dagger)^m e^{-\lambda^* a} a^n] \\ &= (-1)^m \langle (a^\dagger)^m a^n \rangle. \\ (\lambda, \lambda^* = 0) \end{aligned} \quad (13.99)$$

## 第三章 简介：

$P(\alpha)$  性质：

- ①  $\text{Tr}(\hat{\rho})=1 \Rightarrow \sum P(\alpha) = \int d\alpha P(\alpha) = 1$
- ②  $\hat{\rho}^* = \hat{\rho}$  保守  $\Rightarrow P(\alpha) = P(\alpha)^*$  实数  $\rightarrow$  相等
- ③  $P(\alpha)$  可能小于0，一旦发现说明是非经典态  
 $\text{tr}(\hat{\rho}) = p = |\alpha| < n$  时

算法：先算  $C_N(\lambda) = \text{Tr}(\hat{\rho} e^{\lambda \hat{X}} e^{-\lambda \hat{X}})$

$$\text{再 FT} \rightarrow P(\alpha) = \frac{1}{\pi} \int d\lambda e^{\alpha \lambda^* - \lambda \alpha^*} C_N(\lambda)$$

$Q(\alpha)$  性质：

- ①  $\text{Tr}(\hat{\rho})=1 \Rightarrow \sum P(\alpha) = \int d\alpha P(\alpha) = 1$
- ② 正定数  $0 \leq Q(\alpha) \leq \frac{1}{n}$
- ③  $Q(\alpha)$  的最大概率不是1

算法： $Q(\alpha) = \frac{1}{n} \langle \alpha | \hat{\rho} | \alpha \rangle$

$W(\alpha)$  性质：

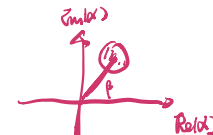
算法：先算  $C_S(\lambda) = \text{Tr}(\hat{\rho} e^{\lambda \hat{X}} e^{-\lambda \hat{X}})$

$$\text{再 FT} \rightarrow P(\alpha) = \frac{1}{\pi} \int d\lambda e^{\alpha \lambda^* - \lambda \alpha^*} C_S(\lambda)$$

例：示例计算  $Q(\alpha)$

相干态  $|p\rangle$        $Q(\alpha) = \frac{1}{n} \langle \alpha | \hat{\rho} | \alpha \rangle = \frac{1}{n} e^{-|\alpha-p|^2}$

Fock态  $|n\rangle$        $Q(\alpha) = \frac{1}{n!} \frac{e^{|\alpha|^2} |\alpha|^{2n}}{n!}$



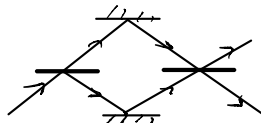
例：单模腔场的  $P(\alpha), Q(\alpha)$

$$P(\alpha) = \frac{1}{2n} \exp\left(-\frac{|\alpha|^2}{n}\right)$$

$$Q(\alpha) = \frac{1}{n+1} \exp\left[-\frac{|\alpha|^2}{n+1}\right] \frac{1}{n}$$

Intro to Chapter 4      子系统  $\leftarrow$  不同部分 能量相加 非平衡 强度相加

例一、M-Z干涉



例二、双光子干涉 (HOM 1982)

# Field–field and photon–photon interferometry

---

Optical interferometry was at the heart of the revolution which ushered in the new era of twentieth century physics. For example, the Michelson interferometer was used to show that there is no detectable motion relative to the ‘ether’; a key experiment in support of special relativity.

It is a wonderful tribute to Michelson that the same interferometer concept is central to the gravity-wave detectors which promise to provide new insights into general relativity and astrophysics in the twenty-first century. Similar tales can be told about the Sagnac and Mach–Zehnder interferometers as discussed in this chapter. We further note that the intensity correlation stellar interferometer of Hanbury-Brown and Twiss\* was a driving force in ushering in the modern era of quantum optics.

We are thus motivated to develop the theory of field (amplitude) and photon (intensity) correlation interferometry. In doing so we will find that the subject provides us with an exquisite probe of the micro and macrocosmos, i.e., quantum mechanics and general relativity.

## 4.1.4 *The Michelson stellar interferometer*

Consider the simple double (i.e., double source) interference setup as in Fig. 4.5. In Fig. 4.5(a), we see a binary star ‘sending’ light to earth with wave vectors  $\mathbf{k}$  and  $\mathbf{k}'$ , and we wish to measure their angular separation,  $\varphi$ .

One way to accomplish this is to collect the light by mirrors  $M_1$  and  $M_2$ , as in Fig. 4.5(b), and to beat the light from two stars on the photodetector located at the point  $P$  chosen so that the two paths

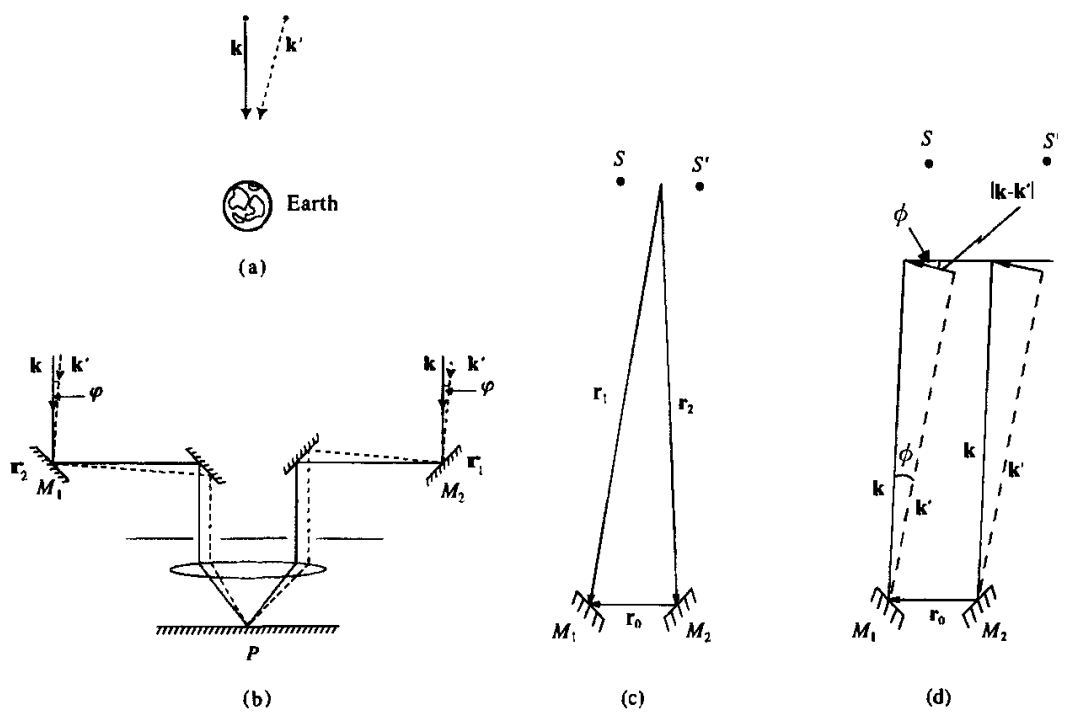
Fig. 4.5

(a) A binary star sending light to earth with wave vectors  $\mathbf{k}$  and  $\mathbf{k}'$ .

(b) Schematics of a Michelson stellar interferometer to measure the angular separation of a binary star.

(c) Filtered light from star  $S$  arrives at mirrors  $M_1$  and  $M_2$  with phase factors  $\exp(-iv_k t + i\mathbf{k} \cdot \mathbf{r}_1)$  and  $\exp(-iv_{k'} t + i\mathbf{k}' \cdot \mathbf{r}_2)$ , respectively, while that from star  $S'$  goes as  $\exp(-iv_{k'} t + i\mathbf{k}' \cdot \mathbf{r}_1)$  and  $\exp(-iv_{k'} t + i\mathbf{k}' \cdot \mathbf{r}_2)$ .

(d) Illustration that for small angles,  $(\mathbf{k} - \mathbf{k}') \cdot (\mathbf{r}_1 - \mathbf{r}_2) = |\mathbf{k} - \mathbf{k}'| r_0 \cos \phi \approx \phi kr_0$ , since  $|\mathbf{k} - \mathbf{k}'| \simeq k\phi$  and  $\cos \phi \simeq 1$ .



$$\star \vec{r}' - \vec{r}_1 = \vec{r}_1 - \vec{r}_2 = \Delta \vec{r}$$

$\overline{M_1 P}$  and  $\overline{M_2 P}$  are equal. The photocurrent is then given by

$$\begin{aligned} I &= \kappa \langle E^* E \rangle \\ &= \kappa \langle |E_{\mathbf{k}}(e^{i\mathbf{k} \cdot \mathbf{r}_1} + e^{i\mathbf{k} \cdot \mathbf{r}_2}) + E_{\mathbf{k}'}(e^{i\mathbf{k}' \cdot \mathbf{r}_1} + e^{i\mathbf{k}' \cdot \mathbf{r}_2})|^2 \rangle \\ &= \kappa \langle 2(|E_{\mathbf{k}}|^2 + |E_{\mathbf{k}'}|^2) + |E_{\mathbf{k}}|^2 [e^{i\mathbf{k} \cdot (\mathbf{r}_1 - \mathbf{r}_2)} + \text{c.c.}] \\ &\quad + |E_{\mathbf{k}'}|^2 [e^{i\mathbf{k}' \cdot (\mathbf{r}_1 - \mathbf{r}_2)} + \text{c.c.}] \rangle, \end{aligned} \quad (4.1.22)$$

where we have made the simplifying assumption that the light from the stars has been filtered so that we may take  $v_k = v_{k'}$  and therefore the temporal factors like  $\exp(iv_k t)$  and  $\exp(iv_{k'} t)$  cancel from Eq. (4.1.22). Furthermore, since the radiation from a star is thermal  $\langle E_{\mathbf{k}} \rangle = \langle E_{\mathbf{k}'} \rangle = 0$  and  $\langle E_{\mathbf{k}}^* E_{\mathbf{k}'} \rangle = \langle E_{\mathbf{k}}^* \rangle \langle E_{\mathbf{k}'} \rangle = 0$ . Finally, we note that  $\kappa$  is an uninteresting constant depending of the characteristics of the photodetector and the distance to the star, etc.

If  $\langle |E_{\mathbf{k}}|^2 \rangle = \langle |E_{\mathbf{k}'}|^2 \rangle = I_0$ , we have

$$\begin{aligned} I &= 2\kappa I_0 \{2 + \cos[\mathbf{k} \cdot (\mathbf{r}_1 - \mathbf{r}_2)] + \cos[\mathbf{k}' \cdot (\mathbf{r}_1 - \mathbf{r}_2)]\} \\ &= 4\kappa I_0 \{1 + \cos[(\mathbf{k} + \mathbf{k}') \cdot (\mathbf{r}_1 - \mathbf{r}_2)/2] \\ &\quad \times \cos[(\mathbf{k} - \mathbf{k}') \cdot (\mathbf{r}_1 - \mathbf{r}_2)/2]\}. \end{aligned} \quad (4.1.23)$$

From Fig. 4.5(d) we see that  $(\mathbf{k} - \mathbf{k}') \cdot (\mathbf{r}_1 - \mathbf{r}_2) \cong \phi kr_0$ , so that (4.1.23) may be written as

$$I = 4\kappa I_0 \left\{1 + \cos[(\mathbf{k} + \mathbf{k}') \cdot (\mathbf{r}_1 - \mathbf{r}_2)/2] \cos\left(\frac{\pi r_0 \phi}{\lambda}\right)\right\}, \quad (4.1.24)$$

where we have noted  $|\mathbf{k}| = |\mathbf{k}'| = 2\pi/\lambda$ . Thus, we see that the photocurrent will contain an interference term which is modulated as we vary  $r_0$  and would serve to determine  $\varphi$  varying  $r_0$  until  $\pi r_0 \varphi / \lambda = \pi$ , etc.

This clever scheme has been applied to several nearby binaries. Unfortunately, atmospheric and instrumental fluctuations enter strongly into the term  $\cos[(\mathbf{k} + \mathbf{k}') \cdot (\mathbf{r}_1 - \mathbf{r}_2)/2]$  in Eq. (4.1.24) and limit the utility of the approach. This is where Hanbury-Brown and Twiss make their dramatic entrance.

#### 4.1.5 Hanbury-Brown-Twiss interferometer 为什么汉布顿和特威斯的干涉仪之前没有说是自己探测自己 太像杨氏双缝

The essence of the Hanbury-Brown-Twiss (HB-T) stellar interferometer is to recognize that if we consider two photodetectors at points  $A_1$  and  $A_2$  with position vectors  $\mathbf{r}_1$  and  $\mathbf{r}_2$ , respectively, as in Fig. 4.6, then we have the photocurrents

$$I(\mathbf{r}_i, t) = \kappa \left\{ |E_{\mathbf{k}}|^2 + |E_{\mathbf{k}'}|^2 + [E_{\mathbf{k}} E_{\mathbf{k}'}^* e^{i(\mathbf{k}-\mathbf{k}') \cdot \mathbf{r}_i} + \text{c.c.}] \right\} \quad (i=1, 2), \quad (4.1.25)$$

and there is phase information in the  $\exp[i(\mathbf{k} - \mathbf{k}') \cdot \mathbf{r}_i]$  terms.

What if we multiply the currents from two detectors (at  $A_1$  and  $A_2$  in Fig. 4.6)? From Eq. (4.1.25) this will yield

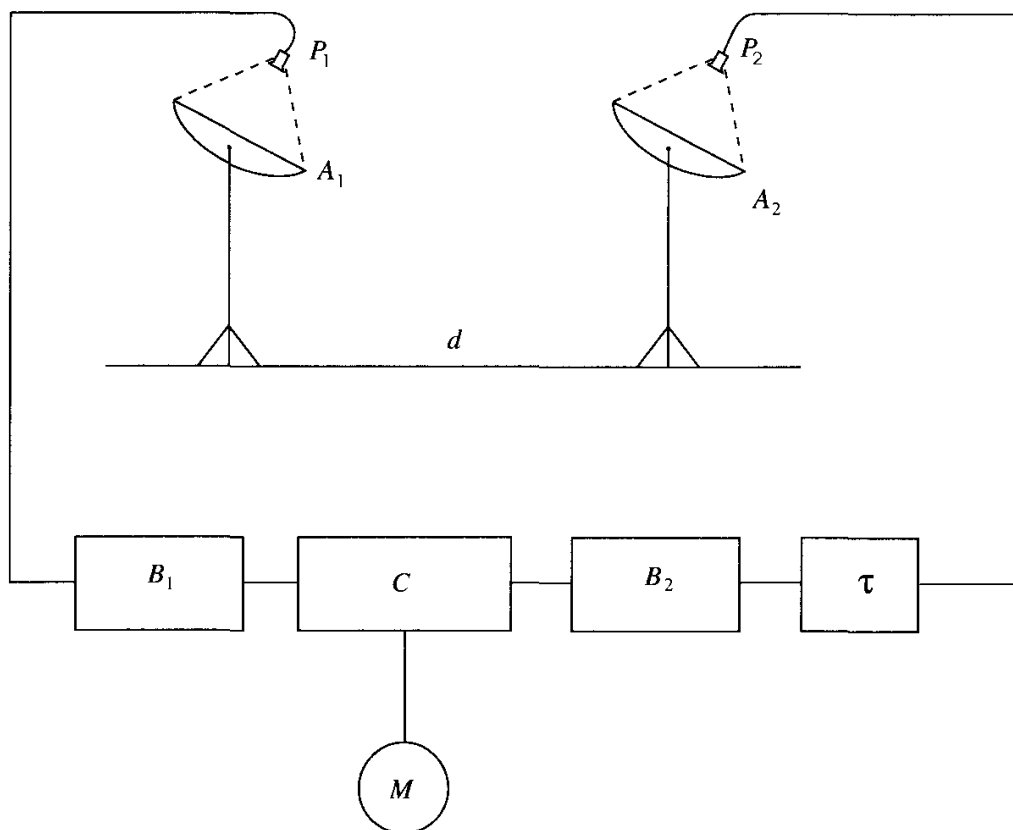
$$\begin{aligned} & \langle I(\mathbf{r}_1, t) I(\mathbf{r}_2, t) \rangle \quad \text{光强干涉!?!} \\ &= \kappa^2 \left\{ \left\{ |E_{\mathbf{k}}|^2 + |E_{\mathbf{k}'}|^2 + [E_{\mathbf{k}} E_{\mathbf{k}'}^* e^{i(\mathbf{k}-\mathbf{k}') \cdot \mathbf{r}_1} + \text{c.c.}] \right\} \right. \\ & \quad \times \left. \left\{ |E_{\mathbf{k}}|^2 + |E_{\mathbf{k}'}|^2 + [E_{\mathbf{k}} E_{\mathbf{k}'}^* e^{i(\mathbf{k}-\mathbf{k}') \cdot \mathbf{r}_2} + \text{c.c.}] \right\} \right\} \\ &= \kappa^2 \left\{ \langle (|E_{\mathbf{k}}|^2 + |E_{\mathbf{k}'}|^2)^2 \rangle \right. \\ & \quad \left. + \langle |E_{\mathbf{k}}|^2 \rangle \langle |E_{\mathbf{k}'}|^2 \rangle [e^{i(\mathbf{k}-\mathbf{k}') \cdot (\mathbf{r}_1 - \mathbf{r}_2)} + \text{c.c.}] \right\}, \end{aligned} \quad (4.1.26)$$

$$4|E|^4 + 2|E|^2 \cdot 2\cos(\angle) + 2|E|^2 (1 + \cos(\angle))$$

where we have used the fact that  $\langle |E_{\mathbf{k}}|^2 E_{\mathbf{k}}^* E_{\mathbf{k}'} \rangle = 0$ , etc. Thus we see that the desired low frequency interference term is present; but atmospherically sensitive terms like  $\cos[(\mathbf{k} + \mathbf{k}') \cdot (\mathbf{r}_1 - \mathbf{r}_2)/2]$  are absent. This is the key insight of Hanbury Brown and Twiss.

It is fair to say, however, that the Hanbury-Brown-Twiss effect created quite a stir when it was first announced. Many questions were voiced, e.g., how can we get phase information by beating photocurrents? Does this not somehow violate quantum mechanics? And what about Dirac's statement that photons only interfere with themselves? The confusion is resolved by considering the quantum theory of photon detection and correlation to which we now turn.

Fig. 4.6  
Schematic diagram of the Hanbury Brown-Twiss stellar intensity interferometer. Here  $P_1$  and  $P_2$  are the photodetectors,  $A_1$  and  $A_2$  are the mirrors,  $B_1$  and  $B_2$  are the amplifiers,  $\tau$  is the delay time,  $C$  is a multiplier, and  $M$  is the integrator.



光子探测 和 量子相干函数

## 4.2 Photon detection and quantum coherence functions

A more complete account of photodetection theory is given in Section 6.5. Here we present a heuristic derivation of photodetection and correlation which is sufficient for the present purposes.

As shown in Chapter 1, the field operator  $\mathbf{E}(\mathbf{r}, t)$  can be separated into the sum of its positive and negative frequency parts

$$\mathbf{E}(\mathbf{r}, t) = \mathbf{E}^{(+)}(\mathbf{r}, t) + \mathbf{E}^{(-)}(\mathbf{r}, t), \quad (4.2.1)$$

where

$$\mathbf{E}^{(+)}(\mathbf{r}, t) = \sum_{\mathbf{k}} \hat{\epsilon}_{\mathbf{k}} \mathcal{E}_{\mathbf{k}} a_{\mathbf{k}} e^{-i\nu_k t + i\mathbf{k} \cdot \mathbf{r}}, \quad (4.2.2)$$

$$\mathbf{E}^{(-)}(\mathbf{r}, t) = \sum_{\mathbf{k}} \hat{\epsilon}_{\mathbf{k}} \mathcal{E}_{\mathbf{k}} a_{\mathbf{k}}^\dagger e^{i\nu_k t - i\mathbf{k} \cdot \mathbf{r}}. \quad (4.2.3)$$

In the following we shall assume, for simplicity, that the field is linearly polarized so that we deal with the scalar quantities  $E^{(+)}(\mathbf{r}, t) = \hat{\epsilon} \cdot \mathbf{E}^{(+)}(\mathbf{r}, t)$  and  $E^{(-)}(\mathbf{r}, t) = \hat{\epsilon} \cdot \mathbf{E}^{(-)}(\mathbf{r}, t)$ .

In the optical region, the detectors usually use the photoelectric effect to make local field measurements. Schematically an atom is

Note: 矢积  $\langle (A-A')(B-B') \rangle$  $A \bar{A} B \bar{B}$   
 $A \bar{A} B \bar{B}$  $A \bar{A} B \bar{B}$   
 $A \bar{A} B \bar{B}$ 不相关  
 $A \bar{A} \downarrow B \bar{B}$   
 $A \bar{A} \downarrow B \bar{B}$ 正相关  
 $A \bar{A} B \bar{B}$   
 $A \bar{A} B \bar{B}$ 反相关  
 $A \bar{A} B \bar{B}$   
 $A \bar{A} B \bar{B}$ 

placed in the radiation field at position  $\mathbf{r}$  in its ground state. The photoelectrons produced by photoionization are then observed. In such absorptive detectors, the measurements are destructive as the photons responsible for producing photoelectrons disappear. In this case, therefore, only the annihilation operator  $E^{(+)}$  contributes. The transition probability of the detector atom for absorbing a photon from the field at position  $\mathbf{r}$  between times  $t$  and  $t + dt$  is proportional to  $w_1(\mathbf{r}, t)dt$ , with

这里从光场角度讲 this is, 从原稿及后添是  
 $k+|\mathbf{r}|i\rangle^2$  但容易写错(方便记忆)

$$\text{Photon counting rate } w_1(\mathbf{r}, t) = |\langle f | E^{(+)}(\mathbf{r}, t) | i \rangle|^2, \quad (4.2.4)$$

where  $|i\rangle$  is the initial state of the field before the detection process and  $|f\rangle$  is the final state in which the field could be found after the process. The final state of the field is never measured. We can therefore sum over all the final states

$$\begin{aligned} w_1(\mathbf{r}, t) &= \sum_f |\langle f | E^{(+)}(\mathbf{r}, t) | i \rangle|^2 \\ &= \sum_f \langle i | E^{(-)}(\mathbf{r}, t) | f \rangle \langle f | E^{(+)}(\mathbf{r}, t) | i \rangle \\ &= \langle i | E^{(-)}(\mathbf{r}, t) E^{(+)}(\mathbf{r}, t) | i \rangle, \end{aligned} \quad (4.2.5)$$

技术上和物理上都

1
2
3

where in the last line we use the completeness relation

$$\sum_f |f\rangle \langle f| = 1. - |i\rangle \langle i| \quad \text{但这项 } \langle i | E^{(+)}(\mathbf{r}, t) | i \rangle \text{ 为 } 0$$

严格说 不包括 |i> 在内.

$$(4.2.6)$$

The photon counting rate  $w_1$  is therefore proportional to the expectation value of the positive definite Hermitian operator  $E^{(-)}(\mathbf{r}, t) E^{(+)}(\mathbf{r}, t)$  taken in the initial state of the field  $|i\rangle$ . In practice, however, we almost never know precisely the state  $|i\rangle$ . Since the precise knowledge of the field does not usually exist, we resort to a statistical description by averaging over all the possible realizations of the initial field

$$w_1(\mathbf{r}, t) = \sum_i P_i \langle i | E^{(-)}(\mathbf{r}, t) E^{(+)}(\mathbf{r}, t) | i \rangle. \quad (4.2.7)$$

If we introduce the density operator for the field

$$\rho = \sum_i P_i |i\rangle \langle i|, \quad (4.2.8)$$

we can rewrite Eq. (4.2.7) as

光场态

$$w_1(\mathbf{r}, t) = \text{Tr}[\rho E^{(-)}(\mathbf{r}, t) E^{(+)}(\mathbf{r}, t)]. \quad (4.2.9)$$

后面可以看为这新量

光强

一阶相干：相位相干  
二阶相干：强度相干

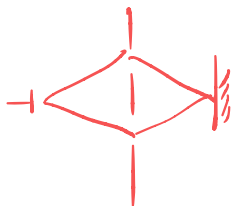
$\propto$  Transition Prob  
光强

We define the first-order correlation function of the field

$$\begin{aligned} \text{-前关联函数} \\ \text{最大 } \sqrt{\langle E_1^{-} \rangle \langle E_1^{+} \rangle} \\ \text{和 } + \end{aligned} \quad G^{(1)}(\mathbf{r}_1, \mathbf{r}_2; t_1, t_2) &= \text{Tr}[\rho E^{(-)}(\mathbf{r}_1, t_1)E^{(+)}(\mathbf{r}_2, t_2)] \\ &= \langle E^{(-)}(\mathbf{r}_1, t_1)E^{(+)}(\mathbf{r}_2, t_2) \rangle. \end{aligned} \quad (4.2.10)$$

Usually we deal with statistically stationary fields in optics, i.e., the correlation functions of the field are invariant under displacements of the time variable. The correlation function  $G^{(1)}(\mathbf{r}_1, \mathbf{r}_2; t_1, t_2)$  then depends on  $t_1$  and  $t_2$  only through the time difference  $\tau = t_2 - t_1$ , i.e.,

平稳光场：



$$G^{(1)}(\mathbf{r}_1, \mathbf{r}_2; t_1, t_2) \equiv G^{(1)}(\mathbf{r}_1, \mathbf{r}_2; \tau). \quad (4.2.11)$$

In terms of  $G^{(1)}$ , the counting rate  $w_1$  is given by

$$\underline{w_1 = G^{(1)}(\mathbf{r}, \mathbf{r}; 0)}. \quad (4.2.12)$$

We now consider the joint counting rate at two photodetectors at  $\mathbf{r}_1$  and  $\mathbf{r}_2$ . The joint probability of observing one photoionization at point  $\mathbf{r}_2$  between  $t_2$  and  $t_2 + dt_2$  and another one at point  $\mathbf{r}_1$  between  $t_1$  and  $t_1 + dt_1$  with  $t_1 \leq t_2$  is proportional to  $w_2(\mathbf{r}_1, t_1; \mathbf{r}_2, t_2)dt_1 dt_2$ , where

$$\underline{w_2(\mathbf{r}_1, t_1; \mathbf{r}_2, t_2) = |\langle f | E^{(+)}(\mathbf{r}_2, t_2)E^{(+)}(\mathbf{r}_1, t_1) | i \rangle|^2}. \quad (4.2.13)$$

It follows, on summing over all the final states and averaging over all the possible realizations of the initial field as before, that

$$\begin{aligned} w_2(\mathbf{r}_1, t_1; \mathbf{r}_2, t_2) \\ = \text{Tr}[\rho E^{(-)}(\mathbf{r}_1, t_1)E^{(-)}(\mathbf{r}_2, t_2)E^{(+)}(\mathbf{r}_2, t_2)E^{(+)}(\mathbf{r}_1, t_1)]. \end{aligned} \quad (4.2.14)$$

The joint probability of photodetection is thus governed by the second-order quantum mechanical correlation function

$$\begin{aligned} G^{(2)}(\mathbf{r}_1, \mathbf{r}_2, \mathbf{r}_3, \mathbf{r}_4; t_1, t_2, t_3, t_4) &= \text{Tr}[\rho E^{(-)}(\mathbf{r}_1, t_1)E^{(-)}(\mathbf{r}_2, t_2) \\ &\quad \times E^{(+)}(\mathbf{r}_3, t_3)E^{(+)}(\mathbf{r}_4, t_4)] \\ &= \langle E^{(-)}(\mathbf{r}_1, t_1)E^{(-)}(\mathbf{r}_2, t_2) \\ &\quad \times E^{(+)}(\mathbf{r}_3, t_3)E^{(+)}(\mathbf{r}_4, t_4) \rangle. \end{aligned} \quad (4.2.15)$$

In general, we can define the  $n$ th-order correlation function

$$\begin{aligned} G^{(n)}(\mathbf{r}_1, \dots, \mathbf{r}_n, \mathbf{r}_{n+1}, \dots, \mathbf{r}_{2n}; t_1, \dots, t_n, t_{n+1}, \dots, t_{2n}) \\ = \text{Tr}[\rho E^{(-)}(\mathbf{r}_1, t_1) \dots E^{(-)}(\mathbf{r}_n, t_n)E^{(+)}(\mathbf{r}_{n+1}, t_{n+1}) \dots E^{(+)}(\mathbf{r}_{2n}, t_{2n})] \\ = \langle E^{(-)}(\mathbf{r}_1, t_1) \dots E^{(-)}(\mathbf{r}_n, t_n)E^{(+)}(\mathbf{r}_{n+1}, t_{n+1}) \dots E^{(+)}(\mathbf{r}_{2n}, t_{2n}) \rangle. \end{aligned} \quad (4.2.16)$$

In this definition of the  $n$ th-order correlation function we have included

equal numbers of creation and destruction operators because such correlation functions are measured in typical multi-photon counting experiments.

It is apparent from the above discussion that the correlation functions of the field operators which are encountered in any photon detection experiment based on the photoelectric effect are in normal order (that is, with all the destruction operators on the right and all the creation operators on the left). For example, the average light intensity at point  $\mathbf{r}$  at time  $t$  is

$$\langle I(\mathbf{r}, t) \rangle = \langle E^{(-)}(\mathbf{r}, t) E^{(+)}(\mathbf{r}, t) \rangle, \quad (4.2.17)$$

$E \rightarrow$   
 $\langle a^\dagger a \rangle$

and the measured intensity-intensity correlation function is equal to  $\langle E^{(-)}(\mathbf{r}, t) E^{(-)}(\mathbf{r}, t) E^{(+)}(\mathbf{r}, t) E^{(+)}(\mathbf{r}, t) \rangle$ , which is different from  $\langle I(\mathbf{r}, t) I(\mathbf{r}, t) \rangle$ . (不同!)

We can define the quantum mechanical first- and second-order degrees of coherence at the position  $\mathbf{r}$  as

$\text{G 相关函数} \rightarrow \text{g 相干度}$

$$g^{(1)}(\mathbf{r}, \tau) = \frac{\langle E^{(-)}(\mathbf{r}, t) E^{(+)}(\mathbf{r}, t + \tau) \rangle}{\sqrt{\langle E^{(-)}(\mathbf{r}, t) E^{(+)}(\mathbf{r}, t) \rangle \langle E^{(-)}(\mathbf{r}, t + \tau) E^{(+)}(\mathbf{r}, t + \tau) \rangle}}, \quad (4.2.18)$$

$$g^{(2)}(\mathbf{r}, \tau) = \frac{\langle E^{(-)}(\mathbf{r}, t) E^{(-)}(\mathbf{r}, t + \tau) E^{(+)}(\mathbf{r}, t + \tau) E^{(+)}(\mathbf{r}, t) \rangle}{\langle E^{(-)}(\mathbf{r}, t) E^{(+)}(\mathbf{r}, t) \rangle \langle E^{(-)}(\mathbf{r}, t + \tau) E^{(+)}(\mathbf{r}, t + \tau) \rangle}, \quad (4.2.19)$$

where we have assumed the field to be statistically stationary. In the definition of  $g^{(2)}(\mathbf{r}, \tau)$ , we have chosen not only the normal ordering of the field operators in the numerator but a certain time ordering. This time ordering is a consequence of the way the photoelectron rate is calculated above (note that  $t_2 \geq t_1$  in Eq. (4.2.14)). Considerably simpler forms for these quantities are obtained in the special case when the radiation field consists of only a single mode. Then most factors cancel when the mode expansions for  $E^{(+)}$  and  $E^{(-)}$  are substituted from Eqs. (4.2.2) and (4.2.3) into Eqs. (4.2.18) and (4.2.19), leaving

$$g^{(1)}(\tau) = \frac{\langle a^\dagger(t) a(t + \tau) \rangle}{\langle a^\dagger a \rangle}, \quad 0 \leq |g^{(1)}| \leq 1 \quad (4.2.20)$$

$$g^{(2)}(\tau) = \frac{\langle a^\dagger(t) a^\dagger(t + \tau) a(t + \tau) a(t) \rangle}{\langle a^\dagger a \rangle^2}. \quad |g^{(2)}| \leq 1 \quad (4.2.21)$$

一阶相干度  $\rightarrow$  二阶相干度

二阶相干度

Since only the normally ordered correlation functions are involved in the photodetection processes, the  $P$ -representation  $P(\alpha, \alpha^*)$  forms a correspondence between classical and quantum coherence theory. This happens because the quantum mechanical expectation values  $g^{(n)}(\tau) = 1$ ,  $g^{(2)}(\tau) = 1$ ,  $g^{(3)}(\tau) = 1$ ,  $g^{(4)}(\tau) = 1$ , ...,  $g^{(n)}(\tau) = 1$  for  $n > 2$ .

例：相干态  
 $g^{(1)}(\tau) = 1$ :  
 $a^\dagger(t) = 1$ :  
 $a(t) = 1$ :  
 $\Rightarrow 1$

of the normally ordered functions can be calculated from the  $P$ -representation just as we would evaluate the corresponding classical coherence function from a classical distribution function. The  $P$ -representation, however, does not have all the properties of a classical distribution function. In particular, as discussed in Section 3.1, the  $P$ -representation is not nonnegative definite. Light fields for which the  $P$ -representation is not a well-behaved distribution will exhibit nonclassical features of light. We will discuss some of them in Section 4.4.

We now derive the normalized correlation function  $g^{(2)}(\tau)$  for thermal and coherent fields within the framework of the quantum theory of coherence. The  $P$ -representation of a single-mode thermal field is given by a Gaussian distribution (Eq. (3.1.26)):

$$P(\alpha, \alpha^*) = \frac{1}{\pi \langle n \rangle} \exp(-|\alpha|^2 / \langle n \rangle). \quad (4.2.22)$$

We then have

$$g^{(2)}(0) = \frac{\int P(\alpha, \alpha^*) |\alpha|^4 d^2\alpha}{[\int P(\alpha, \alpha^*) |\alpha|^2 d^2\alpha]^2} = 2. \quad (4.2.23)$$

However, for a laser operating far above threshold, the field is in a coherent state  $|\alpha_0\rangle$ , for which (see Eq. (3.1.28))

$$P(\alpha, \alpha^*) = \delta^{(2)}(\alpha - \alpha_0). \quad (4.2.24)$$

The normalized correlation then is

$$g^{(2)}(0) = 1. \quad (4.2.25)$$

## 4.3 First-order coherence and Young-type double-source experiments

### 4.3.1 Young's double-slit experiment

One of the classic experiments that exhibits the first-order coherence properties of light is Young's double-slit experiment (see Fig. 4.7). The complex field generated by a quasimonochromatic light source is split at the screen  $S_1$  by placing an opaque screen across the beam with pinholes at points  $P_1$  and  $P_2$ . The positive frequency part of the field operator at a point  $P$  on the screen  $S_2$  at time  $t$  may be approximated by a linear superposition of the field operators present at  $P_1$  and  $P_2$  at earlier times:

$$E^{(+)}(\mathbf{r}, t) = K_1 E^{(+)}(\mathbf{r}_1, t - t_1) + K_2 E^{(+)}(\mathbf{r}_2, t - t_2), \quad (4.3.1)$$

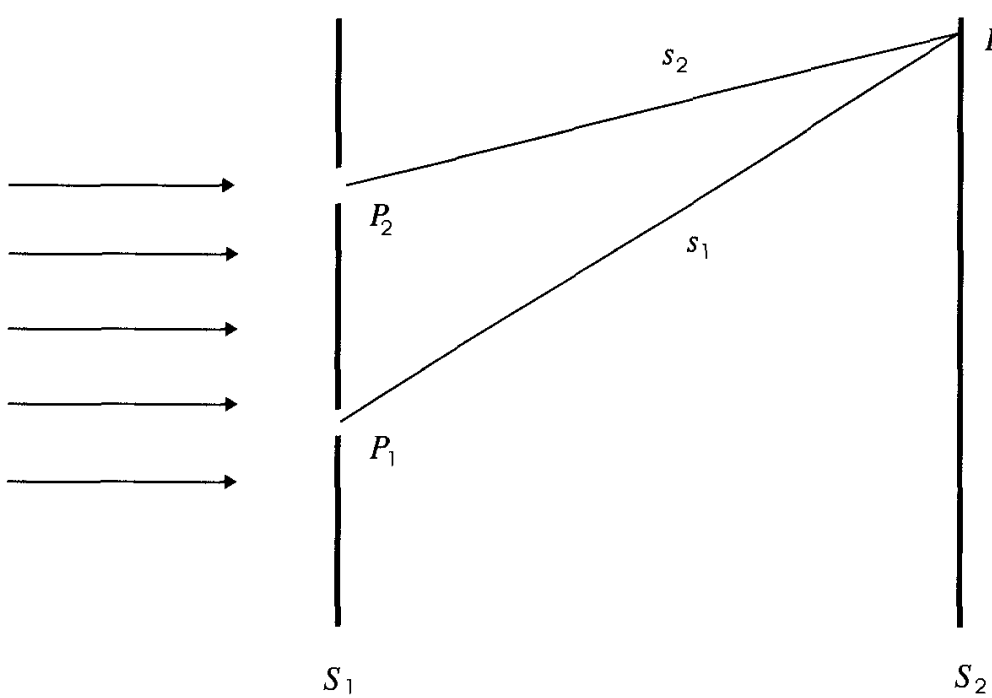


Fig. 4.7  
Schematic diagram of an idealized Young's double-slit experiment.

where  $t_i = s_i/c$  ( $i = 1, 2$ ) is the time needed for the light to travel from the pinhole  $P_i$  to the point  $P$  and  $\mathbf{r}_1$  and  $\mathbf{r}_2$  are the position vectors at the pinholes  $P_1$  and  $P_2$ , respectively. The coefficients  $K_1$  and  $K_2$  depend on the size and geometry of the pinholes. From diffraction theory it follows that  $K_1$  and  $K_2$  are purely imaginary numbers.

A photodetector placed at the point  $P$  measures the intensity

$$\begin{aligned} \langle I(\mathbf{r}, t) \rangle &= \text{Tr}[\rho E^{(-)}(\mathbf{r}, t)E^{(+)}(\mathbf{r}, t)] \\ &= |K_1|^2 \text{Tr}[\rho E^{(-)}(\mathbf{r}_1, t - t_1)E^{(+)}(\mathbf{r}_1, t - t_1)] \\ &\quad + |K_2|^2 \text{Tr}[\rho E^{(-)}(\mathbf{r}_2, t - t_2)E^{(+)}(\mathbf{r}_2, t - t_2)] \\ &\quad + 2\text{Re}\{K_1^* K_2 \text{Tr}[\rho E^{(-)}(\mathbf{r}_1, t - t_1)E^{(+)}(\mathbf{r}_2, t - t_2)]\}. \end{aligned} \quad (4.3.2)$$

We can rewrite this equation in terms of the first-order correlation function

$G^{(1)}(\mathbf{r}_1, \mathbf{r}_2; t_1, t_2)$  in the following way:

$$\begin{aligned} \langle I(\mathbf{r}, t) \rangle &= |K_1|^2 G^{(1)}(\mathbf{r}_1, \mathbf{r}_1; t - t_1, t - t_1) \\ &\quad + |K_2|^2 G^{(1)}(\mathbf{r}_2, \mathbf{r}_2; t - t_2, t - t_2) \\ &\quad + 2\text{Re}[K_1^* K_2 G^{(1)}(\mathbf{r}_1, \mathbf{r}_2; t - t_1, t - t_2)]. \end{aligned} \quad (4.3.3)$$

For statistically stationary fields, expression (4.3.3) for the average intensity at the point  $P$  becomes

$$\begin{aligned} \langle I(\mathbf{r}, t) \rangle &= |K_1|^2 G^{(1)}(\mathbf{r}_1, \mathbf{r}_1; 0) + |K_2|^2 G^{(1)}(\mathbf{r}_2, \mathbf{r}_2; 0) \\ &\quad + 2\text{Re}[K_1^* K_2 G^{(1)}(\mathbf{r}_1, \mathbf{r}_2; \tau)], \end{aligned} \quad (4.3.4)$$

where  $\tau = t_1 - t_2$ . The average intensity  $\langle I(\mathbf{r}, t) \rangle$  is therefore independent of the time  $t$ .

The first two terms in Eq. (4.3.4) represent the average intensities at the point  $P$  due to the light field at the pinholes  $P_1$  and  $P_2$ , respectively. The last term, however, gives a contribution due to fields at both the pinholes and is responsible for the interference. In order to see this clearly we set

$$\langle I^{(i)}(\mathbf{r}) \rangle = |K_i|^2 G^{(1)}(\mathbf{r}_i, \mathbf{r}_i; 0) \quad (i = 1, 2). \quad (4.3.5)$$

We next define the normalized first-order correlation function

$$g^{(1)}(\mathbf{r}_1, \mathbf{r}_2; \tau) = \frac{G^{(1)}(\mathbf{r}_1, \mathbf{r}_2; \tau)}{\sqrt{G^{(1)}(\mathbf{r}_1, \mathbf{r}_1; 0)G^{(1)}(\mathbf{r}_2, \mathbf{r}_2; 0)}}. \quad (4.3.6)$$

In terms of  $g^{(1)}(\mathbf{r}_1, \mathbf{r}_2; \tau)$ , Eq. (4.3.4) can be rewritten as

$$\begin{aligned} \langle I(\mathbf{r}, t) \rangle &= \langle I^{(1)}(\mathbf{r}) \rangle + \langle I^{(2)}(\mathbf{r}) \rangle \\ &+ 2[\langle I^{(1)}(\mathbf{r}) \rangle \langle I^{(2)}(\mathbf{r}) \rangle]^{1/2} \operatorname{Re}[g^{(1)}(\mathbf{r}_1, \mathbf{r}_2; \tau)]. \end{aligned} \quad (4.3.7)$$

Next we set

$$\text{物理意义} \quad \text{两光源相位差} \\ g^{(1)}(\mathbf{r}_1, \mathbf{r}_2; \tau) = |g^{(1)}(\mathbf{r}_1, \mathbf{r}_2; \tau)| e^{i\alpha(\mathbf{r}_1, \mathbf{r}_2; \tau) - iv_0\tau}, \quad (4.3.8)$$

where  $\alpha(\mathbf{r}_1, \mathbf{r}_2; \tau) = \arg[g^{(1)}(\mathbf{r}_1, \mathbf{r}_2; \tau)] + v_0\tau$  and  $v_0$  is the field frequency. We then obtain

$$\begin{aligned} \langle I(\mathbf{r}, t) \rangle &= \langle I^{(1)}(\mathbf{r}) \rangle + \langle I^{(2)}(\mathbf{r}) \rangle + 2[\langle I^{(1)}(\mathbf{r}) \rangle \langle I^{(2)}(\mathbf{r}) \rangle]^{1/2} \\ &\times |g^{(1)}(\mathbf{r}_1, \mathbf{r}_2; \tau)| \cos[\alpha(\mathbf{r}_1, \mathbf{r}_2; \tau) - v_0\tau]. \end{aligned} \quad (4.3.9)$$

For a quasimonochromatic source of light,  $\langle I^{(1)}(\mathbf{r}) \rangle$ ,  $\langle I^{(2)}(\mathbf{r}) \rangle$ ,  $|g^{(1)}(\mathbf{r}_1, \mathbf{r}_2; \tau)|$ , and  $\alpha(\mathbf{r}_1, \mathbf{r}_2; \tau)$  vary slowly with respect to position on the screen. However, the cosine term varies rapidly due to the term  $v_0\tau = v_0(s_1 - s_2)/c$  and will lead to sinusoidal variation of intensity on the screen.

The physical meaning of  $g^{(1)}(\mathbf{r}_1, \mathbf{r}_2; \tau)$  can be understood if we consider the visibility of the interference fringes on the screen. The visibility, which is a measure of the sharpness of the interference fringes, is defined as

$$U = \frac{\langle I(\mathbf{r}) \rangle_{\max} - \langle I(\mathbf{r}) \rangle_{\min}}{\langle I(\mathbf{r}) \rangle_{\max} + \langle I(\mathbf{r}) \rangle_{\min}}, \quad (4.3.10)$$

where  $\langle I(\mathbf{r}) \rangle_{\max}$  and  $\langle I(\mathbf{r}) \rangle_{\min}$  represent the maximum and minimum average intensity, respectively, in the neighborhood of the point  $P$ . To a good approximation for  $\cos[\alpha(\mathbf{r}_1, \mathbf{r}_2; \tau) - v_0\tau]$  they are equal to +1 and -1 in Eq. (4.3.9). We then obtain

$$U = \frac{2[\langle I^{(1)}(\mathbf{r}) \rangle \langle I^{(2)}(\mathbf{r}) \rangle]^{1/2}}{\langle I^{(1)}(\mathbf{r}) \rangle + \langle I^{(2)}(\mathbf{r}) \rangle} |g^{(1)}(\mathbf{r}_1, \mathbf{r}_2; \tau)|, \quad (4.3.11)$$

$g^{(1)}(\mathbf{r}_1, \mathbf{r}_2; \tau)$  复相干度  
大小  $|g| < 1$ , 部分相干  
 $|g|=0$ , 不相干  
 $|g|=1$ , 完全相干.

i.e., the visibility of the fringes is proportional to the magnitude of  $g^{(1)}(\mathbf{r}_1, \mathbf{r}_2; \tau)$ , which is called the complex degree of coherence. In particular, when the averaged intensities of the two beams are equal,  $\langle I^{(1)}(\mathbf{r}) \rangle = \langle I^{(2)}(\mathbf{r}) \rangle$ , the visibility  $U$  is equal to  $|g^{(1)}(\mathbf{r}_1, \mathbf{r}_2; \tau)|$ . Thus when  $g^{(1)}(\mathbf{r}_1, \mathbf{r}_2; \tau) = 0$ , no interference fringes are formed in the region around  $P$  and it would be implied that the two light beams reaching the point  $P$  are mutually incoherent. A maximum visibility of the fringes is obtained around  $P$  when  $|g^{(1)}(\mathbf{r}_1, \mathbf{r}_2; \tau)| = 1$  and the two light beams reaching  $P$  are mutually completely coherent. This happens when

$$\langle E^{(-)}(\mathbf{r}_1, t) E^{(+)}(\mathbf{r}_2, t + \tau) \rangle = \mathcal{E}^*(\mathbf{r}_1, t) \mathcal{E}(\mathbf{r}_2, t + \tau). \quad (4.3.12)$$

The intermediate cases  $0 < |g^{(1)}(\mathbf{r}_1, \mathbf{r}_2; \tau)| < 1$  characterize partial coherence.

As an example, the emission from a Doppler-broadened spectral light source, such as that from a thermal lamp, is described by

$$G^{(1)}(\mathbf{r}_1, \mathbf{r}_2; \tau) = \mathcal{E}_0^2 \exp(-iv_0\tau - \tau^2/2\tau_c^2), \quad (4.3.13)$$

where  $\tau_c$  is a constant. It is therefore clear that as the path difference  $c\tau$  becomes much larger than  $c\tau_c$ ,  $|g^{(1)}(\mathbf{r}_1, \mathbf{r}_2; \tau)| = \exp(-\tau^2/2\tau_c^2)$  goes to zero and the interference fringes disappear. The constant  $\tau_c$ , which will be related to the light bandwidth (shown below), is thus a measure of the coherence time of the light.

An important property of the first-order correlation function

$$G^{(1)}(\mathbf{r}, \mathbf{r}; \tau) = \langle E^{(-)}(\mathbf{r}, t) E^{(+)}(\mathbf{r}, t + \tau) \rangle$$

is that it forms a Fourier transform pair with the power spectrum  $S(\mathbf{r}, v)$  of the statistically stationary field at the position  $\mathbf{r}$ , i.e.,

$$S(\mathbf{r}, v) = \frac{1}{\pi} \operatorname{Re} \int_0^\infty d\tau G^{(1)}(\mathbf{r}, \mathbf{r}; \tau) e^{iv\tau}. \quad (4.3.14)$$

We therefore need the first-order correlation function at positive  $\tau$  to compute the power spectrum.

We consider the example of the Doppler-broadened spectral light source whose first-order correlation function is given by Eq. (4.3.13). The power spectrum for the light source, as computed from Eq. (4.3.14) is therefore equal to

$$S(\mathbf{r}, v) = \frac{\mathcal{E}_0^2 \tau_c}{\sqrt{2\pi}} \exp[-(v - v_0)^2 \tau_c^2 / 2]. \quad (4.3.15)$$

和相干性  
① 相位固定  
② 相位随机

-相干性和不相干性  
-相干性和非相干性

$$S(\mathbf{r}, v) = \frac{1}{\pi} \int_0^\infty d\tau G^{(1)}(\mathbf{r}, \mathbf{r}; \tau) e^{iv\tau}$$

例: 多普勒展宽

$$G^{(1)}(\mathbf{r}_1, \mathbf{r}_2, \tau) = \mathcal{E}_0^2 \exp(-iv_0\tau) \exp\left(-\frac{\tau^2}{2\tau_c^2}\right)$$

$$\Rightarrow S(\mathbf{r}, v) = \frac{\mathcal{E}_0^2 \tau_c}{\sqrt{2\pi}} \exp\left[-\frac{\tau_c^2(v - v_0)^2}{2}\right]$$

完全相干性

$$\langle E_1^{(+)} E_2^{(+)} \rangle$$

$$= \langle E_1^{(+)} \rangle \langle E_2^{(+)} \rangle e^{i\phi}$$

This is a Gaussian spectrum centered around  $\nu = \nu_0$  with a full-width at half-maximum equal to  $2\sqrt{2\ln 2}/\tau_c$ . Thus  $1/\tau_c$ , which is the inverse of the coherence time of the light field, is a measure of the light bandwidth.

一个光子的几率  
幅，自己与自己干涉

### 4.3.2 Young's experiment with light from two atoms\*

Consider the Young-type experiment shown in Fig. 4.8. There we see two atoms at locations  $S$  and  $S'$ . At  $t = 0$  both atoms are allowed to interact with a single photon, designated by  $|\phi\rangle$ , and one or other of the atoms may be excited. In this way we prepare the state

$$\alpha(|a, b'\rangle + |b, a'\rangle)|0\rangle + \beta|b, b'\rangle|\phi\rangle, \quad (4.3.16)$$

where  $|a\rangle$ ,  $|b\rangle$ , and  $|a'\rangle$ ,  $|b'\rangle$  denote the excited and ground states of atoms at  $S$  and  $S'$ , and  $\alpha$  and  $\beta$  are the probability amplitudes for the states associated with excited and ground state atoms, respectively. Thus, with a probability  $|\alpha|^2$  we have prepared the state

$$|\psi(0)\rangle = \frac{1}{\sqrt{2}}(|a, b'\rangle + |b, a'\rangle)|0\rangle \quad (4.3.17)$$

by single-photon absorption. Later in time, this state will decay into the state

$$|\psi(\infty)\rangle = \frac{1}{\sqrt{2}}|b, b'\rangle(|\gamma\rangle + |\gamma'\rangle), \quad (4.3.18)$$

where  $|\gamma\rangle$  and  $|\gamma'\rangle$  denote the photon states associated with emission from sites  $S$  and  $S'$ . For present purposes, it will suffice to take  $|\gamma\rangle$  and  $|\gamma'\rangle$  as plane wave states  $|1_k\rangle$  and  $|1_{k'}\rangle$  where  $\mathbf{k}/k$  and  $\mathbf{k}'/k'$  are the unit vectors from  $S$  and  $S'$  to the detectors at  $\mathbf{r}$ , see Fig. 4.8. However, the question of how to most simply choose the states  $|\gamma\rangle$  and  $|\gamma'\rangle$  while still being faithful to the physics is an important and subtle one, and is treated in Appendix 4.A.\*

The correlation function  $G^{(1)}(\mathbf{r}, \mathbf{r}; t, t)$  now takes the form

$$G^{(1)}(\mathbf{r}, \mathbf{r}; t, t) = \langle \psi(\infty) | E^{(-)}(\mathbf{r}) E^{(+)}(\mathbf{r}) | \psi(\infty) \rangle = G^{(1)}(\mathbf{r}, \mathbf{r}; 0),$$

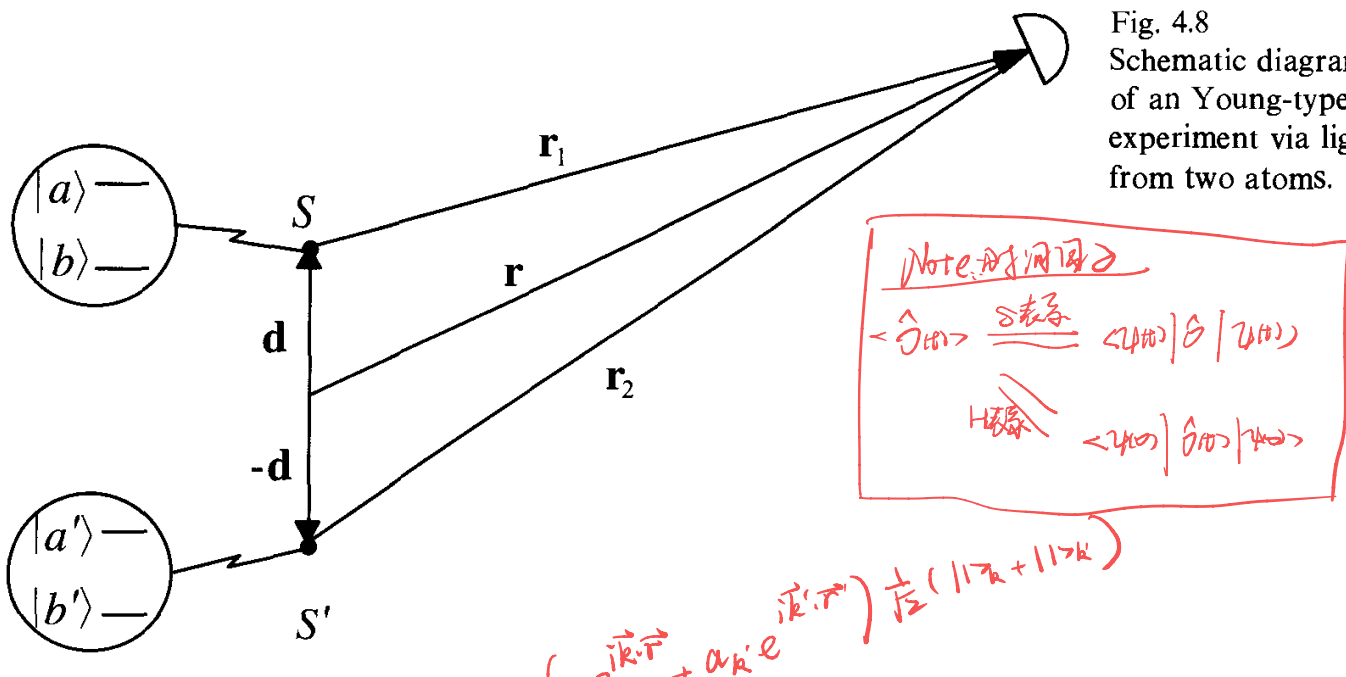
$\uparrow$   
 $\downarrow$   
 $\text{cancel}$

$$(4.3.19)$$

where we have noted that the time-dependent factors cancel because  $\nu_k = \nu_{k'}$ . By completeness as in Eq. (1.5.16), this may be written as

$$G^{(1)}(\mathbf{r}, \mathbf{r}; 0) = \Psi_{\mathcal{E}}^*(\mathbf{r}) \Psi_{\mathcal{E}}(\mathbf{r}), \quad (4.3.20)$$

\* See Scully and Drühl, *Phys. Rev. A* **25**, 2208 (1982).



where

$$\begin{aligned}\Psi_{\text{e}}(\mathbf{r}) &= \langle 0 | E^{(+)}(\mathbf{r}) | \psi(\infty) \rangle \\ &= \frac{\mathcal{E}_k}{\sqrt{2}} (e^{i\mathbf{k} \cdot \mathbf{r}} + e^{i\mathbf{k}' \cdot \mathbf{r}}).\end{aligned}\quad (4.3.21)$$

Thus we see that an interference pattern is obtained which is governed by

$$G^{(1)}(\mathbf{r}, \mathbf{r}; 0) = \mathcal{E}_k^2 \{ 1 + \cos[(\mathbf{k} - \mathbf{k}') \cdot \mathbf{r}] \}, \quad (4.3.22)$$

and as is discussed in Appendix 4.A, this can be written as

$$\begin{aligned}G^{(1)}(\mathbf{r}, \mathbf{r}; 0) &= \mathcal{E}_k^2 \left[ 1 + \cos \left( \frac{2k}{r} d \right) \right] \quad d \text{ 是两源间距} \\ &= \mathcal{E}_k^2 [1 + \cos(2kd/D)],\end{aligned}\quad (4.3.23)$$

which is the usual result.

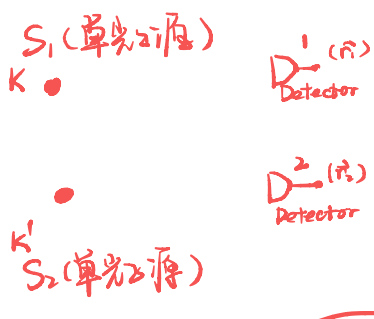
#### 4.4 Second-order coherence

In the previous section we considered the first-order correlation functions and their properties. For fields with identical spectral properties, it is not possible to distinguish the nature of the light source from only the first-order correlation function. For example, a laser beam and the light generated by a conventional thermal source can both have the same first-order coherence properties. The same, however, is not true when we consider the second- and higher-order coherence properties of the light sources. We therefore turn to the applications of the second-order correlation functions of the field.

Fig. 4.8  
Schematic diagram of an Young-type experiment via light from two atoms.

完否?  
 楊拉克 光和電子云 → 一阶干涉  
 塞因斯頓 五十年來不得其解  
 費曼 描述✓ 解決X

物理



#### 4.4.1 The physics behind the Hanbury-Brown-Twiss effect

Armed with a theory of photoelectron correlations, we now return to the Hanbury-Brown-Twiss effect. Let us begin by considering the state  $|\psi\rangle = |1_{\mathbf{k}}, 1_{\mathbf{k}'}\rangle$ , i.e., the case of two independent photons one having momentum  $\mathbf{k}$  and one having momentum  $\mathbf{k}'$ . Now it is clear that the second-order correlation function may be written as

$$G^{(2)}(\mathbf{r}_1, \mathbf{r}_2; t, t) = \langle 1_{\mathbf{k}}, 1_{\mathbf{k}'} | E^{(-)}(\mathbf{r}_1, t) E^{(-)}(\mathbf{r}_2, t) E^{(+)}(\mathbf{r}_2, t) E^{(+)}(\mathbf{r}_1, t) | 1_{\mathbf{k}}, 1_{\mathbf{k}'} \rangle, \quad (4.4.1)$$

and using  $\sum_{\{n\}} |\{n\}\rangle \langle \{n\}| = 1$  this becomes

$$G^{(2)}(\mathbf{r}_1, \mathbf{r}_2; t, t) = \sum_{\{n\}} \langle 1_{\mathbf{k}}, 1_{\mathbf{k}'} | E^{(-)}(\mathbf{r}_1, t) E^{(-)}(\mathbf{r}_2, t) | \{n\} \rangle \times \langle \{n\} | E^{(+)}(\mathbf{r}_2, t) E^{(+)}(\mathbf{r}_1, t) | 1_{\mathbf{k}}, 1_{\mathbf{k}'} \rangle. \quad (4.4.2)$$

As  $|1_{\mathbf{k}}, 1_{\mathbf{k}'}\rangle$  is a two-photon state which is annihilated by  $E^{(+)}(\mathbf{r}_2, t)$   $E^{(+)}(\mathbf{r}_1, t)$ , only the  $|0\rangle\langle 0|$  term survives.

In view of the above, we see that for the case of two single photons we may write

$$G^{(2)}(\mathbf{r}_1, \mathbf{r}_2; t, t) = \Psi^{(2)*}(\mathbf{r}_1, \mathbf{r}_2; t, t) \Psi^{(2)}(\mathbf{r}_1, t; \mathbf{r}_2, t), \quad (4.4.3)$$

where

$$\Psi^{(2)}(\mathbf{r}_1, t; \mathbf{r}_2, t) = \langle 0 | E^{(+)}(\mathbf{r}_2, t) E^{(+)}(\mathbf{r}_1, t) | 1_{\mathbf{k}}, 1_{\mathbf{k}'} \rangle. \quad (4.4.4)$$

From

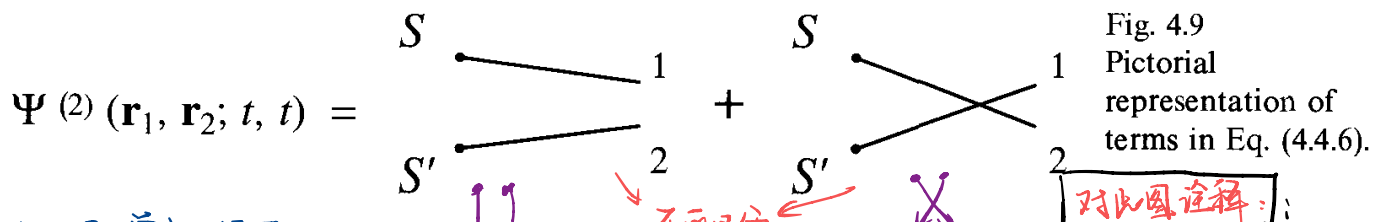
$$E^{(+)}(\mathbf{r}_i, t) = \mathcal{E}_{\mathbf{k}} \left( a_{\mathbf{k}} e^{-i\omega t + i\mathbf{k} \cdot \mathbf{r}_i} + a_{\mathbf{k}'}^* e^{-i\omega t + i\mathbf{k}' \cdot \mathbf{r}_i} \right) \quad (i = 1, 2), \quad (4.4.5)$$

these become

$$\begin{aligned} \Psi^{(2)}(\mathbf{r}_1, t; \mathbf{r}_2, t) &= \mathcal{E}_{\mathbf{k}}^2 e^{-2i\omega t} \langle 0 | a_{\mathbf{k}} e^{i\mathbf{k} \cdot \mathbf{r}_1} a_{\mathbf{k}'}^* e^{i\mathbf{k}' \cdot \mathbf{r}_2} | 1_{\mathbf{k}}, 1_{\mathbf{k}'} \rangle \\ &\quad + \mathcal{E}_{\mathbf{k}}^2 e^{-2i\omega t} \langle 0 | a_{\mathbf{k}'}^* e^{i\mathbf{k}' \cdot \mathbf{r}_1} a_{\mathbf{k}} e^{i\mathbf{k} \cdot \mathbf{r}_2} | 1_{\mathbf{k}}, 1_{\mathbf{k}'} \rangle \\ &= \mathcal{E}_{\mathbf{k}}^2 e^{-2i\omega t} \left( e^{i\mathbf{k} \cdot \mathbf{r}_1 + i\mathbf{k}' \cdot \mathbf{r}_2} + e^{i\mathbf{k}' \cdot \mathbf{r}_1 + i\mathbf{k} \cdot \mathbf{r}_2} \right), \end{aligned} \quad (4.4.6)$$

and

$$G^{(2)}(\mathbf{r}_1, \mathbf{r}_2; t, t) = 2\mathcal{E}_{\mathbf{k}}^4 \left\{ 1 + \cos[(\mathbf{k} - \mathbf{k}') \cdot (\mathbf{r}_1 - \mathbf{r}_2)] \right\}. \quad (4.4.7)$$



完全与HB-T的单光子相同.

### PHOTON-CORRELATION INTERFEROMETRY FROM TWO ATOMS

Consider next the case of two atoms at  $S$  and  $S'$  as in Fig. 4.9 in which both atoms are initially excited, that is,

$$|\psi(0)\rangle = |a, a'\rangle |0\rangle. \quad (4.4.8)$$

Then after many decay times this goes into

$$|\psi(\infty)\rangle = |b, b'\rangle |\gamma, \gamma'\rangle, \quad (4.4.9)$$

where, as in the previous section, we may take  $|\gamma\rangle = |1_{\mathbf{k}}\rangle$ ,  $|\gamma'\rangle = |1_{\mathbf{k}'}\rangle$ . The two-photon correlation function is then identical with that given by Eqs. (4.4.1) and (4.4.7).

Next we turn to incoherent atom excitation in order to display the real power of the HB-T effect. Specifically, suppose we excite the atoms at  $S$  and  $S'$  by electron impact. Then at some instant, call it  $t = 0$ , we will have a state of the form

$$|\psi(0)\rangle = [|\alpha| e^{i\varphi} |a, a'\rangle + |\beta| (e^{i\theta} |a, b'\rangle + e^{i\theta'} |b, a'\rangle) + |\gamma| |b, b'\rangle] \otimes |0\rangle, \quad (4.4.10)$$

which, see Appendix 4.A for a discussion of the spherical-versus plane-wave description of interference physics, evolves into

$$|\psi(\infty)\rangle = [|\alpha| e^{i\varphi} |1_{\mathbf{k}}, 1_{\mathbf{k}'}\rangle + |\beta| (e^{i\theta} |1_{\mathbf{k}}\rangle + e^{i\theta'} |1_{\mathbf{k}'}\rangle) + |\gamma| |0\rangle] \otimes |b, b'\rangle, \quad (4.4.11)$$

where  $\varphi$ ,  $\theta$ , and  $\theta'$  are random phases due, for example, to random excitation times of the atoms.

In such a case, the interference terms in the first-order correlation function will be multiplied by a random phase factor, which we must average over, that is

$$[G^{(1)}(\mathbf{r}, \mathbf{r}; t)]_{\text{interference cross terms}} \rightarrow \langle e^{-i(\theta-\theta')} \rangle e^{-i(\mathbf{k}-\mathbf{k}') \cdot \mathbf{r}}. \quad (4.4.12)$$

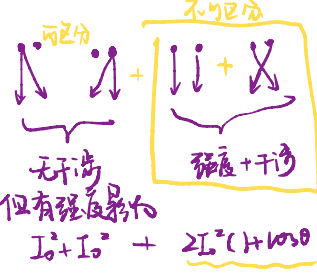
Fig. 4.9  
Pictorial representation of terms in Eq. (4.4.6).

对称注释:

这图不是一个光自己与自己干涉 (两种路径重合), 而是两个不同路径不可区分的状态干涉, 所以才有弱 (+6dB) 干涉 (两光子干涉)

但HB-T的干涉表达式与此略有不同, 因为HB-T不是单光子源, 而是量级.

探测器名探测到两个光子有四种可能:



总结一阶相关、频谱分布. (与光子数无关)  
二阶相关: 光子数的分布. (与光子数有关)  
(HB-T是光子数)

This vanishes due to the random nature of  $\theta$  and  $\theta'$ . Thus one might conclude that atoms described by Eq. (4.4.11) would never yield spatial interference. This is not the case. If we use Eq. (4.4.11) to calculate  $G^{(2)}(\mathbf{r}_1, \mathbf{r}_2; t, t)$ , we find

$$\begin{aligned} G^{(2)}(\mathbf{r}_1, \mathbf{r}_2; t, t) &= |\alpha|^2 \langle 1_{\mathbf{k}}, 1_{\mathbf{k}'} | E^{(-)}(\mathbf{r}_1) E^{(-)}(\mathbf{r}_2) E^{(+)}(\mathbf{r}_2) E^{(+)}(\mathbf{r}_1) | 1_{\mathbf{k}}, 1_{\mathbf{k}'} \rangle \\ &= 2|\alpha|^2 \mathcal{E}_{\mathbf{k}}^4 \{1 + \cos[(\mathbf{k} - \mathbf{k}') \cdot (\mathbf{r}_1 - \mathbf{r}_2)]\}. \end{aligned} \quad (4.4.13)$$

Here we see again that the random phases which destroy first-order coherence do not affect second-order HB-T type coherences.

### THE HANBURY-BROWN-TWISS EFFECT FOR THERMAL AND LASER LIGHT 热光场及激光

We now turn to the case of many-photon states associated with thermal and laser light and calculate the HB-T correlations for two such sources at  $S$  and  $S'$ .

As before, we look for the rate of coincidences in the photocount rates of detectors at  $\mathbf{r}_1$  and  $\mathbf{r}_2$  governed by the second-order correlation function

$$G^{(2)}(\mathbf{r}_1, \mathbf{r}_2; t, t) = \langle E^{(-)}(\mathbf{r}_1, t) E^{(-)}(\mathbf{r}_2, t) E^{(+)}(\mathbf{r}_2, t) E^{(+)}(\mathbf{r}_1, t) \rangle, \quad (4.4.14)$$

不能插  $|n>$  因为不是单光子，只是  $|0><0|$   
没有  $|1><1|$  ...

and consider the case in which the essential terms in the electric field operators  $E(\mathbf{r}_i, t)$  ( $i = 1, 2$ ) are given by

$$E^{(+)}(\mathbf{r}_i, t) = \mathcal{E}_{\mathbf{k}} \left( a_{\mathbf{k}} e^{-ivt+i\mathbf{k}\cdot\mathbf{r}_i} + a_{\mathbf{k}'}^{\dagger} e^{-ivt+i\mathbf{k}'\cdot\mathbf{r}_i} \right), \quad (4.4.15)$$

where  $\mathbf{k}$  and  $\mathbf{k}'$  are the wave vectors of light from the two sources  $S$  and  $S'$ . Furthermore, as before, we are considering only equal frequency intervals such that  $v = c|\mathbf{k}| = c|\mathbf{k}'|$ . Noting that only 'pairwise' operator orderings remain for thermal light, phase-diffused laser light, and light from two atoms (see Appendix 4.B), we have

热光场是时间相关的

??这个还要考虑

$$\begin{aligned} G^{(2)}(\mathbf{r}_1, \mathbf{r}_2; t, t) &= \mathcal{E}_{\mathbf{k}}^4 \langle (a_{\mathbf{k}}^{\dagger} e^{-i\mathbf{k}\cdot\mathbf{r}_1} + a_{\mathbf{k}'}^{\dagger} e^{-i\mathbf{k}'\cdot\mathbf{r}_1}) (a_{\mathbf{k}}^{\dagger} e^{-i\mathbf{k}\cdot\mathbf{r}_2} + a_{\mathbf{k}'}^{\dagger} e^{-i\mathbf{k}'\cdot\mathbf{r}_2}) \\ &\quad \times (a_{\mathbf{k}} e^{i\mathbf{k}\cdot\mathbf{r}_2} + a_{\mathbf{k}'} e^{i\mathbf{k}'\cdot\mathbf{r}_2}) (a_{\mathbf{k}} e^{i\mathbf{k}\cdot\mathbf{r}_1} + a_{\mathbf{k}'} e^{i\mathbf{k}'\cdot\mathbf{r}_1}) \rangle \\ &= \mathcal{E}_{\mathbf{k}}^4 \langle a_{\mathbf{k}}^{\dagger} a_{\mathbf{k}}^{\dagger} a_{\mathbf{k}} a_{\mathbf{k}} + a_{\mathbf{k}'}^{\dagger} a_{\mathbf{k}}^{\dagger} a_{\mathbf{k}'} a_{\mathbf{k}'} \\ &\quad + a_{\mathbf{k}}^{\dagger} a_{\mathbf{k}}^{\dagger} a_{\mathbf{k}} a_{\mathbf{k}'} [1 + e^{-i(\mathbf{k}-\mathbf{k}') \cdot (\mathbf{r}_1 - \mathbf{r}_2)}] \\ &\quad + a_{\mathbf{k}'}^{\dagger} a_{\mathbf{k}}^{\dagger} a_{\mathbf{k}'} a_{\mathbf{k}} [1 + e^{i(\mathbf{k}-\mathbf{k}') \cdot (\mathbf{r}_1 - \mathbf{r}_2)}] \rangle. \end{aligned} \quad (4.4.16)$$

16页

If we assume  $\langle n_{\mathbf{k}} \rangle = \langle n_{\mathbf{k}'} \rangle \equiv \langle n \rangle$  and likewise  $\langle n_{\mathbf{k}}^2 \rangle = \langle n_{\mathbf{k}'}^2 \rangle \equiv \langle n^2 \rangle$ , we may write Eq. (4.4.16) as

$$\begin{aligned} G^{(2)}(\mathbf{r}_1, \mathbf{r}_2; t, t) &= \langle a^\dagger a^\dagger a a \rangle = \langle n^2 \rangle - \langle n \rangle \\ &= 2\mathcal{E}_{\mathbf{k}}^4 (\langle n^2 \rangle - \langle n \rangle + \langle n \rangle^2 \{ 1 + \cos [(\mathbf{k} - \mathbf{k}') \cdot (\mathbf{r}_1 - \mathbf{r}_2)] \}). \end{aligned} \quad (4.4.17)$$

干涉可观察 = 光子统计

Next we calculate  $\langle n^2 \rangle$  for the two different cases in question: stars and phase-diffused laser light.

(a) Stars: the light from stars is thermal, therefore

thermal

$$\langle n^2 \rangle = 2\langle n \rangle^2 + \langle n \rangle, \quad \langle n \rangle = [\exp(\hbar\nu/k_B T) - 1]^{-1},$$

and Eq. (4.4.17) yields

$$\begin{aligned} G^{(2)}(\mathbf{r}_1, \mathbf{r}_2; t, t) &= 2\mathcal{E}_{\mathbf{k}}^4 (2\langle n \rangle^2 + \langle n \rangle^2 \{ 1 + \cos [(\mathbf{k} - \mathbf{k}') \cdot (\mathbf{r}_1 - \mathbf{r}_2)] \}). \end{aligned} \quad (4.4.18)$$

The last term in Eq. (4.4.18) is the Hanbury-Brown-Twiss term which allows us to measure the angle between  $\mathbf{k}$  and  $\mathbf{k}'$  as in the discussion following Eq. (4.1.24).

(c)  $|\mathbf{k}, \mathbf{k}'\rangle$

$$\Rightarrow \langle n^2 \rangle = \langle n \rangle$$

(b) Lasers: far above threshold, the photon statistics for the lasers are coherent Poissonian, therefore,  $\langle n^2 \rangle = \langle n \rangle^2 + \langle n \rangle$ , and we have

$$\begin{aligned} G^{(2)}(\mathbf{r}_1, \mathbf{r}_2; t, t) &= 2\mathcal{E}_{\mathbf{k}}^4 (\langle n \rangle^2 + \langle n \rangle^2 \{ 1 + \cos [(\mathbf{k} - \mathbf{k}') \cdot (\mathbf{r}_1 - \mathbf{r}_2)] \}). \end{aligned} \quad (4.4.19)$$

$$\Rightarrow \langle n^2 \rangle = \langle n \rangle^2 \{ 1 + \cos [(\mathbf{k} - \mathbf{k}') \cdot (\mathbf{r}_1 - \mathbf{r}_2)] \}$$

干涉可观察取决于光子统计  
二相干场：

相干场：  
干涉 干涉干涉强度。

So, in both cases, we can measure the angular separation without the troublesome  $\cos [(\mathbf{k} + \mathbf{k}') \cdot (\mathbf{r}_1 - \mathbf{r}_2)/2]$ -type terms which plague the Michelson stellar interferometer.

## THE HANBURY-BROWN-TWISS SPATIAL INTERFERENCE EFFECT FOR NEUTRONS

对易  $\Rightarrow$  反对易

By now, it is clear (contrary to what one frequently hears and reads) that the HB-T interference pattern, i.e., the interference cross terms in  $G^{(2)}(\mathbf{r}_1, \mathbf{r}_2)$ , has nothing to do with the boson nature of the photons. That is, the HB-T interference cross terms are present for radiation emitted by two independent atoms or lasers as shown in the previous two sections. In both of these cases, ‘boson clumping’ is absent.

Furthermore, it is clear from Eq. (4.4.4) and Fig. 4.9 that the effect carries over for neutrons as well. In such a case, the photon annihilation operators such as that given by Eq. (4.4.5) are replaced by a fermion operator of the form

↑  
測量  
真態

$$\hat{\psi}(\mathbf{r}_i, t) = c_{\mathbf{k}} e^{-i\omega t + i\mathbf{k} \cdot \mathbf{r}_i} + c_{\mathbf{k}'} e^{-i\omega t + i\mathbf{k}' \cdot \mathbf{r}_i}, \quad (4.4.20)$$

where the relevant fermion annihilation operators  $c_{\mathbf{k}}$  and  $c_{\mathbf{k}'}$  now obey the anticommutation relations

$$c_{\mathbf{k}} c_{\mathbf{k}'}^\dagger + c_{\mathbf{k}'}^\dagger c_{\mathbf{k}} = \delta_{\mathbf{k}, \mathbf{k}'}, \rightarrow [c_{\mathbf{k}}, c_{\mathbf{k}'}] = \delta_{\mathbf{k}, \mathbf{k}'} \quad (4.4.21)$$

$$c_{\mathbf{k}}^\dagger c_{\mathbf{k}'}^\dagger + c_{\mathbf{k}'}^\dagger c_{\mathbf{k}} = 0, \rightarrow [c_{\mathbf{k}'}^\dagger, c_{\mathbf{k}}] = 0 \quad (4.4.22)$$

$$c_{\mathbf{k}} c_{\mathbf{k}'} + c_{\mathbf{k}'} c_{\mathbf{k}} = 0. \rightarrow [c_{\mathbf{k}}, c_{\mathbf{k}'}] = 0 \quad (4.4.23)$$

Now Eq. (4.4.4) is replaced by the two-fermion wave function

$$\begin{aligned} \Psi^{(2)}(\mathbf{r}_1, t; \mathbf{r}_2, t) &= \langle 0 | \hat{\psi}(\mathbf{r}_2, t) \hat{\psi}(\mathbf{r}_1, t) | \psi \rangle \\ &= e^{-2i\omega t} \langle 0 | c_{\mathbf{k}} e^{i\mathbf{k} \cdot \mathbf{r}_2} c_{\mathbf{k}'} e^{i\mathbf{k}' \cdot \mathbf{r}_1} | 1_{\mathbf{k}}, 1_{\mathbf{k}'} \rangle \\ &\quad + e^{-2i\omega t} \langle 0 | c_{\mathbf{k}'} e^{i\mathbf{k}' \cdot \mathbf{r}_2} c_{\mathbf{k}} e^{i\mathbf{k} \cdot \mathbf{r}_1} | 1_{\mathbf{k}}, 1_{\mathbf{k}'} \rangle, \end{aligned} \quad (4.4.24)$$

and because

???

$$\begin{aligned} \langle 0 | c_{\mathbf{k}} c_{\mathbf{k}'} | 1_{\mathbf{k}}, 1_{\mathbf{k}'} \rangle &= \langle 0 | c_{\mathbf{k}} c_{\mathbf{k}'} c_{\mathbf{k}}^\dagger c_{\mathbf{k}'}^\dagger | 0 \rangle \\ &= -\langle 0 | c_{\mathbf{k}} c_{\mathbf{k}'}^\dagger | 0 \rangle \langle 0 | c_{\mathbf{k}'} c_{\mathbf{k}}^\dagger | 0 \rangle \\ &= -1, \end{aligned} \quad (4.4.25)$$

while an equivalent operator algebra for the second term in (4.4.24) yields +1, the fermion–fermion correlation function takes the form

二阶干涉  
光子数统计  
被泡探测  
二次量分析

$$G^{(2)}(\mathbf{r}_1, \mathbf{r}_2; t, t) = 2 \left\{ 1 - \cos[(\mathbf{k} - \mathbf{k}') \cdot (\mathbf{r}_1 - \mathbf{r}_2)] \right\}. \quad (4.4.26)$$

Thus we see that the Hanbury-Brown-Twiss effect works as well for two radiative point sources,  $S$  and  $S'$  of Fig. 4.9, emitting neutrons or  $\beta$  particles, as it does for  $\gamma$  rays or  $\alpha$  particles. The only difference is the sign of the interference term.

#### 4.4.2 Detection and measurement of squeezed states via homodyne detection

As seen earlier, direct photon count experiments, in which light of photon number distribution  $p(n)$  falls directly on a photodetector, provide information about the mean photon number and higher-order moments only. Such intensity measurements, therefore, are not particularly sensitive to squeezing but to antibunching and sub- or super-Poissonian statistics, which can also occur for nonsqueezed fields. Detection of squeezed states, on the other hand, requires a phase-sensitive scheme that measures the variance of a quadrature of the field. In this section, we consider the problem of detection of squeezed states of radiation via homodyne detection.

The schematic arrangement for homodyne detection is shown in

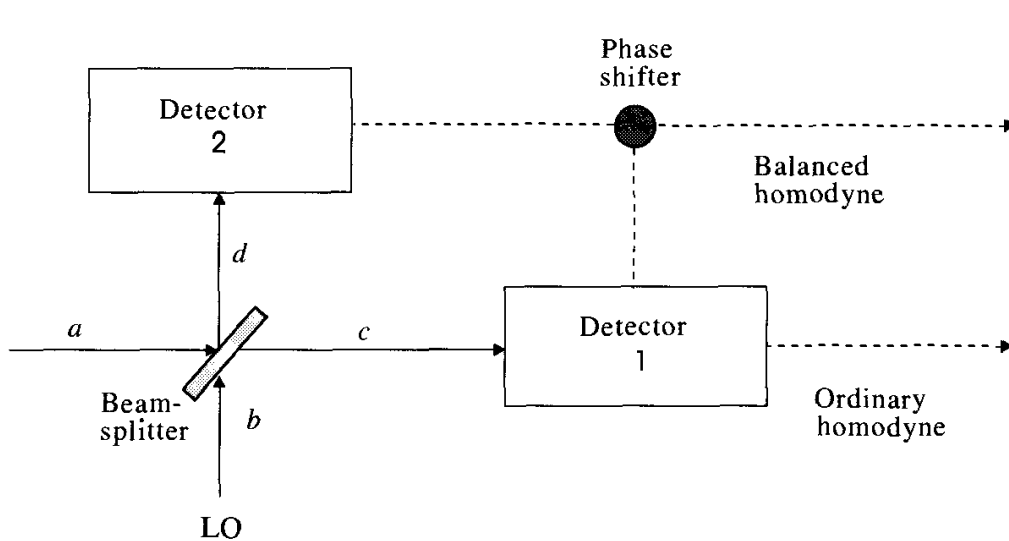


Fig. 4.10  
Schematic diagram  
for homodyne  
detection.

Fig. 4.10. The input field is superimposed on the field from a local oscillator (LO) at a lossless beam-splitter of transmissivity  $T$  and reflectivity  $R$  such that  $R + T = 1$ . The input and the oscillator modes are described by the annihilation operators  $a$  and  $b$ , respectively. Then denoting the two out-modes reaching photodetectors 1 and 2 by  $c$  and  $d$ , respectively, we have

$$c = \sqrt{T} a + i\sqrt{1-T} b, \quad (4.4.27)$$

$$d = i\sqrt{1-T} a + \sqrt{T} b. \quad (4.4.28)$$

There is a  $\pi/2$  phase shift between the reflected and the transmitted waves for a symmetric beam-splitter which we have included by the factor  $i$  in Eqs. (4.4.27) and (4.4.28). The signals measured by the two detectors are determined by the operators

$$c^\dagger c = T a^\dagger a + (1 - T) b^\dagger b + i\sqrt{T(1-T)}(a^\dagger b - b^\dagger a), \quad (4.4.29)$$

$$d^\dagger d = (1 - T) a^\dagger a + T b^\dagger b - i\sqrt{T(1-T)}(a^\dagger b - b^\dagger a). \quad (4.4.30)$$

The frequency of the LO is equal to the input frequency so that the above operators do not have any time dependence. In the following we discuss the ordinary and balanced homodyne detectors.

### ORDINARY HOMODYNE DETECTION

In ordinary homodyne detection, the transmissivity of the beam-splitter is close to unity, i.e.,

$$T \gg R, \quad (4.4.31)$$

and only the photocurrent from detector 1 is measured. The LO mode is excited into a large amplitude coherent state  $|\beta_l\rangle$  with phase  $\phi_l$ . From Eq. (4.4.29) the signal reaching detector 1 is obtained as

$$\langle c^\dagger c \rangle = T \langle a^\dagger a \rangle + (1-T)|\beta_l|^2 - 2\sqrt{T(1-T)}|\beta_l| \langle X(\phi_l + \pi/2) \rangle, \quad (4.4.32)$$

where

$$X(\phi) \equiv X_\phi = \frac{1}{2}(ae^{-i\phi} + a^\dagger e^{i\phi}). \quad (4.4.33)$$

We see that the signal contains the transmitted part of the input photons, reflected LO field, and most importantly, an interference term between the input field and the LO field. It is precisely this interference term that contains a quadrature of the input field depending upon the phase of the LO. In this detection scheme, a strong LO is used so that

$$(1-T)|\beta_l|^2 \gg T \langle a^\dagger a \rangle. \quad (4.4.34)$$

The inequalities (4.4.31) and (4.4.34) together imply that almost all the input field reaches the photodetector but the fraction of the LO field reaching the detector is still dominant. We can, therefore, neglect the first term in Eq. (4.4.32) and the mean number of photons in mode  $c$  is

$$\langle n_c \rangle = (1-T)|\beta_l|^2 - 2\sqrt{T(1-T)}|\beta_l| \langle X(\phi_l + \pi/2) \rangle. \quad (4.4.35)$$

The first term constitutes a known constant value which can be subtracted from the signal and the remaining signal contains the quadrature of the input only.

The input and the LO modes are independent, i.e.,  $\langle ab \rangle = \langle a \rangle \langle b \rangle$ . The photon number fluctuations can then be calculated in a straightforward manner using Eqs. (4.4.29) and (4.4.30)

$$(\Delta n_c)^2 = (1-T)|\beta_l|^2 \{(1-T) + 4T[\Delta X(\phi_l + \pi/2)]^2\}. \quad (4.4.36)$$

In obtaining Eq. (4.4.36), we have used the inequality (4.4.34) and retained terms of second order in  $|\beta_l|$ . The signal noise is now seen to contain reflected LO noise (first term) and the transmitted input quadrature noise (second term). When the input is incoherent (or vacuum),  $[\Delta X(\phi_l + \pi/2)]^2 = 1/4$ , and the remaining term represents the LO shot noise. The squeezing condition for the input is

$$[\Delta X(\phi_l + \pi/2)]^2 < 1/4 \quad (4.4.37)$$

for certain values of the LO phase  $\phi_l$  for which either quadrature  $X_1$  or  $X_2$  is squeezed.

In practice, the input is first blocked to determine the shot-noise level. The input is then allowed to reach the beam-splitter and the variance is determined with reference to the shot-noise level. Squeezing therefore manifests itself in sub-Poissonian statistics in homodyne detection.

Note, however, that intensity measurements in homodyne detection are quite different from those in direct detection, i.e., (a) intensity fluctuations in this case directly measure the fluctuations in a quadrature of the input, and (b) the signal and its variance depend upon the local oscillator phase angle, which is an external parameter.

### BALANCED HOMODYNE DETECTION

In the discussion following Eq. (4.4.35), we assumed a perfectly coherent LO field and the oscillator excess noise has been neglected. The LO shot noise and the excess noise that enter through the reflectivity of the beam-splitter cannot be suppressed in ordinary homodyne detection because  $T$ , in principle, can never be 1. The LO noise can therefore limit ordinary homodyne detection. In particular, the detection is not quantum limited if the transmitted input noise is smaller than the reflected oscillator noise, as may be the case when the input noise is too small.

An alternative scheme is based on two-port homodyne detection which balances the output from the two ports of the beam-splitter. The fact that the noninterference terms at the two ports have the same sign and the interference terms appear with opposite signs (see Eqs. (4.4.29) and (4.4.30)) can be exploited to completely eliminate the noninterference terms. In this scheme, a 50/50 beam-splitter is used and the difference of two photodetector measurements is obtained. The output signal is determined by the operator

$$n_{cd} = c^\dagger c - d^\dagger d = -i(a^\dagger b - b^\dagger a). \quad (4.4.38)$$

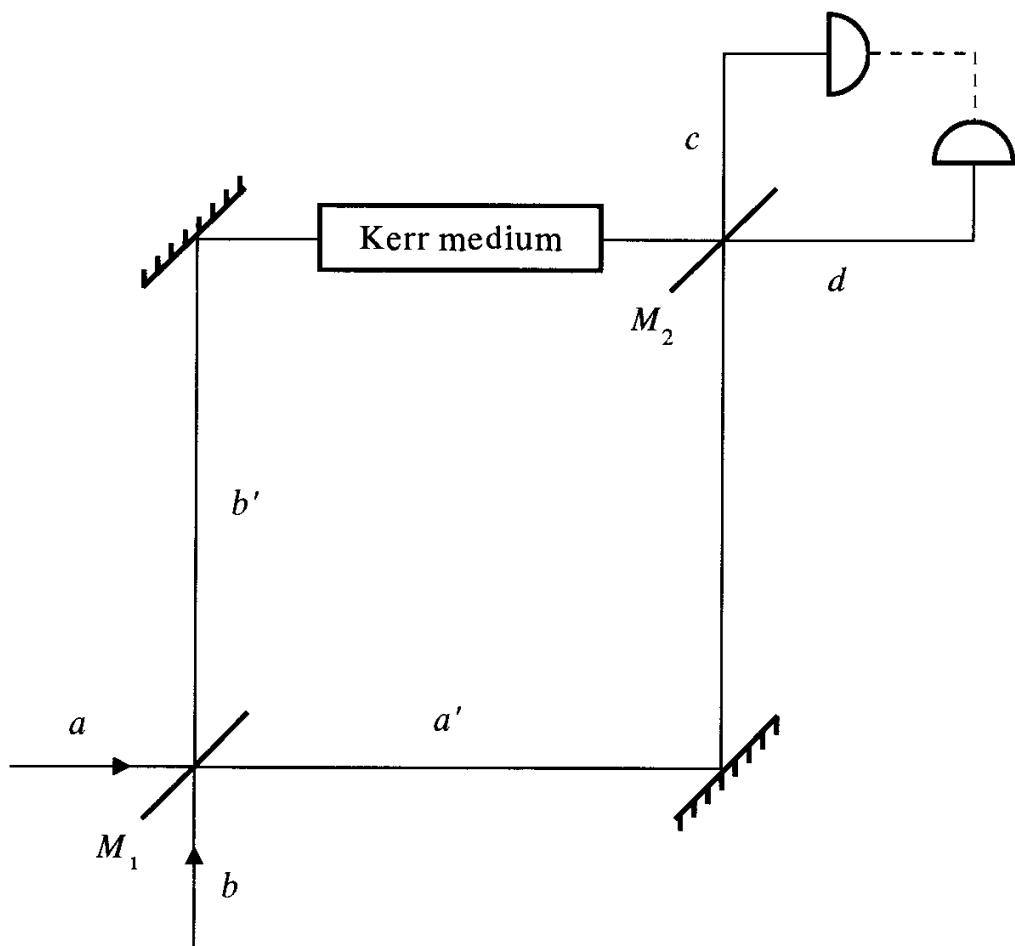
The measured signal then is

$$\langle n_{cd} \rangle = -2|\beta_l| \langle X(\phi_l + \pi/2) \rangle. \quad (4.4.39)$$

We see that the LO contribution to the signal has been eliminated and only the interference between the LO mean field and the input quadrature survives. The variance of the output signal can be found to be

$$(\Delta n_{cd})^2 = 4|\beta_l|^2 [\Delta X(\phi_l + \pi/2)]^2. \quad (4.4.40)$$

**Fig. 4.11**  
A Mach-Zehnder interferometer with a phase sensitive element in the upper arm operating in the balanced mode. The operators  $a$  and  $b$  are the annihilation operators for the signal and local oscillator modes.



Here once again we assume a strong LO. The dominant term now is only due to the interference between the input signal noise and the LO power, and the LO noise is eliminated completely. This makes the strong LO condition less stringent in this case.

#### MEASUREMENT OF PHASE UNCERTAINTY\*

The use of balanced homodyne detection in precision interferometry yields several interesting results. Here we discuss the application of balanced homodyne detection in the measurement of phase uncertainty of optical signals.

The system is depicted in Fig. 4.11, where we see a Mach-Zehnder interferometer with a phase sensitive element in the upper arm operating in the balanced mode. The phase sensitive element introduces a phase shift  $\phi_p$ , e.g., by a Kerr effect medium discussed in Section 19.2.

We assume  $M_1$  and  $M_2$  in Fig. 4.11 to be 50/50 beam-splitters

\* This section follows, in part, the unpublished lecture notes of B. Yurke, to whom the authors are indebted.

and assume the two path lengths between them to be equal. The annihilation operators of the various modes in Fig. 4.11 are related to each other via

$$a' = \frac{1}{\sqrt{2}}(a + ib), \quad (4.4.41)$$

$$b' = \frac{1}{\sqrt{2}}(ia + b), \quad (4.4.42)$$

and

$$\begin{aligned} c &= \frac{1}{\sqrt{2}}(a' + ib'e^{i\phi_p}) \\ &= \frac{1}{2}[(1 - e^{i\phi_p})a + i(1 + e^{i\phi_p})b], \end{aligned} \quad (4.4.43)$$

$$\begin{aligned} d &= \frac{1}{\sqrt{2}}(ia' + b'e^{i\phi_p}) \\ &= \frac{1}{2}[i(1 + e^{i\phi_p})a - (1 - e^{i\phi_p})b]. \end{aligned} \quad (4.4.44)$$

Here, as before, we assume a  $\pi/2$  phase shift for the reflected field.

The output signal in the balanced homodyne detector is given by the operator

$$\begin{aligned} n_{cd} &= c^\dagger c - d^\dagger d \\ &= (b^\dagger b - a^\dagger a) \cos \phi_p - (a^\dagger b + b^\dagger a) \sin \phi_p. \end{aligned} \quad (4.4.45)$$

If the local oscillator mode is in a large amplitude coherent state  $|\beta_l\rangle$  and the signal mode is in a vacuum state  $|0\rangle$ , the signal is

$$\langle n_{cd} \rangle = n_l \cos \phi_p, \quad (4.4.46)$$

where  $n_l = |\beta_l|^2$ .

It is interesting to note that, for  $\phi_p = \pi/2$ ,

$$n_{cd} = -(a^\dagger b + b^\dagger a), \quad (4.4.47)$$

i.e.,  $n_{cd}$  does not depend on the photon number operators and the system in Fig. 4.11 is essentially equivalent to a balanced homodyne detector of Fig. 4.10.

Now, for the signal mode in a vacuum state, the difference operator (4.4.47) has a variance

$$(\Delta n_{cd})^2 = |\beta_l|^2 = n_l. \quad (4.4.48)$$

This can be related to the phase error by noting that, from Eq. (4.4.46), we have

$$\frac{\partial \langle n_{cd} \rangle}{\partial \phi_p} = -n_l \sin \phi_p, \quad (4.4.49)$$

and, since on balance ( $\phi_p = \pi/2$ ),

$$\left| \frac{\partial \langle n_{cd} \rangle}{\partial \phi_p} \right| = n_l. \quad (4.4.50)$$

Hence the phase error is given by

$$\begin{aligned} \Delta\phi &= \frac{\Delta n_{cd}}{|\partial \langle n_{cd} \rangle / \partial \phi_p|} = \frac{\sqrt{n_l}}{n_l} \\ &= \frac{1}{\sqrt{n_l}}. \end{aligned} \quad (4.4.51)$$

If we now take the signal to be a squeezed vacuum state,  $|0, \xi\rangle$  with  $\xi = r \exp(i\theta)$ ,

$$\begin{aligned} \langle n_{cd} \rangle &= (n_l + \sinh^2 r) \cos \phi_p \\ &\cong n_l \cos \phi_p. \end{aligned} \quad (4.4.52)$$

On balance,  $\phi_p = \pi/2$ ,  $|\partial \langle n_{cd} \rangle / \partial \phi_p| = n_l$ , and

$$(\Delta n_{cd})^2 = n_l [\cosh 2r - \cos(\theta - 2\phi_l) \sinh 2r] + \sinh^2 r, \quad (4.4.53)$$

where we have used Eqs. (2.7.11)–(2.7.13). If we take  $\theta = 2\phi_l$ , Eq. (4.4.53) becomes

$$(\Delta n_{cd})^2 = n_l e^{-2r} + \sinh^2 r, \quad (4.4.54)$$

and, for  $n_l \gg 1$ , we may neglect the  $\sinh^2 r$  term in Eq. (4.4.54) to yield the reduced phase noise

$$\begin{aligned} \Delta\phi &= \frac{\Delta n_{cd}}{|\partial \langle n_{cd} \rangle / \partial \phi_p|} \\ &= \frac{e^{-r}}{\sqrt{n_l}}. \end{aligned} \quad (4.4.55)$$

HOM干擾

Hong - Ou - Mandel

#### 4.4.3 Interference of two photons

We now describe an experiment in which the joint probability for the detection of two photons at two points is measured as a function of the separation between the points. This two-photon interference experiment is an example of the intensity correlation experiment where the predictions of the quantum theoretical analysis are quite different from the corresponding predictions of the classical coherence theory. The experimental results agree with the predictions of the quantum coherence theory for the choice of parameters where the classical and quantum theories yield different results. The existence of nonclassical effects in two-photon interference is just one example of a large number of related phenomena where the quantum nature of light is exhibited

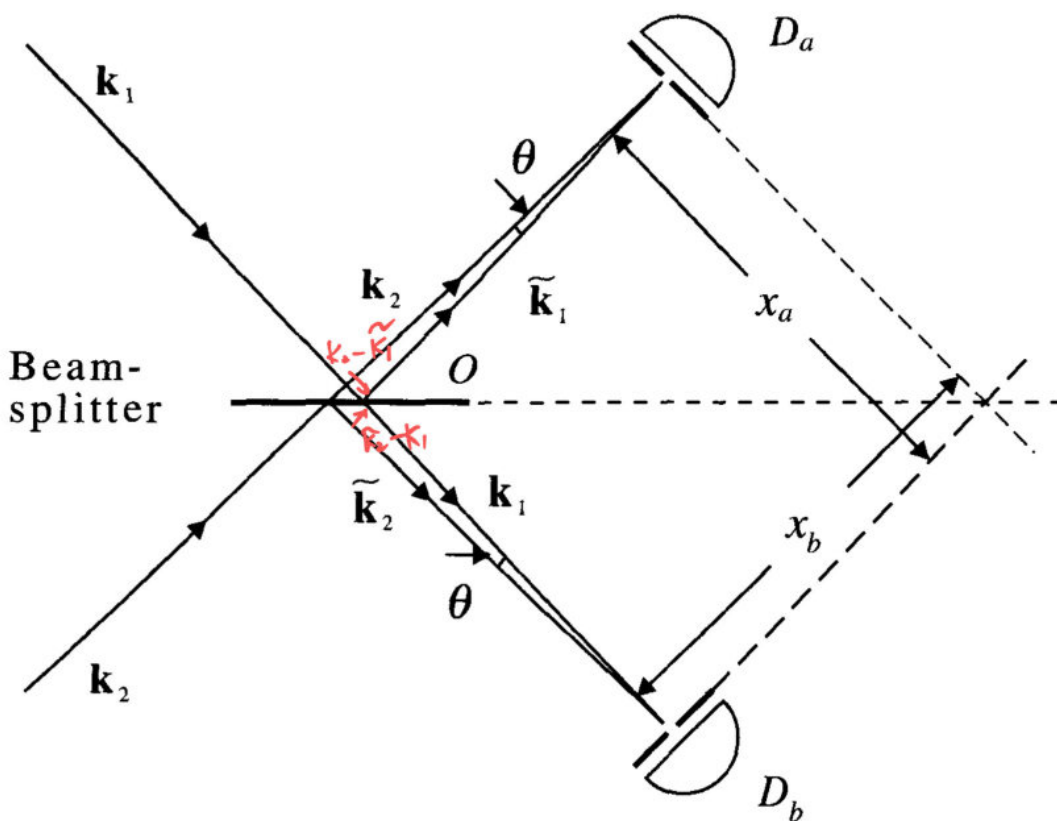


Fig. 4.12  
Schematic diagram for the two-photon interference experiment. (From Z. Y. Ou and L. Mandel, *Phys. Rev. Lett.* **62**, 2941 (1989).)

explicitly. Some of these phenomena will be discussed later in this book, particularly in Chapter 21.

In the two-photon interferometer, two randomly phased light waves of narrow bandwidth impinge simultaneously on the surface of a beam-splitter. The reflected and transmitted waves are brought together on the detectors  $D_a$  and  $D_b$  located at  $\mathbf{r}_a$  and  $\mathbf{r}_b$ , respectively, as shown in Fig. 4.12. The outputs, after amplification, are sent to a correlator. The measured coincidence rate provides a measure of the joint detection probability  $P(x_a, x_b)\delta x_a \delta x_b$  of detection at  $x_a$  and  $x_b$  within  $\delta x_a$  and  $\delta x_b$ , respectively. Here  $x_a$  and  $x_b$  are the projections of  $\mathbf{r}_a$  and  $\mathbf{r}_b$  onto the vectors  $\mathbf{k}_2 - \tilde{\mathbf{k}}_1$  and  $\mathbf{k}_2 - \tilde{\mathbf{k}}_1$ , respectively (see Fig. 4.12), where  $\mathbf{k}_1$ ,  $\mathbf{k}_2$  are the wave vectors corresponding to  $\mathbf{k}_1$ ,  $\mathbf{k}_2$  after reflection at the beam-splitter.

As discussed in Section 4.2, the joint detection probability is governed by  $w_2$ . We thus have

$$P(x_a, x_b) = \kappa_a \kappa_b \langle E^{(-)}(x_a) E^{(-)}(x_b) E^{(+)}(x_b) E^{(+)}(x_a) \rangle, \quad (4.4.56)$$

where  $\kappa_a$  and  $\kappa_b$  are factors which depend on the characteristics of the detectors. We now calculate the joint detection probability for incident correlated photons within the framework of both quantum and classical coherence theories.

If we treat  $O$  (see Fig. 4.12) as the origin, we can express the positive frequency part of the fields  $E^{(+)}(x_a)$  and  $E^{(+)}(x_b)$  in the form

$$E^{(+)}(x_a) = \mathcal{E} \left( i\sqrt{R}a_1 e^{i\tilde{\mathbf{k}}_1 \cdot \mathbf{r}_a} + \sqrt{T}a_2 e^{i\tilde{\mathbf{k}}_2 \cdot \mathbf{r}_a} \right), \quad (4.4.57)$$

$$E^{(+)}(x_b) = \mathcal{E} \left( \sqrt{T}a_1 e^{i\tilde{\mathbf{k}}_1 \cdot \mathbf{r}_b} + i\sqrt{R}a_2 e^{i\tilde{\mathbf{k}}_2 \cdot \mathbf{r}_b} \right), \quad (4.4.58)$$

where  $R$  and  $T$  are the reflectivity and the transmittivity of the beam-splitter,  $a_1$  and  $a_2$  are the destruction operators for the input fields at the beam-splitter, and  $\mathcal{E} = (\hbar v / 2\epsilon_0 V)^{1/2}$ . If the beam-splitter is 50/50, then  $R = T = 1/2$ . Equations (4.4.57) and (4.4.58) then simplify and are given in the form

$$E^{(+)}(x_a) = \frac{\mathcal{E}}{\sqrt{2}} (ia_1 e^{i\tilde{\mathbf{k}}_1 \cdot \mathbf{r}_a} + a_2 e^{i\tilde{\mathbf{k}}_2 \cdot \mathbf{r}_a}), \quad (4.4.59)$$

$$E^{(+)}(x_b) = \frac{\mathcal{E}}{\sqrt{2}} (a_1 e^{i\tilde{\mathbf{k}}_1 \cdot \mathbf{r}_b} + ia_2 e^{i\tilde{\mathbf{k}}_2 \cdot \mathbf{r}_b}). \quad (4.4.60)$$

The initial state of the field for single photons is the two-photon Fock state  $|1_1, 1_2\rangle$ . Such a state can be prepared in the process of degenerate parametric amplification in a nonlinear medium (Chapter 16). The joint detection probability density, Eq. (4.4.56), is therefore given by

$$\begin{aligned} P(x_a, x_b) &= \kappa_a \kappa_b \langle 1_1, 1_2 | E^{(-)}(x_a) E^{(-)}(x_b) E^{(+)}(x_b) E^{(+)}(x_a) | 1_1, 1_2 \rangle \\ &= \frac{1}{2} \kappa_a \kappa_b \mathcal{E}^4 \\ &\quad \{1 - \cos[(\mathbf{k}_2 - \tilde{\mathbf{k}}_1) \cdot \mathbf{r}_a - (\tilde{\mathbf{k}}_2 - \mathbf{k}_1) \cdot \mathbf{r}_b]\} \end{aligned} \quad (4.4.61)$$

where we have substituted for  $E^{(+)}(x_a)$  and  $E^{(+)}(x_b)$  and their Hermitian conjugates from Eqs. (4.4.59) and (4.4.60). If the angles  $\theta$  between  $\tilde{\mathbf{k}}_1$  and  $\mathbf{k}_2$  and between  $\tilde{\mathbf{k}}_2$  and  $\mathbf{k}_1$  are very small, then the associated interference pattern has a fringe spacing given by

$$L \approx \frac{2\pi}{|\tilde{\mathbf{k}}_1 - \mathbf{k}_2|} = \frac{2\pi}{|\tilde{\mathbf{k}}_2 - \mathbf{k}_1|} \approx \frac{2\pi}{k\theta}, \quad \text{red note: } \tilde{\mathbf{k}}_2 - \mathbf{k}_1 \approx \tilde{\mathbf{k}}_1 \text{ and } \tilde{\mathbf{k}}_2 \approx \mathbf{k}_2 \quad (4.4.62)$$

圆柱波有凹凸 where  $k = |\mathbf{k}_1| = |\mathbf{k}_2|$ , and we obtain (\vec{r}\_a - \vec{r}\_b) \hat{\mathbf{k}}\_a = x\_a - x\_b.

$$P(x_a, x_b) = \frac{1}{2} \kappa_a \kappa_b \mathcal{E}^4 \{1 - \cos[2\pi(x_a - x_b)/L]\}. \quad (4.4.63)$$

Thus the joint detection probability exhibits a cosine modulation in  $x_a - x_b$  with visibility

$$U = \frac{P_{\max} - P_{\min}}{P_{\max} + P_{\min}} = 1. \quad (4.4.64)$$

Therefore, there is an interference between two two-photon amplitudes associated with both photons being reflected and both photons being transmitted.

A unity visibility implies that if a photon is detected at the position  $x_a$  then there are certain positions  $x_b$  where the other photon cannot be found, and vice versa. This situation is in contrast to classical optics (as seen below) which predicts a nonvanishing optical field at both positions  $x_a$  and  $x_b$ .

Next we calculate the visibility by treating the incident fields classically. We can replace the operators  $a_1$  and  $a_2$  in Eqs. (4.4.59) and (4.4.60) by the classical  $c$ -number amplitudes  $\alpha_1$  and  $\alpha_2$ , respectively. We also assume that the fields have random phases. This is a reasonable assumption because the single-photon states have arbitrary phase. The classical ensemble averages of phase-dependent quantities, such as  $\alpha_1$  and  $|\alpha_1|^2\alpha_2$ , therefore vanish.

The joint detection probability  $P(x_a, x_b)$  is now given by Eq. (4.4.56) where  $E^{(+)}$  and  $E^{(-)}$  are classical  $c$ -number fields and the angle brackets indicate the classical ensemble average. It is readily seen that

$$P(x_a, x_b) = \frac{1}{4}\kappa_a\kappa_b\{\langle(I_1 + I_2)^2\rangle - 2\langle I_1 I_2 \rangle \cos[2\pi(x_a - x_b)/2]\}, \quad (4.4.65)$$

*二阶干涉:*

where  $I_1 = \mathcal{E}^2|\alpha_1|^2$  and  $I_2 = \mathcal{E}^2|\alpha_2|^2$ . The visibility  $U$  of the interference is given by

$$U = \frac{2\langle I_1 I_2 \rangle}{\langle I_1^2 \rangle + \langle I_2^2 \rangle + 2\langle I_1 I_2 \rangle}. \quad (4.4.66)$$

As  $\langle I_1^2 \rangle + \langle I_2^2 \rangle \geq 2\langle I_1 I_2 \rangle$ , it follows that

$$U \leq \frac{1}{2}, \quad (4.4.67)$$

which gives a classical limit. This shows that the visibility cannot exceed 50 percent in contradiction to the prediction of the quantum mechanical result.

An observation of a larger than 50 percent visibility therefore corresponds to nonclassical behavior. A visibility of over 75 percent has been observed in the two-photon interference experiments.

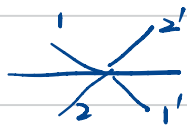
#### 4.4.4 Photon antibunching, Poissonian, and sub-Poissonian light

In Section 4.2 we showed that a correspondence between the quantum and classical coherence theories can be established via  $P$ -representation.

*经典教科书  
是二次量的结果，不能用经典方法完全解释。*

补充:

BS



多光子模型 - 干涉计算

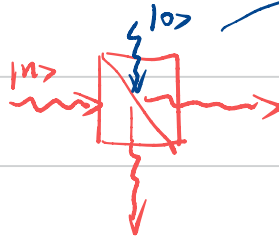
$$\text{半透半反 } \begin{pmatrix} a'_1 \\ a'_2 \end{pmatrix} = \frac{1}{\sqrt{2}} \begin{pmatrix} 1 & i \\ i & 1 \end{pmatrix} \begin{pmatrix} a_1 \\ a_2 \end{pmatrix}$$

$a$  是  $a^\dagger$  和  $a$ .

一般情形

$$\begin{pmatrix} a'_1 \\ a'_2 \end{pmatrix} = \begin{pmatrix} \sqrt{i}R & iI \\ iI & \sqrt{i}R \end{pmatrix} \begin{pmatrix} a_1 \\ a_2 \end{pmatrix}$$

8.4.22 中, Ketterle 提到



若是这样则要加上一次  $\text{tr}$ , 因为真空流动.

否则不足以完美解释一些现象

Therefore, there is an interference between two two-photon amplitudes associated with both photons being reflected and both photons being transmitted.

A unity visibility implies that if a photon is detected at the position  $x_a$  then there are certain positions  $x_b$  where the other photon cannot be found, and vice versa. This situation is in contrast to classical optics (as seen below) which predicts a nonvanishing optical field at both positions  $x_a$  and  $x_b$ .

Next we calculate the visibility by treating the incident fields classically. We can replace the operators  $a_1$  and  $a_2$  in Eqs. (4.4.59) and (4.4.60) by the classical  $c$ -number amplitudes  $\alpha_1$  and  $\alpha_2$ , respectively. We also assume that the fields have random phases. This is a reasonable assumption because the single-photon states have arbitrary phase. The classical ensemble averages of phase-dependent quantities, such as  $\alpha_1$  and  $|\alpha_1|^2\alpha_2$ , therefore vanish.

The joint detection probability  $P(x_a, x_b)$  is now given by Eq. (4.4.56) where  $E^{(+)}$  and  $E^{(-)}$  are classical  $c$ -number fields and the angle brackets indicate the classical ensemble average. It is readily seen that

$$P(x_a, x_b) = \frac{1}{4}\kappa_a\kappa_b\{\langle(I_1 + I_2)^2\rangle - 2\langle I_1 I_2 \rangle \cos[2\pi(x_a - x_b)/2]\}, \quad (4.4.65)$$

二阶干涉:

where  $I_1 = \mathcal{E}^2|\alpha_1|^2$  and  $I_2 = \mathcal{E}^2|\alpha_2|^2$ . The visibility  $U$  of the interference is given by

$$U = \frac{2\langle I_1 I_2 \rangle}{\langle I_1^2 \rangle + \langle I_2^2 \rangle + 2\langle I_1 I_2 \rangle}. \quad (4.4.66)$$

经典极限

• 是二次量的结果，不能用经典方法解释。

As  $\langle I_1^2 \rangle + \langle I_2^2 \rangle \geq 2\langle I_1 I_2 \rangle$ , it follows that

$$U \leq \frac{1}{2}, \quad (4.4.67)$$

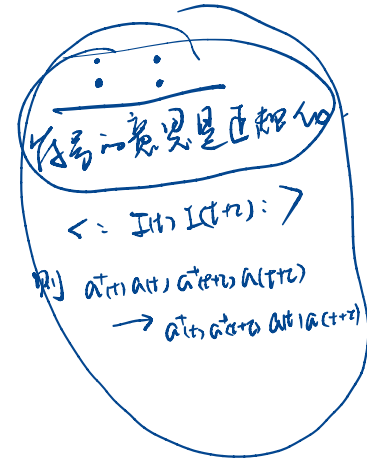
which gives a classical limit. This shows that the visibility cannot exceed 50 percent in contradiction to the prediction of the quantum mechanical result.

An observation of a larger than 50 percent visibility therefore corresponds to nonclassical behavior. A visibility of over 75 percent has been observed in the two-photon interference experiments.

#### 4.4.4 Photon antibunching, Poissonian, and sub-Poissonian light

非经典光，还有压低态（3个典型）

In Section 4.2 we showed that a correspondence between the quantum and classical coherence theories can be established via  $P$ -representation.



However, as we discussed, the  $P$ -representation does not have all the properties of a classical distribution function. Thus it is possible that certain inequalities for the correlation functions which implicitly assume a well-defined probability distribution may not be satisfied. A violation of these inequalities for certain radiation fields would therefore provide explicit evidence for the quantum nature of light. In this section we consider some examples of such fields.

In the classical coherence theory, the field operators are replaced by  $c$ -number fields. For such classical fields, it follows from the Schwarz inequality,  $|\langle a^* b \rangle|^2 \leq \langle |a|^2 \rangle \langle |b|^2 \rangle$  (with  $a = I(\mathbf{r}, t)$  and  $b = I(\mathbf{r}, t + \tau)$ ), that

$$|\langle I(\mathbf{r}, t)I(\mathbf{r}, t + \tau) \rangle|^2 \leq \langle I^2(\mathbf{r}, t) \rangle \langle I^2(\mathbf{r}, t + \tau) \rangle. \quad (4.4.68)$$

The corresponding inequality in the quantum coherence theory is obtained by replacing the product of intensities within the angle brackets by the corresponding normally ordered operators, i.e.,

$$|\langle :I(\mathbf{r}, t)I(\mathbf{r}, t + \tau): \rangle|^2 \leq \langle :I^2(\mathbf{r}, t): \rangle \langle :I^2(\mathbf{r}, t + \tau): \rangle, \quad (4.4.69)$$

where  $:$  represents normal ordering, i.e., the creation operators to the left and the annihilation operators to the right. This inequality is satisfied for fields with a well-defined  $P$ -representation. It follows from the definition of  $g^{(2)}(\tau)$  (Eq. (4.2.21)), that, for statistically stationary fields, this inequality can be recast in the following simple form

$$g^{(2)}(\tau) \leq g^{(2)}(0). \quad (4.4.70)$$

This inequality was seen to be satisfied by thermal and coherent light. We recall from the definition of  $g^{(2)}(\tau)$  that it is a measure of the photon correlations between some time  $t$  and a later time  $t + \tau$ . When the field satisfies the inequality  $g^{(2)}(\tau) < g^{(2)}(0)$  for  $\tau < \tau_c$ , the photons exhibit excess correlations for times less than the correlation time  $\tau_c$ . This is called *photon bunching* as the photons tend to distribute themselves preferentially in bunches rather than at random. When such a light beam falls on a photodetector, more photon pairs are detected close together than further apart (Fig. 4.13(a)). The thermal field is an example of photon bunching. 单光子源

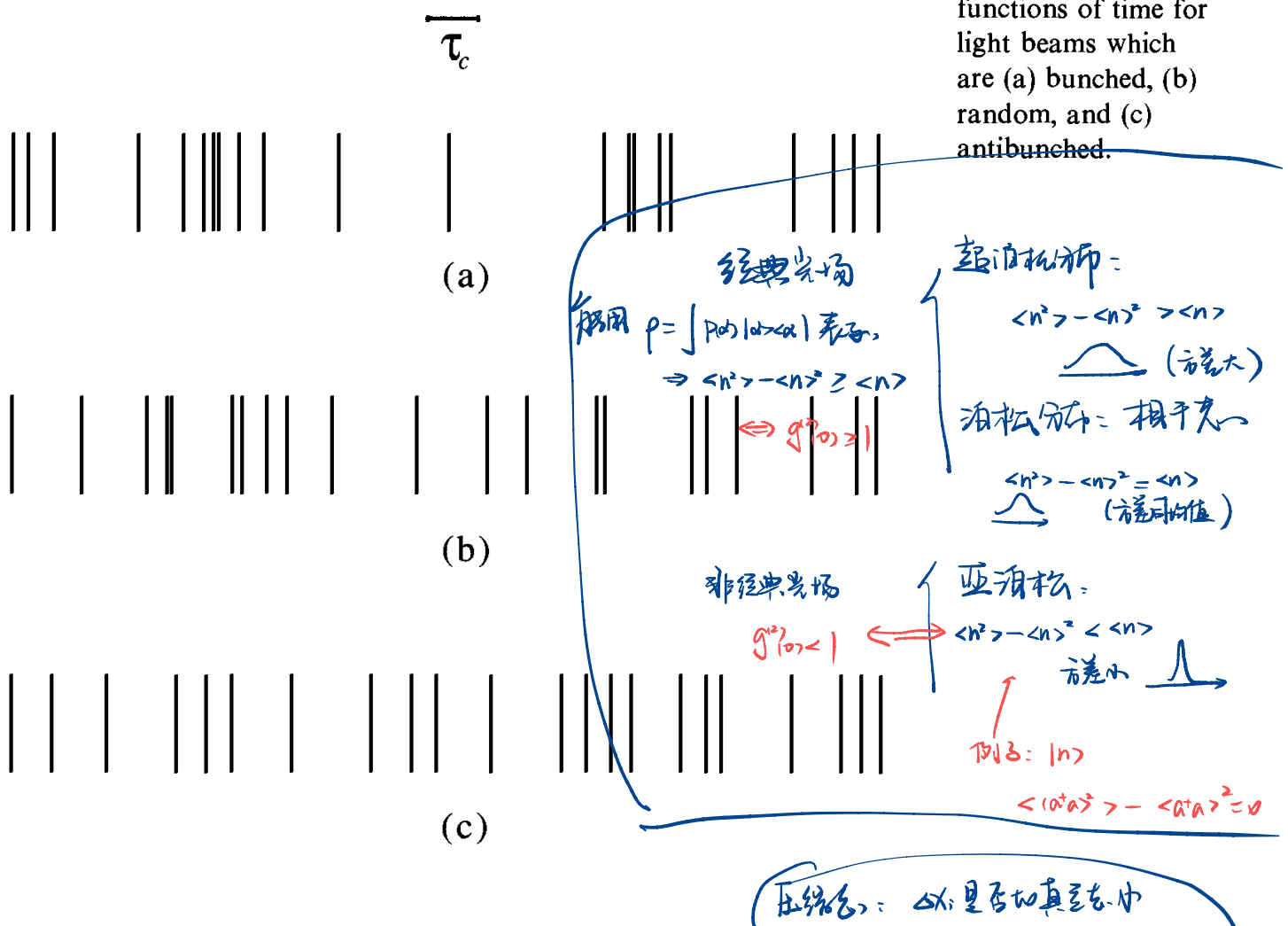
In certain quantum optical systems, the inequality (4.4.70) may be violated with the result

反聚束判据  $\rightarrow g^{(2)}(\tau) > g^{(2)}(0).$

反聚束  $g^{(2)}(\tau) > g^{(2)}(0) \rightarrow$  非经典光场  
聚束  $g^{(2)}(\tau) < g^{(2)}(0) \rightarrow$  经典光场  
随机  $g^{(2)}(\tau) = g^{(2)}(0)$

This would correspond to the phenomenon of *photon antibunching*. This is the opposite effect, in which fewer photon pairs are detected

相干度  $g^{(2)}(0) = g^{(2)}(0)$   
还是经典光场



close together than further apart (Fig. 4.13(c)). Photon antibunching will be discussed in the process of resonance fluorescence from an atom in Section 10.6.

Another nonclassical inequality is given by

$$g^{(2)}(0) < 1. \quad (4.4.72)$$

This nonclassical inequality is satisfied by fields whose  $P$ -representation is not nonnegative definite. To see this explicitly, we first rewrite this inequality, after some rearrangement, in the form (see Eq. (4.2.21))

$$(\langle a^\dagger a^\dagger a a \rangle - \langle a^\dagger a \rangle^2) < 0, \quad (4.4.73)$$

or, in terms of the  $P$ -representation,

$$\int P(\alpha, \alpha^*) (|\alpha|^2 - \langle a^\dagger a \rangle)^2 d^2\alpha < 0. \quad (4.4.74)$$

Since  $(|\alpha|^2 - \langle a^\dagger a \rangle)^2$  is positive definite for all values of  $\alpha$ , the only way this inequality may be satisfied is if  $P(\alpha, \alpha^*)$  is negative for at

least some values of  $\alpha$ . Thus  $P(\alpha, \alpha^*)$  does not satisfy the properties of a classical distribution function. The inequality (4.4.72) is satisfied by fields whose photon distribution function is narrower than the Poisson distribution. Such fields are referred to as *sub-Poissonian*. Fields for which  $g^{(2)}(0) = 1$  and  $g^{(2)}(0) > 1$  are similarly referred to as *Poissonian* and *super-Poissonian*, respectively. For example, a thermal field for which  $g^{(2)}(0) = 2$  is super-Poissonian, a field in a coherent state  $|\alpha_0\rangle$  for which  $g^{(2)}(0) = 1$  is Poissonian, and the field in a number state  $|n_0\rangle$  for which  $g^{(2)}(0) = 1 - 1/n_0$  is sub-Poissonian.

It is evident from the above discussion that many other field states can be constructed for which the  $P$ -representation will not be well-behaved. One such state is the squeezed state of the radiation field. To show this, we express  $(\Delta X_i)^2$  ( $i = 1, 2$ ) as an average with respect to the  $P$ -representation:

$$\begin{aligned} (\Delta X_i)^2 &= \frac{1}{4} + (: \Delta X_i :)^2 \\ &= \frac{1}{4} \left\{ 1 + \int d^2\alpha P(\alpha, \alpha^*) [(\alpha + \alpha^*) - (\langle \alpha \rangle + \langle \alpha^* \rangle)]^2 \right\}. \end{aligned} \quad (4.4.75)$$

The condition for squeezing  $(\Delta X_i)^2 < 1/4$  ( $i = 1$  or  $2$ ) requires that  $P(\alpha, \alpha^*)$  is negative for at least some values of  $\alpha$ , i.e., it is not “non-negative definite”. A squeezed state of the radiation field, therefore, is a nonclassical state.

## 4.5 Photon counting and photon statistics

In this section we determine the photoelectron counting statistics produced by a fully quantum mechanical field. The problem of obtaining the photocount distribution from the photon statistics can be solved in a completely quantum mechanical fashion. Here we give a simple derivation of this relationship based on a simple probabilistic argument.

Let the probability of having a photoelectron ejected from a detector interacting with a field having just one photon  $|1\rangle$  for a certain time be given by  $\eta$ . The *quantum efficiency*  $\eta$  depends on the characteristics of the detector atoms and the interaction time. Now, if the state of the radiation field is  $|n\rangle$ , the probability of observing  $m$  photoelectrons,  $P_m^{(n)}$ , is proportional to  $\eta^m$  which is to be multiplied by the probability that  $(n - m)$  quanta were not absorbed, i.e.,  $(1 - \eta)^{n-m}$ . This gives

$$P_m^{(n)} \propto \eta^m (1 - \eta)^{n-m}. \quad (4.5.1)$$

However, we do not know which  $m$  photons of the original number  $n$  were absorbed, so we must include a combinatorial factor:

$$P_m^{(n)} = \binom{n}{m} \eta^m (1 - \eta)^{n-m}. \quad (4.5.2)$$

只考虑吸收 < 1. 不考虑

暗背景

This is Bernoulli's distribution for  $m$  successful events (counts) and  $n - m$  failures, each event having a probability  $\eta$ . Since we have a distribution of  $n$  values given by the photon distribution function  $\rho_{nn}$ , we must multiply Eq. (4.5.2) by  $\rho_{nn}$  and sum over  $n$ :

$$P_m = \sum_n P_m^{(n)} \rho_{nn}, \quad (4.5.3)$$

which yields the following expression for the photoelectron counting distribution:

$$P_m = \sum_{n=m}^{\infty} \binom{n}{m} \eta^m (1 - \eta)^{n-m} \rho_{nn}. \quad (4.5.4)$$

This expression is valid for all  $\eta$  ( $0 \leq \eta \leq 1$ ). Clearly, if we wish to obtain the photon statistics by counting photoelectrons, we must require  $\eta = 1$ . In that case, we obtain from Eq. (4.5.4)

$$P_m = \rho_{mm}. \quad (4.5.5)$$

In all other cases,  $\eta < 1$ , and the measured photoelectron statistics can be very different from the photon statistics.

Alternatively, we can write  $P_m$  in terms of the  $P$ -representation,  $P(\alpha, \alpha^*)$ , of the field by noting that

$$\rho_{nn} = \int d^2\alpha P(\alpha, \alpha^*) \frac{|\alpha|^{2n}}{n!} e^{-|\alpha|^2}, \quad (4.5.6)$$

so that Eq. (4.5.4) becomes

$$P_m = \int d^2\alpha \sum_{n=m}^{\infty} \binom{n}{m} P(\alpha, \alpha^*) \frac{|\alpha|^{2n}}{n!} e^{-|\alpha|^2} \eta^m (1 - \eta)^{n-m}. \quad (4.5.7)$$

By changing  $n$  to  $\ell + m$  and summing over  $\ell$ , we obtain

$$P_m = \int d^2\alpha P(\alpha, \alpha^*) \frac{(\eta|\alpha|^2)^m}{m!} e^{-\eta|\alpha|^2}. \quad (4.5.8)$$

It may be pointed out that this equation can be inverted, i.e., it is possible to derive the  $P$ -representation of the field from the knowledge of  $P_m$ , given that  $\rho$  is diagonal in the  $n$  representation.

## 4.A Classical and quantum descriptions of two-source interference

Classically, the radiation from the two slits in Young's experiment is correctly described by two spherical waves. In the notation of Fig. 4.14, the intensity at the screen then goes as

$$I(\mathbf{r}) = \left| \frac{\mathcal{E}e^{ikr_1}}{r_1} + \frac{\mathcal{E}e^{ikr_2}}{r_2} \right|^2, \quad (4.A.1)$$

and the interference cross term is given by

$$I_{12} = \frac{\mathcal{E}^* \mathcal{E}}{r_1 r_2} e^{ik(r_1 - r_2)} + \text{c.c.} \quad (4.A.2)$$

Noting that  $r_{1,2} = \sqrt{D^2 + (x \mp d)^2} \cong D + d^2/(2D) \mp xd/D$ , where the ‘−’ goes with source 1 and the ‘+’ with source 2, we have

$$I_{12} \cong \frac{\mathcal{E}^* \mathcal{E}}{r^2} e^{-2ikxd/D} + \text{c.c.} \quad (4.A.3)$$

However, some texts give a plane-wave treatment of Young's setup, in which it is argued that the radiation at the detector site  $\mathbf{r}$  consists of two plane waves. In such a case, we have

$$I(\mathbf{r}) = |\mathcal{E}_0 e^{\mathbf{k}_1 \cdot \mathbf{r}} + \mathcal{E}_0 e^{\mathbf{k}_2 \cdot \mathbf{r}}|^2, \quad (4.A.4)$$

and the interference cross term is

$$I_{12}(\mathbf{r}) = \mathcal{E}_0^* \mathcal{E}_0 e^{i(\mathbf{k}_1 - \mathbf{k}_2) \cdot \mathbf{r}} + \text{c.c.} \quad (4.A.5)$$

Hence if, in the notation of Fig. 4.14, we write  $\mathbf{k}_i = k(\hat{z} \cos \theta_i + \hat{x} \sin \theta_i)$ , then  $\mathbf{k}_i \cdot \mathbf{r} = k(D \cos \theta_i + x \sin \theta_i) \cong k(D \mp xd/D)$ , where the ‘−’ signs go with 1 and 2, and we find

$$I_{12}(\mathbf{r}) \cong \mathcal{E}_0^* \mathcal{E}_0 e^{-2ikxd/D} + \text{c.c.}, \quad (4.A.6)$$

in agreement with the spherical-wave treatment.

The quantum field theoretic description of Young's experiment is well illustrated by replacing the two slits by two atoms as in Section 4.3.2 and Section 21.1. There the state vector for the photon emitted by the  $i$ th atom is given by

$$|\gamma_i\rangle = \sum_{\mathbf{k}} \frac{g_{\mathbf{k}} e^{-i\mathbf{k} \cdot \mathbf{d}_i}}{(v_{\mathbf{k}} - \omega) + i\Gamma/2} |1_{\mathbf{k}}\rangle, \quad (4.A.7)$$

where  $g_{\mathbf{k}}$  is a constant depending on the strength of atom-field coupling,  $\omega$  is the atomic frequency between levels  $|a\rangle$  and  $|b\rangle$ ,  $\Gamma$  is the

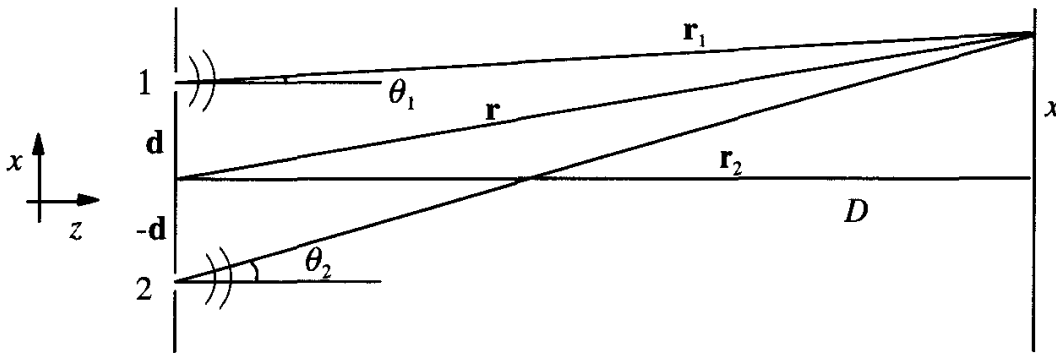


Fig. 4.14  
Schematic diagram for a plane-wave treatment of Young's setup.

decay rate for the  $|a\rangle \rightarrow |b\rangle$  transition, and  $\mathbf{d}_i$  is the position of the  $i$ th atom. The correlation function for the scattered field is then found to be

$$\begin{aligned} G^{(1)}(\mathbf{r}, \mathbf{r}; 0) &= \frac{1}{2} \left| \langle 0 | E^{(+)}(\mathbf{r}, t) | \gamma_1 \rangle + \langle 0 | E^{(+)}(\mathbf{r}, t) | \gamma_2 \rangle \right|^2 \\ &= \left| \frac{\tilde{\mathcal{E}} e^{i k r_1}}{r_1} + \frac{\tilde{\mathcal{E}} e^{i k r_2}}{r_2} \right|^2, \end{aligned} \quad (4.A.8)$$

where  $\tilde{\mathcal{E}}$  is an effective electric field. Thus we have the same result as in the classical spherical-wave problem.

Finally, we note that single photon plane-wave states can be used to demonstrate the two-source interference fringes. At the risk of belaboring the obvious, we note that if we consider the radiation from source 1 to be described by the single photon state  $|1_{\mathbf{k}_1}\rangle$ , and that from source 2 by  $|1_{\mathbf{k}_2}\rangle$ , then we have  $|\psi\rangle = (|1_{\mathbf{k}_1}\rangle + |1_{\mathbf{k}_2}\rangle)/\sqrt{2}$  and

$$\begin{aligned} G^{(1)}(\mathbf{r}, \mathbf{r}; 0) &= \langle \psi | E^{(-)}(\mathbf{r}, t) E^{(+)}(\mathbf{r}, t) | \psi \rangle \\ &= \frac{1}{2} \left| \langle 0 | E^{(+)}(\mathbf{r}, t) | 1_{\mathbf{k}_1} \rangle + \langle 0 | E^{(+)}(\mathbf{r}, t) | 1_{\mathbf{k}_2} \rangle \right|^2 \\ &= \mathcal{E}_0^* \mathcal{E}_0 \left| e^{i \mathbf{k}_1 \cdot \mathbf{r}} + e^{i \mathbf{k}_2 \cdot \mathbf{r}} \right|^2. \end{aligned} \quad (4.A.9)$$

Here again, interference is observed as in the classical case, and the utilization of both states  $|\gamma_i\rangle$  and  $|1_{\mathbf{k}_i}\rangle$  in Young-type experiments is justified.

## 4.B Calculation of the second-order correlation function

From Eqs. (4.4.14) and (4.4.15), we have (note that some terms are underlined)

$$\begin{aligned}
G^{(2)}(\mathbf{r}_1, \mathbf{r}_2; t, t) &= \mathcal{E}_{\mathbf{k}}^4 \langle [a_{\mathbf{k}}^\dagger(1) + a_{\mathbf{k}'}^\dagger(1)][a_{\mathbf{k}}^\dagger(2) + a_{\mathbf{k}'}^\dagger(2)][a_{\mathbf{k}}(2) + a_{\mathbf{k}'}(2)] \\
&\quad [a_{\mathbf{k}}(1) + a_{\mathbf{k}'}(1)] \rangle \\
&= \mathcal{E}_{\mathbf{k}}^4 \langle \underline{a_{\mathbf{k}}^\dagger(1)a_{\mathbf{k}}^\dagger(2)a_{\mathbf{k}}(2)a_{\mathbf{k}}(1)} \\
&\quad + \underline{[a_{\mathbf{k}}^\dagger(1)a_{\mathbf{k}}^\dagger(2)a_{\mathbf{k}}(2)a_{\mathbf{k}'}(1) + a_{\mathbf{k}}^\dagger(1)a_{\mathbf{k}}^\dagger(2)a_{\mathbf{k}'}(2)a_{\mathbf{k}}(1)}} \\
&\quad + \underline{a_{\mathbf{k}}^\dagger(1)a_{\mathbf{k}}^\dagger(2)a_{\mathbf{k}'}(2)a_{\mathbf{k}'}(1)} \\
&\quad + \underline{a_{\mathbf{k}}^\dagger(1)a_{\mathbf{k}'}^\dagger(2)a_{\mathbf{k}}(2)a_{\mathbf{k}'}(1) + a_{\mathbf{k}}^\dagger(1)a_{\mathbf{k}'}^\dagger(2)a_{\mathbf{k}'}(2)a_{\mathbf{k}}(1)} \\
&\quad + \underline{[a_{\mathbf{k}}^\dagger(1)a_{\mathbf{k}'}^\dagger(2)a_{\mathbf{k}}(2)a_{\mathbf{k}}(1) + a_{\mathbf{k}}^\dagger(1)a_{\mathbf{k}'}^\dagger(2)a_{\mathbf{k}'}(2)a_{\mathbf{k}'}(1)]} \\
&\quad + \underline{a_{\mathbf{k}'}^\dagger(1)a_{\mathbf{k}}^\dagger(2)a_{\mathbf{k}}(2)a_{\mathbf{k}'}(1) + a_{\mathbf{k}'}^\dagger(1)a_{\mathbf{k}}^\dagger(2)a_{\mathbf{k}'}(2)a_{\mathbf{k}}(1)} \\
&\quad + \underline{[a_{\mathbf{k}'}^\dagger(1)a_{\mathbf{k}'}^\dagger(2)a_{\mathbf{k}}(2)a_{\mathbf{k}'}(1) + a_{\mathbf{k}'}^\dagger(1)a_{\mathbf{k}'}^\dagger(2)a_{\mathbf{k}'}(2)a_{\mathbf{k}'}(1)]} \\
&\quad + \underline{a_{\mathbf{k}'}^\dagger(1)a_{\mathbf{k}'}^\dagger(2)a_{\mathbf{k}'}(2)a_{\mathbf{k}'}(1)} \\
&\quad + \underline{[a_{\mathbf{k}'}^\dagger(1)a_{\mathbf{k}'}^\dagger(2)a_{\mathbf{k}}(2)a_{\mathbf{k}'}(1) + a_{\mathbf{k}'}^\dagger(1)a_{\mathbf{k}'}^\dagger(2)a_{\mathbf{k}'}(2)a_{\mathbf{k}}(1)]} \\
&\quad + \underline{a_{\mathbf{k}'}^\dagger(1)a_{\mathbf{k}'}^\dagger(2)a_{\mathbf{k}}(2)a_{\mathbf{k}}(1)]} \rangle, \tag{4.B.1}
\end{aligned}$$

where

$$\begin{aligned}
a_{\mathbf{k}}^\dagger(i) &= a_{\mathbf{k}}^\dagger e^{-i\mathbf{k}\cdot\mathbf{r}_i}, \\
a_{\mathbf{k}'}^\dagger(i) &= a_{\mathbf{k}'}^\dagger e^{-i\mathbf{k}'\cdot\mathbf{r}_i}. \tag{4.B.2}
\end{aligned}$$

Note that all the terms in square brackets for the final equation vanish when averaged for stars, phase-diffused lasers, thermal light, and atoms. Therefore, keeping only the underlined terms, we find

$$\begin{aligned}
G^{(2)}(\mathbf{r}_1, \mathbf{r}_2; t, t) &= \mathcal{E}_{\mathbf{k}}^4 \langle a_{\mathbf{k}}^\dagger a_{\mathbf{k}}^\dagger a_{\mathbf{k}} a_{\mathbf{k}} + a_{\mathbf{k}'}^\dagger a_{\mathbf{k}'}^\dagger a_{\mathbf{k}'} a_{\mathbf{k}'}' \\
&\quad + a_{\mathbf{k}}^\dagger a_{\mathbf{k}'}^\dagger a_{\mathbf{k}} a_{\mathbf{k}'} [1 + e^{-i(\mathbf{k}-\mathbf{k}')\cdot(\mathbf{r}_1-\mathbf{r}_2)}] \\
&\quad + a_{\mathbf{k}'}^\dagger a_{\mathbf{k}}^\dagger a_{\mathbf{k}'} a_{\mathbf{k}} [1 + e^{i(\mathbf{k}-\mathbf{k}')\cdot(\mathbf{r}_1-\mathbf{r}_2)}] \rangle. \tag{4.B.3}
\end{aligned}$$

## Problems

- 4.1** Show that the radiation field state which is a linear superposition of the vacuum state and a single photon state, i.e.,

$$|\psi\rangle = a_0|0\rangle + a_1|1\rangle,$$

where  $a_0$  and  $a_1$  are complex coefficients, is a nonclassical state.

- 4.2** Let  $m_n = \langle a^{\dagger n} a^n \rangle$  be the  $n$ th-order moment of the intensity variable. Consider the matrix defined by

$$\mathcal{M} = \begin{bmatrix} 1 & m_1 & m_2 \\ m_1 & m_2 & m_3 \\ m_2 & m_3 & m_4 \end{bmatrix}.$$

Show that for a classical  $P$ -representation  $\det \mathcal{M}$  must be positive definite. (Hint: see G. S. Agarwal and K. Tara, *Phys. Rev. A* **46**, 485 (1992).)

- 4.3** Consider a state described by the density operator

$$\rho = \mathcal{N} a^{\dagger m} e^{-\kappa a^\dagger a} a^m,$$

where  $\mathcal{N}$  is a normalization constant and  $\kappa = \hbar v / k_B T$ .

- (a) Show that it goes over to a Fock state if  $\kappa \rightarrow \infty$  and to a thermal state if  $\kappa \rightarrow 0$ .
- (b) Find  $g^{(2)}(0)$  and show that the photon statistics are sub-Poissonian if

$$\bar{n} < \sqrt{\frac{m}{m+1}},$$

where  $\bar{n} = [\exp(\kappa) - 1]^{-1}$ .

- 4.4** Find the photoelectron distribution function  $P_m$  for the coherent state  $|\alpha\rangle$ , the number state  $|n\rangle$ , and the single-mode thermal field at temperature  $T$ .

# Atom–field interaction – semiclassical theory

---

One of the simplest nontrivial problems involving the atom–field interaction is the coupling of a two-level atom with a single mode of the electromagnetic field. A two-level atom description is valid if the two atomic levels involved are resonant or nearly resonant with the driving field, while all other levels are highly detuned. Under certain realistic approximations, it is possible to reduce this problem to a form which can be solved exactly; allowing essential features of the atom–field interaction to be extracted.

In this chapter we present a semiclassical theory of the interaction of a single two-level atom with a single mode of the field in which the atom is treated as a quantum two-level system and the field is treated classically. A fully quantum mechanical theory will be presented in Chapter 6.

A two-level atom is formally analogous to a spin-1/2 system with two possible states. In the dipole approximation, when the field wavelength is larger than the atomic size, the atom–field interaction problem is mathematically equivalent to a spin-1/2 particle interacting with a time-dependent magnetic field. Just as the spin-1/2 system undergoes the so-called Rabi oscillations between the spin-up and spin-down states under the action of an oscillating magnetic field, the two-level atom also undergoes *optical* Rabi oscillations under the action of the driving electromagnetic field. These oscillations are damped if the atomic levels decay. An understanding of this simple model of the atom–field interaction enables us to consider more complicated problems involving an ensemble of atoms interacting with the field. Perhaps the most important

example of such a problem is the laser, which we discuss later in this chapter.\*

## 5.1 Atom–field interaction Hamiltonian

An electron of charge  $e$  and mass  $m$  interacting with an external electromagnetic field is described by a minimal-coupling Hamiltonian

$$\mathcal{H} = \frac{1}{2m} [\mathbf{p} - e\mathbf{A}(\mathbf{r}, t)]^2 + eU(\mathbf{r}, t) + V(r), \quad (5.1.1)$$

where  $\mathbf{p}$  is the canonical momentum operator,  $\mathbf{A}(\mathbf{r}, t)$  and  $U(\mathbf{r}, t)$  are the vector and scalar potentials of the external field, respectively, and  $V(r)$  is an electrostatic potential that is normally the atomic binding potential. In this section, we first derive this Hamiltonian from a gauge invariance point of view, before reducing it to a simple form suitable for describing the interaction of a two-level atom with the radiation field.

### 5.1.1 Local gauge (phase) invariance and minimal-coupling Hamiltonian

The motion of a free electron is described by the Schrödinger equation

$$\frac{-\hbar^2}{2m} \nabla^2 \psi = i\hbar \frac{\partial \psi}{\partial t}, \quad (5.1.2)$$

such that

$$P(\mathbf{r}, t) = |\psi(\mathbf{r}, t)|^2 \quad (5.1.3)$$

gives the probability density of finding an electron at position  $\mathbf{r}$  and time  $t$ . In Eq. (5.1.2), if  $\psi(\mathbf{r}, t)$  is a solution so is  $\psi_1(\mathbf{r}, t) = \psi(\mathbf{r}, t) \exp(i\chi)$  where  $\chi$  is an arbitrary constant phase. The probability density  $P(\mathbf{r}, t)$  would also remain unaffected by an arbitrary choice of  $\chi$ . Thus the choice of the phase of the wave function  $\psi(\mathbf{r}, t)$  is completely arbitrary, and two functions differing only by a constant phase factor represent the same physical state.

The situation is different, however, if the phase is allowed to vary *locally*, i.e. to be a function of space and time variables, i.e.,

$$\psi(\mathbf{r}, t) \rightarrow \psi(\mathbf{r}, t) e^{i\chi(\mathbf{r}, t)}. \quad (5.1.4)$$

\* The semiclassical theory of laser behavior as developed by the schools of Lamb and Haken (see Lamb [1963,1964] and Haken [1964]) are the pioneering treatments of the problem. Lamb begins from the coupled Maxwell–Schrödinger equations, while Haken and co-workers take a semiclassical (factorized) limit of quantum fields.



The probability  $P(\mathbf{r}, t)$  remains unaffected by this transformation, but the Schrödinger equation (5.1.2) is no longer satisfied. If we want to satisfy *local gauge (phase)* invariance, then the Schrödinger equation must be modified by adding new terms to Eq. (5.1.2)

$$\left\{ -\frac{\hbar^2}{2m} \left[ \nabla - i\frac{e}{\hbar} \mathbf{A}(\mathbf{r}, t) \right]^2 + eU(\mathbf{r}, t) \right\} \psi = i\hbar \frac{\partial \psi}{\partial t}, \quad (5.1.5)$$

where  $\mathbf{A}(\mathbf{r}, t)$  and  $U(\mathbf{r}, t)$  are functions which must be inserted into (5.1.2) if we want to be able to make the transformation (5.1.4), and are given by

*电场场强和相位已变换后*

*全空间相位变了 e<sup>iχ(r,t)</sup>*

*仍满足 Schrödinger 方程*

$$\mathbf{A}(\mathbf{r}, t) \rightarrow \mathbf{A}(\mathbf{r}, t) + \frac{\hbar}{e} \nabla \chi(\mathbf{r}, t), \quad (5.1.6)$$

$$U(\mathbf{r}, t) \rightarrow U(\mathbf{r}, t) - \frac{\hbar}{e} \frac{\partial \chi}{\partial t}(\mathbf{r}, t). \quad (5.1.7)$$

The functions  $\mathbf{A}(\mathbf{r}, t)$  and  $U(\mathbf{r}, t)$  are identified as the vector and scalar potentials of the electromagnetic field, respectively. These are the gauge-dependent potentials. The gauge-independent quantities are the electric and magnetic fields

$$\mathbf{E} = -\nabla U - \frac{\partial \mathbf{A}}{\partial t}, \quad (5.1.8)$$

$$\mathbf{B} = \nabla \times \mathbf{A}. \quad (5.1.9)$$

Equation (5.1.5), which is the logical extension of Eq. (5.1.2) due to the requirement of local gauge (phase) invariance, has the form

$$\mathcal{H}\psi = i\hbar \frac{\partial \psi}{\partial t}, \quad (5.1.10)$$

with  $\mathcal{H}$  being the minimal-coupling Hamiltonian (recall  $\mathbf{p} = -i\hbar \nabla$ ) described in Eq. (5.1.1). The Schrödinger equation (5.1.5) represents the interaction of an electron with a given electromagnetic field. The electrons are described by the wave function  $\psi(\mathbf{r}, t)$  whereas the field is described by the vector and scalar potentials  $\mathbf{A}$  and  $U$ , respectively.

It is interesting to note that the Hamiltonian (5.1.1) has been ‘derived’ from a gauge invariance argument and is expressed in terms of the gauge-dependent quantities  $\mathbf{A}(\mathbf{r}, t)$  and  $U(\mathbf{r}, t)$ . The vector and scalar potentials have therefore a larger physical significance than is usually attributed to them. They are not merely introduced for the sake of mathematical simplicity in problems dealing with ‘observable’ electric and magnetic fields. Instead, they arise naturally in any gauge (phase) invariance argument as shown above.

We also note that the Schrödinger equation plus the concept of local gauge invariance has led us to the introduction of the electromagnetic field. In this way, we can and do argue that the ‘photon’ (in our

derivation, the classical field limit of the same) has been ‘derived’ from the Schrödinger equation plus the local gauge invariance arguments.

We have here a taste of one of the most fundamental concepts in modern physics, namely, that of the gauge field theory. Gauge theory, in the hands of Steven Weinberg and Abdus Salam, led to the unification of the weak and the electromagnetic interactions.

### 5.1.2 Dipole approximation and $\mathbf{r} \cdot \mathbf{E}$ Hamiltonian

We now examine the problem of an electron bound by a potential  $V(r)$  to a force center (nucleus) located at  $\mathbf{r}_0$ . The minimal-coupling Hamiltonian (5.1.1) for an interaction between an atom and the radiation field can be reduced to a simple form by using the dipole approximation. The entire atom is immersed in a plane electromagnetic wave described by a vector potential  $\mathbf{A}(\mathbf{r}_0 + \mathbf{r}, t)$ . This vector potential may be written in the dipole approximation,  $\mathbf{k} \cdot \mathbf{r} \ll 1$ , as

$$\begin{aligned}\mathbf{A}(\mathbf{r}_0 + \mathbf{r}, t) &= \mathbf{A}(t) \exp[i\mathbf{k} \cdot (\mathbf{r}_0 + \mathbf{r})] \\ &= \mathbf{A}(t) \exp(i\mathbf{k} \cdot \mathbf{r}_0)(1 + i\mathbf{k} \cdot \mathbf{r} + \dots) \\ &\simeq \mathbf{A}(t) \exp(i\mathbf{k} \cdot \mathbf{r}_0).\end{aligned}\quad (5.1.11)$$



The Schrödinger equation for this problem (in the dipole approximation) is given by Eq. (5.1.5) with  $\mathbf{A}(\mathbf{r}, t) \equiv \mathbf{A}(\mathbf{r}_0, t)$ , i.e.,

$$\left\{ -\frac{\hbar^2}{2m} \left[ \nabla - \frac{ie}{\hbar} \mathbf{A}(\mathbf{r}_0, t) \right]^2 + V(r) \right\} \psi(\mathbf{r}, t) = i\hbar \frac{\partial \psi(\mathbf{r}, t)}{\partial t}, \quad (5.1.12)$$

where we have added a binding potential  $V(r)$ . We note that in Eq. (5.1.12), and elsewhere in this book, we are working in the radiation gauge, in which

$$U(\mathbf{r}, t) = 0, \quad (5.1.13)$$

and

$$\nabla \cdot \mathbf{A} = 0. \quad (5.1.14)$$

We have added the term  $V(r)$  in the Hamiltonian which arises from the electrostatic potential that binds the electron to the nucleus.

We proceed to simplify Eq. (5.1.12) by defining a new wave function  $\phi(\mathbf{r}, t)$  as

$$\psi(\mathbf{r}, t) = \exp \left[ \frac{ie}{\hbar} \mathbf{A}(\mathbf{r}_0, t) \cdot \mathbf{r} \right] \phi(\mathbf{r}, t). \quad (5.1.15)$$

*相当子做了规范化操作*

*下 A 与 F.E 有关  
但波函数差个相因子  
(5.1.3)*

*以后只用 F.E*

Inserting Eq. (5.1.15) into Eq. (5.1.12), we find

$$\begin{aligned} i\hbar \left[ \frac{ie}{\hbar} \dot{\mathbf{A}} \cdot \mathbf{r} \phi(\mathbf{r}, t) + \dot{\phi}(\mathbf{r}, t) \right] \exp \left( \frac{ie}{\hbar} \mathbf{A} \cdot \mathbf{r} \right) \\ = \exp \left( \frac{ie}{\hbar} \mathbf{A} \cdot \mathbf{r} \right) \left[ \frac{p^2}{2m} + V(r) \right] \phi(\mathbf{r}, t). \end{aligned} \quad (5.1.16)$$

This equation, after the cancellation of the exponential factor and some rearrangement, takes the simple form

$$i\hbar \dot{\phi}(\mathbf{r}, t) = [\mathcal{H}_0 - e\mathbf{r} \cdot \mathbf{E}(\mathbf{r}_0, t)]\phi(\mathbf{r}, t), \quad (5.1.17)$$

where

$$\mathcal{H}_0 = \frac{p^2}{2m} + V(r), \quad (5.1.18)$$

is the unperturbed Hamiltonian of the electron and we use  $\mathbf{E} = -\dot{\mathbf{A}}$ . Notice that the total Hamiltonian

$$\mathcal{H} = \mathcal{H}_0 + \mathcal{H}_1 \quad (5.1.19)$$

with

$$\mathcal{H}_1 = -e\mathbf{r} \cdot \mathbf{E}(\mathbf{r}_0, t), \quad (5.1.20)$$

is given in terms of the gauge-independent field  $\mathbf{E}$ . We shall use this Hamiltonian in our subsequent studies of atom–field interaction. Note also that this Hamiltonian has been obtained from the radiation gauge Hamiltonian (5.1.12) by applying the gauge transformation  $\chi(\mathbf{r}, t) = -e\mathbf{A}(\mathbf{r}_0, t) \cdot \mathbf{r}/\hbar$ .

### 5.1.3 $\mathbf{p} \cdot \mathbf{A}$ Hamiltonian

In many textbooks one finds the atom–field Hamiltonian expressed in terms of the canonical momentum  $\mathbf{p}$  and the vector potential  $\mathbf{A}$  instead of the simple gauge invariant expression (5.1.17). This has resulted in considerable confusion, and we therefore consider the problem in some detail. We again choose a radiation gauge in which  $U(\mathbf{r}, t) = 0$  and  $\nabla \cdot \mathbf{A} = 0$ . The condition  $\nabla \cdot \mathbf{A} = 0$  implies, in quantum mechanics, that  $[\mathbf{p}, \mathbf{A}] = 0$ . The total Hamiltonian (5.1.1) can, therefore, be written as

$$\mathcal{H}' = \mathcal{H}_0 + \mathcal{H}_2, \quad (5.1.21)$$

where  $\mathcal{H}_0$  is given by Eq. (5.1.18) and, in the dipole approximation (5.1.11),

$$\mathcal{H}_2 = -\frac{e}{m} \mathbf{p} \cdot \mathbf{A}(\mathbf{r}_0, t) + \frac{e^2}{2m} A^2(\mathbf{r}_0, t), \quad (5.1.22)$$

and the Schrödinger equation reads

$$\left[ \mathcal{H}_0 - \frac{e}{m} \mathbf{p} \cdot \mathbf{A}(\mathbf{r}_0, t) + \frac{e^2}{2m} A^2(\mathbf{r}_0, t) \right] \psi(\mathbf{r}, t) = i\hbar \frac{\partial}{\partial t} \psi(\mathbf{r}, t). \quad (5.1.23)$$

The  $A^2$  term in Eq. (5.1.23) is usually small and can be ignored. The wave function  $\psi(\mathbf{r}, t)$  then obeys the equation of motion

$$i\hbar \frac{\partial}{\partial t} \psi(\mathbf{r}, t) = \left[ \mathcal{H}_0 - \frac{e}{m} \mathbf{p} \cdot \mathbf{A}(\mathbf{r}_0, t) \right] \psi(\mathbf{r}, t), \quad (5.1.24)$$

corresponding to a Hamiltonian

$$\mathcal{H}' = \mathcal{H}_0 - \frac{e}{m} \mathbf{p} \cdot \mathbf{A}(\mathbf{r}_0, t), \quad (5.1.25)$$

and

$$\mathcal{H}_2 = -\frac{e}{m} \mathbf{p} \cdot \mathbf{A}(\mathbf{r}_0, t). \quad (5.1.26)$$

The two different Hamiltonians  $\mathcal{H}_1$  and  $\mathcal{H}_2$  given in Eqs. (5.1.20) and (5.1.26), respectively, seem to give different physical results since the matrix elements of these Hamiltonians, calculated between the eigenstates of the *unperturbed* Hamiltonian  $\mathcal{H}_0$ , given by Eq. (5.1.18), are not the same. In order to show this explicitly, we consider a linearly polarized monochromatic plane-wave field interacting with an atom placed at  $\mathbf{r}_0 = 0$ . The electric field then takes the form

$$\mathbf{E}(0, t) = \mathcal{E} \cos \nu t, \quad (5.1.27)$$

and the corresponding vector potential in the radiation gauge is

$$\mathbf{A}(0, t) = -\frac{1}{\nu} \mathcal{E} \sin \nu t. \quad (5.1.28)$$

Consider now the time-independent amplitudes associated with  $\mathcal{H}_1$  and  $\mathcal{H}_2$ ,

$$W_1 = -e \mathbf{r} \cdot \mathcal{E}, \quad (5.1.29a)$$

$$W_2 = \frac{e}{mv} \mathbf{p} \cdot \mathcal{E}. \quad (5.1.29b)$$

We may relate  $W_1$  and  $W_2$  by noting that

$$\mathbf{p} = mv = -m \left( \frac{i}{\hbar} \right) [\mathbf{r}, \mathcal{H}_0]. \quad (5.1.30)$$

We then find for the matrix elements of  $W_1$  and  $W_2$ , calculated between an initial eigenstate  $|i\rangle$  of  $\mathcal{H}_0$  (with  $\mathcal{H}_0|i\rangle = \hbar\omega_i|i\rangle$ ) and a

final eigenstate  $|f\rangle$  (with  $\mathcal{H}_0|f\rangle = \hbar\omega_f|f\rangle$ ), the ratio

$$\begin{aligned} \left| \frac{\langle f | W_2 | i \rangle}{\langle f | W_1 | i \rangle} \right| &= \left| - \frac{(e/mv) \langle f | \mathbf{p} | i \rangle \cdot \mathcal{E}}{e \langle f | \mathbf{r} | i \rangle \cdot \mathcal{E}} \right| \\ &= \frac{\omega}{v}, \end{aligned} \quad (5.1.31)$$

where  $\omega = \omega_f - \omega_i$  is the transition frequency. Hence, the matrix elements of the two interaction Hamiltonians  $\mathcal{H}_1$  and  $\mathcal{H}_2$  differ by the ratio of the transition frequency over the field frequency. As was first pointed out by Lamb, this makes a difference in measurable quantities like transition rates. We present a resolution of this in Appendix 5.A.

## 5.2 Interaction of a single two-level atom with a single-mode field

### 5.2.1 Probability amplitude method

Consider the interaction of a single-mode radiation field of frequency  $v$  with a two-level atom (Fig. 5.1). Let  $|a\rangle$  and  $|b\rangle$  represent the upper and lower level states of the atom, i.e., they are eigenstates of the unperturbed part of the Hamiltonian  $\mathcal{H}_0$  with the eigenvalues  $\hbar\omega_a$  and  $\hbar\omega_b$ , respectively. The wave function of a two-level atom can be written in the form

$$|\psi(t)\rangle = C_a(t)|a\rangle + C_b(t)|b\rangle, \quad (5.2.1)$$

where  $C_a$  and  $C_b$  are the probability amplitudes of finding the atom in states  $|a\rangle$  and  $|b\rangle$ , respectively. The corresponding Schrödinger equation is

$$|\dot{\psi}(t)\rangle = -\frac{i}{\hbar}\mathcal{H}|\psi(t)\rangle, \quad (5.2.2)$$

with

$$\mathcal{H} = \mathcal{H}_0 + \mathcal{H}_1, \quad (5.2.3)$$

where  $\mathcal{H}_0$  and  $\mathcal{H}_1$  represent the unperturbed and interaction parts of the Hamiltonian, respectively. By using the completeness relation  $|a\rangle\langle a| + |b\rangle\langle b| = \mathbf{1}$ , we can write  $\mathcal{H}_0$  as

$$\begin{aligned} \mathcal{H}_0 &= (|a\rangle\langle a| + |b\rangle\langle b|)\mathcal{H}_0(|a\rangle\langle a| + |b\rangle\langle b|) \\ &= \hbar\omega_a|a\rangle\langle a| + \hbar\omega_b|b\rangle\langle b|, \end{aligned} \quad (5.2.4)$$

where we use  $\mathcal{H}_0|a\rangle = \hbar\omega_a|a\rangle$  and  $\mathcal{H}_0|b\rangle = \hbar\omega_b|b\rangle$ . Similarly, the part of the Hamiltonian  $\mathcal{H}_1$  that represents the interaction of the atom

with the radiation field can be written as

$$\begin{aligned}\mathcal{H}_1 &= -exE(t) \\ &= -e(|a\rangle\langle a| + |b\rangle\langle b|)x(|a\rangle\langle a| + |b\rangle\langle b|)E(z, t) \\ &= -(\wp_{ab}|a\rangle\langle b| + \wp_{ba}|b\rangle\langle a|)E(t),\end{aligned}\quad \begin{array}{l} \text{不满足偶/奇对称} \\ \text{总是有 } \int_{-\infty}^{\infty} x \cdot \text{偶 } dx = 0 \end{array} \quad (5.2.5)$$

where  $\wp_{ab} = \wp_{ba}^* = e\langle a|x|b\rangle$  is the matrix element of the electric dipole moment and  $E(t)$  is the field at the atom. Here, we assume that the electric field is linearly polarized along the  $x$ -axis. In the dipole approximation, the field can be expressed as

$$E(t) = \mathcal{E} \cos vt, \quad (5.2.6)$$

where  $\mathcal{E}$  is the amplitude and  $v = ck$  is the frequency of the field. The equations of motion for the amplitudes  $C_a$  and  $C_b$  may be written as

$$\dot{C}_a = -i\omega_a C_a + i\Omega_R e^{-i\phi} \cos(vt) C_b, \quad (5.2.7)$$

$$\dot{C}_b = -i\omega_b C_b + i\Omega_R e^{i\phi} \cos(vt) C_a, \quad (5.2.8)$$

where the Rabi frequency  $\Omega_R$  is defined as

$$\Omega_R = \frac{|\wp_{ba}| \mathcal{E}}{\hbar}, = \frac{\langle a | \hat{H}' | b \rangle}{\hbar} \quad (5.2.9)$$

and  $\phi$  is the phase of the dipole matrix element  $\wp_{ba} = |\wp_{ba}| \exp(i\phi)$ . In order to solve for  $C_a$  and  $C_b$ , we first write the equations of motion for the slowly varying amplitudes:

$$c_a = C_a e^{i\omega_a t}, \quad (5.2.10)$$

$$c_b = C_b e^{i\omega_b t}. \quad (5.2.11)$$

It then follows from Eqs. (5.2.7) and (5.2.8) that

$$\dot{c}_a = i \frac{\Omega_R}{2} e^{-i\phi} c_b e^{i(\omega-v)t} + \dots \quad (5.2.12)$$

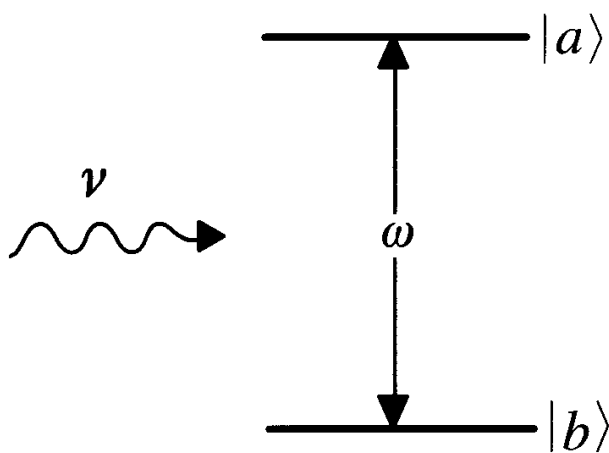
$$\dot{c}_b = i \frac{\Omega_R}{2} e^{i\phi} c_a e^{-i(\omega-v)t} + \dots \quad (5.2.13)$$

where  $\omega = \omega_a - \omega_b$  is the atomic transition frequency. In deriving Eqs. (5.2.12) and (5.2.13), we have ignored counter-rotating terms proportional to  $\exp[\pm i(\omega + v)t]$  on the right-hand side in the *rotating-wave approximation*. This is generally a very good approximation. Furthermore, in some cases the counter-rotating terms never appear (as seen later in section 5.2.3) and Eqs. (5.2.12) and (5.2.13) are exact.

可化成二阶单未知数方程

随自旋进动  
W-Y  
不随自旋进动  
W+Y

Fig. 5.1  
Interaction of a  
two-level atom with a  
single-mode field.



The solutions for  $c_a$  and  $c_b$  can be written as

$$c_a(t) = (a_1 e^{i\Omega t/2} + a_2 e^{-i\Omega t/2}) e^{i\Delta t/2}, \quad (5.2.14)$$

$$c_b(t) = (b_1 e^{i\Omega t/2} + b_2 e^{-i\Omega t/2}) e^{-i\Delta t/2}, \quad (5.2.15)$$

*S<sub>R</sub> 不打擾 Rabi: 有 3/2*

*S<sub>R</sub> Rabi 1/2*

where  $\Delta = \omega - \nu$ ,

$$\Rightarrow \Omega = \sqrt{\Omega_R^2 + (\omega - \nu)^2}, \quad (5.2.16)$$

and  $a_1$ ,  $a_2$ ,  $b_1$ , and  $b_2$  are constants of integration which are determined from the initial conditions:

$$a_1 = \frac{1}{2\Omega} [(\Omega - \Delta)c_a(0) + \Omega_R e^{-i\phi} c_b(0)], \quad (5.2.17)$$

$$a_2 = \frac{1}{2\Omega} [(\Omega + \Delta)c_a(0) - \Omega_R e^{-i\phi} c_b(0)], \quad (5.2.18)$$

$$b_1 = \frac{1}{2\Omega} [(\Omega + \Delta)c_b(0) + \Omega_R e^{i\phi} c_a(0)], \quad (5.2.19)$$

$$b_2 = \frac{1}{2\Omega} [(\Omega - \Delta)c_b(0) - \Omega_R e^{i\phi} c_a(0)]. \quad (5.2.20)$$

We then have

$$c_a(t) = \left\{ c_a(0) \left[ \cos\left(\frac{\Omega t}{2}\right) - \frac{i\Delta}{\Omega} \sin\left(\frac{\Omega t}{2}\right) \right] + i \frac{\Omega_R}{\Omega} e^{-i\phi} c_b(0) \sin\left(\frac{\Omega t}{2}\right) \right\} e^{i\Delta t/2}, \quad (5.2.21)$$

$$c_b(t) = \left\{ c_b(0) \left[ \cos\left(\frac{\Omega t}{2}\right) + \frac{i\Delta}{\Omega} \sin\left(\frac{\Omega t}{2}\right) \right] + i \frac{\Omega_R}{\Omega} e^{i\phi} c_a(0) \sin\left(\frac{\Omega t}{2}\right) \right\} e^{-i\Delta t/2}. \quad (5.2.22)$$

It is not difficult to verify that

$$|c_a(t)|^2 + |c_b(t)|^2 = 1, \quad (5.2.23)$$

which is a simple statement of the conservation of probability since the atom is in state  $|a\rangle$  or  $|b\rangle$ .

If we assume that the atom is initially in the state  $|a\rangle$  then  $c_a(0) = 1, c_b(0) = 0$ . The probabilities of the atom being in states  $|a\rangle$  and  $|b\rangle$  at time  $t$  are then given by  $|c_a(t)|^2$  and  $|c_b(t)|^2$ . The inversion is given by

布居反转

$$\begin{aligned} W(t) &= |c_a(t)|^2 - |c_b(t)|^2 \\ &= \left( \frac{\Delta^2 - \Omega_R^2}{\Omega^2} \right) \sin^2 \left( \frac{\Omega t}{2} \right) + \cos^2 \left( \frac{\Omega t}{2} \right). \end{aligned} \quad (5.2.24)$$

Under the action of the incident field, a dipole moment is induced between the two atomic levels. This induced dipole moment is given by the expectation value of the dipole moment operator

$$P(t) = e \langle \psi(t) | r | \psi(t) \rangle = C_a^* C_b \delta_{ab} + \text{c.c.} = c_a^* c_b \delta_{ab} e^{i\omega t} + \text{c.c.} \quad (5.2.25)$$

On substituting Eqs. (5.2.21) and (5.2.22) into Eq. (5.2.25), we obtain, for an atom initially in the upper level,

$$\begin{aligned} P(t) &= 2 \operatorname{Re} \left\{ \frac{i\Omega_R}{\Omega} \delta_{ab} \left[ \cos \left( \frac{\Omega t}{2} \right) + \frac{i\Delta}{\Omega} \sin \left( \frac{\Omega t}{2} \right) \right] \sin \left( \frac{\Omega t}{2} \right) e^{i\phi} e^{ivt} \right\}. \end{aligned} \quad (5.2.26)$$

The dipole moment therefore oscillates with the frequency of the incident field.

电偶极振荡. 已跃迁且电偶极扭曲。

In the special case when the atom is at resonance with the incident field ( $\Delta = 0$ ), we get  $\Omega = \Omega_R$  and

$$W(t) = \cos(\Omega_R t). \quad \text{布居反转了.} \quad (5.2.27)$$

The inversion oscillates between  $-1$  and  $1$  at a frequency  $\Omega_R$  (see Fig. 5.2).

In 1937, Rabi considered the problem of a spin-1/2 magnetic dipole undergoing precessions in a magnetic field and obtained an expression for the probability that a spin-1/2 atom incident on a Stern-Gerlach apparatus would be flipped from the  $(1)_0$  or  $(0)_1$  state to the  $(0)_1$  or  $(1)_0$  state, respectively, by an applied radio-frequency magnetic field. In the present problem, the atom undergoes a Rabi ‘flopping’ between the *upper and lower levels under the action of the electromagnetic field in complete analogy with the spin-1/2 system*.

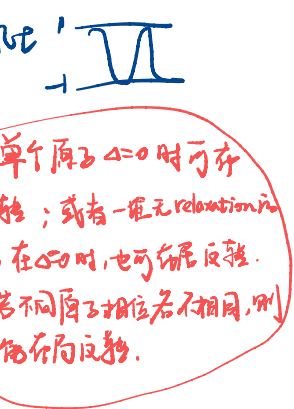
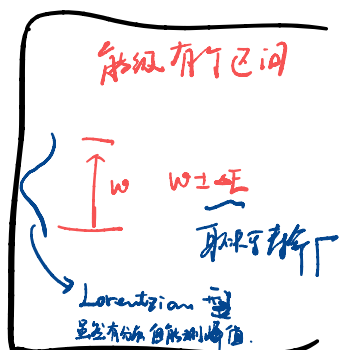
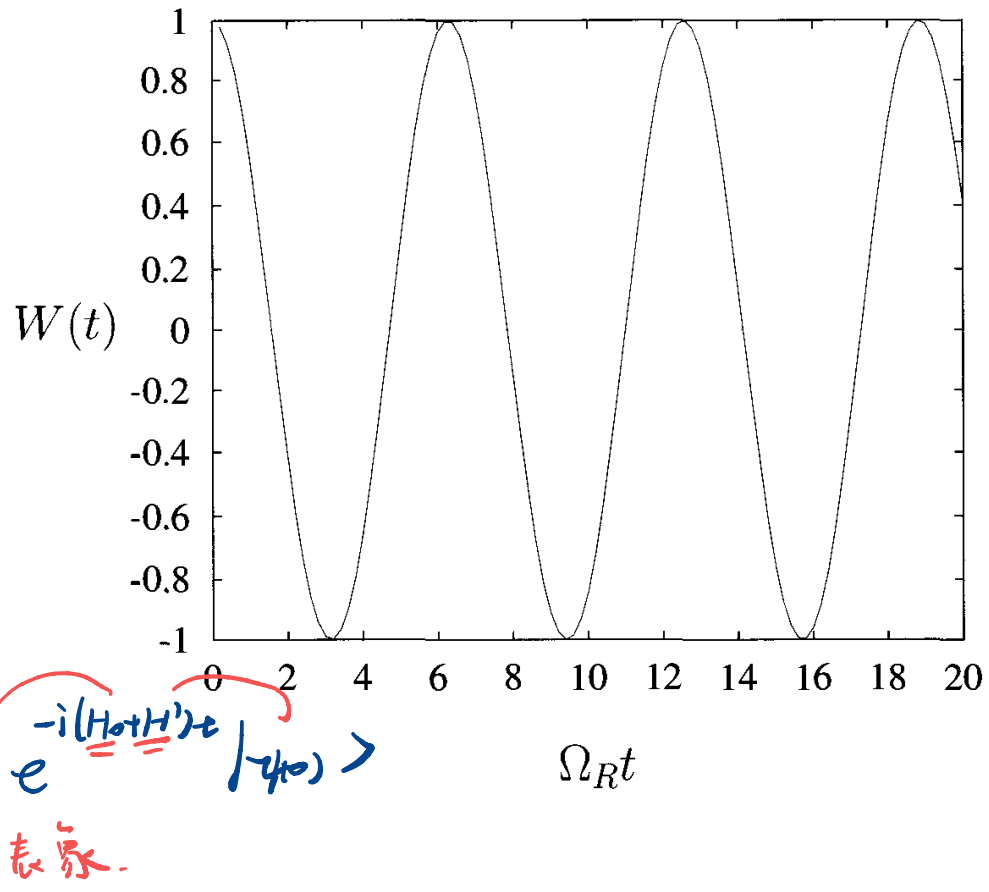


Fig. 5.2  
Oscillations of the population inversion  $W(t)$  as a function of time.



### 5.2.2 Interaction picture

Consider the Schrödinger equation

$$\frac{\partial}{\partial t} |\psi(t)\rangle = -\frac{i}{\hbar} \mathcal{H} |\psi(t)\rangle. \quad (5.2.28)$$

This equation can be integrated formally to give

$$|\psi(t)\rangle = U(t)|\psi(0)\rangle, \quad (5.2.29)$$

where the unitary time-evolution operator is defined by

$$\dot{U}(t) = -\frac{i}{\hbar} \mathcal{H} U(t), \quad (5.2.30)$$

and  $U(0) = 1$ .

A useful approach to the atom–field interaction problem exists in the *interaction picture* in which we assign to the state vector the time dependence due only to the interaction energy. This is accomplished by defining the state vector  $|\psi_I\rangle$  in the interaction picture via

$$|\psi_I(t)\rangle = U_0^\dagger(t)|\psi(t)\rangle, \quad (5.2.31)$$

where

$$U_0(t) = \exp\left(-\frac{i}{\hbar} \mathcal{H}_0 t\right). \quad (5.2.32)$$

It then follows that

$$\frac{\partial}{\partial t}|\psi_I(t)\rangle = \left[ \frac{\partial}{\partial t} U_0^\dagger(t) \right] |\psi(t)\rangle + U_0^\dagger(t) \frac{\partial}{\partial t} |\psi(t)\rangle, \quad (5.2.33)$$

and hence, from Eqs. (5.2.28), (5.2.31), and (5.2.32), we obtain

$$\boxed{\frac{\partial}{\partial t}|\psi_I(t)\rangle = -\frac{i}{\hbar}\mathcal{V}(t)|\psi_I(t)\rangle} \quad \text{态演化方程} \quad (5.2.34)$$

Here

$$\mathcal{V}(t) = U_0^\dagger(t)\mathcal{H}_1 U_0(t), \quad \hat{U}_0(t) = \exp(-i\frac{\hat{H}_0}{\hbar}t) \quad (5.2.35)$$

is the interaction picture Hamiltonian. An operator  $O$  in the Schrödinger picture will accordingly transform as

$$\boxed{O_I(t) = U_0^\dagger(t)O_s U_0(t).} \quad | \psi_I(t) = \hat{U}_0(t)|\psi_s(t)\rangle \quad (5.2.36)$$

This can be seen from the expectation value

$$\begin{aligned} \langle O \rangle &= \langle \psi(t) | O | \psi(t) \rangle \\ &= \langle \psi_I(t) | U_0^\dagger(t) O U_0(t) | \psi_I(t) \rangle \\ &= \langle \psi_I(t) | O_I(t) | \psi_I(t) \rangle. \end{aligned} \quad (5.2.37)$$

物理相当于在 Schrödinger 算符的本征基上  
添入  $e^{i\frac{\hat{H}_0}{\hbar}t}$   
因为子 S 本来是  $e^{i(\hat{H}_0+\hat{H}_I)t}$ , 故相当于  
正影响  $\hat{H}_I$  的演化.

A formal solution of Eq. (5.2.34) is

$$|\psi_I(t)\rangle = U_I(t)|\psi_I(0)\rangle, \quad \text{态演化方程} \quad (5.2.38)$$

where

$$U_I(t) = \mathcal{T} \exp \left[ -\frac{i}{\hbar} \int_0^t \mathcal{V}(\tau) d\tau \right] \quad (5.2.39)$$

is the time-evolution operator in the interaction picture, and  $\mathcal{T}$  is the 时间算符, which is a shorthand notation for

$$\mathcal{T} \exp \left[ -\frac{i}{\hbar} \int_0^t \mathcal{V}(\tau) d\tau \right]$$

$$\Rightarrow = 1 - \frac{i}{\hbar} \int_0^t dt_1 \mathcal{V}(t_1) + \left( -\frac{i}{\hbar} \right)^2 \int_0^t dt_1 \int_0^{t_1} dt_2 \mathcal{V}(t_1) \mathcal{V}(t_2) + \dots$$

计算机

In order to demonstrate the usefulness of the above formalism, we consider the interaction of a two-level atom with a monochromatic field of frequency  $\nu$ . The Hamiltonian for this problem is given by Eqs. (5.2.3), (5.2.4), and (5.2.5). It follows, on using

$$\mathcal{H}_0^n = (\hbar\omega_a)^n |a\rangle\langle a| + (\hbar\omega_b)^n |b\rangle\langle b|, \quad (5.2.41)$$

that

$$\begin{aligned} \mathcal{I} &= |a\rangle\langle a| + |b\rangle\langle b| \\ U_0(t) &= \exp\left(-\frac{i}{\hbar}\mathcal{H}_0 t\right) \\ &= \exp(-i\omega_a t)|a\rangle\langle a| + \exp(-i\omega_b t)|b\rangle\langle b|. \end{aligned} \quad (5.2.42)$$

For an atom at  $z = 0$ , the interaction picture Hamiltonian is, therefore, given by

$$\begin{aligned} \mathcal{V}(t) &= -\hbar\Omega_R U_0^\dagger(t)(e^{-i\phi}|a\rangle\langle b| + e^{i\phi}|b\rangle\langle a|)U_0(t) \cos vt \\ &= -\frac{\hbar\Omega_R}{2}[e^{-i\phi}|a\rangle\langle b|e^{i\Delta t} + e^{i\phi}|b\rangle\langle a|e^{-i\Delta t} \\ &\quad + e^{-i\phi}|a\rangle\langle b|e^{i(\omega+v)t} + e^{i\phi}|b\rangle\langle a|e^{-i(\omega+v)t}], \end{aligned} \quad (5.2.43)$$

where  $\Delta = \omega - v$ . The terms proportional to  $\exp[\pm i(\omega + v)t]$  vary very rapidly and their average over a time scale larger than  $1/v$  is zero. These terms can therefore be neglected in the *rotating-wave approximation*. The simplified interaction picture Hamiltonian is

$$\rightarrow \mathcal{V}(t) = -\frac{\hbar\Omega_R}{2}(e^{-i\phi}|a\rangle\langle b| + e^{i\phi}|b\rangle\langle a|), \quad (5.2.44)$$

where we assume resonance,  $\Delta = 0$ . The time-evolution operator in the interaction picture  $U_I(t)$  can be obtained simply from Eq. (5.2.39) by using

$$\begin{aligned} \mathcal{V}^{2n}(t) &= \left(\frac{\hbar\Omega_R}{2}\right)^{2n}(|a\rangle\langle a| + |b\rangle\langle b|)^n, \\ \mathcal{V}^{2n+1}(t) &= -\left(\frac{\hbar\Omega_R}{2}\right)^{2n+1}(e^{-i\phi}|a\rangle\langle b| + e^{i\phi}|b\rangle\langle a|). \end{aligned} \quad (5.2.45)$$

The resulting expression for  $U_I(t)$  is

$$\rightarrow U_I(t) = \cos\left(\frac{\Omega_R t}{2}\right)(|a\rangle\langle a| + |b\rangle\langle b|) + i \sin\left(\frac{\Omega_R t}{2}\right)(e^{-i\phi}|a\rangle\langle b| + e^{i\phi}|b\rangle\langle a|). \quad (5.2.46)$$

If the atom is initially in the excited state ( $|\psi(0)\rangle \equiv |a\rangle$ ),

$$\begin{aligned} |\psi(t)\rangle &= U_I(t)|a\rangle \\ &= \cos\left(\frac{\Omega_R t}{2}\right)|a\rangle + i \sin\left(\frac{\Omega_R t}{2}\right)e^{i\phi}|b\rangle, \end{aligned} \quad (5.2.47)$$

and we obtain the probability amplitudes

$$c_a(t) = \langle a|\psi\rangle = \cos\left(\frac{\Omega_R t}{2}\right), \quad (5.2.48a)$$

$$c_b(t) = \langle b|\psi\rangle = i \sin\left(\frac{\Omega_R t}{2}\right)e^{i\phi}, \quad (5.2.48b)$$

in agreement with Eqs. (5.2.21) and (5.2.22).

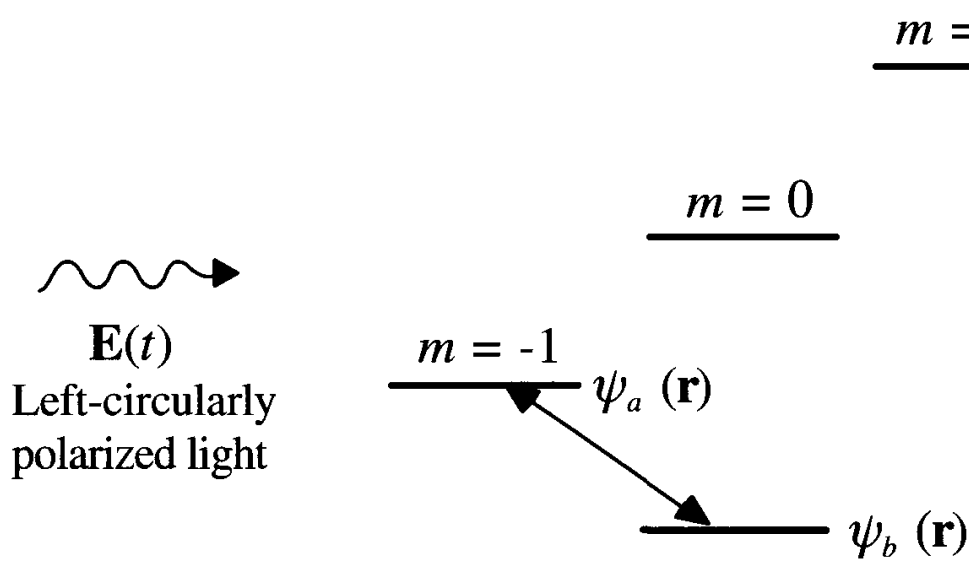


Fig. 5.3  
Figure illustrating an incident electric field interacting with a hydrogen (Rydberg) atom such that the energy difference  $\epsilon_{m=1} - \epsilon_b$  is much larger than  $\epsilon_{m=-1} - \epsilon_b$ .

### 5.2.3 Beyond the rotating-wave approximation

In quantum optics, the so-called rotating-wave approximation, as discussed in connection with Eq. (5.2.13), is frequently encountered. Of course, it is a very good approximation and amounts to keeping only energy-conserving terms in the Hamiltonian.

Moreover, as we show here, there are situations in which it is “exact”, i.e., for all practical purposes the ‘counter-rotating terms’ never show up. Consider the case of a hydrogen atom in a strong magnetic field interacting with a monochromatic field as shown in Fig. 5.3. If the levels are sharp and well separated, we may focus on only the two levels, see Problem 5.7, for which

$$\psi_a(\mathbf{r}) = \frac{1}{\sqrt{64\pi a_0^3}} \frac{1}{a_0} (x - iy) \exp(-r/2a_0), \quad (5.2.49a)$$

$$\psi_b(\mathbf{r}) = \frac{1}{\sqrt{\pi a_0^3}} \exp(-r/a_0), \quad (5.2.49b)$$

where  $a_0$  is the Bohr radius.

Using the dipole approximation (see Section 5.1.2) and placing the atom at the origin so that  $\mathbf{R} = 0$ , we have the interaction picture Hamiltonian

$$\mathcal{V} = -e\mathbf{r}(t) \cdot \mathbf{E}(t), \quad (5.2.50a)$$

where

$$\mathbf{r}(t) = e^{i\mathcal{H}_0 t} \mathbf{r} e^{-i\mathcal{H}_0 t}, \quad (5.2.50b)$$

and therefore

$$\mathcal{V}_{ab}(t) = -e\mathbf{r}_{ab}(t) \cdot \mathbf{E}(t) = -e\mathbf{r}_{ab} \cdot \mathbf{E}(t)e^{i\omega t}, \quad (5.2.51a)$$

$$\mathcal{V}_{ba}(t) = -e\mathbf{r}_{ba}(t) \cdot \mathbf{E}(t) = -e\mathbf{r}_{ba} \cdot \mathbf{E}(t)e^{-i\omega t}, \quad (5.2.51b)$$

where  $\omega$  is the atomic frequency.

Now, for the case of linear polarization in which

$$\mathbf{E}(t) = \hat{x}\mathcal{E} \cos vt, \quad (5.2.52)$$

Eqs. (5.2.51a, 5.2.51b) and (5.2.52) imply

$$\begin{aligned} \mathcal{V}_{ab}(t) &= -ex_{ab}\mathcal{E} \cos vt e^{i\omega t} \\ &= -ex_{ab} \frac{\mathcal{E}}{2} [e^{i(v+\omega)t} + e^{-i(v-\omega)t}] \\ &\cong -ex_{ab} \frac{\mathcal{E}}{2} e^{-i(v-\omega)t}, \end{aligned} \quad (5.2.53)$$

and likewise

$$\begin{aligned} \mathcal{V}_{ba}(t) &= -ex_{ba}\mathcal{E} \cos vt e^{-i\omega t} \\ &= -ex_{ba} \frac{\mathcal{E}}{2} [e^{i(v-\omega)t} + e^{-i(v+\omega)t}] \\ &\cong -ex_{ba} \frac{\mathcal{E}}{2} e^{i(v-\omega)t}. \end{aligned} \quad (5.2.54)$$

Thus we make the rotating-wave approximation in neglecting counter terms that go like  $\exp[\pm i(\omega + v)t]$ .

Now consider the case of left-circular polarization (LCP), which connects  $\psi_a(r)$  and  $\psi_b(r)$ , as given by Eqs. (5.2.49). The electric field is given by

$$\mathbf{E}(t) = \hat{x}\mathcal{E} \cos vt - \hat{y}\mathcal{E} \sin vt. \quad (5.2.55)$$

Equations (5.2.53) and (5.2.54) now take the form

$$\mathcal{V}_{ab}(t) = -e\mathcal{E}(x_{ab} \cos vt + y_{ab} \sin vt)e^{i\omega t} \quad (5.2.56a)$$

$$\mathcal{V}_{ba}(t) = -e\mathcal{E}(x_{ba} \cos vt + y_{ba} \sin vt)e^{-i\omega t} \quad (5.2.56b)$$

where, in view of Eqs. (5.2.49a) and (5.2.49b), we can write

$$ex_{ab} = \int \psi_a^*(\mathbf{r}) x \psi_b(\mathbf{r}) d\mathbf{r} = \varphi, \quad (5.2.57a)$$

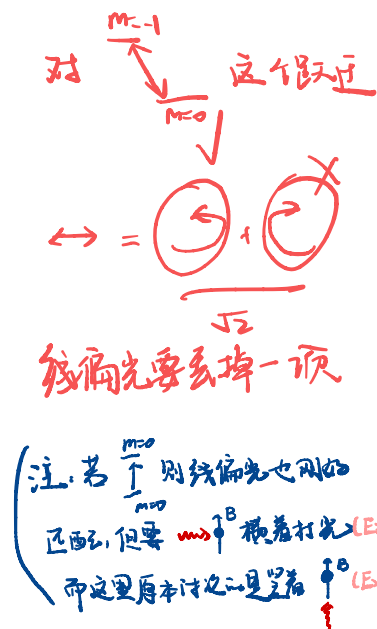
$$ey_{ab} = \int \psi_a^*(\mathbf{r}) y \psi_b(\mathbf{r}) d\mathbf{r} = -i\varphi, \quad (5.2.57b)$$

and similarly,  $ex_{ba} = \varphi$  and  $ey_{ba} = i\varphi$ . Therefore Eqs. (5.2.56a) and (5.2.56b) take the simple form

$$\mathcal{V}_{ab}(t) = -\varphi\mathcal{E}(\cos vt - i \sin vt)e^{i\omega t} = -\varphi\mathcal{E}e^{-i(v-\omega)t} \quad (5.2.58a)$$

$$\mathcal{V}_{ba}(t) = -\varphi\mathcal{E}(\cos vt + i \sin vt)e^{-i\omega t} = -\varphi\mathcal{E}e^{i(v-\omega)t}, \quad (5.2.58b)$$

and the counter-rotating terms never appear.



左旋光场用的匹配，无高斯场  
而右旋光全靠高斯场，无法匹配

本节总结：  
进阶理解  $\leftrightarrow$  简单理解  
Rotating frame  $\leftrightarrow$  相互作用场

Finally, we note that although there are no counter terms of the form  $e^{i(v+\omega)t}$  associated with the LCP light inducing  $\Delta m = -1$  transitions, there are counter terms associated with LCP and transitions to a state  $n = 2, l = 1, m_l = +1$ , i.e.,  $\Delta m = +1$ . Such transitions are usually said to vanish due to angular momentum selection rules. Here they are seen to ‘vanish’ since they go as counter rotating terms. That is, they are allowed in the sense of an atom making a transition to an excited state with the emission of a photon. Such terms can be much smaller than the usual counter-rotating terms; see Problem 5.7.

### 5.3 Density matrix for a two-level atom\*

For a given physical system, there exists a state vector  $|\psi\rangle$  which contains all possible information about the system. If we want to extract a piece of the system’s information, we must calculate the expectation value of the corresponding operator  $O$ ,

$$\langle O \rangle_{QM} = \langle \psi | O | \psi \rangle. \quad (5.3.1)$$

In many situations we may not know  $|\psi\rangle$ ; we may only know the probability  $P_\psi$  that the system is in the state  $|\psi\rangle$ . For such a situation, we not only need to take the quantum mechanical average but also the ensemble average over many identical systems that have been similarly prepared. Instead of Eq. (5.3.1), we now have (see Section 3.1)

$$\langle\langle O \rangle_{QM} \rangle_{\text{ensemble}} = \text{Tr}(O\rho), \quad (5.3.2)$$

where the density operator  $\rho$  is defined by

$$\rho = \sum_{\psi} P_{\psi} |\psi\rangle \langle \psi|. \quad (5.3.3)$$

It can be seen that

$$\text{Tr}(O\rho) = \text{Tr}(\rho O). \quad (5.3.4)$$

In the particular case where all  $P_\psi$  are zero except the one for a state  $|\psi_0\rangle$ , then

$$\rho = |\psi_0\rangle \langle \psi_0|, \quad (5.3.5)$$

and the state is called a pure state. It follows from the conservation of probability that  $\text{Tr}(\rho) = 1$ . Also, for a pure state,

$$\text{Tr}(\rho^2) = 1. \quad (5.3.6)$$

*Also  $\text{Tr}(\rho^2) < 1$*

\* The more complete picture of stimulated emission as developed by Lamb and Scully [1971] is found in Chapter III of Sargent, Scully and Lamb [1974].

### 5.3.1 Equation of motion for the density matrix

We can obtain the equation of motion for the density matrix from the Schrödinger equation,

$$|\dot{\psi}\rangle = -\frac{i}{\hbar} \mathcal{H} |\psi\rangle. \quad (5.3.7)$$

Taking the time derivative of  $\rho$  (Eq. (5.3.3)) we have

$$\dot{\rho} = \sum_{\psi} P_{\psi} (|\dot{\psi}\rangle\langle\psi| + |\psi\rangle\langle\dot{\psi}|), \quad (5.3.8)$$

where  $P_{\psi}$  is time independent. Using Eq. (5.3.7) to replace  $|\dot{\psi}\rangle$  and  $\langle\dot{\psi}|$  in Eq. (5.3.8) we get

$$\Rightarrow \dot{\rho} = -\frac{i}{\hbar} [\mathcal{H}, \rho]. \quad (5.3.9)$$

Equation (5.3.9) is often called the Liouville or Von Neumann equation of motion for the density matrix. It is more general than the Schrödinger equation since it uses the density operator instead of a specific state vector and can therefore give statistical as well as quantum mechanical information.

In Eq. (5.3.9), we have not included the decay of the atomic levels due to spontaneous emission. The excited atomic levels can also decay because of collisions and other phenomena. The finite lifetime of the atomic levels can be described very well by adding phenomenological decay terms to the density operator equation (5.3.9) (see also Problem 5.2).

The decay rates can be incorporated in Eq. (5.3.9) by a relaxation matrix  $\Gamma$ , which is defined by the equation

$$\dot{C}_n = \pm i\omega C_n - \gamma C_n \quad \langle n | \Gamma | m \rangle = \gamma_n \delta_{nm}. \quad (5.3.10)$$

$\Rightarrow -\Gamma_i \text{ 对应 } \omega_i - \Gamma_j \text{ 对应 } \omega_j$  With this addition, the density matrix equation of motion becomes

$$\dot{\rho} = -\frac{i}{\hbar} [\mathcal{H}, \rho] - \frac{1}{2} \underbrace{\{\Gamma, \rho\}}_{\substack{\text{衰减矩阵} \\ \text{对称}}} \underbrace{\Gamma}_{\substack{\text{对称} \\ \text{FWHM}}}, \quad (5.3.11)$$

where  $\{\Gamma, \rho\} = \Gamma \rho + \rho \Gamma$ . In general, the relaxation processes are more complicated.

The  $ij$ th matrix element of Eq. (5.3.11) is

$$\dot{\rho}_{ij} = -\frac{i}{\hbar} \sum_k (\mathcal{H}_{ik} \rho_{kj} - \rho_{ik} \mathcal{H}_{kj}) - \frac{1}{2} \sum_k (\Gamma_{ik} \rho_{kj} + \rho_{ik} \Gamma_{kj}). \quad (5.3.12)$$

This formula is useful in the treatment of many-level systems.

### 5.3.2 Two-level atom

*微光场中有限能级矩阵  
不是密度矩阵 ( $\text{Tr}(\rho) \neq 1$ )  
 $(\text{Tr}(\rho) < 1)$*

We now consider the two-level atomic system again where the state of the system is a linear combination of states  $|a\rangle$  and  $|b\rangle$ , i.e.,  $|\psi\rangle = C_a|a\rangle + C_b|b\rangle$ . Then the density matrix operator can be written as

$$\begin{aligned}\rho &= |\psi\rangle\langle\psi| = [C_a(t)|a\rangle + C_b(t)|b\rangle] [C_a^*(t)\langle a| + C_b^*(t)\langle b|] \\ &= |C_a|^2|a\rangle\langle a| + C_a C_b^*|a\rangle\langle b| + C_b C_a^*|b\rangle\langle a| + |C_b|^2|b\rangle\langle b|.\end{aligned}\quad (5.3.13)$$

Taking the matrix elements, we get

$$\rho_{aa} = \langle a|\rho|a\rangle = |C_a(t)|^2, \quad (5.3.14)$$

$$\rho_{ab} = \langle a|\rho|b\rangle = C_a(t)C_b^*(t), \quad (5.3.15)$$

$$\rho_{ba} = \rho_{ab}^*, \quad (5.3.16)$$

$$\rho_{bb} = \langle b|\rho|b\rangle = |C_b(t)|^2. \quad (5.3.17)$$

The matrix form of the density operator is

$$\rho = \begin{pmatrix} \rho_{aa} & \rho_{ab} \\ \rho_{ba} & \rho_{bb} \end{pmatrix}. \quad (5.3.18)$$

It is obvious that  $\rho_{aa}$  and  $\rho_{bb}$  are the probabilities of being in the upper and lower states, respectively. For the meaning of the off-diagonal elements we need to remember that the atomic polarization, see Eq. (5.2.25), of the two-level atom (at  $z$ ) is

$$\langle a|\vec{e}_r|b\rangle + \langle b|\vec{e}_r|a\rangle$$

$$P(z, t) = C_a C_b^* \rho_{ba} + \text{c.c.} = \rho_{ab}(z, t) \rho_{ba} + \text{c.c.} \quad (5.3.19)$$

So we see that the off-diagonal elements determine the atomic polarization.

We could have found this form for  $\rho$  more directly from Eq. (5.3.5) by remembering that in spinor notation

$$|\psi\rangle = \begin{pmatrix} C_a \\ C_b \end{pmatrix}; \quad \langle\psi| = (C_a^* \ C_b^*). \quad (5.3.20)$$

Then by matrix multiplication

$$\rho = \begin{pmatrix} C_a \\ C_b \end{pmatrix} (C_a^* \ C_b^*) = \begin{pmatrix} |C_a|^2 & C_a C_b^* \\ C_b C_a^* & |C_b|^2 \end{pmatrix}. \quad (5.3.21)$$

We can derive the equations of motion for the density matrix elements from Eq. (5.3.12) with the Hamiltonian given by Eqs. (5.2.4)

and (5.2.5). The resulting equations are

$$\dot{\rho}_{aa} = -\gamma_a \rho_{aa} + \frac{i}{\hbar} [\delta_{ab} E \rho_{ba} - \text{c.c.}], \quad (5.3.22)$$

$$\dot{\rho}_{bb} = -\gamma_b \rho_{bb} - \frac{i}{\hbar} [\delta_{ab} E \rho_{ba} - \text{c.c.}], \quad (5.3.23)$$

$$\dot{\rho}_{ab} = -(i\omega + \gamma_{ab}) \rho_{ab} - \frac{i}{\hbar} \delta_{ab} E (\rho_{aa} - \rho_{bb}), \rightarrow \text{会微 (5.3.20) 换掉} \quad (5.3.24)$$

$$\langle a | b \rangle = 0 \quad \text{(不写)} \\ \langle a | P | b \rangle \quad \text{(a \neq b)}$$

where  $\gamma_{ab} = (\gamma_a + \gamma_b)/2$  with  $\gamma_a$  and  $\gamma_b$  defined by Eq. (5.3.10) and  $E(t)$  is given by Eq. (5.2.6). In the rotating-wave approximation,  $\cos(\omega t)$  is replaced by  $\exp(-i\omega t)/2$  in Eqs. (5.3.22)–(5.3.24).

Note:  $\rho_{aa} + \rho_{bb} \neq 0$

因为是两能级不封闭。

不只有两能级，还有其他能级。

若该其他能级后阵系封闭。  
•故不平移各反身性，而是闭合的。

### 5.3.3 Inclusion of elastic collisions between atoms

The physical interpretation of the elements of the density matrix allows us to include in these equations terms associated with certain processes. One such process is the elastic collision between atoms in a gas.

In particular, during an atom–atom collision the energy levels experience random Stark shifts without a change of state and the decay rate for  $\rho_{ab}$  is increased without much change in  $\gamma_a$  and  $\gamma_b$ . The change in the decay rate of  $\rho_{ab}$  may be computed in a simple way as follows.

We assume that the random Stark shifts are included in Eq. (5.3.24) by adding a random shift  $\delta\omega(t)$  to the energy difference  $\omega$ . Ignoring the atom–field interactions for simplicity, we can write the equation of motion for the density matrix element  $\rho_{ab}$  as

$$\dot{\rho}_{ab} = -[i\omega + \underbrace{i\delta\omega(t)}_{\text{随机}} + \gamma_{ab}] \rho_{ab}. \quad (5.3.25)$$

Integrating Eq. (5.3.25) formally, we have

$$\rho_{ab}(t) = \exp \left[ -(i\omega + \gamma_{ab})t - i \int_0^t dt' \delta\omega(t') \right] \rho_{ab}(0). \quad (5.3.26)$$

We now perform an ensemble average of (5.3.26) over the random variations in  $\delta\omega(t)$ . This average affects only the  $\delta\omega(t)$  factor, so that we find  $\langle \exp[-i \int_0^t dt' \delta\omega(t')] \rangle$ .

The function  $\delta\omega$  is as often positive as negative. Hence the ensemble average  $\langle \delta\omega(t) \rangle$  is zero. Furthermore, as the variations in  $\delta\omega(t)$  are usually rapid compared to other changes which occur in times like  $1/\gamma_{ab}$ , we take

$$\text{假设} \rightarrow \langle \delta\omega(t) \delta\omega(t') \rangle = 2\gamma_{ph} \delta(t - t'), \quad (5.3.27)$$

where  $\gamma_{ph}$  is a constant. We also assume that  $\delta\omega(t)$  is described by a Gaussian random process, so that the well-known moment theorem

随机性：

of Gaussian processes is valid. Under these conditions we obtain

$$\left\langle \exp \left[ -i \int_0^t dt' \delta \omega(t') \right] \right\rangle = \exp(-\gamma_{ph} t), \quad (5.3.28)$$

which gives for the average of (5.3.26)

$$\rho_{ab}(t) = \exp[-(i\omega + \gamma_{ab} + \gamma_{ph})t] \rho_{ab}(0). \quad (5.3.29)$$

It follows, on differentiating this equation and including the interaction term, that we have the modified equation of motion for  $\rho_{ab}$ :

$$\dot{\rho}_{ab} = -(i\omega + \gamma) \rho_{ab} - \frac{i}{\hbar} \delta_{ab} E(z, t) (\rho_{aa} - \rho_{bb}), \quad (5.3.30)$$

where  $\gamma = \gamma_{ab} + \gamma_{ph}$  is the new decay rate. Equation (5.3.30) is an average equation with respect to collisions.

## 5.4 Maxwell–Schrödinger equations

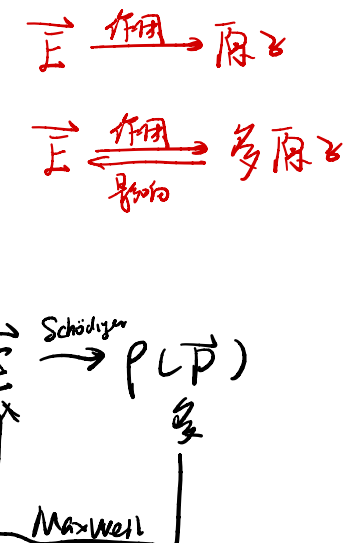
The interaction of a single atom with the single-mode field, which was discussed in the previous sections, represents a simple, idealized system. In many problems of interest in quantum optics, one is interested in the interaction of the radiation field with a large number of atoms. The prime example of such a system is a single-mode laser where atoms pumped into the excited level interact with the electromagnetic field inside a cavity. Other examples include coherent pulse propagation and optical bistability.

In this section, we develop a mathematical framework to treat such problems based on a self-consistent set of equations for the matter and the field. This set of equations and its extensions enable us to deal with many semiclassical problems where the atoms are treated quantum mechanically and the field is treated classically.

In the present semiclassical atom–field interaction, the classical field induces electric dipole moments in the medium according to the laws of quantum mechanics. The density matrix is used to facilitate the statistical summations involved in obtaining the macroscopic polarization of the medium for the individual dipole moments. The semiclassical approach, though remarkably good for many problems of interest in the study of a given system, is however inadequate to provide information about the quantum statistical features of light. These aspects will be presented in later chapters where the radiation field will be treated quantum mechanically.

其中

$$\begin{aligned} & \left\langle \int_0^t dt_1 \delta w_1(t_1) \int_0^{t_1} dt_2 \delta w_2(t_2) \right\rangle \\ &= \int_0^t dt_1 \int_0^{t_1} dt_2 \langle \delta w_1(t_1) \delta w_2(t_2) \rangle \\ &= \int_0^t dt_1 \int_0^{t_1} dt_2 \langle \delta w_1(t_1) \rangle 2\gamma_{ph} \\ &= \int_0^t dt_1 2\gamma_{ph} = 2\gamma_{ph} t. \end{aligned}$$



### 5.4.1 Population matrix and its equation of motion

We consider the interaction of an electromagnetic field with a medium which consists of two-level homogeneously broadened atoms. The individual atoms are described by the density operator (see Eqs. (5.3.14)–(5.3.17))

$$\rho(z, t, t_0) = \sum_{\alpha, \beta} \rho_{\alpha\beta}(z, t, t_0) |\alpha\rangle\langle\beta|, \quad (5.4.1)$$

原点から始まる。

where  $\alpha, \beta = a, b$  and  $\rho_{\alpha\beta}(z, t, t_0)$  are the density matrix elements for an individual atom at time  $t$  and position  $z$ , which starts interacting with the field at an initial time  $t_0$ . The initial time  $t_0$  can be random. The single-atom density matrix elements  $\rho_{\alpha\beta}(z, t, t_0)$  obey the equations of motion (5.3.22), (5.3.23), and (5.3.30). If the state of the atom at the time of injection is described by

$$\rho(z, t_0, t_0) = \sum_{\alpha, \beta} \rho_{\alpha\beta}^{(0)} |\alpha\rangle\langle\beta|, \quad (5.4.2)$$

then

$$\rho_{\alpha\beta}(z, t_0, t_0) = \rho_{\alpha\beta}^{(0)}$$

$r_a(z, t_0)$  が  $\rho_{\alpha\beta}$  の元

The effect of all the atoms which are pumped at the rate  $r_a(z, t_0)$  atoms per second per unit volume is obtained by summing over initial times. The resulting population matrix is defined as

激光照射下  $\Rightarrow$

$$\begin{aligned} \rho(z, t) &= \int_{-\infty}^t dt_0 r_a(z, t_0) \rho(z, t, t_0) \\ &= \sum_{\alpha, \beta} \int_{-\infty}^t dt_0 r_a(z, t_0) \rho_{\alpha\beta}(z, t, t_0) |\alpha\rangle\langle\beta|. \end{aligned} \quad (5.4.4)$$

当前时刻的密度是以前时刻的积累和

Generally the excitation  $r_a(z, t_0)$  varies slowly and can be taken to be a constant. The macroscopic polarization of the medium,  $P(z, t)$ , will be produced by an ensemble of atoms that arrive at  $z$  at time  $t$ , regardless of their time of excitation, i.e.,

$$\begin{aligned} P(z, t) &= \int_{-\infty}^t dt_0 r_a(z, t_0) \text{Tr}[\hat{\rho}(z, t, t_0)] \\ &= \sum_{\alpha, \beta} \int_{-\infty}^t dt_0 r_a(z, t_0) \rho_{\alpha\beta}(z, t, t_0) \delta_{\beta\alpha}, + \text{C.C.} \end{aligned} \quad (5.4.5)$$

where  $\hat{\rho}$  is the dipole moment operator and, in the second line, we have substituted for  $\rho(z, t, t_0)$  from Eq. (5.4.1). For a two-level atom, with  $\rho_{ab} = \rho_{ba} = \rho$ , we obtain

簡単化  $\Rightarrow P(z, t) = \rho [\rho_{ab}(z, t) + \text{c.c.}]$

$$(5.4.6)$$

Thus the off-diagonal elements of the population matrix determine the macroscopic polarizations.

The equations of motion for the elements of the population matrix  $\rho(z, t)$  can be obtained by taking the time derivative of Eq. (5.4.4) and using Eqs. (5.3.22), (5.3.23), and (5.3.30). For example, if the atoms are incoherently excited to levels  $|a\rangle$  and  $|b\rangle$  at a constant rate  $r_a$  ( $\rho_{ab}^{(0)} = \rho_{ba}^{(0)} = 0$ ), we obtain

$$\dot{\rho}_{aa} = (\lambda_a - \gamma_a \rho_{aa}) + \frac{i}{\hbar} (\wp E \rho_{ba} - \text{c.c.}), \quad (5.4.7)$$

$$\dot{\rho}_{bb} = \lambda_b - \gamma_b \rho_{bb} - \frac{i}{\hbar} (\wp E \rho_{ba} - \text{c.c.}), \quad (5.4.8)$$

$$\dot{\rho}_{ab} = -(i\omega + \gamma) \rho_{ab} - \frac{i}{\hbar} \wp E (\rho_{aa} - \rho_{bb}), \quad (5.4.9)$$

where  $\lambda_a = r_a \rho_{aa}^{(0)}$  and  $\lambda_b = r_b \rho_{bb}^{(0)}$ . These equations for the two-level atomic medium are coupled to the field  $E$ . The condition of self-consistency requires that the equation of motion for the field  $E$  is driven by the atomic population matrix elements. In the following section, we derive such an equation for a single-mode running wave.

### 5.4.2 Maxwell's equations for slowly varying field functions

The electromagnetic field radiation is described by Maxwell's equations:

$$\nabla \cdot \mathbf{D} = 0, \quad \nabla \times \mathbf{E} = -\frac{\partial \mathbf{B}}{\partial t}, \quad (5.4.10)$$

$$\nabla \cdot \mathbf{B} = 0, \quad \nabla \times \mathbf{H} = \mathbf{J} + \frac{\partial \mathbf{D}}{\partial t}, \quad (5.4.11)$$

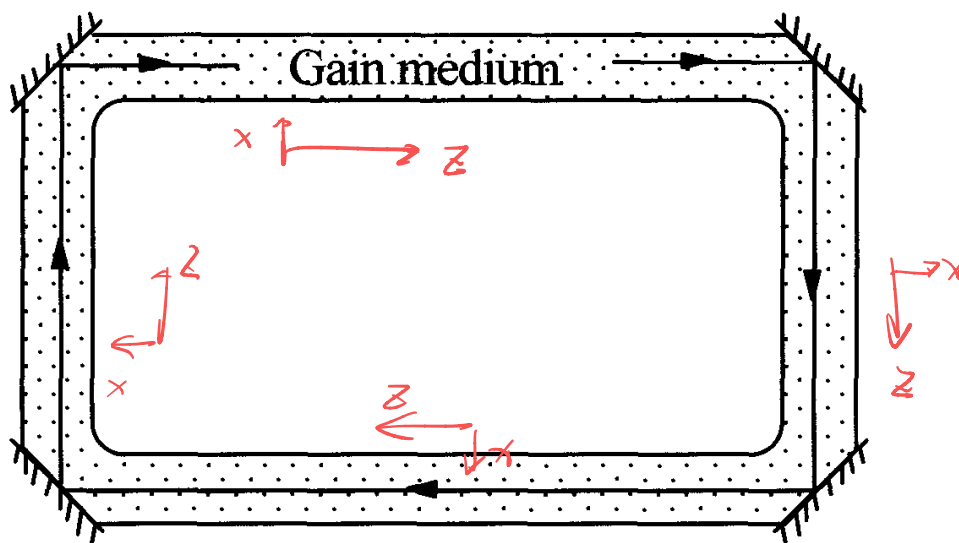
where

$$\mathbf{D} = \epsilon_0 \mathbf{E} + \mathbf{P}, \quad \mathbf{B} = \mu_0 \mathbf{H}, \quad \mathbf{J} = \sigma \mathbf{E}. \quad (5.4.12)$$

Here  $\mathbf{P}$  is the macroscopic polarization of the medium. In order to avoid a complicated boundary-value problem, we assume the presence of a medium with conductivity  $\sigma$ . This conductivity is intended to take into account phenomenologically the linear losses due to any absorbing background medium, and also those losses due to diffraction and mirror transmission. Combining the curl equations, taking the appropriate time derivatives, and using Eq. (5.4.12), we get the wave equation

$$\nabla \times (\nabla \times \mathbf{E}) + \mu_0 \sigma \frac{\partial \mathbf{E}}{\partial t} + \mu_0 \epsilon_0 \frac{\partial^2 \mathbf{E}}{\partial t^2} = -\mu_0 \frac{\partial^2 \mathbf{P}}{\partial t^2}. \quad (5.4.13)$$

Fig. 5.4  
Schematic diagram of a laser in a unidirectional ring configuration.



The polarization  $\mathbf{P}(\mathbf{r}, t)$  thus acts as a source term in the equation for the radiation field. We have in mind a situation in which the radiation field interacts with two-level atoms inside a unidirectional ring cavity as shown in Fig. 5.4. Usually both running waves exist inside the cavity. The unidirectional situation is achieved by the insertion of a device with high loss for one running wave. The variations in the field intensity transverse to the laser axis are typically slowly varying on the scale of the optical wavelength. Hence, we neglect the  $x$ - and  $y$ -dependence of  $\mathbf{E}$ , i.e.,

$$\mathbf{E}(\mathbf{r}, t) = E(z, t)\hat{\mathbf{x}}. \quad (5.4.14)$$

Equation (5.4.13) then reduces to

$$-\frac{\partial^2 E}{\partial z^2} + \mu_0 \sigma \frac{\partial E}{\partial t} + \frac{1}{c^2} \frac{\partial^2 E}{\partial t^2} = -\mu_0 \frac{\partial^2 P}{\partial t^2}. \quad (5.4.15)$$

The field of frequency  $v$  is represented as a running wave

$$\overbrace{\text{~~~~~}}^{E(z,t)} = \frac{1}{2} \underbrace{\mathcal{E}(z,t)}_{\text{慢变幅}} e^{-i[vt-kz+\phi(z,t)]} + \text{c.c.}, \quad (5.4.16)$$

where  $\mathcal{E}(z, t)$  and  $\phi(z, t)$  are slowly varying functions of position and time with  $k = v/c$ . For the problem of laser oscillation,  $k = v_c/c$  where  $v_c$  is the cavity frequency. In general,  $\mathcal{E}(z, t)$  is a complex function; however, in the present and in the next section, we assume it to be real. 若更复杂，而把相位加到 中去。

If the field is written as in Eq. (5.4.16) then the response of the medium, neglecting higher harmonics, is given by the polarization

$$P(z, t) = \frac{1}{2} \mathcal{P}(z, t) e^{-i[vt-kz+\phi(z,t)]} + \text{c.c.}, \quad (5.4.17)$$

where  $\mathcal{P}(z, t)$  is a slowly varying function of position and time.

The slowly varying complex polarization  $\mathcal{P}(z, t)$  is given in terms of the population matrix by identification of the positive frequency parts in Eqs. (5.4.6) and (5.4.17):

$$\mathcal{P}(z, t) = 2\wp \rho_{ab} e^{i[vt - kz + \phi(z, t)]}. \quad (5.4.18)$$

The expressions for  $E(z, t)$  and  $P(z, t)$  are substituted from Eqs. (5.4.16) and (5.4.17) in Eq. (5.4.15), and the following approximations are made

**慢變量：**  $\frac{\partial \mathcal{E}}{\partial t} = \frac{\partial \mathcal{E}}{\partial v} \frac{1}{v} \ll \mathcal{E}, \quad \frac{\partial \mathcal{E}}{\partial z} \ll k\mathcal{E}, \quad \frac{\partial \phi}{\partial t} \ll v, \quad \frac{\partial \phi}{\partial z} \ll k, \quad (5.4.19)$

$$\frac{\partial \mathcal{P}}{\partial t} = \frac{\partial \mathcal{P}}{\partial v} \frac{1}{v} \ll \mathcal{P}, \quad \frac{\partial \mathcal{P}}{\partial z} \ll k\mathcal{P}. \quad \frac{\partial \phi}{\partial t} = \frac{\partial \phi}{\partial v} \frac{1}{v} \ll 1 \quad (5.4.20)$$

These slowly varying amplitude and phase approximations are justified when  $\mathcal{E}$ ,  $\phi$ , and  $\mathcal{P}$  do not change appreciably in an optical frequency period. By noting that Eq. (5.4.15) can be rewritten as

$$\left( \frac{\partial}{\partial z} + \frac{1}{c} \frac{\partial}{\partial t} \right) \left( -\frac{\partial}{\partial z} + \frac{1}{c} \frac{\partial}{\partial t} \right) E = -\mu_0 \sigma \frac{\partial E}{\partial t} - \mu_0 \frac{\partial^2 P}{\partial t^2}, \quad (5.4.21)$$

and

$$\left( -\frac{\partial}{\partial z} + \frac{1}{c} \frac{\partial}{\partial t} \right) E \cong -2ikE, \quad \text{而且}$$

we obtain

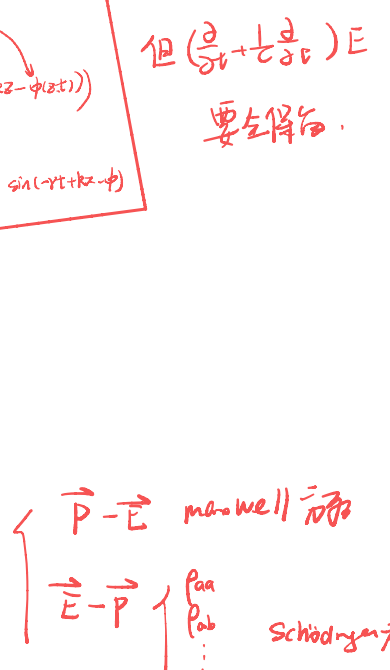
$$(5.4.16 \sim 5.4.22) \quad \frac{\partial \mathcal{E}}{\partial z} + \frac{1}{c} \frac{\partial \mathcal{E}}{\partial t} = -\kappa \mathcal{E} - \frac{1}{2\epsilon_0} k \operatorname{Im} \mathcal{P}, \quad (5.4.23)$$

$$5.4.24 \quad \frac{\partial \phi}{\partial z} + \frac{1}{c} \frac{\partial \phi}{\partial t} = k - \frac{v}{c} - \frac{1}{2\epsilon_0} k \mathcal{E}^{-1} \operatorname{Re} \mathcal{P}, \quad (5.4.24)$$

where  $\kappa = \sigma / 2\epsilon_0 c$  is the linear loss coefficient.

Equations (5.4.7)–(5.4.9), (5.4.23), and (5.4.24) form a self-consistent set of equations. This set of equations is the starting point of the study of many systems involving the interaction of the radiation field with an ensemble of atoms. The generalization of this set of equations to a multi-level atomic system and a multi-mode field is straightforward.

As an important example of the applications of this set of equations, we present the semiclassical theory of the laser in the next section.



## 5.5 Semiclassical laser theory

In this section, we first outline the basic principle of laser operation and then present a theory of the laser as developed principally by Lamb and co-workers. The threshold condition for a laser and the evolution equation of the electromagnetic field is also derived.

### 5.5.1 Basic principle

In 1954, Gordon, Zeiger, and Townes showed that coherent electromagnetic radiation can be generated in the radio frequency range by the so-called maser (microwave amplification by stimulated emission of radiation). The first maser action was observed in ammonia.

The maser principle was extended by Schawlow and Townes, and also by Prokhorov, to the optical domain, thus obtaining a laser (light amplification by stimulated emission of radiation). A laser consists of a set of atoms interacting with an electromagnetic field inside a cavity. The cavity supports only a specific set of modes corresponding to a discrete sequence of eigenfrequencies. The active atoms, i.e., the ones that are pumped to the upper level of the laser transition, are in resonance with one of the eigenfrequencies of the cavity. A resonant electromagnetic field gives rise to stimulated emission, and the atoms transfer their excitation energy to the radiation field. The emitted radiation is still at resonance. If the upper level is sufficiently populated, this radiation gives rise to further transitions in other atoms. In this way all the excitation energy of the atoms is transferred to a single mode of the radiation field.

The first pulsed laser operation was demonstrated by Maiman in ruby. The first continuous wave (cw) laser, a He–Ne gas laser, was built by Javan. Since then, a large variety of systems have been demonstrated to exhibit lasing action; generating coherent light over a frequency domain ranging from infrared to ultraviolet. These include dye lasers, chemical lasers, and semiconductor lasers. A new class of lasers which uses electrons in a periodic magnetic field (called free-electron lasers) has also been developed.

From our discussion of the laser principle, it is clear that a laser theory should incorporate three basic elements, an active medium (two-level atoms with population inversion), pumping to the upper lasing level, and the radiation losses due to the cavity. A systematic semiclassical theory of the laser was developed by Lamb.

### 5.5.2 Lamb's semiclassical theory

环型单向腔

We consider the semiclassical laser theory for the simple case of a linearly polarized electric field in a unidirectional ring cavity and two-level homogeneously broadened, active atoms.

The time dependence of the electric field  $\mathcal{E}(z, t)$  can be separated from the spatial part by expanding the field in the normal modes

of the cavity. In a ring cavity only certain discrete modes achieve appreciable magnitude, namely, those with the frequencies

$$\nu_m = \frac{m\pi c}{S} = k_m c, \quad (5.5.1)$$

where  $S$  is the circumference of the ring,  $m$  is a large integer (typically of the order  $10^6$ ), and  $k_m$  is the corresponding wave number. Here, we consider a single mode with unidirectional (running-wave) mode functions  $U(z) = \exp(ikz)$  (Fig. 5.4).

The equations of motion for the field amplitude (5.4.23) and phase (5.4.24) for the present problem reduce to

$$\frac{\partial \mathcal{E}}{\partial t} = -\frac{1}{2} \mathcal{C} \mathcal{E} - \frac{1}{2} \left( \frac{\nu}{\epsilon_0} \right) \text{Im} \mathcal{P}, \quad (5.5.2a)$$

$$\frac{\partial \phi}{\partial t} = (\nu_c - \nu) - \frac{1}{2} \left( \frac{\nu}{\epsilon_0} \right) \mathcal{E}^{-1} \text{Re} \mathcal{P}, \quad (5.5.2b)$$

where  $\nu_c$  is the cavity frequency and  $\gamma = (\gamma_a + \gamma_b)/2$ . In Eq. (5.5.2a),  $\kappa$  has been replaced by  $\mathcal{C}/2c$  where  $\mathcal{C} = \nu_c/Q$  (where  $Q$  is the quality factor of the cavity) to account for the field losses through the mirrors of the cavity. The driving polarization  $\mathcal{P}$  (Eq. (5.4.18)) is determined by Eq. (5.4.9) which yields

$$\begin{aligned} \mathcal{P}(z, t) &= \frac{-i\wp^2}{\hbar} \int_{-\infty}^t \exp[-\gamma(t-t') - i(\omega-\nu)(t-t')] \\ &\times \mathcal{E}(t')[\rho_{aa}(t') - \rho_{bb}(t')] dt'. \end{aligned} \quad (5.5.3)$$

The integral (5.5.3) can be simply performed, provided the amplitude  $\mathcal{E}(t')$  and the population difference  $\rho_{aa} - \rho_{bb}$  do not change appreciably in the time  $1/\gamma$ , for then these terms can be factored outside the integral. This solution leads to rate equations for the atomic populations. These approximations are exact in steady state ( $\dot{\mathcal{P}} = 0$ ). This gives

$$\text{Im} \mathcal{P}(t) = \frac{-\wp^2}{\hbar} \mathcal{E}(t) \gamma \frac{\rho_{aa}(t) - \rho_{bb}(t)}{\gamma^2 + (\omega - \nu)^2}, \quad (5.5.4a)$$

$$\text{Re} \mathcal{P}(t) = \frac{-\wp^2}{\hbar} \mathcal{E}(t) (\omega - \nu) \frac{\rho_{aa}(t) - \rho_{bb}(t)}{\gamma^2 + (\omega - \nu)^2}. \quad (5.5.4b)$$

On substituting Eqs. (5.5.4) into the equations of motion for  $\rho_{aa}$  and  $\rho_{bb}$  ((5.4.7) and (5.4.8)), we obtain the rate equations

$$\dot{\rho}_{aa} = \lambda_a - \gamma_a \rho_{aa} - R(\rho_{aa} - \rho_{bb}), \quad (5.5.5a)$$

$$\dot{\rho}_{bb} = \lambda_b - \gamma_b \rho_{bb} + R(\rho_{aa} - \rho_{bb}), \quad (5.5.5b)$$

where the rate constant is

$$R = \frac{1}{2} \left( \frac{\wp \mathcal{E}}{\hbar} \right)^2 \frac{\gamma}{\gamma^2 + (\omega - \nu)^2}. \quad (5.5.6)$$

$\mathcal{E}$  是腔场本征场  
 $\mathcal{P}$  是实际光场

It is evident that the rate constant  $R$ , which determines the rate at which the population difference varies in time, depends primarily on the rate at which the total field intensity varies. Hence, the rate-equation approximation consists of the assumption that the electric field envelope varies slowly in atomic lifetimes. We can determine the population difference in the steady state from Eqs. (5.5.5). This difference can be substituted in turn back into the equations for  $\text{Im}\mathcal{P}$  and  $\text{Re}\mathcal{P}$ , thus determining the polarization components.

*激光器正负输出*

→ *输出*

In the steady state ( $\dot{\rho}_{aa} = \dot{\rho}_{bb} = 0$ ), Eqs. (5.5.5) yield

$$\text{输出反差} = \rho_{aa} - \rho_{bb} = \frac{N_0}{1 + R/R_s}, \quad (\text{R为总衰减系数}) \quad (5.5.7)$$

where  $N_0 = \lambda_a \gamma_a^{-1} - \lambda_b \gamma_b^{-1}$  and  $R_s = \gamma_a \gamma_b / 2\gamma$ . The population difference is therefore given by  $N_0$ , which appears in the absence of the field, divided by a factor which increases as the intensity of the electric field increases.

Combining Eq. (5.5.7) with Eqs. (5.5.4) and (5.5.2) we obtain the amplitude and frequency determining equations

$$\dot{\mathcal{E}} = -\frac{\mathcal{C}}{2}\mathcal{E} + \frac{\mathcal{A}\mathcal{E}}{2[1 + \frac{\mathcal{B}}{\mathcal{A}}(\frac{\epsilon_0 V}{2\hbar\nu})\mathcal{E}^2]}, \quad (5.5.8)$$

$$\nu + \dot{\phi} = \nu_c + \frac{(\omega - \nu)\mathcal{A}}{2\gamma[1 + \frac{\mathcal{B}}{\mathcal{A}}(\frac{\epsilon_0 V}{2\hbar\nu})\mathcal{E}^2]}, \quad (5.5.9)$$

where  $V$  is the volume of the cavity and

$$\mathcal{A} = \left( \frac{\wp^2 \nu \gamma}{\epsilon_0 \hbar} \right) \frac{N_0}{\gamma^2 + (\omega - \nu)^2}, \quad \text{线性增益} \quad (5.5.10a)$$

$$\mathcal{B} = \left( \frac{4\wp^2}{\hbar^2} \right) \left( \frac{\gamma^2}{\gamma_a \gamma_b} \right) \frac{\mathcal{A}}{\gamma^2 + (\omega - \nu)^2} \left( \frac{\hbar\nu}{2\epsilon_0 V} \right). \quad \text{饱和参数} \quad (5.5.10b)$$

Here  $\mathcal{A}$  is the linear gain parameter and  $\mathcal{B}$  is the saturation parameter.

We now define a dimensionless intensity

$$n = \frac{\epsilon_0 \mathcal{E}^2 V}{2\hbar\nu}, \quad (5.5.11)$$

which corresponds to the ‘number of photons’ in the laser. (Here,  $\epsilon_0 \mathcal{E}^2 V / 2$  is the total energy in the laser beam and  $\hbar\nu$  is the energy associated with a single photon.) This statement will be sharpened when we study the quantum theory of the laser in Chapter 11. It follows from Eqs. (5.5.8) and (5.5.9) that

$$\dot{n} = -\mathcal{C}n + \frac{\mathcal{A}n}{1 + \frac{\mathcal{B}}{\mathcal{A}}n}, \quad (5.5.12)$$

$$\nu + \dot{\phi} = \nu_c + \frac{(\omega - \nu)\mathcal{A}}{2\gamma(1 + \frac{\mathcal{B}}{\mathcal{A}}n)}. \quad (5.5.13)$$

$$\begin{aligned} \text{左端} &= \frac{\epsilon_0 \mathcal{E}^2 V}{2\hbar\nu} \\ &= \frac{\epsilon_0 \mathcal{E}^2}{2} \sin^2 \theta + \frac{B^2 \cos^2 \theta}{2\hbar\nu} \\ &= \frac{\epsilon_0 \mathcal{E}^2}{2} \end{aligned}$$

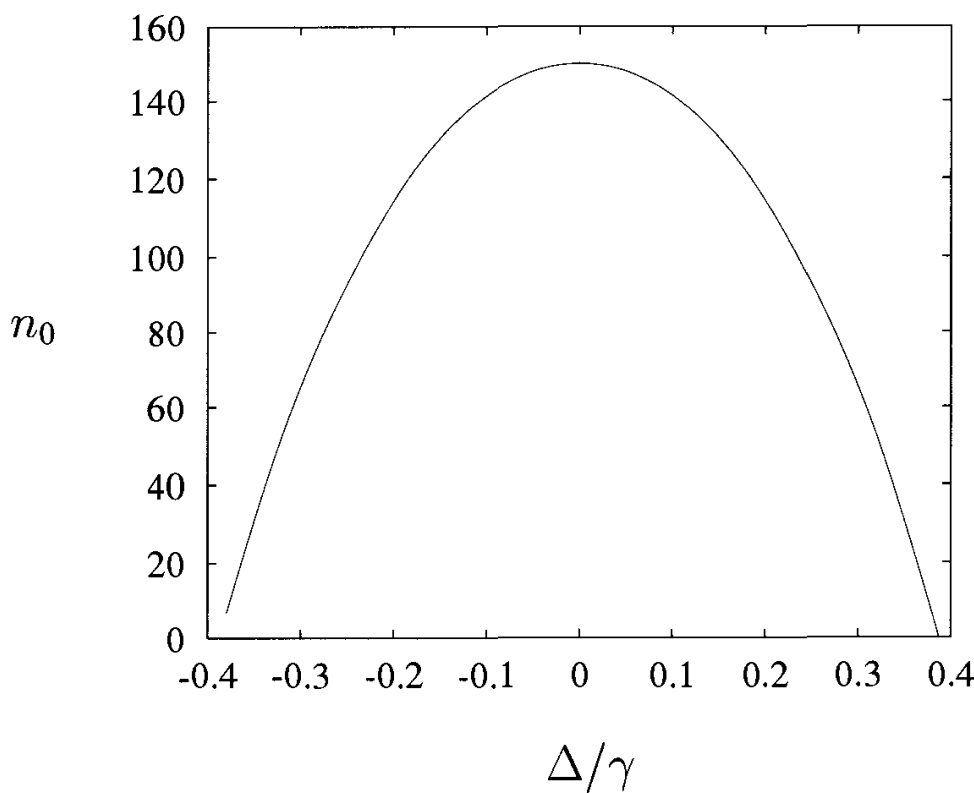


Fig. 5.5  
A plot of the steady-state intensity  $n_0$  versus the detuning  $\delta/\gamma$ . Here  $\mathcal{C} = 1\mu\text{sec}^{-1}$ ,  $\phi^2 v N_0 / \epsilon_0 \hbar \gamma = 1.15\mu\text{sec}^{-1}$ , and  $2\phi^4 v^2 N_0 / \epsilon_0^2 \hbar^2 \gamma_a \gamma_b \gamma V = 10^{-3}\mu\text{sec}^{-1}$ .

小贴士

For small excitations ( $\mathcal{B}n/\mathcal{A} \ll 1$ ), a perturbation theory is obtained by expanding the denominator in Eqs. (5.5.12) and (5.5.13), resulting in

$$\dot{n} = (\mathcal{A} - \mathcal{C}) n - \mathcal{B}n^2, \quad (5.5.14)$$

$$v + \dot{\phi} = v_c + \left( \frac{\omega - v}{2\gamma} \right) (\mathcal{A} - \mathcal{B}n). \quad (5.5.15)$$

Equations (5.5.14) and (5.5.15) are the basic equations for the laser. As shown below, they yield the laser threshold condition, the steady-state and transient intensity of the laser, and the frequency pulling due to the presence of the gain medium.

It is easily seen from Eq. (5.5.14) that, in steady state ( $\dot{n} = 0$ ),  $n = 0$  unless  $\mathcal{A} > \mathcal{C}$ . When  $\mathcal{A} > \mathcal{C}$ , the steady-state intensity is given by

$$n_0 \equiv n = \frac{\mathcal{A} - \mathcal{C}}{\mathcal{B}}. \quad (5.5.16)$$

Thus, the laser threshold condition is  $\mathcal{A} = \mathcal{C}$ , i.e., when the gain is equal to the cavity losses.

In Fig. 5.5, the steady-state intensity is plotted against the detuning  $\Delta = \omega - v$ . According to Eq. (5.5.15), the oscillation frequency  $v$  itself depends on the intensity. A good approximation, however, results from taking  $v = v_c$  in the calculation of the various coefficients.

The frequency determining Eq. (5.5.15) predicts a pulling of the oscillation frequency from the passive cavity frequency towards line

center. Specifically, in steady state ( $\dot{\phi} = 0$ )

$$v = \frac{v_c + \mathcal{S}\omega}{1 + \mathcal{S}}, \quad (5.5.17)$$

where the stabilization factor

$$\mathcal{S} = \frac{\mathcal{A} - \mathcal{B}n_0}{2\gamma} = \frac{\mathcal{C}}{2\gamma}. \quad (5.5.18)$$

Equation (5.5.17) can be interpreted as a center-of-mass equation in which the oscillation frequency  $v$  assumes the average value of  $v_c$  and  $\omega$  with weights 1 and  $\mathcal{S}$ , respectively. In the typical case,  $\mathcal{C} \ll 2\gamma$  and therefore  $v \cong v_c$ , but  $v$  is pulled closer to the atomic frequency  $\omega$ . This is called mode pulling.

频率牵引，腔决定走向

## 5.6 A physical picture of stimulated emission and absorption

In order to better appreciate the physics behind stimulated emission and absorption, let us consider an atom at the point  $z = 0$  interacting with the field  $E(z, t) = \mathcal{E}(z, t) \cos(\nu t - kz)$ . As before, the amplitudes  $C_a$  and  $C_b$  are determined by Eqs. (5.2.7) and (5.2.8), and the slowly varying amplitudes  $c_a = C_a e^{i\omega_a t}$  and  $c_b = C_b e^{i\omega_b t}$  are determined by Eqs. (5.2.12) and (5.2.13), respectively. For simplicity, we assume exact resonance  $\Delta = \omega - \nu = 0$ . Then the solution (5.2.21)–(5.2.22) becomes

$$c_a(t) = \left[ c_a(0) \cos\left(\frac{\Omega_R t}{2}\right) + i c_b(0) \sin\left(\frac{\Omega_R t}{2}\right) \right], \quad (5.6.1a)$$

$$c_b(t) = \left[ c_b(0) \cos\left(\frac{\Omega_R t}{2}\right) + i c_a(0) \sin\left(\frac{\Omega_R t}{2}\right) \right], \quad (5.6.1b)$$

where we have assumed a real dipole matrix element  $\rho_{ab} = \rho_{ba} \equiv \rho$ . Now, to the lowest order, we may trivially calculate  $\rho_{ab} = c_a c_b^* e^{-i\omega t}$  for the cases of atom in the excited state and the ground state.

For the first case (stimulated emission), in which  $c_a(0) = 1$  and  $c_b(0) = 0$ , we find to lowest order for an atom which passes through the laser cavity in a time  $\tau$

$$c_a(\tau) \cong 1, \quad (5.6.2a)$$

$$c_b(\tau) \cong i \frac{\Omega_R \tau}{2}, \quad (5.6.2b)$$

and the polarization is then (see Eq. (5.4.18))

$$\begin{aligned} \mathcal{P} &= 2\rho \rho_{ab} e^{i\nu\tau} \\ &\cong -i\rho \Omega_R \tau. \end{aligned} \quad (5.6.3)$$

For the case of absorption, initially  $c_a(0) = 0$ ,  $c_b(0) = 1$ , to the lowest order one gets

$$c_a(\tau) \cong i \frac{\Omega_R \tau}{2}, \quad (5.6.4a)$$

$$c_b(\tau) \cong 1, \quad (5.6.4b)$$

and

$$\mathcal{P} \cong i \wp \Omega_R \tau. \quad (5.6.5)$$

Now, using Eq. (5.4.23), for the atom initially in the excited state we have

$$\frac{1}{c} \frac{\partial \mathcal{E}}{\partial t} = \frac{k}{2\epsilon_0} \frac{\wp^2}{\hbar} \mathcal{E} \tau, \quad (5.6.6)$$

where we have neglected the cavity loss. It follows from Eq. (5.6.6) that the change in the electric field during the time  $\tau$  is

$$\Delta \mathcal{E} \cong \frac{ck}{2\epsilon_0} \frac{\wp^2}{\hbar} \mathcal{E} \tau^2, \quad (5.6.7)$$

i.e., the incident field experiences gain.

Likewise for the atom initially in the ground state, we have

$$\frac{1}{c} \frac{\partial \mathcal{E}}{\partial t} = -\frac{k}{2\epsilon_0} \frac{\wp^2}{\hbar} \mathcal{E} \tau, \quad (5.6.8)$$

and therefore

$$\Delta \mathcal{E} \cong -\frac{ck}{2\epsilon_0} \frac{\wp^2}{\hbar} \mathcal{E} \tau^2, \quad (5.6.9)$$

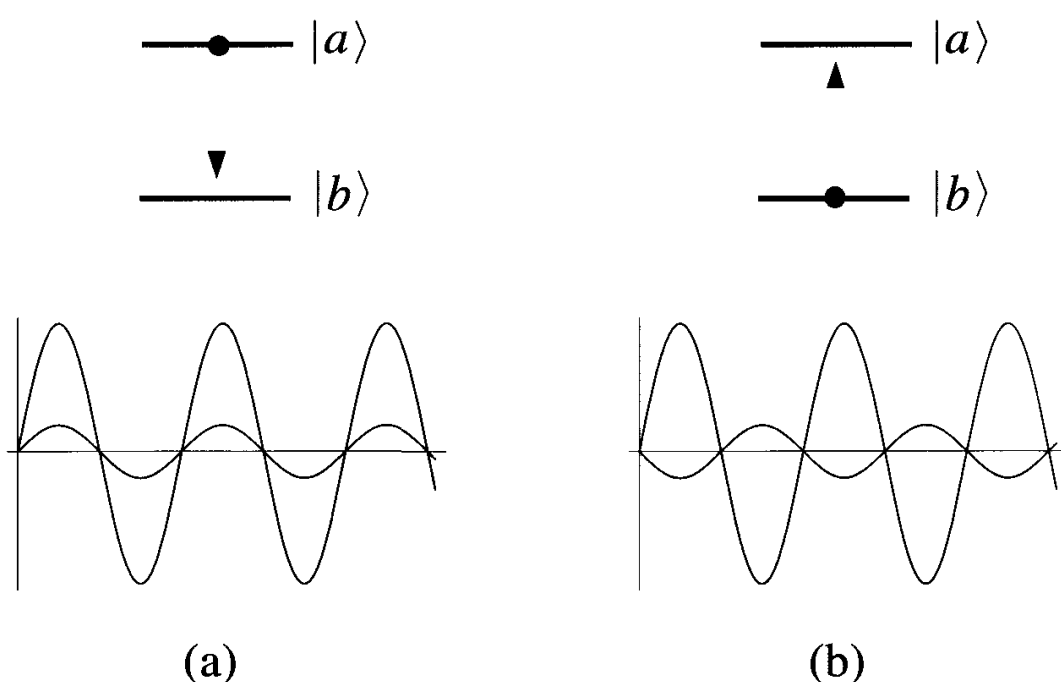
i.e., the incident field experiences loss. Thus the atom acts essentially as a tiny oscillating electronic current induced by the incident light field. Attenuation of an incident field is then the result of the radiation from this current interfering destructively with the incident light (see Fig. 5.6). This simple physical picture of stimulated emission and absorption can be expanded to explain more complicated phenomena, e.g., lasing without inversion, as we shall see in Section 7.3.1.

## 5.7 Time delay spectroscopy

In the previous section, we saw how simple and intuitively pleasing the concepts of stimulated emission and absorption are when treated within the framework of semiclassical radiation theory. As an example

Fig. 5.6

- (a) Emission:  
induced dipole  
radiation interferes  
constructively with  
incident radiation.  
(b) Absorption:  
induced dipole  
radiation interferes  
destructively with  
incident radiation.



of unusual and counter-intuitive physics within the framework of semiclassical theory, we conclude this chapter with a discussion of time delay spectroscopy.

In conventional spectroscopy, the limit of resolution of the energy between two levels  $|a\rangle$  and  $|b\rangle$  is governed by the sum of the decay rates  $\gamma_a$  and  $\gamma_b$  out of these levels.

In this section we present a spectroscopic technique which provides resolution beyond the natural linewidth. These considerations are based on the fact that in the *transient regime*, the probability for induced transitions in a two-level system interacting with a monochromatic electromagnetic field is not governed by a Lorentzian of width  $(\gamma_a + \gamma_b)/2 \equiv \gamma_{ab}$ , but rather by  $(\gamma_a - \gamma_b)/2 \equiv \delta_{ab}$ . The Lorentzian width  $\gamma_{ab}$ , which usually appears in atomic physics, is regained only in the proper limits.

We proceed by considering the experimental situation in which an ensemble of two-level atoms is excited at time  $t = t_0$  into the  $|b\rangle$  state by some ‘instantaneous’ excitation mechanism, e.g., a picosecond optical pulse. The excited atoms are then driven by a monochromatic but tunable radiation field.

Consider the level scheme illustrated in Fig. 5.7. There we see an atom with two unstable levels  $|a\rangle$  and  $|b\rangle$  and a weak field driving the atom from the lower level  $|b\rangle$  to the upper level  $|a\rangle$ . If one includes the lower levels ( $|c\rangle$  and  $|d\rangle$ ) to which  $|a\rangle$  and  $|b\rangle$  decay, this may be considered as a four-level atom. That is, we prepare the atom in level  $|b\rangle$  at  $t_0$ , drive the atom to level  $|a\rangle$ , and count the number of atoms accumulating in level  $|c\rangle$ , starting a finite time  $t$  after the atom is

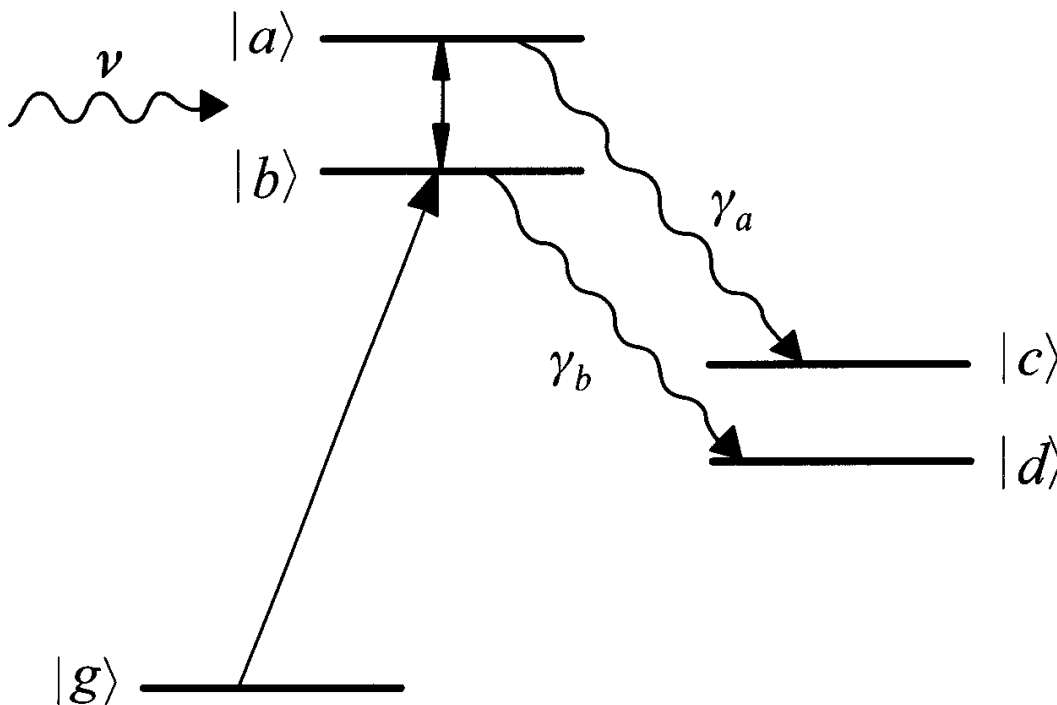


Fig. 5.7  
Level diagram indicating excitation of atom from ground state to  $|b\rangle$ , subsequent interaction with resonant radiation promoting atom from  $|b\rangle$  to  $|a\rangle$  with attendant decays to states  $|d\rangle$  and  $|c\rangle$  at rates  $\gamma_b$  and  $\gamma_a$ , respectively.

prepared. The counting rate is measured as a function of the detuning between the laser and atomic frequencies.

We proceed by solving the density matrix equations of motion (5.3.22)–(5.3.24) for  $\rho_{aa}(t)$  to lowest nonvanishing order. This yields

$$\begin{aligned} \rho_{aa}(t) \\ = \frac{\Omega_R^2}{\Delta^2 + \delta_{ab}^2} [e^{-\gamma_a(t-t_0)} + e^{-\gamma_b(t-t_0)} - 2e^{-\gamma_{ab}(t-t_0)} \cos \Delta(t-t_0)], \end{aligned} \quad (5.7.1)$$

where  $\delta_{ab} = (\gamma_a - \gamma_b)/2$ ,  $\Omega_R$  is the Rabi frequency of the driven transition and  $\Delta$  is the detuning between the laser and  $\omega_{ab}$ . The key point is that the Lorentzian factor in (5.7.1) goes as  $\gamma_a - \gamma_b$  not  $\gamma_a + \gamma_b$ .

Now suppose we count the number of photons emitted when the excited atom makes the  $|a\rangle \rightarrow |c\rangle$  transition. This will be equal to the total number of atoms accumulated in level  $|c\rangle$  which is determined by the simple rate equation

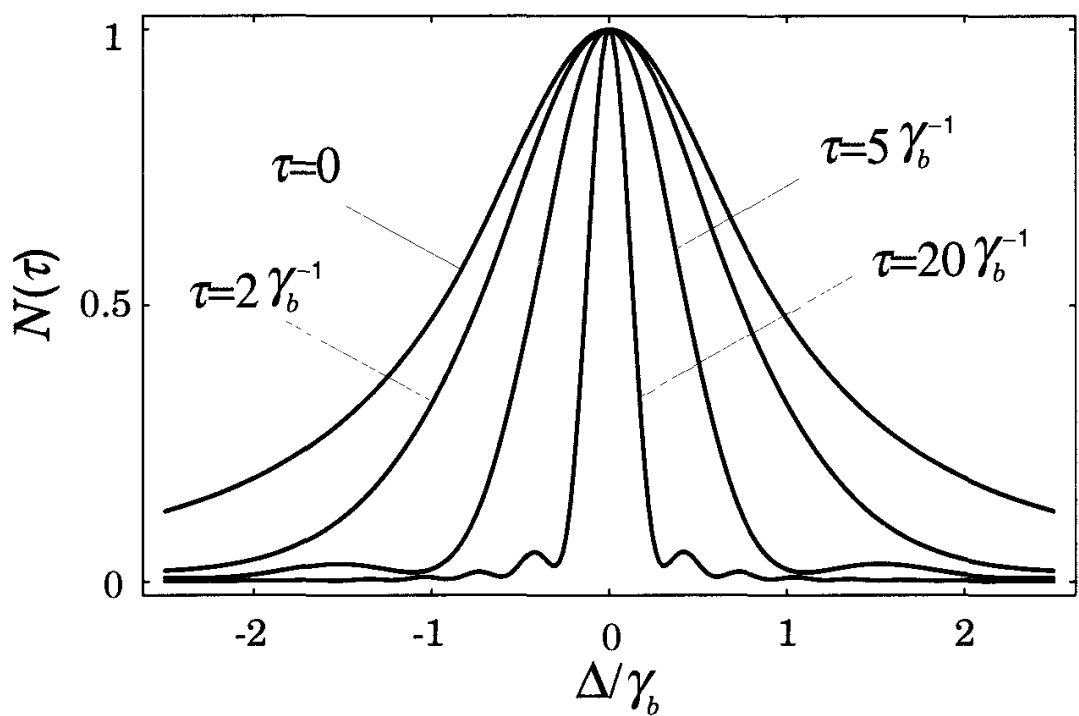
$$\dot{\rho}_{cc}(t, t_0) = \gamma \rho_{aa}(t, t_0), \quad (5.7.2)$$

where the notation reminds us that the atoms are initially excited at time  $t_0$ . Then the total number of spontaneously emitted photons from time  $t_0$  to a time long after the initial excitation to level  $|b\rangle$  is given by

$$N(\Delta, t_0) = \eta \gamma_a \int_{t_0}^{\infty} \rho_{aa}(\Delta, t, t_0) dt, \quad (5.7.3)$$

where  $\eta$  is a constant determined by the efficiency of photon detection.

**Fig. 5.8**  
 Time delay  
 spectroscopy signal  
 $N(\tau)$  for different  $\tau$ . The different curves have been  
 normalized for  
 simplicity. In fact the  
 peak heights of the  
 curves corresponding  
 to larger  $\tau$  are  
 strongly reduced as  
 indicated by  
 Eq. (5.7.6).  
 Nevertheless the line  
 narrowing can be  
 useful as discussed  
 by Figger and  
 Walther (1974).



Inserting (5.7.1) into (5.7.3) we find

$$N(\Delta, t_0) = \frac{\eta\gamma_a\Omega_R^2}{\Delta^2 + \gamma_{ab}^2} \frac{2\gamma_{ab}}{\gamma_a\gamma_b}. \quad (5.7.4)$$

That is, when we carry out the above procedure, collecting the  $|a\rangle \rightarrow |c\rangle$  photons from  $t_0$  onwards we regain the usual Lorentzian of width  $\gamma_{ab}$ . This is reassuring since in most experiments it is indeed  $\gamma_{ab}$  that governs the resolution of our experiments.

However, let us now wait for a time  $t_0 + \tau$  before accepting any counts. That is let us measure

$$N(\Delta, t_0 + \tau) = \eta\gamma_a \int_{t_0+\tau}^{\infty} \rho_{aa}(\Delta, t, t_0) dt. \quad (5.7.5)$$

Inserting (5.7.1) into (5.7.5) we now find\*

$$\begin{aligned} N(\Delta, t_0 + \tau) &= \frac{\eta\gamma_a\Omega_R^2}{\Delta^2 + \delta_{ab}^2} \left[ \frac{\exp(-\gamma_a\tau)}{\gamma_a} + \frac{\exp(-\gamma_b\tau)}{\gamma_b} \right. \\ &\quad \left. + \frac{2\exp(-\gamma_{ab}\tau)}{\Delta^2 + \gamma_{ab}^2} (\Delta \sin \Delta\tau - \gamma_{ab} \cos \Delta\tau) \right]. \end{aligned} \quad (5.7.6)$$

The point is clear. When we delay observation we find a line narrowing as is seen by comparing Eqs. (5.7.4) and (5.7.6). Equation (5.7.6) is plotted for various values of time delay in Fig. 5.8.

We conclude by noting that, as pointed out explicitly by Figger and Walther, the line narrowing in time delay spectroscopy provides a

\* See Meystre, Scully, and Walther [1980].

high spectral *resolution* in the sense that we can separate closely spaced lines. However, this higher resolution does not always lead to a higher experimental *accuracy* in the final result for the atomic transition frequencies  $\omega_{ab}$ . The reason for this is the exponential damping of the signal with the time delay  $\tau$  by means of the prefactors  $\exp(-\gamma_a \tau)$  and  $\exp(-\gamma_b \tau)$  in Eq. (5.7.6) which decrease the signal. We will return to the question of enhancing spectroscopic resolution in later chapters, e.g., in Section 21.7.

## 5.A Equivalence of the $\mathbf{r} \cdot \mathbf{E}$ and the $\mathbf{p} \cdot \mathbf{A}$ interaction Hamiltonians

In Section 5.1 we noted that in the radiation gauge (*R*-gauge) and in the dipole approximation  $(\mathbf{A}(\mathbf{r}, t), U(\mathbf{r}, t)) \equiv (\mathbf{A}(t), 0)$ , the gauge transformation

$$\chi(\mathbf{r}, t) = -\frac{e}{\hbar} \mathbf{A}(t) \cdot \mathbf{r} \quad (5.A.1)$$

yields the gauge  $(0, -\mathbf{E}(t) \cdot \mathbf{r})$ . We observe that the gauge  $(0, -\mathbf{E}(t) \cdot \mathbf{r})$  leads to the electric-dipole interaction  $\mathcal{H}$  (Eq. (5.1.19)), and thus we call it the electric field gauge (*E*-gauge). The two Hamiltonians  $\mathcal{H}$  (Eq. (5.1.19)) and  $\mathcal{H}'$  (Eq. (5.1.21)) are therefore related via the gauge transformation (5.A.1). A gauge transformation requires a transformation of the potentials according to Eqs. (5.1.6) and (5.1.7) and of the wave functions according to Eq. (5.1.4). Nonidentical, *wrong* results are obtained for physically measurable quantities in different gauges if only one of these two transformations is carried out. We will discuss how we have to handle the wave functions in the two different gauges in order to obtain gauge-invariant physical predictions. Before this, however, let us briefly discuss some examples of physical quantities.

### 5.A.1 Form-invariant physical quantities

A form-invariant physical quantity is defined as a quantity whose corresponding operator  $G_\chi = G(A_\chi, U_\chi)$  is form invariant under a unitary transformation  $T(\mathbf{r}, t) = \exp[i\chi(\mathbf{r}, t)]$ , i.e.,

$$G_{\chi'} = T G_\chi T^\dagger, \quad (5.A.2)$$

where the wave function in the gauge  $\chi$  is transformed to the gauge  $\chi'$  by the unitary transformation

$$\psi_{\chi'}(\mathbf{r}, t) = T(\mathbf{r}, t) \psi_\chi(\mathbf{r}, t). \quad (5.A.3)$$

The difference between physical and nonphysical quantities lies in the gauge invariance of the eigenvalues. The eigenvalues of a physical quantity are identical in all gauges, whereas the eigenvalues of nonphysical quantities depend on the chosen gauge. In order to show this, we denote the eigenvalues and eigenstates of the operator  $G_\chi$  by  $g_n$  and  $|\xi_{\chi,n}\rangle$ , respectively:

$$G_\chi |\xi_{\chi,n}\rangle = g_n |\xi_{\chi,n}\rangle. \quad (5.A.4)$$

Only for physical quantities are the eigenvalues  $g_n$  gauge invariant, i.e.,

$$\begin{aligned} G_{\chi'} |\xi_{\chi',n}\rangle &= T G_\chi T^\dagger T |\xi_{\chi,n}\rangle \\ &= T g_n |\xi_{\chi,n}\rangle \\ &= g_n |\xi_{\chi',n}\rangle. \end{aligned} \quad (5.A.5)$$

Hence, nonphysical quantities can only be used as calculational tools.

We next consider some examples of physical and nonphysical quantities. The starting point for these considerations is the fact that the operators  $\mathbf{r}$  and  $\mathbf{p}$  ( $\mathbf{p} = -i\hbar\nabla$ ), associated with the position and the canonical momentum of the particle, are the same in all gauges, by which we mean that  $\mathbf{p}$  is represented by  $-i\hbar\nabla$  in all gauges. This ensures that, in any gauge, the commutation relation  $[\mathbf{r}_j, \mathbf{p}_k] = i\hbar\delta_{jk}$  is satisfied. With this rule the operator for the mechanical momentum,

$$\pi_\chi = \mathbf{p} - e\mathbf{A}_\chi(\mathbf{r}, t), \quad (5.A.6)$$

is a physical, measurable quantity since

$$\begin{aligned} T\pi_\chi T^\dagger &= T[\mathbf{p} - e\mathbf{A}_\chi(\mathbf{r}, t)]T^\dagger \\ &= \mathbf{p} - e\mathbf{A}_\chi - \hbar\nabla\chi \\ &= \mathbf{p} - e\mathbf{A}_{\chi'} \\ &= \pi_{\chi'}. \end{aligned} \quad (5.A.7)$$

Similarly, the instantaneous energy operator of the system, consisting of the kinetic energy and the static potential (normally the atomic binding potential)

$$\mathcal{E}_\chi = \frac{1}{2m} [\mathbf{p} - e\mathbf{A}_\chi(\mathbf{r}, t)]^2 + V(r), \quad (5.A.8)$$

represents a physical quantity as well as any other operator which is only a function of other physical quantities like  $\pi_\chi$ .

On the other hand, the canonical momentum  $\mathbf{p}$  is not a physical quantity since

$$T\mathbf{p}T^\dagger = \mathbf{p} - \hbar\nabla\chi \neq \mathbf{p}. \quad (5.A.9)$$

In a similar way, the operator  $\mathcal{H}_0 = p^2/2m$  (which does not depend on potentials) is not a physical quantity because

$$T\mathcal{H}_0 T^\dagger = \mathcal{H}_0 - \frac{\hbar}{2m} [\mathbf{p} \cdot \nabla \chi + (\nabla \chi) \cdot \mathbf{p}] + \frac{\hbar^2}{2m} (\nabla \chi)^2 \neq \mathcal{H}_0. \quad (5.A.10)$$

In general, any operator which is a function of nonphysical quantities alone, like the canonical momentum  $\mathbf{p}$  or the vector or the scalar potentials  $\mathbf{A}_\chi$  or  $U_\chi$ , represents a nonphysical quantity. The total Hamiltonian

$$\mathcal{H}_\chi = \frac{1}{2m} [\mathbf{p} - e\mathbf{A}_\chi(\mathbf{r}, t)]^2 + eU_\chi(\mathbf{r}, t) + V(r) \quad (5.A.11)$$

is also a nonphysical quantity, since it depends on the scalar potential  $U_\chi$ .

We therefore conclude that the time evolution of a physical system is determined by Hamiltonians such as  $\mathcal{H}_\chi$  or  $\mathcal{H}_0$ , which in general are not observable quantities. The physical quantities are, for example, the mechanical momentum and the instantaneous energy of the system.

### 5.A.2 Transition probabilities in a two-level atom

In this subsection we restrict the discussion to the large-wavelength dipole approximation (LWA) in which  $\mathbf{A}$  may be considered to be independent of  $\mathbf{r}$ , i.e.,  $\mathbf{A}(\mathbf{r}, t) \equiv \mathbf{A}(t)$ . Since the energy operator  $\mathcal{E}_\chi$  (as given by Eq. (5.A.8)) is time dependent, its eigenstates  $|\alpha_\chi(t)\rangle$ , where  $\alpha = a, b$ , and its eigenvalues  $E_\alpha = \hbar\omega_\alpha$  are also time dependent in general, namely

$$\mathcal{E}_\chi |\alpha_\chi(t)\rangle = E_\alpha |\alpha_\chi(t)\rangle. \quad (5.A.12)$$

However, in the LWA the eigenvalues of  $\mathcal{E}_\chi$  are time independent. This can be seen with the help of the gauge transformation (5.A.1). In the LWA

$$\exp \left[ -\frac{ie\mathbf{A}(t) \cdot \mathbf{r}}{\hbar} \right] [\mathbf{p} - e\mathbf{A}(t)]^2 \exp \left[ \frac{ie\mathbf{A}(t) \cdot \mathbf{r}}{\hbar} \right] = p^2, \quad (5.A.13)$$

so that

$$\exp \left[ -\frac{ie\mathbf{A}(t) \cdot \mathbf{r}}{\hbar} \right] \mathcal{E}_\chi \exp \left[ \frac{ie\mathbf{A}(t) \cdot \mathbf{r}}{\hbar} \right] = \mathcal{H}_0. \quad (5.A.14)$$

The eigenstate  $|\alpha_\chi\rangle$  is then related to the eigenstate  $|\alpha(t)\rangle$  of  $\mathcal{H}_0$  by

$$|\alpha_\chi\rangle = \exp \left[ \frac{ie\mathbf{A}_\chi(t) \cdot \mathbf{r}}{\hbar} \right] |\alpha(t)\rangle, \quad (5.A.15)$$

and the eigenvalues  $E_\alpha$  of  $\mathcal{E}_\chi$  coincide with the time-independent eigenvalues  $E_\alpha$  of  $\mathcal{H}_0$  since the eigenvalues of physical quantities are gauge independent.

In the  $E$ -gauge the unperturbed energy operator  $\mathcal{E}_E$  is equal to the *unperturbed* Hamiltonian  $\mathcal{H}_0$ . Hence the eigenstates of  $\mathcal{H}_0$  are also the eigenstates of  $\mathcal{E}_E$ . Therefore, only in the  $E$ -gauge is the wave function expanded in terms of energy eigenstates, and the coefficients  $c_\alpha(t)$ , where  $\alpha = a, b$ , in Eqs. (5.2.10) and (5.2.11) are interpreted as probability amplitudes for finding the system in an eigenstate of the observable energy. In any other gauge,  $\mathcal{H}_0$  is a nonphysical quantity and its eigenstates are not the energy eigenstates of the system. The expansion coefficients  $c_\alpha(t)$  in Eqs. (5.2.10) and (5.2.11) are then the probability amplitudes for finding the system in an eigenstate of  $\mathcal{H}_0$ . However, if  $\mathcal{H}_0$  is a nonphysical quantity, this *probability* is gauge dependent and has to be distinguished from the measurable, gauge-invariant probability of finding the system in an energy eigenstate.

It is, therefore, useful to expand the wave function of the system in terms of eigenstates of the energy operator  $\mathcal{E}_\chi$

$$|\psi_\chi(t)\rangle = d_a(t)e^{-i\omega_a t}|a_\chi\rangle + d_b(t)e^{-i\omega_b t}|b_\chi\rangle. \quad (5.A.16)$$

The expansion coefficients  $d_a$  and  $d_b$  then coincide with the probability amplitudes for transitions of the system to the eigenstates  $|a_\chi\rangle$  and  $|b_\chi\rangle$ , respectively of the energy operator  $\mathcal{E}_\chi$  with energies  $\hbar\omega_a$  and  $\hbar\omega_b$ :

$$d_a(t) = \langle a_\chi | \psi_\chi(t) \rangle e^{i\omega_a t}, \quad (5.A.17)$$

$$d_b(t) = \langle b_\chi | \psi_\chi(t) \rangle e^{i\omega_b t}. \quad (5.A.18)$$

We will now show explicitly that these amplitudes are gauge invariant.

In the  $E$ -gauge, the probability amplitude  $d_a(t)$  is given by

$$d_a^E(t) = \langle a | U_0(t) U_I^{(1)}(t) | b \rangle e^{i\omega_a t} \quad (5.A.19)$$

and, in the  $R$ -gauge, by

$$\begin{aligned} d_a^R(t) &= \langle a | \exp \left[ -\frac{ie}{\hbar} \mathbf{A}(t) \cdot \mathbf{r} \right] U_0(t) U_I^{(2)}(t) \exp \left[ \frac{ie}{\hbar} \mathbf{A}(0) \cdot \mathbf{r} \right] | b \rangle e^{i\omega_a t}, \\ &\quad (5.A.20) \end{aligned}$$

where  $U_0(t) = \exp(-i\mathcal{H}_0 t/\hbar)$  and

$$U_I^{(i)}(t) = \mathcal{T} \exp \left[ -\frac{i}{\hbar} \int_0^t d\tau U_0^\dagger(\tau) \mathcal{H}_i(\tau) U_0(\tau) \right]. \quad (5.A.21)$$

Here, we assume that the atom is initially in the ground state  $|b\rangle$ . Similar expressions exist for the amplitudes  $d_b^E(t)$  and  $d_b^R(t)$ . In the first order of perturbation theory, the time-evolution operator  $U_I^{(1)}$  becomes

$$U_I^{(1)} = 1 - \frac{i}{\hbar} \int_0^t d\tau U_0^\dagger(\tau) \mathcal{H}_1 U_0(\tau), \quad (5.A.22)$$

and the probability amplitude of the excited state in the  $E$ -gauge takes the form

$$\begin{aligned} d_a^E(t) &= -\frac{i}{\hbar} \langle a | \int_0^t d\tau U_0^\dagger(\tau) \mathcal{H}_1 U_0(\tau) | b \rangle \\ &= \frac{ie}{2\hbar} \mathcal{E} \cdot \langle a | \mathbf{r} | b \rangle \int_0^t d\tau e^{i(\omega-v)\tau} \\ &= \frac{e}{2\hbar} \mathcal{E} \cdot \mathbf{r}_{ab} \frac{e^{i\Delta t} - 1}{\Delta}. \end{aligned} \quad (5.A.23)$$

This result is now compared to the corresponding result in the  $R$ -gauge. In first-order perturbation theory,

$$\begin{aligned} d_a^R(t) &= \langle a | \left[ 1 - \frac{ie}{\hbar} \mathbf{A}(t) \cdot \mathbf{r} \right] U_0(t) \left[ 1 - \frac{i}{\hbar} \int_0^t d\tau U_0^\dagger(\tau) \mathcal{H}_2 U_0(\tau) \right] \\ &\quad \times \left[ 1 + \frac{ie}{\hbar} \mathbf{A}(0) \cdot \mathbf{r} \right] | b \rangle \exp(i\omega_a t). \end{aligned} \quad (5.A.24)$$

Using (5.1.26) and (5.2.32) and  $A(t) = \frac{1}{2}\mathcal{A}e^{-ivt}$ , to lowest order in  $\mathcal{A}$ , yields

$$d_a^R(t) = -\frac{ie}{\hbar} \frac{\mathcal{A}}{2} \left[ -\mathbf{r}_{ab} e^{-i(\omega-v)t} + \mathbf{p}_{ab} \frac{e^{-i(\omega-v)t} - 1}{i(\omega - v)} + \mathbf{r}_{ab} \right].$$

From (5.1.30) we have  $\mathbf{p}_{ab} = +im\omega \mathbf{r}_{ab}$  and defining  $\mathcal{E} = iv\mathcal{A}$  yields

$$d_a^R(t) = \frac{e}{2\hbar} \mathcal{E} \cdot \mathbf{r}_{ab} \frac{e^{i\Delta t} - 1}{\Delta}. \quad (5.A.25)$$

Thus, the amplitudes  $d_a^E(t)$  and  $d_a^R(t)$  are seen to be identical. This resolves\* the apparent contradiction pointed out at the end of Section 5.1.

\* The present treatment is oversimplified in that the effects of atomic decay are not included. For the more general case, see Lamb, Schlicher and Scully [1987].

## 5.B Vector model of the density matrix

A physical picture of the density matrix is provided by reducing Eqs. (5.3.22), (5.3.23), and (5.3.30) into a form equivalent to the Bloch equations appearing in nuclear magnetic resonance. The present problem of a two-level atom interacting with an electromagnetic field is similar to that of a spin-1/2 magnetic dipole undergoing precession in a magnetic field. This formal similarity has led to the prediction, observation, and physical understanding of a number of phenomena associated with coherent pulse propagation in a system of two-level atoms.

We introduce the real quantities

$$R_1 = \rho_{ab}e^{i\gamma t} + \text{c.c.}, \quad (5.B.1)$$

$$R_2 = i\rho_{ab}e^{i\gamma t} + \text{c.c.}, \quad (5.B.2)$$

$$R_3 = \rho_{aa} - \rho_{bb}. \quad (5.B.3)$$

These quantities are components of the vector  $\mathbf{R}$ , given by

$$\mathbf{R} = R_1\hat{\mathbf{e}}_1 + R_2\hat{\mathbf{e}}_2 + R_3\hat{\mathbf{e}}_3. \quad (5.B.4)$$

where  $\hat{\mathbf{e}}_1$ ,  $\hat{\mathbf{e}}_2$ , and  $\hat{\mathbf{e}}_3$  form a set of mutually perpendicular unit vectors. Here,  $R_1$  and  $R_2$  represent the atom's dipole moment, and  $R_3$  is the population difference between the levels  $|a\rangle$  and  $|b\rangle$ .

It follows from Eqs. (5.3.22), (5.3.23), and (5.3.30) that, in the rotating-wave approximation, (with  $\phi = 0$ )

$$\dot{R}_1 = -\Delta R_2 - \frac{1}{T_2}R_1, \quad (5.B.5)$$

$$\dot{R}_2 = \Delta R_1 - \frac{1}{T_2}R_2 + \Omega_R R_3, \quad (5.B.6)$$

$$\dot{R}_3 = -\frac{1}{T_1}R_3 - \Omega_R R_2, \quad (5.B.7)$$

where we have assumed  $\gamma_a = \gamma_b = 1/T_1$  and  $\gamma = 1/T_2$ . The quantities  $T_1$  and  $T_2$  are called the longitudinal and the transverse relaxation times, respectively, in analogy with the corresponding quantities in the Bloch equations. Equations (5.B.5)–(5.B.7) are referred to as the optical Bloch equations.

When  $T_1 = T_2$ , these equations can be written in the following compact form

$$\dot{\mathbf{R}} = -\frac{1}{T_1}\mathbf{R} + \mathbf{R} \times \boldsymbol{\Omega}, \quad (5.B.8)$$

where the effective field is given by

$$\boldsymbol{\Omega} = \Omega_R \hat{\mathbf{e}}_1 - \Delta \hat{\mathbf{e}}_3. \quad (5.B.9)$$

The time dependence of  $\mathbf{R}$ , as given by Eq. (5.B.8), is well known from classical mechanics. The vector  $\mathbf{R}$  precesses clockwise about the effective field  $\boldsymbol{\Omega}$  with diminishing amplitude. The precessions for resonance and slightly off resonance are depicted in Fig. 5.9. Physically  $\mathbf{R}$  pointing along  $\hat{\mathbf{e}}_3$  ( $R_3 = 1$ ,  $R_1 = R_2 = 0$ ) represents a system in its upper level,  $\rho_{aa} = 1$ ,  $\rho_{bb} = 0$ . Similarly,  $\mathbf{R}$  pointing along  $-\hat{\mathbf{e}}_3$  represents a system in its lower level.

## 5.C Quasimode laser physics based on the modes of the universe\*

Most laser theories, e.g., that of Section 5.5, describe the electromagnetic field in terms of a discrete set of quasimodes of the laser cavity, each of which has a finite quality factor  $Q$ . In the present section, this theory is generalized for a laser with a cavity modeled by a semi-transparent wall as one of the mirrors so that there are now many modes of the ‘universe’ corresponding to each quasimode. Here we show that the normal modes of the universe associated with a single ‘mode’ may, under proper conditions, lock together and the  $\delta$ -function laser lineshape may be regained.

We consider the normal modes for a combined system of a laser cavity coupled to the outside world. We represent the ‘universe’ by a much larger cavity having perfectly reflecting walls. A simple one-dimensional model which carries the essential features of such a combined system is illustrated in Fig. 5.10. The mirrors at  $z = L$  and  $-L_0$  are completely reflective, while the one at  $z = 0$  is semitransparent. Region 1 corresponds to a laser cavity and region 2 to the rest of the universe.

We represent a semitransparent mirror by a very thin plate with a very large dielectric constant. As an idealization of such a mirror we choose the dielectric constant around  $z = 0$  to be

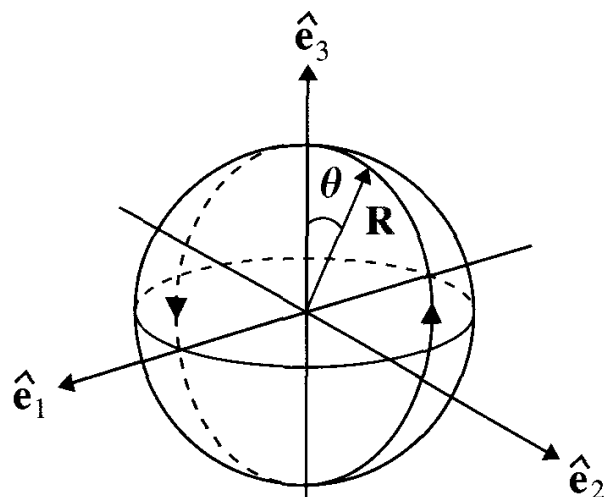
$$\epsilon(z) = \epsilon_0[1 + \eta\delta(z)], \quad (5.C.1)$$

where  $\eta$  is a parameter with the dimension of length which determines the transparency of this plate.

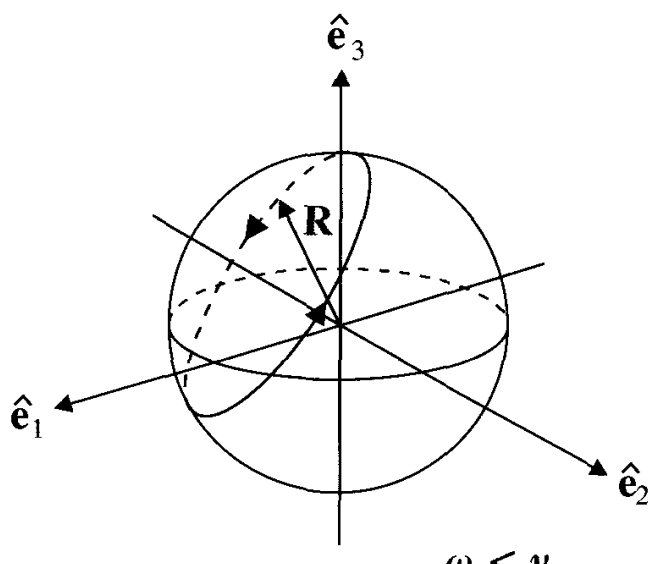
The normal mode functions of this system can be obtained by solving Maxwell’s equations with the proper boundary conditions (see Problem 5.6). For those normal modes having frequency  $v_k (= ck)$  close

\* For further reading, see Lang, Scully and Lamb [1973].

Fig. 5.9  
Precession of Bloch vector  $\mathbf{R}$  about the effective field  $\Omega$  for  
(a)  $\Delta = 0$  and  
(b)  $\Delta \neq 0$ .



(a)

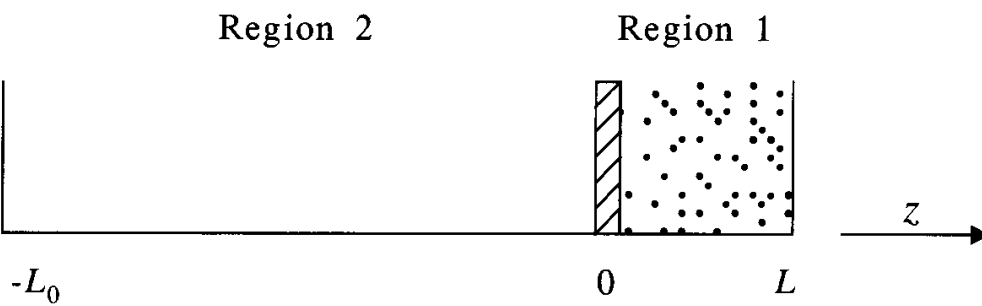


(b)

to a ‘resonant’ frequency  $\nu_0 (= ck_0)$ , the eigenfunctions of the entire cavity are

$$U_k(z) = \begin{cases} M_k \sin k(z - L) & (z > 0), \\ \xi_k \sin k(z + L) & (z < 0), \end{cases} \quad (5.C.2)$$

where  $\xi_k$  is a phase factor which alternates between 1 and -1 as  $k$  increases from one value to the next. The coefficients  $M_k$  in (5.C.2) are



$$M_k = \frac{\mathcal{C}\Lambda}{2} \left[ (v_k - v_0)^2 + \frac{\mathcal{C}^2}{4} \right]^{-1/2}, \quad (5.C.3)$$

where  $\mathcal{C}$  is the bandwidth associated with the mirror transparency and is given by

$$\mathcal{C} = 2c/\eta^2 k_0^2 L = 2c/\Lambda^2 L, \quad (5.C.4)$$

with

$$\Lambda = \eta v_0 / c = \eta k_0, \quad (5.C.5)$$

and the frequency  $v_0$  of the  $n$ th quasimode is given by

$$v_0 = ck_0 = (n\pi + 1/\Lambda)c/L. \quad (5.C.6)$$

An arbitrary undriven field in the entire cavity can be expressed as the positive frequency part of the field

$$E^{(+)}(z, t) = \sum_k \mathcal{E}_k(0) U_k(z) e^{-i\omega t} = \sum_k \mathcal{E}_k(t) U_k(z), \quad (5.C.7)$$

which is to be understood as a sum over modes of the large cavity, i.e., ‘the universe’.

We now demonstrate that the semitransparency of the mirror leads to a damping of free oscillations in the laser cavity. Let us assume that, at  $t = 0$ , the laser cavity (region 1) contains a field of the form

$$E^{(+)}(z, 0) = |\mathcal{E}_0| e^{-i\varphi} \sin k_0(z - L), \quad (5.C.8)$$

whereas no field exists outside the cavity, i.e., in region 2. The coefficients  $\mathcal{E}_k(0)$  for this case are obtained by multiplying (5.C.8) by  $U_k(z)$  defined in (5.C.2) and integrating over  $z$ . We find

$$\mathcal{E}_k(t) = (|\mathcal{E}_0| M_k L / L_0) e^{-i(v_k t + \varphi)}. \quad (5.C.9)$$

Therefore at later times,  $t > 0$ ,

$$E(z, t) = (|\mathcal{E}_0| L / L_0) \sum_k M_k U_k(z) e^{-i(v_k t + \varphi)}. \quad (5.C.10)$$

Fig. 5.10  
Leaky cavity  
bounded by a perfect  
mirror at  $z = L$  and  
a semitransparent  
mirror at  $z = 0$ . The  
auxiliary cavity  
which, along with the  
leaky cavity,  
constitutes the  
universe, is bounded  
by a perfect mirror  
at  $z = -L_0$  ( $L_0 \rightarrow \infty$ )  
and the mirror at  
 $z = 0$ .

The summation can be approximated by an integral if the frequency separation between the normal modes is small compared to  $\mathcal{C}$ . Carrying out the integration over  $k$  in (5.C.10), the explicit form of  $E(z, t)$  in the maser cavity turns out to be

$$E^{(+)}(z, 0) = |\mathcal{E}_0| \sin k_0(z - L) e^{-i(v_k t + \phi) - \mathcal{C}t/2}. \quad (5.C.11)$$

Equation (5.C.11) indicates that the field localized in the maser cavity decays exponentially owing to leakage through the mirror at a rate  $\mathcal{C}/2$ .

## Problems

- 5.1** Show that the Schrödinger equation (5.1.5) is invariant under local gauge transformations (5.1.4), (5.1.6), and (5.1.7).
- 5.2** The finite lifetime of the atomic levels can be described by adding phenomenological decay terms to the probability amplitude equations (5.2.12) and (5.2.13):

$$\begin{aligned}\dot{c}_a &= -\frac{\gamma}{2} c_a + \frac{i\Omega_R}{2} e^{-i\phi} c_b, \\ \dot{c}_b &= -\frac{\gamma}{2} c_b + \frac{i\Omega_R}{2} e^{i\phi} c_a,\end{aligned}$$

where  $\gamma$  is the decay constant and  $\omega = v$ . For an atom initially in the state  $|a\rangle$ , show that the inversion at time  $t$  is

$$W(t) = e^{-\gamma t} \cos(\Omega_R t).$$

- 5.3** Find the solution of Eq. (5.B.8) (with  $T_1 \rightarrow \infty$ ):

$$\dot{\mathbf{R}} = \mathbf{R} \times \boldsymbol{\Omega}$$

for  $\mathbf{R}(0) = 0$ . Give a physical interpretation of this solution.

- 5.4** Show that, in general,

$$\text{Tr}(\rho^2) \leq 1,$$

where the equality is valid only for a pure state.

- 5.5** Consider a three-level atom interacting with a classical field of frequency  $\nu$ . The transitions  $|a\rangle \rightarrow |b\rangle$  and  $|b\rangle \rightarrow |c\rangle$  are allowed whereas the transition  $|a\rangle \rightarrow |c\rangle$  is forbidden. It is also assumed that  $\omega_a - \omega_b = \omega_b - \omega_c = \nu$ . Assuming the atom to be initially in level  $|c\rangle$ , find the probabilities for the atom to be in levels  $|a\rangle$  and  $|c\rangle$  after making the rotating-wave approximation.
- 5.6** The electromagnetic field in the entire cavity (region 1 and region 2 in Fig. 5.10) is governed by the Maxwell wave equation

$$\frac{\partial^2 E}{\partial z^2} - \mu_0 \epsilon_0 [1 + \eta \delta(z)] \frac{\partial^2 E}{\partial t^2} = 0,$$

where  $E$  can be written as

$$E = U_k(z) e^{-iv_k t}.$$

- (a) Find  $U_k(z)$  in the form (5.C.2) and prove that

$$\frac{M_k^2}{\xi_k^2} = \frac{\tan^2 kL + 1}{\tan^2 kL + (\Lambda \tan kL - 1)^2},$$

where  $\Lambda$  is given by Eq. (5.C.5). Derive Eq. (5.C.3).

- (b) Show that

$$(v_k - v_{k'})^2 \int_{-L_0}^L dz U_k(z) U_{k'}(z) \epsilon(z) = 0,$$

where  $\epsilon(z) = \epsilon_0[1 + \eta \delta(z)]$ . (Hint: see R. Lang, M. O. Scully, and W. E. Lamb, Jr., *Phys. Rev. A* **7**, 1788 (1973).)

- 5.7** The  $m = +1$  level of Fig. 5.3 is weakly coupled to the  $\psi_b(r)$  level by the left-circular polarized light of Eq. (5.2.55) via counter rotating terms. Note that in such a case ( $m = 0$  to  $m = +1$ ) we normally rule out such coupling on the grounds that right-circularly polarized light is needed for the  $m = 0$  to  $m = +1$  transition.

(a) Show that if we define

$$\begin{aligned}\psi_{a'}(\mathbf{r}) &= \psi_{n=2, l=1, m_l=+1}(\mathbf{r}) \\ &= \eta(x + iy)e^{-r/2a_0},\end{aligned}$$

where  $\eta$  is the uninteresting constant  $[\sqrt{64\pi a_0^3}a_0]^{-1}$ , then

$$\begin{aligned}\mathcal{V}_{a'b}(t) &= -e\mathcal{E} \int d\mathbf{r} \psi_a^*(\mathbf{r}) \mathbf{r} \cdot (\hat{x} \cos vt - \hat{y} \sin vt) \\ &\quad \psi_b(\mathbf{r}) e^{i\omega_{a'b} t} \\ &= -\phi\mathcal{E} e^{i(\omega_{a'b} + v)t}.\end{aligned}$$

(b) Show, by specific example, that the counter terms associated with the  $|b\rangle \rightarrow |a'\rangle$  transitions, which go like  $[\omega_{a'b} + v]^{-1}$  can be much smaller than the usual counter terms  $[\omega_{ab} + v]^{-1}$ . Hint: consider a Rydberg atom in which  $\omega_{ab} = \omega_{a'b} \cong 10^9$ Hz. If we now apply a field of around  $10^4$  Gauss, we could arrange for the Zeeman shifted  $\omega_{ab} \sim 10^3$ Hz while  $\omega_{a'b} \sim 10^{10}$ Hz.

# Atom–field interaction – quantum theory

---

In the preceding chapters concerning the interaction of a radiation field with matter, we assumed the field to be classical. In many situations this assumption is valid. There are, however, many instances where a classical field fails to explain experimentally observed results and a quantized description of the field is required. This is, for example, true of spontaneous emission in an atomic system which was described phenomenologically in Chapter 5. For a rigorous treatment of the atomic level decay in free space, we need to consider the interaction of the atom with the vacuum modes of the universe. Even in the simplest system involving the interaction of a single-mode radiation field with a single two-level atom, the predictions for the dynamics of the atom are quite different in the semiclassical theory and the fully quantum theory. In the absence of the decay process, the semiclassical theory predicts Rabi oscillations for the atomic inversion whereas the quantum theory predicts certain *collapse* and *revival* phenomena due to the quantum aspects of the field. These interesting quantum field theoretical predictions have been experimentally verified.

 In this chapter we discuss the interaction of the quantized radiation field with the two-level atomic system described by a Hamiltonian in the dipole and the rotating-wave approximations. For a single-mode field it reduces to a particularly simple form. This is a very interesting Hamiltonian in quantum optics for several reasons. First, it can be solved exactly for arbitrary coupling constants and exhibits some true quantum dynamical effects such as collapse followed by periodic revivals of the atomic inversion. Second, it provides the simplest illustration of spontaneous emission and thus explains the effects of various kinds of quantum statistics of the field in more complicated systems such as a micromaser and a laser, which we shall study in

later chapters. Third, and perhaps most importantly,\* it has become possible to realize it experimentally through the spectacular advances in the development of high- $Q$  microwave cavities.

The spontaneous decay of an atomic level is treated by considering the interaction of the two-level atom with the modes of the universe in the vacuum state. We examine the state of the field that is generated in the process of emission of a quantum of energy equal to the energy difference between the atomic levels. Such a state may be regarded as a single-photon state.

## 6.1 Atom–field interaction Hamiltonian

The interaction of a radiation field  $\mathbf{E}$  with a single-electron atom can be described by the following Hamiltonian in the dipole approximation:

$$\mathcal{H} = \mathcal{H}_A + \mathcal{H}_F - e\mathbf{r} \cdot \mathbf{E}. \quad \text{17.7 A dipole approx} \quad (6.1.1)$$

Here  $\mathcal{H}_A$  and  $\mathcal{H}_F$  are the energies of the atom and the radiation field, respectively, in the absence of the interaction, and  $\mathbf{r}$  is the position vector of the electron. In the dipole approximation, the field is assumed to be uniform over the whole atom.

The energy of the free field  $\mathcal{H}_F$  is given in terms of the creation and destruction operators by

$$\mathcal{H}_F = \sum_{\mathbf{k}} \hbar v_k \left( a_{\mathbf{k}}^\dagger a_{\mathbf{k}} + \frac{1}{2} \right). \quad (6.1.2)$$

We can express  $\mathcal{H}_A$  and  $e\mathbf{r}$  in terms of the atom transition operators

$$\sigma_{ij} = \underbrace{|i\rangle\langle j|}_{\text{atom transition operators}}. \quad (6.1.3)$$

As before  $\{|i\rangle\}$  represents a complete set of atomic energy eigenstates, i.e.,  $\sum_i |i\rangle\langle i| = 1$ . It then follows from the eigenvalue equation  $\mathcal{H}_A|i\rangle = E_i|i\rangle$  that

$$\mathcal{H}_A = \sum_i E_i |i\rangle\langle i| = \sum_i E_i \sigma_{ii}. \quad \square \quad (6.1.4)$$

Also

$$e\mathbf{r} = \sum_{i,j} e |i\rangle\langle i| \mathbf{r} |j\rangle\langle j| = \sum_{i,j} \wp_{ij} \sigma_{ij}, \quad (6.1.5)$$

\* Especially the micromaser of H. Walther and coworkers as discussed in Chapter 13. See also the Physics Today article by Haroche and Kleppner [1989] which presents the physics of cavity QED very nicely.

where  $\phi_{ij} = e\langle i|\mathbf{r}|j \rangle$  is the electric-dipole transition matrix element. The electric field operator is evaluated in the dipole approximation at the position of the point atom. It follows from Eq. (1.1.27) that, for the atom at the origin, we have

$$\begin{aligned} & \text{ae}^{-i\omega t} + a^\dagger e^{i\omega t} \\ & \xrightarrow{\text{是因由 Heisenberg 算子}} \mathbf{E} = \sum_{\mathbf{k}} \hat{e}_{\mathbf{k}} \epsilon_{\mathbf{k}} (a_{\mathbf{k}} + a_{\mathbf{k}}^\dagger), \quad \epsilon_{\mathbf{k}} = \sqrt{\frac{\hbar v_k}{2\epsilon_0 V}} \end{aligned} \quad (6.1.6)$$

$a \rightarrow e^{-i\omega t}$     $a^\dagger \rightarrow e^{i\omega t}$

where  $\epsilon_{\mathbf{k}} = (\hbar v_k / 2\epsilon_0 V)^{1/2}$ . Here, for simplicity, we have taken a linear polarization basis and the polarization unit vectors to be real.

It now follows, on substituting for  $\mathcal{H}_F$ ,  $\mathcal{H}_A$ ,  $e\mathbf{r}$ , and  $\mathbf{E}$  from Eqs. (6.1.2), (6.1.4), (6.1.5), and (6.1.6) into Eq. (6.1.1), that

$$\mathcal{H} = \sum_{\mathbf{k}} \hbar v_k a_{\mathbf{k}}^\dagger a_{\mathbf{k}} + \sum_i E_i \sigma_{ii} + \hbar \sum_{i,j} \sum_{\mathbf{k}} g_{\mathbf{k}}^{ij} \sigma_{ij} (a_{\mathbf{k}} + a_{\mathbf{k}}^\dagger), \quad (6.1.7)$$

where

$$g_{\mathbf{k}}^{ij} = -\frac{\phi_{ij} \cdot \hat{e}_{\mathbf{k}} \epsilon_{\mathbf{k}}}{\hbar}. \quad (6.1.8)$$

In Eq. (6.1.7), we have omitted the zero-point energy from the first term. For the sake of simplicity, we will assume  $\phi_{ij}$  to be real throughout this chapter.

$\xrightarrow{\text{二能級}}$  We now proceed to the case of a two-level atom. For  $\phi_{ab} = \phi_{ba}$ , we write

$$g_{\mathbf{k}} = g_{\mathbf{k}}^{ab} = g_{\mathbf{k}}^{ba}. \quad (6.1.9)$$

The following form of the Hamiltonian is obtained

$$\begin{aligned} \mathcal{H} = & \sum_{\mathbf{k}} \hbar v_k a_{\mathbf{k}}^\dagger a_{\mathbf{k}} + (E_a \sigma_{aa} + E_b \sigma_{bb}) \\ & + \hbar \sum_{\mathbf{k}} g_{\mathbf{k}} (\sigma_{ab} + \sigma_{ba})(a_{\mathbf{k}} + a_{\mathbf{k}}^\dagger). \end{aligned} \quad (6.1.10)$$

The second term in Eq. (6.1.10) can be rewritten as

$$E_a \sigma_{aa} + E_b \sigma_{bb} = \frac{1}{2} \hbar \omega (\sigma_{aa} - \sigma_{bb}) + \frac{1}{2} (E_a + E_b), \quad (6.1.11)$$

where we use  $(E_a - E_b) = \hbar \omega$  and  $\sigma_{aa} + \sigma_{bb} = 1$ . The constant energy term  $(E_a + E_b)/2$  can be ignored. If we use the notation

$$\sigma_z = \sigma_{aa} - \sigma_{bb} = |a\rangle\langle a| - |b\rangle\langle b|, \quad (6.1.12)$$

$$\sigma_+ = \sigma_{ab} = |a\rangle\langle b|, \quad (6.1.13)$$

$$\sigma_- = \sigma_{ba} = |b\rangle\langle a|, \quad (6.1.14)$$

the Hamiltonian (6.1.10) takes the form

$$\mathcal{H} = \sum_{\mathbf{k}} \hbar v_k a_{\mathbf{k}}^\dagger a_{\mathbf{k}} + \frac{1}{2} \hbar \omega \sigma_z + \hbar \sum_{\mathbf{k}} g_{\mathbf{k}} (\sigma_+ + \sigma_-) (a_{\mathbf{k}} + a_{\mathbf{k}}^\dagger). \quad (6.1.15)$$

It follows from the identity

$$[\sigma_{ij}, \sigma_{kl}] = \sigma_{il}\delta_{jk} - \sigma_{kj}\delta_{il}, \quad \square$$

① 不是反交换子  
( $\sigma_{il}, \sigma_{jk}$ )  
② 也不是交换子  
反交换子是泡利矩阵的性质  
(Fermi's Golden Rule)  
这里不是直接用 Hamiltonian  
(Rob. 泡利).

that  $\sigma_+$ ,  $\sigma_-$ , and  $\sigma_z$  satisfy the spin-1/2 algebra of the Pauli matrices, i.e.,

$$[\sigma_-, \sigma_+] = -\sigma_z, \quad (6.1.17)$$

$$[\sigma_-, \sigma_z] = 2\sigma_-. \quad (6.1.18)$$

In the matrix notation,  $\sigma_-$ ,  $\sigma_+$ , and  $\sigma_z$  are given by

$$\sigma_- = \begin{pmatrix} 0 & 0 \\ 1 & 0 \end{pmatrix}, \quad \sigma_+ = \begin{pmatrix} 0 & 1 \\ 0 & 0 \end{pmatrix}, \quad \sigma_z = \begin{pmatrix} 1 & 0 \\ 0 & -1 \end{pmatrix}. \quad (6.1.19)$$

The  $\sigma_-$  operator takes an atom in the upper state into the lower state whereas  $\sigma_+$  takes an atom in the lower state into the upper state.

The interaction energy in Eq. (6.1.15) consists of four terms. The term  $a_{\mathbf{k}}^\dagger \sigma_-$  describes the process in which the atom is taken from the upper state into the lower state and a photon of mode  $\mathbf{k}$  is created. The term  $a_{\mathbf{k}} \sigma_+$  describes the opposite process. The energy is conserved in both the processes. The term  $a_{\mathbf{k}} \sigma_-$  describes the process in which the atom makes a transition from the upper to the lower level and a photon is annihilated, resulting in the loss of approximately  $2\hbar\omega$  in energy. Similarly  $a_{\mathbf{k}}^\dagger \sigma_+$  results in the gain of  $2\hbar\omega$ . Dropping the energy nonconserving terms corresponds to the rotating-wave approximation. The resulting simplified Hamiltonian is

$$\mathcal{H} = \sum_{\mathbf{k}} \hbar v_k a_{\mathbf{k}}^\dagger a_{\mathbf{k}} + \frac{1}{2} \hbar \omega \sigma_z + \hbar \sum_{\mathbf{k}} g_{\mathbf{k}} (\sigma_+ a_{\mathbf{k}} + a_{\mathbf{k}}^\dagger \sigma_-). \quad (6.1.20)$$

This form of the Hamiltonian describing the interaction of a single two-level atom with a multi-mode field is the starting point of many calculations in the field of quantum optics.

(至此，用了慢辐射，放波近似)

## 6.2 Interaction of a single two-level atom with a single-mode field

It follows from Eq. (6.1.20) that the interaction of a single-mode quantized field of frequency  $v$  with a single two-level atom is described

by the Hamiltonian

$$\mathcal{H} = \mathcal{H}_0 + \mathcal{H}_1, \quad (6.2.1)$$

where

$$\mathcal{H}_0 = \hbar v a^\dagger a + \frac{1}{2} \hbar \omega \sigma_z, \quad (6.2.2)$$

$$\mathcal{H}_1 = \hbar g (\sigma_+ a + a^\dagger \sigma_-). \quad (6.2.3)$$

Here we have removed the subscript from the coupling constant  $g$ . The Hamiltonian, given by Eqs. (6.2.1)–(6.2.3), describes the atom–field interaction in the dipole and rotating-wave approximations. As we show below, this important Hamiltonian of quantum optics provides us with an exactly solvable example of the field–matter interaction.

It is convenient to work in the interaction picture. The Hamiltonian, in the interaction picture, is given by

$$\mathcal{V} = e^{i\mathcal{H}_0 t/\hbar} \mathcal{H}_1 e^{-i\mathcal{H}_0 t/\hbar}. \quad (6.2.4)$$

Using

  $e^{\alpha A} B e^{-\alpha A} = B + \alpha [A, B] + \frac{\alpha^2}{2!} [A, [A, B]] + \dots, \quad (6.2.5)$

it can be readily seen that

$$e^{iv a^\dagger a t} a e^{-iv a^\dagger a t} = a e^{-iv t}, \quad (6.2.6)$$

$$e^{i\omega \sigma_z t/2} \sigma_+ e^{-i\omega \sigma_z t/2} = \sigma_+ e^{i\omega t}. \quad (6.2.7)$$

Combining Eqs. (6.2.1)–(6.2.3), (6.2.4), (6.2.6), and (6.2.7), we have

$$\mathcal{V} = \hbar g (\sigma_+ a e^{i\Delta t} + a^\dagger \sigma_- e^{-i\Delta t}), \quad (6.2.8)$$

where  $\Delta = \omega - v$ .

In this section, we present three different but equivalent methods to solve for the evolution of the atom–field system described by the Hamiltonian (6.2.1)–(6.2.3) based on the solutions of the probability amplitudes, the Heisenberg field and atomic operators, and the unitary time-evolution operator.

下面是求解方法 (Schrödinger 方程)

### 6.2.1 Probability amplitude method

We first proceed to solve the equation of motion for  $|\psi\rangle$ , i.e.,

$$i\hbar \frac{\partial |\psi\rangle}{\partial t} = \mathcal{V} |\psi\rangle. \quad (6.2.9)$$

At any time  $t$ , the state vector  $|\psi(t)\rangle$  is a linear combination of the states  $|a, n\rangle$  and  $|b, n\rangle$ . Here  $|a, n\rangle$  is the state in which the atom is in

the excited state  $|a\rangle$  and the field has  $n$  photons. A similar description exists for the state  $|b, n\rangle$ . As we are using the interaction picture, we use the slowly varying probability amplitudes  $c_{a,n}$  and  $c_{b,n}$ . The state vector is therefore

$$|\psi(t)\rangle = \sum_n [c_{a,n}(t)|a, n\rangle + c_{b,n}(t)|b, n\rangle]. \quad (6.2.10)$$

The interaction energy (6.2.8) can only cause transitions between the states  $|a, n\rangle$  and  $|b, n+1\rangle$ . We therefore consider the evolution of the amplitudes  $c_{a,n}$  and  $c_{b,n+1}$ . The equations of motion for the probability amplitudes  $c_{a,n}$  and  $c_{b,n+1}$  are obtained by first substituting for  $|\psi(t)\rangle$  and  $\mathcal{V}$  from Eqs. (6.2.10) and (6.2.8) in Eq. (6.2.9) and then projecting the resulting equations onto  $\langle a, n|$  and  $\langle b, n+1|$ , respectively. We then obtain

$$\dot{c}_{a,n} = -ig\sqrt{n+1} e^{i\Delta t} c_{b,n+1}, \quad (6.2.11)$$

$$\dot{c}_{b,n+1} = -ig\sqrt{n+1} e^{-i\Delta t} c_{a,n}. \quad (6.2.12)$$

This coupled set of equations is very similar to that obtained in the semiclassical treatment (cf. Eqs. (5.2.12) and (5.2.13)). These equations can be solved exactly subject to certain initial conditions. A general solution for the probability amplitudes is

$$c_{a,n}(t) = \left\{ c_{a,n}(0) \left[ \cos\left(\frac{\Omega_n t}{2}\right) - \frac{i\Delta}{\Omega_n} \sin\left(\frac{\Omega_n t}{2}\right) \right] - \frac{2ig\sqrt{n+1}}{\Omega_n} c_{b,n+1}(0) \sin\left(\frac{\Omega_n t}{2}\right) \right\} e^{i\Delta t/2}, \quad (6.2.13)$$

$$c_{b,n+1}(t) = \left\{ c_{b,n+1}(0) \left[ \cos\left(\frac{\Omega_n t}{2}\right) + \frac{i\Delta}{\Omega_n} \sin\left(\frac{\Omega_n t}{2}\right) \right] - \frac{2ig\sqrt{n+1}}{\Omega_n} c_{a,n}(0) \sin\left(\frac{\Omega_n t}{2}\right) \right\} e^{-i\Delta t/2}, \quad (6.2.14)$$

where

$$\Omega_n^2 = \Delta^2 + 4g^2(n+1). \quad (6.2.15)$$

高频率  
Rabi频率  
与 g 相关
与 Δ 有关  
与 n 有关，光越强，振幅越大  
与 Cn(0) 无关  
场强无关

If initially the atom is in the excited state  $|a\rangle$  then  $c_{a,n}(0) = c_n(0)$  and  $c_{b,n+1}(0) = 0$ . Here  $c_n(0)$  is the probability amplitude for the field alone. We then obtain

$$c_{a,n}(t) = c_n(0) \left[ \cos\left(\frac{\Omega_n t}{2}\right) - \frac{i\Delta}{\Omega_n} \sin\left(\frac{\Omega_n t}{2}\right) \right] e^{i\Delta t/2}, \quad (6.2.16)$$

$$c_{b,n+1}(t) = -c_n(0) \frac{2ig\sqrt{n+1}}{\Omega_n} \sin\left(\frac{\Omega_n t}{2}\right) e^{-i\Delta t/2}. \quad (6.2.17)$$

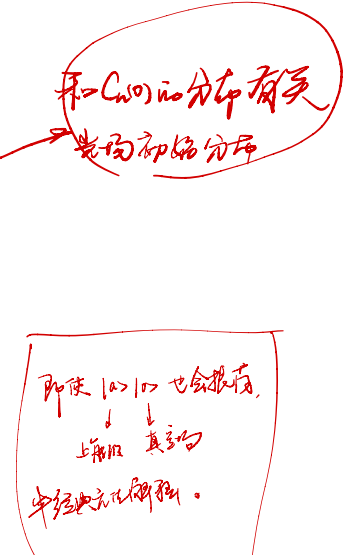
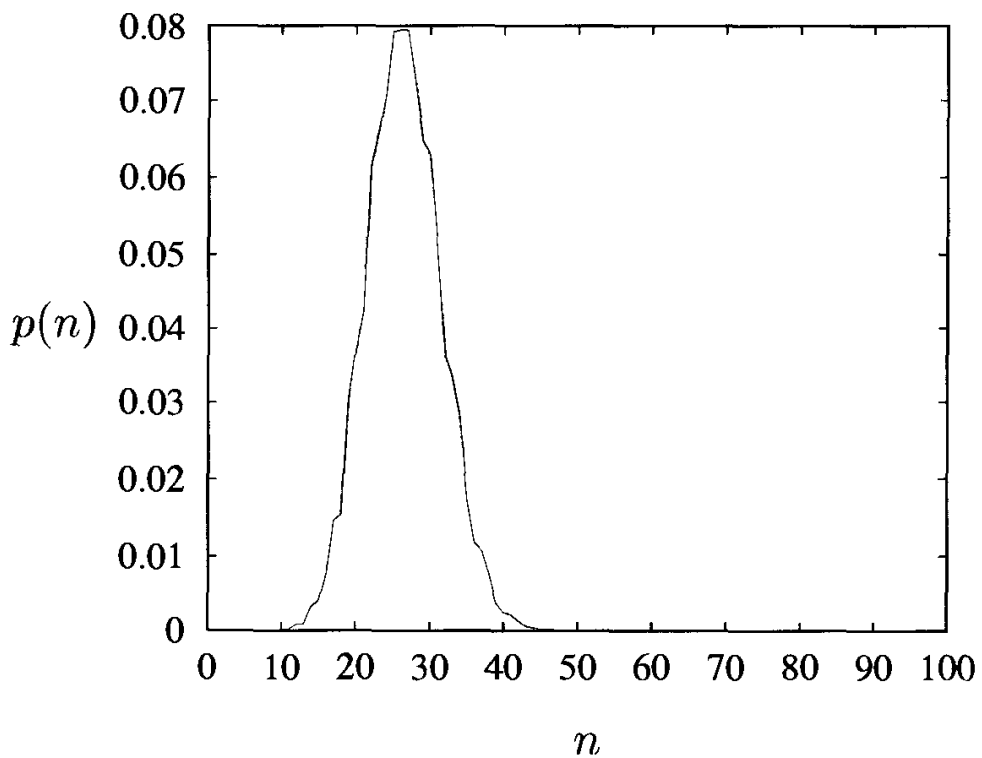


**Fig. 6.1**  
Behavior of  $p(n)$ , as given by Eq. (6.2.18), for an initially coherent state. The value of the various parameters are  $\Delta = 0$ ,  $\langle n \rangle = 25$ , and  $gt = 1$ .



These equations give us a complete solution of the problem. All the physically relevant quantities relating to the quantized field and the atom can be obtained from them.

The expressions  $|c_{a,n}(t)|^2$  and  $|c_{b,n}(t)|^2$  represent the probabilities that, at time  $t$ , the field has  $n$  photons present and the atom is in levels  $|a\rangle$  and  $|b\rangle$ , respectively. The probability  $p(n)$  that there are  $n$  photons in the field at time  $t$  is therefore obtained by taking the trace over the atomic states, i.e.,

$$\begin{aligned} \text{时间场中有 } n \text{ 光子} \Rightarrow p(n) &= |c_{a,n}(t)|^2 + |c_{b,n}(t)|^2 \\ &= \rho_{nn}(0) \left[ \cos^2 \left( \frac{\Omega_n t}{2} \right) + \left( \frac{\Delta}{\Omega_n} \right)^2 \sin^2 \left( \frac{\Omega_n t}{2} \right) \right] \\ &\quad + \rho_{n-1,n-1}(0) \left( \frac{4g^2 n}{\Omega_{n-1}^2} \right) \sin^2 \left( \frac{\Omega_{n-1} t}{2} \right), \end{aligned} \quad (6.2.18)$$

where  $\rho_{nn}(0) = |c_n(0)|^2$  is the probability that there are  $n$  photons present in the field at time  $t = 0$ . In Fig. 6.1, we plot  $p(n)$  for an initial coherent state

$$\rho_{nn}(0) = \frac{\langle n \rangle^n e^{-\langle n \rangle}}{n!}. \quad (6.2.19)$$

Another important quantity is the inversion  $W(t)$  which is related to the probability amplitudes  $c_{a,n}(t)$  and  $c_{b,n}(t)$  by the expression

$$\text{时间场有 } n \text{ 光子} \quad W(t) = \sum_n [|c_{a,n}(t)|^2 - |c_{b,n}(t)|^2]. \quad (6.2.20)$$

Ramsey 分裂 不影响

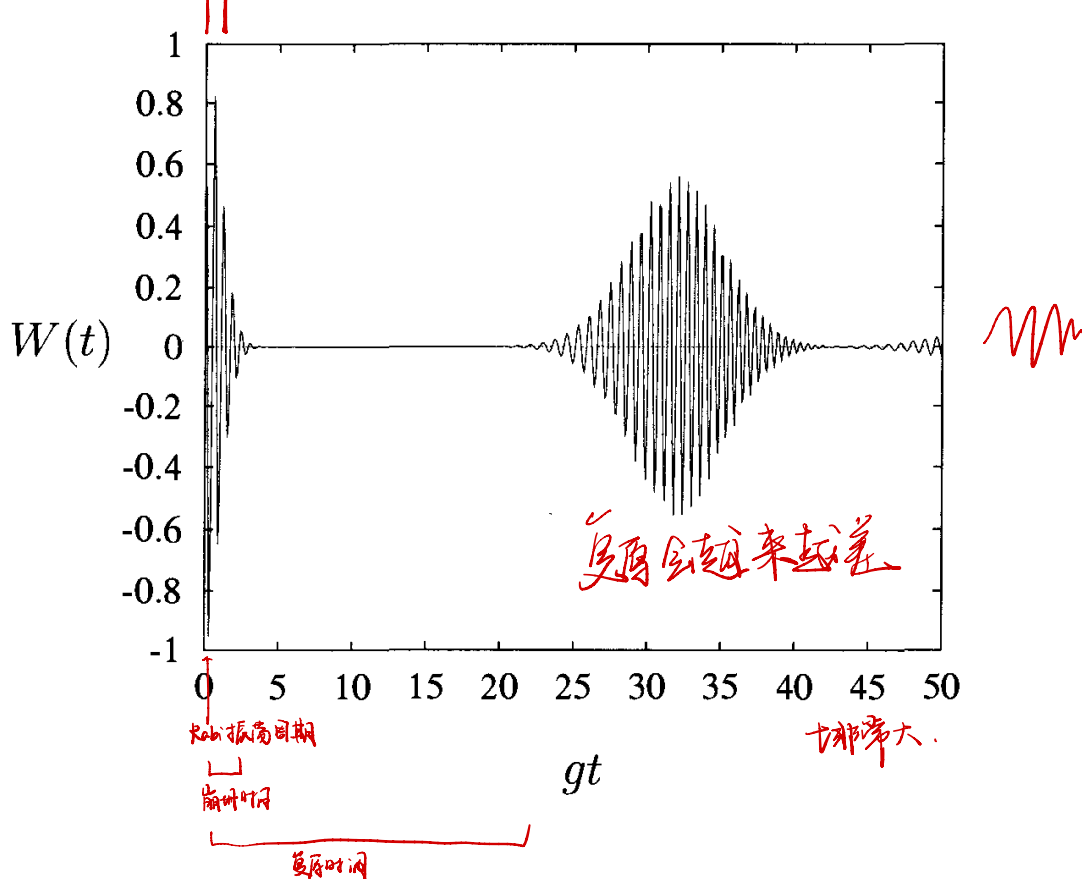


Fig. 6.2  
Time evolution of the population inversion  $W(t)$  for an initially coherent state with  $\langle n \rangle = 25$  and  $\Delta = 0$ .

On substituting for  $c_{a,n}(t)$  and  $c_{b,n}(t)$  from Eqs. (6.2.16) and (6.2.17) and making some rearrangements, we obtain

$$W(t) = \sum_{n=0}^{\infty} \rho_{nn}(0) \left[ \frac{\Delta^2}{\Omega_n^2} + \frac{4g^2(n+1)}{\Omega_n^2} \cos(\Omega_n t) \right]. \quad (6.2.21)$$

It is interesting to note that even for initial vacuum field ( $\rho_{nn}(0) = \delta_{n0}$ ),

$$W(t) = \frac{1}{\Delta^2 + 4g^2} \left\{ \Delta^2 + 4g^2 \cos \left[ (\Delta^2 + 4g^2)^{1/2} t \right] \right\}, \quad (6.2.22)$$

i.e., the Rabi oscillations take place. This result is drastically different from the predictions of the semiclassical theory of Chapter 5. In the semiclassical theory, the atom in the excited state cannot make a transition to the lower level in the absence of a driving field. In the fully quantum mechanical treatment, the transition from the upper level to the lower level in the *vacuum* becomes possible due to spontaneous emission. Equation (6.2.22) is the simplest example of spontaneous emission in which the spontaneously emitted photon contributes to the single mode of the field considered. A detailed analysis of spontaneous emission by an atom in free space due to the presence of infinitely many vacuum modes will be discussed in the next section.

In Fig. 6.2,  $W(t)$  is plotted as a function of the normalized time  $\tau = gt$  for an initial coherent state. The behavior of  $W(t)$  is quite different

崩塌复原效应

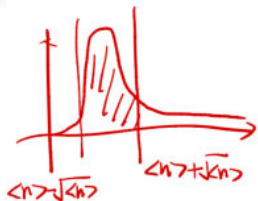
from the corresponding curve (Fig. 5.2) in the semiclassical theory. In the present case the envelope of the sinusoidal Rabi oscillations ‘collapses’ to zero. However as time increases we encounter a ‘revival’ of the collapsed inversion. This behavior of collapse and revival of inversion is repeated with increasing time, with the amplitude of Rabi oscillations decreasing and the time duration in which revival takes place increasing and ultimately overlapping with the earlier revival.

The phenomena of collapse and revival can be physically understood from Eq. (6.2.21). Each term in the summation represents Rabi oscillations for a definite value of  $n$ . The photon distribution function  $\rho_{nn}(0)$  determines the relative weight for each value of  $n$ . At the initial time,  $t = 0$ , the atom is prepared in a definite state and therefore all the terms in the summation are correlated. As time increases the Rabi oscillations associated with different excitations have different frequencies and therefore become uncorrelated leading to a collapse of inversion. As time is further increased, the correlation is restored and revival occurs. This behavior continues and an infinite sequence of revivals is obtained. The important thing is that revivals occur only because of the granular structure of the photon distribution. Revival is thus a pure quantum phenomenon. A continuous photon distribution (without zeros) would give a collapse, as would a classical random field, but no revivals.

Simple expressions for the times  $t_R$ ,  $t_c$ , and  $t_r$  associated with the sinusoidal Rabi oscillations, the collapse of these oscillations and their revival, respectively, can be determined from Eq. (6.2.21) in the limit  $\langle n \rangle \gg 1$ . The **time period  $t_R$  of the Rabi oscillations** is given by the inverse of the Rabi frequency  $\Omega_n$  at  $n = \langle n \rangle$ , i.e.,

$$t_R \sim \frac{1}{\Omega_{\langle n \rangle}} = \frac{1}{(\Delta^2 + 4g^2 \underbrace{\langle n \rangle}_{(n>+1)})^{1/2}}. \quad (6.2.23)$$

周期性振荡



As mentioned earlier, these Rabi oscillations continue until a collapse time  $t_c$ , when the oscillations associated with different values of  $n$  become uncorrelated. Now, for the Poisson distribution (6.2.19) for the initial coherent field, the root-mean-square deviation in the photon number  $\Delta n$  is equal to  $\sqrt{\langle n \rangle}$ . An estimate of  $t_c$  can therefore be obtained from the condition

$$\left( \Omega_{\langle n \rangle + \sqrt{\langle n \rangle}} - \Omega_{\langle n \rangle - \sqrt{\langle n \rangle}} \right) t_c \sim 1. \quad (6.2.24)$$

Since  $\langle n \rangle \gg \sqrt{\langle n \rangle}$  in the limit  $\langle n \rangle \gg 1$ , Eq. (6.2.24) yields

$$\begin{aligned} t_c &\sim \frac{1}{\Omega_{\langle n \rangle + \sqrt{\langle n \rangle}} - \Omega_{\langle n \rangle - \sqrt{\langle n \rangle}}} \quad \text{[复习时间]} \\ &\simeq \frac{1}{[\Delta^2 + 4g^2 (\langle n \rangle + \sqrt{\langle n \rangle})]^{1/2} - [\Delta^2 + 4g^2 (\langle n \rangle - \sqrt{\langle n \rangle})]^{1/2}} \\ &\simeq \frac{1}{2g} \left(1 + \frac{\Delta^2}{4g^2 \langle n \rangle}\right)^{1/2}. \xrightarrow{\text{Resonance}} \frac{1}{2g} \end{aligned} \quad (6.2.25)$$

Under the conditions of exact resonance,  $\Delta = 0$ , the collapse time  $t_c$  is equal to  $1/2g$  and is independent of the mean number of photons  $\langle n \rangle$ . For nonzero detuning,  $t_c$  decreases with increasing  $\langle n \rangle$ . The interval between revivals,  $t_r$ , can be found from the condition

$$(\Omega_{\langle n \rangle} - \Omega_{\langle n \rangle - 1})t_r = 2\pi m \quad (m = 1, 2, \dots), \quad (6.2.26)$$

i.e., the revivals take place when the phases of oscillation of the neighboring terms in Eq. (6.2.21) differ by an integral multiple of  $2\pi$ . Again, in the limit  $\langle n \rangle \gg 1$ , we obtain

$$\begin{aligned} t_r &= \frac{2\pi m}{\Omega_{\langle n \rangle} - \Omega_{\langle n \rangle - 1}} \quad \text{[复习时间]} \\ &\simeq \frac{2\pi m \sqrt{\langle n \rangle}}{g} \left(1 + \frac{\Delta^2}{4g^2 \langle n \rangle}\right)^{1/2}, \end{aligned} \quad (6.2.27)$$

where  $m$  is an integer. This shows that revivals take place at regular intervals.

### 6.2.2 Heisenberg operator method

So far we have considered the problem of the interaction of a single-mode quantized field with a single two-level atom in the interaction picture. In the following we give the solution of the same problem in the Heisenberg picture. In particular we solve the operator equations for the atomic and field operators  $a(t)$  and  $\sigma_{\pm}(t)$ . These solutions may be particularly useful in the calculation of the multi-time correlation functions necessary in the study of the spectral properties of the field.

The Heisenberg equations for the operators  $a$ ,  $\sigma_-$ , and  $\sigma_z$  are obtained from the atom-field Hamiltonian (6.2.1)

$$\dot{a} = \frac{1}{i\hbar} [a, \mathcal{H}] = -i\nu a - ig\sigma_-, \quad (6.2.28)$$

$$\dot{\sigma}_- = -i\omega\sigma_- + ig\sigma_z a, \quad (6.2.29)$$

$$\dot{\sigma}_z = 2ig(a^\dagger\sigma_- - \sigma_+a). \quad (6.2.30)$$

→ 解释1:

$$\text{对易}, \dot{N} = [N, H] = 0$$

→ 解释2:

$$\sigma_+ \sigma_- \text{ 对易} \quad \text{下同上式}$$

In order to facilitate a solution of these coupled operator equations we define the following constants of motion:

$$N = a^\dagger a + \sigma_+ \sigma_-, \quad \begin{array}{l} \text{总激发数} \\ \text{不变} \end{array} \quad (6.2.31)$$

$$C = \frac{1}{2} \Delta \sigma_z + g(\sigma_+ a + a^\dagger \sigma_-), \quad \begin{array}{l} \leftarrow \text{激发放} \\ \leftarrow \text{交换常数} \end{array} \quad (6.2.32)$$

i.e.,  $N$  and  $C$  commute with the Hamiltonian  $[N, \mathcal{H}] = [C, \mathcal{H}] = 0$ . Here  $N$  is an operator that represents the total excitation in the atom-field system, and  $C$  is an exchange constant.

We first derive an equation of motion for the atomic lowering operator  $\sigma_-$ . It follows from Eq. (6.2.29) that

$$\begin{aligned} \ddot{\sigma}_- &= -i\omega \dot{\sigma}_- + ig(\dot{\sigma}_z a + \sigma_z \dot{a}) \\ &= -i\omega \dot{\sigma}_- - 2g^2(a^\dagger \sigma_- a - \sigma_+ a^2) + v g \sigma_z a - g^2 \sigma_-, \end{aligned} \quad (6.2.33)$$

where, in the second line, we substituted for  $\dot{\sigma}_z$  and  $\dot{a}$  from Eqs. (6.2.30) and (6.2.28), respectively. It is readily verified that

$$\begin{aligned} g^2(a^\dagger \sigma_- a - \sigma_+ a^2) &= -i \left( \frac{\Delta}{2} + C \right) \dot{\sigma}_- \\ &\quad + \left( vC - \frac{1}{2}\Delta^2 + \frac{1}{2}\omega\Delta \right) \sigma_-, \end{aligned} \quad (6.2.34)$$

$$g \sigma_z a = -i \dot{\sigma}_- + \omega \sigma_-. \quad (6.2.29) \quad (6.2.35)$$

On substituting these expressions in Eq. (6.2.33), we obtain the desired equation for  $\sigma_-$ :

$$\ddot{\sigma}_- + 2i(v - C)\dot{\sigma}_- + (2vC - v^2 + g^2)\sigma_- = 0. \quad (6.2.36)$$

In a similar manner, we obtain

$$\ddot{a} + 2i(v - C)\dot{a} + (2vC - v^2 + g^2)a = 0. \quad (6.2.37)$$

These equations can be solved in a straightforward manner and the resulting expressions for  $\sigma_-(t)$  and  $a(t)$  are (6.2.29)

$$\begin{aligned} \sigma_-(t) &= [\sigma_+(t)]^\dagger \quad \text{初态为 } \sigma_+(0) = -i\omega \sigma_- + i g \sigma_z a \xrightarrow{\text{代入}} \text{利用 (6.2.42)} \\ &= e^{-ivt} e^{iCt} \left[ \left( \cos \kappa t + iC \frac{\sin \kappa t}{\kappa} \right) \sigma_-(0) - ig \frac{\sin \kappa t}{\kappa} a(0) \right], \end{aligned} \quad (6.2.38)$$

$$a(t) = e^{-ivt} e^{iCt} \left[ \left( \cos \kappa t - iC \frac{\sin \kappa t}{\kappa} \right) a(0) - ig \frac{\sin \kappa t}{\kappa} \sigma_-(0) \right], \quad (6.2.39)$$

where  $\kappa$  is a constant operator

$$\kappa = \left[ \frac{\Delta^2}{4} + g^2(N+1) \right]^{1/2}, \quad (6.2.40)$$

$\kappa = \sqrt{g^2 + C^2}$

which commutes with  $C$ , i.e.,  $[C, \kappa] = 0$ . In deriving Eqs. (6.2.38) and (6.2.39), we used

$$C^2 = \frac{\Delta^2}{4} + g^2 N, \quad (\text{原开脚面}) \quad (6.2.41)$$

$$g\sigma_z a = 2C\sigma_- + \Delta\sigma_- - ga. \quad (6.2.42)$$

Equations (6.2.38) and (6.2.39) provide a complete solution of the problem involving interaction of a two-level atom with a single-mode field in the Heisenberg picture. All quantities of interest can be obtained from these solutions. For example, the expression for the inversion  $W(t)$  (Eq. (6.2.21)) can be recovered from Eq. (6.2.38) via

$$\begin{aligned} W(t) &= \langle a, \alpha | \sigma_z(t) | a, \alpha \rangle, & \xrightarrow{\text{why?}} \text{Schrödinger pict. } \Phi(6.2.20) \\ &= 2\langle a, \alpha | \sigma_+(t)\sigma_-(t) | a, \alpha \rangle - 1. & W(t) = (a^\dagger - |a\rangle)(c_a^\dagger c_a) \begin{pmatrix} 1 & 0 \\ 0 & -1 \end{pmatrix} \begin{pmatrix} c_a \\ c_b \end{pmatrix} = \langle a| \sigma_+ | \Psi \rangle = \langle \Psi | \sigma_+ \rangle = \langle \Psi | \Psi \rangle \end{aligned} \quad (6.2.43)$$

Here we have assumed that the atom is initially in the excited state  $|a\rangle$  and the field is initially in the coherent state  $|\alpha\rangle$ .

As mentioned earlier, a particular advantage of working in the Heisenberg picture is that the evaluation of multi-time correlation functions is straightforward. As an example, we can use Eq. (6.2.38) to construct the dipole-dipole correlation function (Problem 6.5)

$$\begin{aligned} &\langle a, \alpha | \sigma_+(t)\sigma_-(t+\tau) | a, \alpha \rangle \quad \text{不再相关子项} \\ &= e^{-i\tau - |\alpha|^2} \sum_{n=0}^{\infty} \frac{|\alpha|^{2n}}{n!} \\ &\times \frac{1}{4\Omega_n^2} \left[ \cos(\Omega_{n-1}\tau/2) - \frac{i\Delta}{2\Omega_{n-1}} \sin(\Omega_{n-1}\tau/2) \right] \\ &\times \{(\Omega_n + \Delta)^2 e^{-i\Omega_n\tau/2} + (\Omega_n - \Delta)^2 e^{i\Omega_n\tau/2} \\ &+ 8g^2(n+1) \cos[\Omega_n(\tau+2t)/2]\}, \end{aligned} \quad (6.2.44)$$

where  $\Omega_n$  is given in Eq. (6.2.15).

Schrödinger pict. 也成立

$$\begin{aligned} &\langle A(t)B(t+\tau) \rangle + \langle B(t)A(t+\tau) \rangle \\ &= \underbrace{\langle \Psi(t) |}_{\langle \Psi(t) |} \underbrace{e^{i\frac{\Delta t}{2}}}_A \underbrace{e^{-i\frac{\Delta t}{2}}}_B \underbrace{e^{i\frac{\Delta(t+\tau)}{2}}}_B \underbrace{e^{-i\frac{\Delta(t+\tau)}{2}}}_A \underbrace{| \Psi(t+\tau) \rangle}_{\langle \Psi(t+\tau) |} \\ &= \langle \Psi(t) | \hat{A} \left( e^{i\frac{\Delta t}{2}} \hat{B} \right) | \Psi(t+\tau) \rangle \end{aligned}$$

若  $\hat{A}$  合时，换成时序算符  $\hat{T}$  会出错

### 6.2.3 Unitary time-evolution operator method

Another equivalent approach to deal with the problem of atom-field interaction is through the unitary time-evolution operator. In many problems where the evolution of the system is unitary, i.e., there is no dissipation, this approach may prove to be the simplest.

For the present problem of the interaction of a two-level atom with a single-mode quantized radiation field, the unitary time-evolution operation is given by

$$U(t) = \exp(-i\mathcal{V}t/\hbar), \quad (6.2.45)$$

where the interaction picture Hamiltonian  $\mathcal{V}$ , at exact resonance, is given by (Eq. (6.2.8) with  $\Delta = 0$ )

*Ansatz*  $\rightarrow \mathcal{V} = \hbar g(\sigma_+ a + a^\dagger \sigma_-).$  (6.2.46)

Here  $\sigma_+ = |a\rangle\langle b|$  and  $\sigma_- = |b\rangle\langle a|$ . It follows, on using

$$(\sigma_+ a + a^\dagger \sigma_-)^{\ell} = (aa^\dagger)^\ell |a\rangle\langle a| + (a^\dagger a)^\ell |b\rangle\langle b|, \quad (6.2.47)$$

$$\underline{(\sigma_+ a + a^\dagger \sigma_-)^{\ell+1}} = \underline{(aa^\dagger)^\ell a |a\rangle\langle b|} + \underline{a^\dagger (aa^\dagger)^\ell |b\rangle\langle a|}, \quad (6.2.48)$$

that

$$\begin{aligned} U(t) &= \cos(gt\sqrt{a^\dagger a + 1})|a\rangle\langle a| + \cos(gt\sqrt{a^\dagger a})|b\rangle\langle b| \\ &\quad - i \frac{\sin(gt\sqrt{a^\dagger a + 1})}{\sqrt{a^\dagger a + 1}} a|a\rangle\langle b| - ia^\dagger \frac{\sin(gt\sqrt{a^\dagger a + 1})}{\sqrt{a^\dagger a + 1}} |b\rangle\langle a|. \end{aligned} \quad (6.2.49)$$

The wave vector at time  $t$  in terms of the wave vector at time  $t = 0$  is simply given by

$$|\psi(t)\rangle = U(t)|\psi(0)\rangle. \quad (6.2.50)$$

As an example of the equivalence of this method with earlier approaches we evaluate the probability amplitudes  $c_{a,n}(t)$  and  $c_{b,n+1}(t)$  for an atom initially in the excited state  $|a\rangle$  and the field as a linear combination of number states, i.e.,

$$|\psi(0)\rangle = \sum_{n=0}^{\infty} c_n(0)|a, n\rangle. \quad (6.2.51)$$

On substituting for  $U(t)$  and  $|\psi(0)\rangle$  from Eqs. (6.2.49) and (6.2.51), respectively, in Eq. (6.2.50), we obtain

$$\begin{aligned} |\psi(t)\rangle &= \sum_{n=0}^{\infty} c_n(0) \left[ \cos(gt\sqrt{n+1})|a, n\rangle \right. \\ &\quad \left. - i \sin(gt\sqrt{n+1})|b, n+1\rangle \right]. \end{aligned} \quad (6.2.52)$$

We thus have

$$c_{a,n}(t) = \langle a, n | \psi(t) \rangle = c_n(0) \cos(gt\sqrt{n+1}), \quad (6.2.53)$$

$$c_{b,n+1}(t) = -ic_n(0) \sin(gt\sqrt{n+1}), \quad (6.2.54)$$

in full agreement with Eqs. (6.2.16) and (6.2.17) for  $\Delta = 0$ .

### 6.3 Weisskopf–Wigner theory of spontaneous emission between two atomic levels

In the previous section, we showed that an atom in the upper level can make transitions back and forth to the lower state in time even in the absence of an applied field. However, it is seen experimentally that an atom in an excited state decays to the ground state with a characteristic lifetime but it does not make back and forth transitions. The atomic decay has been added into the atomic density matrix equations (see Problem 5.2) phenomenologically. In our model of spontaneous emission discussed in the previous section, the decay is not included because we have considered only one mode of the field. For a proper account of the atomic decay a continuum of modes, corresponding to a quantization cavity which is infinite in extent, needs to be included.

The interaction picture Hamiltonian, in the rotating-wave approximation, for this system is

$$\mathcal{V} = \hbar \sum_{\mathbf{k}} [g_{\mathbf{k}}^*(\mathbf{r}_0) \sigma_+ a_{\mathbf{k}} e^{i(\omega - \nu_{\mathbf{k}})t} + \text{H.c.}], \quad (6.3.1)$$

*以下不考虑场  
为简并态  
只取一个*  
where  $g_{\mathbf{k}}(\mathbf{r}_0) = g_{\mathbf{k}} \exp(-i\mathbf{k} \cdot \mathbf{r}_0)$ , i.e., we have included the spatial dependence explicitly. Here,  $\mathbf{r}_0$  is the location of the atom. The interaction picture Hamiltonian is obtained following the same method as outlined in the beginning of Section 6.2. We assume that at time  $t = 0$  the atom is in the excited state  $|a\rangle$  and the field modes are in the vacuum state  $|0\rangle$ . The state vector is therefore

$$|\psi(t)\rangle = c_a(t)|a, 0\rangle + \sum_{\mathbf{k}} c_{b,\mathbf{k}}|b, 1_{\mathbf{k}}\rangle, \quad (6.3.2)$$

with

$$c_a(0) = 1, \quad c_{b,\mathbf{k}}(0) = 0. \quad (6.3.3)$$

We want to determine the state of the atom and the state of the radiation field at some later time when the atom begins to emit photons and we do so in the Weisskopf–Wigner approximation.

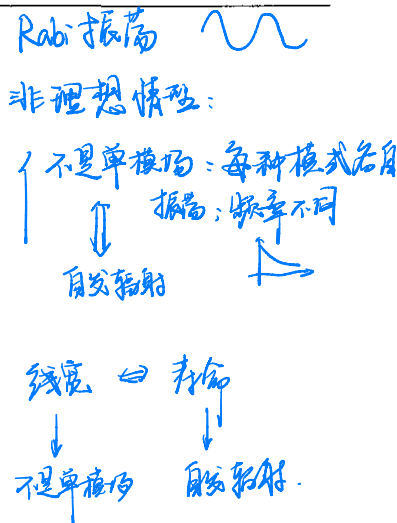
From the Schrödinger equation

$$|\dot{\psi}(t)\rangle = -\frac{i}{\hbar} \mathcal{V} |\psi(t)\rangle, \quad (6.3.4)$$

we get the equations of motion for the probability amplitudes  $c_a$  and  $c_{b,\mathbf{k}}$ : *看似双重本征，但由于只作用在自己模式上，故少一个项。*

$$\dot{c}_a(t) = -i \sum_{\mathbf{k}} g_{\mathbf{k}}^*(\mathbf{r}_0) e^{i(\omega - \nu_{\mathbf{k}})t} c_{b,\mathbf{k}}(t), \quad (6.3.5)$$

$$\dot{c}_{b,\mathbf{k}}(t) = -ig_{\mathbf{k}}(\mathbf{r}_0) e^{-i(\omega - \nu_{\mathbf{k}})t} c_a(t). \quad (6.3.6)$$



*对技术和是双频腔的设置  
与所有方向*

In order to get an equation that involves  $c_a$  only, we first integrate Eq. (6.3.6),

$$c_{b,\mathbf{k}}(t) = -ig_{\mathbf{k}}(\mathbf{r}_0) \int_0^t dt' e^{-i(\omega - v_k)t'} c_a(t'). \quad (6.3.7)$$

On substituting this expression of  $c_{b,\mathbf{k}}(t)$  into Eq. (6.3.5), we obtain

$$\dot{c}_a(t) = - \sum_{\mathbf{k}} |g_{\mathbf{k}}(\mathbf{r}_0)|^2 \int_0^t dt' e^{i(\omega - v_k)(t-t')} c_a(t'). \quad (6.3.8)$$

This is still an exact equation. We have replaced two linear differential equations by one linear differential-integral equation. Next we make some approximations.

Assuming that the modes of the field are closely spaced in frequency, we can replace the summation over  $\mathbf{k}$  by an integral:

$$\sum_{\mathbf{k}} \rightarrow 2 \frac{V}{(2\pi)^3} \int_0^{2\pi} d\phi \int_0^\pi d\theta \sin \theta \int_0^\infty dk k^2, \quad (6.3.9)$$

where  $V$  is the quantization volume. It follows from Eq. (6.1.8) that

$$|g_{\mathbf{k}}(\mathbf{r}_0)|^2 = \frac{v_k}{2\hbar\epsilon_0 V} \wp_{ab}^2 \cos^2 \theta, \quad (6.3.10)$$

where  $\theta$  is the angle between the atomic dipole moment  $\wp_{ab}$  and the electric field polarization vector  $\hat{\mathbf{e}}_{\mathbf{k}}$ . Equation (6.3.8) therefore becomes

$$\dot{c}_a(t) = - \frac{4\wp_{ab}^2}{(2\pi)^2 6\hbar\epsilon_0 c^3} \int_0^\infty dv_k v_k^3 \int_0^t dt' e^{i(\omega - v_k)(t-t')} c_a(t'), \quad (6.3.11)$$

*课本笔记*

where integrations over  $\theta$  and  $\phi$  have been carried out and we have used  $k = v_k/c$ . In the emission spectrum, the intensity of light associated with the emitted radiation is going to be centered about the atomic transition frequency  $\omega$ . The quantity  $v_k^3$  varies little around  $v_k = \omega$  for which the time integral in Eq. (6.3.11) is not negligible. We can therefore replace  $v_k^3$  by  $\omega^3$  and the lower limit in the  $v_k$  integration by  $-\infty$ . The integral

$$\int_{-\infty}^\infty dv_k e^{i(\omega - v_k)(t-t')} = 2\pi\delta(t - t'), \quad (6.3.12)$$

yields the following equation for  $c_a(t)$ , in the Weisskopf–Wigner approximation:

$$N = N e^{-\Gamma t} \downarrow |C_a|^2 \quad \dot{c}_a(t) = -\frac{\Gamma}{2} c_a(t), \quad (6.3.13)$$

where the decay constant

$$\Gamma = \frac{1}{4\pi\epsilon_0} \frac{4\omega^3 \wp_{ab}^2}{3\hbar c^3}. \quad (6.3.14)$$

A solution of Eq. (6.3.13) gives

$$\rho_{aa} \equiv |c_a(t)|^2 = \exp(-\Gamma t), \quad (6.3.15)$$

i.e., an atom in the excited state  $|a\rangle$  in vacuum decays exponentially in time with the lifetime  $\tau = 1/\Gamma$ .

During the process of spontaneous emission, the atom emits a quantum of energy equal to  $E_a - E_b = \hbar\nu$ . We now calculate the state of the field emitted during the spontaneous emission process.

We first calculate the coefficient  $c_{b,k}(t)$ . Substituting the solution for  $c_a(t)$  into Eq. (6.3.7) we find

$$\begin{aligned} c_{b,k}(t) &= -ig_k(r_0) \int_0^t dt' e^{-i(\omega-\nu_k)t'-\Gamma t'/2} \\ &= g_k(r_0) \left[ \frac{1 - e^{-i(\omega-\nu_k)t-\Gamma t/2}}{(\nu_k - \omega) + i\Gamma/2} \right], \end{aligned} \quad (6.3.16)$$

so that

$$\begin{aligned} |\psi(t)\rangle &= e^{-\Gamma t/2} |a, 0\rangle \\ &\quad + |b\rangle \sum_k g_k e^{-ik \cdot r_0} \left[ \frac{1 - e^{i(\omega-\nu_k)t-\Gamma t/2}}{(\nu_k - \omega) + i\Gamma/2} \right] |1_k\rangle. \end{aligned} \quad (6.3.17)$$

Upon introducing the field state

$$|\gamma_0\rangle = \sum_k g_k \frac{e^{-ik \cdot r_0}}{(\nu_k - \omega) + i\Gamma/2} |1_k\rangle, \quad (6.3.18)$$

for times long compared to the radiative decay  $t \gg \Gamma^{-1}$  we have  $|\psi\rangle \rightarrow |b\rangle|\gamma_0\rangle$ . Here the index ‘0’ in  $|\gamma_0\rangle$  reminds us that this state corresponds to an atom located at position  $r_0$ . This is a linear superposition of the single-photon states with different wave vectors associated with them.

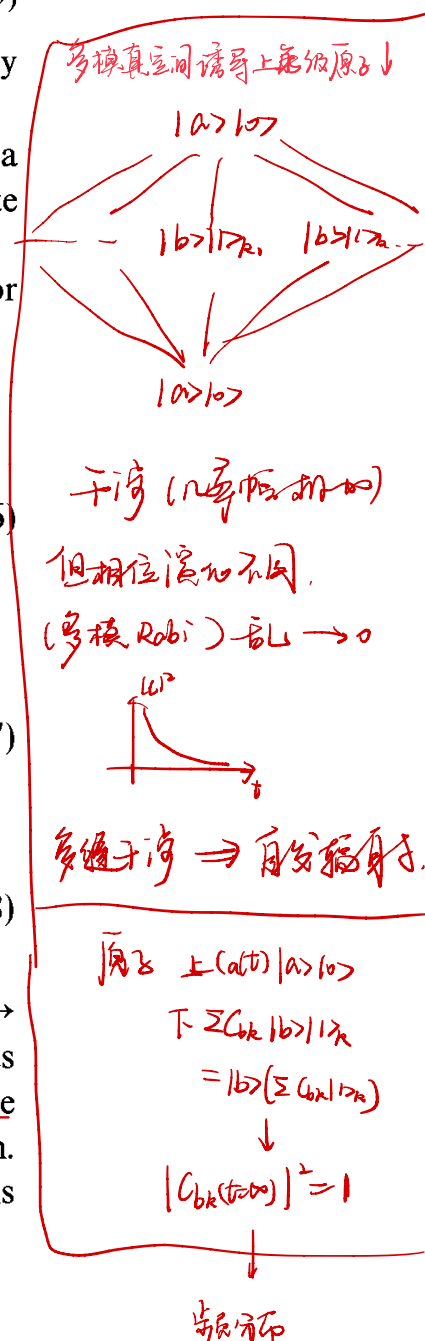
The first-order correlation function  $G^{(1)}(\mathbf{r}, \mathbf{r}; t, t)$  for large times is given by

~~物理意义?~~

$$\begin{aligned} G^{(1)}(\mathbf{r}, \mathbf{r}; t, t) &= \langle \psi | E^{(-)}(\mathbf{r}, t) E^{(+)}(\mathbf{r}, t) | \psi \rangle \\ &= \langle \gamma_0 | E^{(-)}(\mathbf{r}, t) E^{(+)}(\mathbf{r}, t) | \gamma_0 \rangle \\ &\stackrel{\text{在 } t \rightarrow \infty}{=} \langle \gamma_0 | E^{(-)}(\mathbf{r}, t) | 0 \rangle \langle 0 | E^{(+)}(\mathbf{r}, t) | \gamma_0 \rangle. \end{aligned} \quad (6.3.19)$$

Here a complete set of states is inserted and since only the vacuum state survives while the other states lead to zero, we keep the vacuum state only. We have also assumed, that the field is linearly polarized, say along the  $x$ -axis. As discussed in Section 4.2,  $G^{(1)}(\mathbf{r}, \mathbf{r}; t, t)$  is proportional to the probability of registering a photon at time  $t$  by a photodetector located at the position  $\mathbf{r}$ . According to Eq. (6.3.19),  $G^{(1)}(\mathbf{r}, \mathbf{r}; t, t) = |\langle 0 | E^{(+)}(\mathbf{r}, t) | \gamma_0 \rangle|^2$ . Thus the function

$$\Psi_\gamma(\mathbf{r}, t) = \langle 0 | E^{(+)}(\mathbf{r}, t) | \gamma_0 \rangle \quad (6.3.20)$$



can be interpreted as a kind of **wave function** for a photon. This is in analogy with the corresponding wave function for particles (see Section 1.5).

From the definitions of  $E^{(+)}(\mathbf{r}, t)$  and  $|\gamma_0\rangle$  (Eqs. (1.1.30) and (6.3.18)), we find

$$\begin{aligned}\langle 0 | E^{(+)}(\mathbf{r}, t) | \gamma_0 \rangle &= \\ &= \sqrt{\frac{\hbar}{2\epsilon_0 V}} \sum_{\mathbf{k}, \mathbf{k}'} \langle 0 | (v_{k'})^{1/2} a_{\mathbf{k}'} e^{-iv_{k'} t + i\mathbf{k}' \cdot \mathbf{r}} g_{\mathbf{k}} \frac{e^{-i\mathbf{k} \cdot \mathbf{r}_0}}{(v_k - \omega) + i\Gamma/2} | 1_{\mathbf{k}} \rangle \\ &= \sqrt{\frac{\hbar}{2\epsilon_0 V}} \sum_{\mathbf{k}} (v_k)^{1/2} g_{\mathbf{k}} e^{-iv_k t} e^{i\mathbf{k} \cdot (\mathbf{r} - \mathbf{r}_0)} \frac{1}{(v_k - \omega) + i\Gamma/2}. \quad (6.3.21)\end{aligned}$$

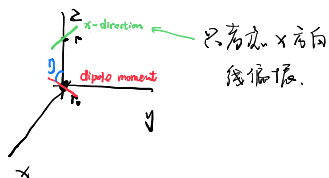
(光子的)

假定光场为一向向波函数

下一下方向为飞物

原偶极矩在x平面内

轴成角



We now evaluate this function by first converting the sum into an integral via Eq. (6.3.9). We however do not include the factor 2 from there as the field is assumed to be polarized along the  $x$ -axis. The  $\phi$ - and  $\theta$ -integrations can be carried out by choosing a coordinate system in which the vector  $\mathbf{r} - \mathbf{r}_0$  points along the  $z$ -axis, the atomic dipole moment forms an angle  $\eta$  with the  $z$ -axis in the  $x$ - $z$  plane, and the wave vector  $\mathbf{k}$  has components

$$\mathbf{k} = k(\sin \theta \cos \phi \hat{x} + \sin \theta \sin \phi \hat{y} + \cos \theta \hat{z}). \quad (6.3.22)$$

The resulting expression for  $\langle 0 | E^{(+)}(\mathbf{r}, t) | \gamma_0 \rangle$  is\*

$$\begin{aligned}\langle 0 | E^{(+)}(\mathbf{r}, t) | \gamma_0 \rangle &= \frac{ic \rho_{ab} \sin \eta}{8\pi^2 \epsilon_0 \Delta r} \\ &\times \int_0^\infty dk k^2 (e^{ik\Delta r} - e^{-ik\Delta r}) \frac{e^{-iv_k t}}{(v_k - \omega) + i\Gamma/2}, \quad (6.3.23)\end{aligned}$$

$$k = \frac{p}{c}$$

where  $\Delta r = |\mathbf{r} - \mathbf{r}_0|$ . In the above integral the term  $\exp[-i(k\Delta r + v_k t)]$  represents an incoming wave and we will therefore neglect it. As in the Weisskopf–Wigner theory of spontaneous emission, we assume that the quantity  $v_k^2$  varies little around  $v_k = \omega$  and therefore can be replaced by  $\omega^2$  and the lower limit of integration can be extended to  $-\infty$ . Making these approximations we are left with the integral

$$\int_{-\infty}^{\infty} dv_k \frac{e^{-iv_k t + iv_k \Delta r/c}}{(v_k - \omega) + i\Gamma/2}.$$

$$\text{奇数: } \omega - i\Gamma/2 = v_k$$

积分图: 圆弧加0

$t < \frac{\Delta r}{c}$  上半圆弧加0  
过上

$t > \frac{\Delta r}{c}$  下半圆弧加0

This integral is evaluated by using the contour method (see Fig. 6.3).

For  $t < \Delta r/c$ , the contour lies in the upper half-plane and if  $t > \Delta r/c$ , in the lower half-plane. On performing the integration, we find that

\* Equation (6.3.23) can be derived in a more complete and rigorous way using the method in Appendix 10.A.

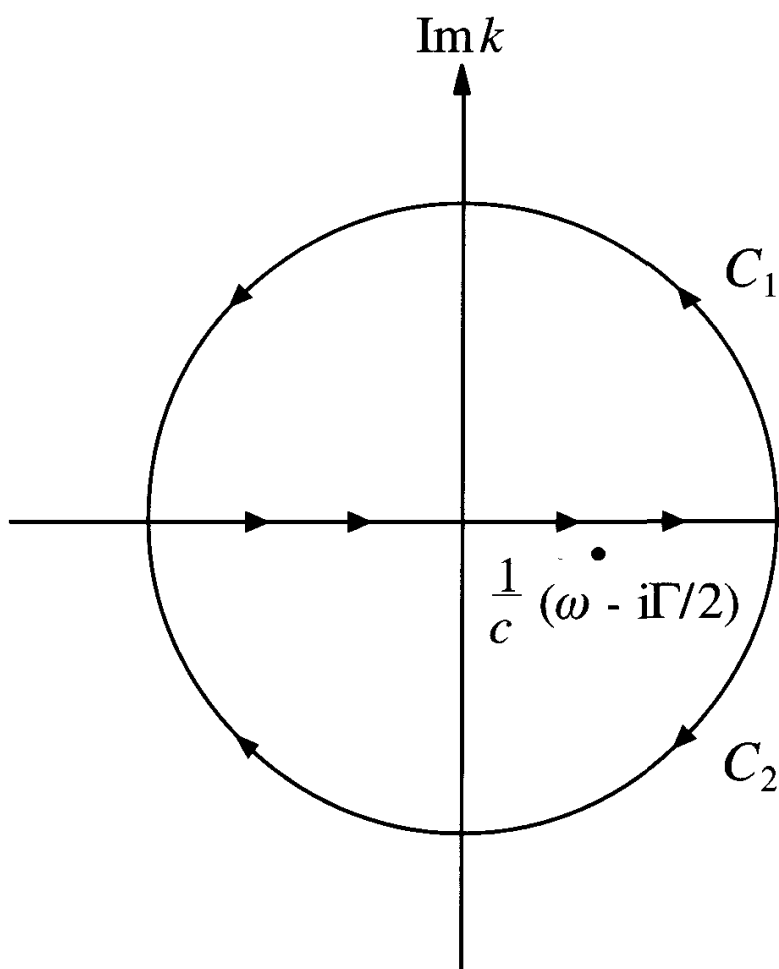


Fig. 6.3  
Contours used for evaluating the integral in Eq. (6.3.23):  $C_1$  if  $t < \Delta r/c$  and  $C_2$  if  $t > \Delta r/c$ .

角放宣祖：上半為0，下限圖

$$\oint = 2\pi i \operatorname{Res} [f(z), a], \quad \gamma_k = \omega - \frac{iP}{z}$$

$$\Rightarrow \operatorname{Res} [f(z), a] = \frac{1}{(m-1)!} \frac{d^{m-1}}{dz^{m-1}} (z-a)^m f(z)$$

$$f(z) = \frac{\omega z}{(z-a)^m}$$

Step function

$$\Theta(x) = \begin{cases} 1, & x > 0 \\ 0, & x \leq 0 \end{cases}$$

$$\langle 0 | E^{(+)}(\mathbf{r}, t) | \gamma_0 \rangle = \frac{\mathcal{E}_0}{\Delta r} \Theta \left( t - \frac{\Delta r}{c} \right) e^{-i(t-\frac{\Delta r}{c})(\omega - i\Gamma/2)}, \quad (6.3.24)$$

where  $\Theta$  is a unit step function and

$$\mathcal{E}_0 = -\frac{\omega^2 \rho_{ab} \sin \eta}{4\pi \epsilon_0 c^2}. \quad (6.3.25)$$

We then find that

$$G^{(1)}(\mathbf{r}, \mathbf{r}; t, t) = \frac{|\mathcal{E}_0|^2}{|\mathbf{r} - \mathbf{r}_0|^2} \Theta \left( t - \frac{|\mathbf{r} - \mathbf{r}_0|}{c} \right) e^{-\Gamma(t - |\mathbf{r} - \mathbf{r}_0|/c)}. \quad (6.3.26)$$

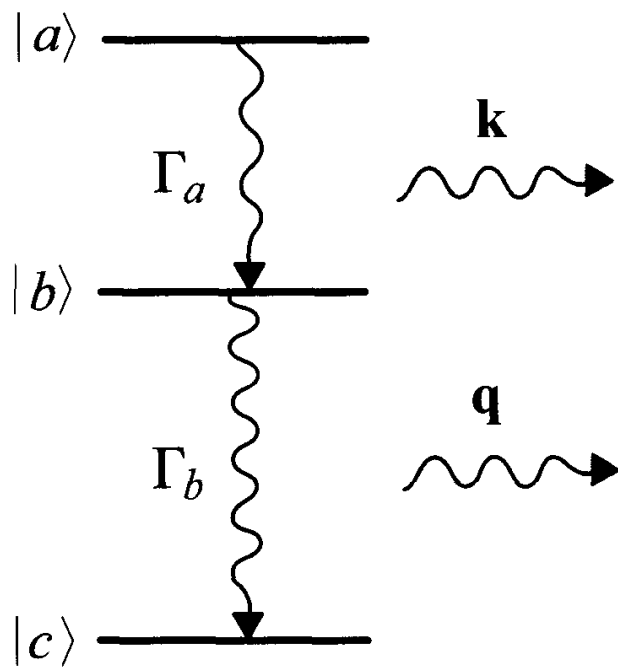
Here the step function is a manifestation of the fact that the signal cannot move faster than the speed of light.

Lorentzian  
而該步進是 6.3.23  
或將 6.3.24 作 Fourier 变换

## 6.4 Two-photon cascades

In this section we consider the spontaneous emission in a three-level atom in cascade configuration, as shown in Fig. 6.4. The atom in upper state  $|a\rangle$  emits a  $\mathbf{k}$  photon of frequency  $\nu_k$  and decays to state

**Fig. 6.4**  
Level scheme for atomic decay due to spontaneous emission in a three-level atom in cascade configuration.



$|b\rangle$  which decays to ground state  $|c\rangle$ , via emission of a  $\mathbf{q}$  photon of frequency  $\nu_q$ . The interaction picture Hamiltonian for the system is

$$\begin{aligned} \mathcal{V} = \hbar \sum_{\mathbf{k}} & \left[ g_{a,\mathbf{k}}^*(\mathbf{r}_0) \sigma_+^{(1)} a_{\mathbf{k}} e^{i(\omega_{ab} - \nu_k)t} + \text{H.c.} \right] \\ & + \hbar \sum_{\mathbf{q}} \left[ g_{b,\mathbf{q}}^*(\mathbf{r}_0) \sigma_+^{(2)} a_{\mathbf{q}} e^{i(\omega_{bc} - \nu_q)t} + \text{H.c.} \right], \end{aligned} \quad (6.4.1)$$

where  $\sigma_+^{(1)} = |a\rangle\langle b|$ ,  $\sigma_+^{(2)} = |b\rangle\langle c|$ , and  $g_{a,\mathbf{k}}(\mathbf{r}_0)$  and  $g_{b,\mathbf{q}}(\mathbf{r}_0)$  are the appropriate coupling constants for  $|a\rangle \rightarrow |b\rangle$  and  $|b\rangle \rightarrow |c\rangle$  transitions, respectively.

The state of the atom-field system is now described by

$$|\psi(t)\rangle = c_a(t)|a, 0\rangle + \sum_{\mathbf{k}} c_{b,\mathbf{k}}|b, 1_{\mathbf{k}}\rangle + \sum_{\mathbf{k}, \mathbf{q}} c_{c,\mathbf{k}, \mathbf{q}}|c, 1_{\mathbf{k}}, 1_{\mathbf{q}}\rangle. \quad (6.4.2)$$

As in Section 6.3, the probability amplitudes  $c_a$ ,  $c_{b,\mathbf{k}}$ , and  $c_{c,\mathbf{k}, \mathbf{q}}$  obey the equations of motion

$$\dot{c}_a = -i \sum_{\mathbf{k}} g_{a,\mathbf{k}}^*(\mathbf{r}_0) c_{b,\mathbf{k}} e^{i(\omega_{ab} - \nu_k)t}, \quad (6.4.3)$$

$$\dot{c}_{b,\mathbf{k}} = -ig_{a,\mathbf{k}}(\mathbf{r}_0) c_a e^{-i(\omega_{ab} - \nu_k)t} - i \sum_{\mathbf{q}} g_{b,\mathbf{q}}^*(\mathbf{r}_0) c_{c,\mathbf{k}, \mathbf{q}} e^{i(\omega_{bc} - \nu_q)t}, \quad (6.4.4)$$

$$\dot{c}_{c,\mathbf{k}, \mathbf{q}} = -ig_{b,\mathbf{q}}(\mathbf{r}_0) c_{b,\mathbf{k}} e^{-i(\omega_{bc} - \nu_q)t}. \quad (6.4.5)$$

Following the lead of Section 6.3, we recognize that, in the Weisskopf–Wigner approximation,

$$-i \sum_{\mathbf{k}} g_{a,\mathbf{k}}^*(\mathbf{r}_0) c_{b,\mathbf{k}} e^{i(\omega_{ab} - \nu_k)t} = -\frac{\Gamma_a}{2} c_a, \quad (6.4.6)$$

where  $\Gamma_a$  is the atomic decay rate from state  $|a\rangle$  to state  $|b\rangle$ . Furthermore, it is clear that the second term in Eq. (6.4.4) represents decay from  $|b\rangle$  to  $|c\rangle$  and we may write

$$-i \sum_{\mathbf{q}} g_{b,\mathbf{q}}^*(\mathbf{r}_0) c_{c,\mathbf{k},\mathbf{q}} e^{i(\omega_{bc} - \nu_q)t} = -\frac{\Gamma_b}{2} c_{b,\mathbf{k}}, \quad (6.4.7)$$

where  $\Gamma_b$  is the decay rate from state  $|b\rangle$  to state  $|c\rangle$ . Upon inserting Eqs. (6.4.6) and (6.4.7) into (6.4.3)–(6.4.5), we obtain the useful final form for the atom–field equations of motion

$$\dot{c}_a = -\frac{\Gamma_a}{2} c_a, \quad (6.4.8)$$

$$\dot{c}_{b,\mathbf{k}} = -ig_{a,\mathbf{k}}(\mathbf{r}_0) e^{-i(\omega_{ab} - \nu_k)t - \frac{\Gamma_a}{2}t} - \frac{\Gamma_b}{2} c_{b,\mathbf{k}}, \quad (6.4.9)$$

$$\dot{c}_{c,\mathbf{k},\mathbf{q}} = -ig_{b,\mathbf{q}}(\mathbf{r}_0) c_{b,\mathbf{k}} e^{-i(\omega_{bc} - \nu_q)t}, \quad (6.4.10)$$

where we have substituted  $\exp(-\Gamma_a t/2)$  for  $c_a(t)$  in the first term of Eq. (6.4.9).

We are most interested in the state of the field for times  $t \gg \Gamma_a^{-1}$  and  $\Gamma_b^{-1}$ , i.e., we want to know  $c_{c,\mathbf{k},\mathbf{q}}(\infty)$  as  $c_a(\infty)$  and  $c_{b,\mathbf{k}}(\infty)$  tend to zero.

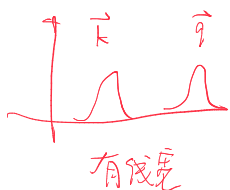
It follows, on carrying out the simple integration implied by Eq. (6.4.9), that

$$\begin{aligned} c_{b,\mathbf{k}}(t) &= -ig_{a,\mathbf{k}}(\mathbf{r}_0) \int_0^t dt' e^{-i(\omega_{ab} - \nu_k)t' - \Gamma_a t'/2} e^{-\Gamma_b(t-t')/2} \\ &= -ig_{a,\mathbf{k}}(\mathbf{r}_0) \frac{e^{i(\nu_k - \omega_{ab})t - \Gamma_a t/2} - e^{-\Gamma_b t/2}}{i(\nu_k - \omega_{ab}) - \frac{1}{2}(\Gamma_a - \Gamma_b)}. \end{aligned} \quad (6.4.11)$$

This expression for  $c_{b,\mathbf{k}}(t)$  can now be substituted into Eq. (6.4.10), and the resulting equation can be integrated to yield the following long time limit of  $c_{c,\mathbf{k},\mathbf{q}}(t)$ :

$$\begin{aligned} c_{c,\mathbf{k},\mathbf{q}}(\infty) &= g_{a,\mathbf{k}} g_{b,\mathbf{q}} e^{-i(\mathbf{k}+\mathbf{q}) \cdot \mathbf{r}_0} \frac{1}{i(\nu_k - \omega_{ab}) - \frac{1}{2}(\Gamma_a - \Gamma_b)} \\ &\quad \times \left[ \frac{1}{i(\nu_k + \nu_q - \omega_{ac}) - \frac{1}{2}\Gamma_a} - \frac{1}{i(\nu_q - \omega_{bc}) - \frac{1}{2}\Gamma_b} \right] \\ &= \frac{-g_{a,\mathbf{k}} g_{b,\mathbf{q}} e^{-i(\mathbf{k}+\mathbf{q}) \cdot \mathbf{r}_0}}{[i(\nu_k + \nu_q - \omega_{ac}) - \frac{1}{2}\Gamma_a][i(\nu_q - \omega_{bc}) - \frac{1}{2}\Gamma_b]}. \end{aligned} \quad (6.4.12)$$

As in the long time limit, both  $c_a(t)$  and  $c_{b,\mathbf{k}}(t)$  are zero, we insert  $c_{c,\mathbf{k},\mathbf{q}}(\infty)$ , as given by Eq. (6.4.12), into Eq. (6.4.2) and find that the



state of the radiation field is given by

$$|\gamma, \phi\rangle = \sum_{\mathbf{k}, \mathbf{q}} \frac{-g_{a,\mathbf{k}} g_{b,\mathbf{q}} e^{-i(\mathbf{k}+\mathbf{q}) \cdot \mathbf{r}_0}}{[i(v_k + v_q - \omega_{ac}) - \frac{1}{2}\Gamma_a][i(v_q - \omega_{bc}) - \frac{1}{2}\Gamma_b]} |1_{\mathbf{k}}, 1_{\mathbf{q}}\rangle, \quad (6.4.13)$$

where  $|\gamma, \phi\rangle$  represents the two-photon state.

We shall make detailed use of this result in Chapter 21 when we utilize two-photon correlation functions in order to gain insight into the foundations of quantum mechanics.

$\Gamma_a > \Gamma_b$  高光子数很区分  
 $\Gamma_a \ll \Gamma_b$  二者的不同区分 → 早年用双波干涉.

## 6.5 Excitation probabilities for single and double photoexcitation events

In Section 4.2 we presented heuristic arguments to show that the photodetection probability is governed by the normally ordered field correlation functions. Here we derive the excitation probability for single and double photoelectron events using the atom–field interaction formalism developed in this chapter.\*

Consider the interaction of linearly polarized light, described by the field operators  $E^{(+)}(\mathbf{r}, t)$  and  $E^{(-)}(\mathbf{r}, t)$ , with an atomic system consisting of a lower level  $|b\rangle$  and a set of excited levels  $|a_j\rangle$  (Fig. 6.5). We assume that the atom is initially in state  $|b\rangle$  and the field is in state  $|i\rangle$ . The interaction picture Hamiltonian, in the rotating-wave approximation, is

$$\mathcal{V} = - \sum_j \wp_{a_j b} \sigma_{a_j b} E^{(+)}(\mathbf{r}, t) \exp(i\omega_{a_j} t) + \text{H.c.} \quad (6.5.1)$$

The state of the atom–field system at time  $t$  is given by

$$\begin{aligned} |\psi(t)\rangle &= U_I(t)|\psi(0)\rangle \\ &\simeq \left[ 1 - \frac{i}{\hbar} \int_0^t dt' \mathcal{V}(t') \right] |b\rangle \otimes |i\rangle. \end{aligned} \quad (6.5.2)$$

The probability of exciting the atom to level  $|a_j\rangle$  is found by calculating the expectation value of the projection operator  $|a_j\rangle\langle a_j|$ , i.e.,

$$\begin{aligned} P_j(t) &= \langle \psi(t) | a_j \rangle \langle a_j | \psi(t) \rangle \\ &= \frac{\wp_{a_j b}^2}{\hbar^2} \int_0^t \int_0^t dt_1 dt_2 \exp[i\omega_{a_j}(t_1 - t_2)] \langle i | E^{(-)}(\mathbf{r}, t_2) E^{(+)}(\mathbf{r}, t_1) | i \rangle, \end{aligned} \quad (6.5.3)$$

where we substitute for  $|\psi(t)\rangle$  from Eq. (6.5.2). If we want only the probability of excitation, we should sum over all excited levels  $|a_j\rangle$ .

\* For an excellent treatment see the Les Houches lectures of Glauber [1965].

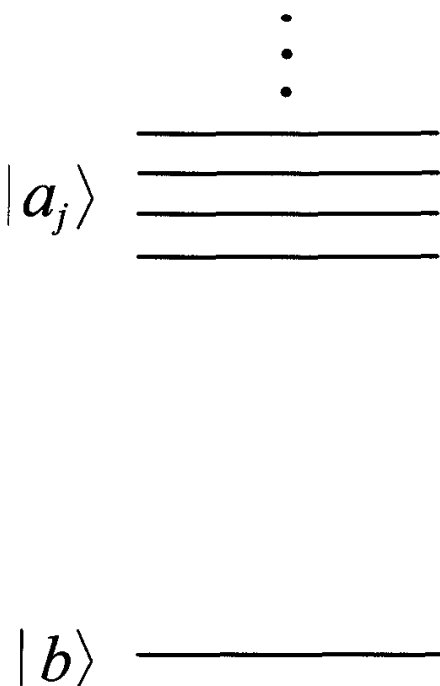


**Fig. 6.5**  
Level scheme for photodetection. The atom makes a transition from state  $|b\rangle$  to the manifold of excited states  $|a_j\rangle$ .

If  $\wp_{aj}^2$  is largely independent of  $j$ , we can take  $\wp_{aj}^2 \simeq \wp^2$ . Hence, for a broad-band detector the summation over  $j$  of the function  $\exp[i\omega_{aj}(t_1 - t_2)]$  introduces an effective  $\delta(t_1 - t_2)$  function and we obtain

$$\begin{aligned} P(t) &= \sum_j P_j(t) \\ &= \kappa \int_0^t dt_1 \langle i | E^{(-)}(\mathbf{r}, t_1) E^{(+)}(\mathbf{r}, t_1) | i \rangle, \end{aligned} \quad (6.5.4)$$

where  $\kappa$  is a constant. For mixed states, Eq. (6.5.4) becomes

$$P(t) = \kappa \int_0^t dt_1 \text{Tr} [\rho E^{(-)}(\mathbf{r}, t_1) E^{(+)}(\mathbf{r}, t_1)]. \quad (6.5.5)$$

Next, we consider atoms at the points  $\mathbf{r}_1$  and  $\mathbf{r}_2$  and find the joint-count probability  $P_{12}$  of double photoexcitation, i.e., we want the expectation value of the photoexcitation operator

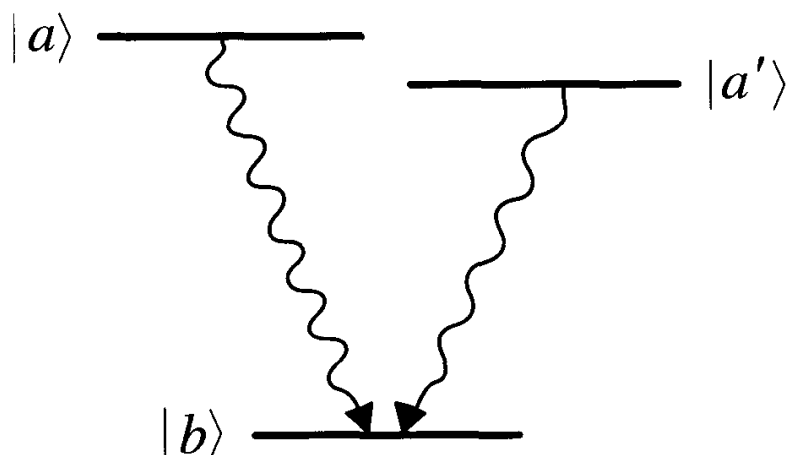
$$\left( \sum_j |a_j\rangle \langle a_j| \right)_\alpha$$

for both atoms, i.e.,  $\alpha = 1$  and 2. Similarly to Eq. (6.5.5), we obtain

$$\begin{aligned} P_{12} &= \kappa' \int_0^t dt_1 \int_0^t dt_2 \\ &\times \text{Tr} [\rho E^{(-)}(\mathbf{r}_1, t_1) E^{(-)}(\mathbf{r}_2, t_2) E^{(+)}(\mathbf{r}_2, t_2) E^{(+)}(\mathbf{r}_1, t_1)]. \end{aligned} \quad (6.5.6)$$

Thus  $P_{12}$  is governed by the second-order correlation function of the field operators.

**Fig. 6.6**  
Radiative decay of two closely lying levels  $|a\rangle$  and  $|a'\rangle$  to a common level  $|b\rangle$ .



## Problems

- 6.1** A model sometimes considered to study the atom–field coupling in a lossless cavity is represented by the Hamiltonian

$$\mathcal{H} = \hbar v a^\dagger a + \hbar \omega \sigma_z + \hbar g \left[ \sigma_+ a(a^\dagger a)^{1/2} + (a^\dagger a)^{1/2} a^\dagger \sigma_- \right],$$

in the usual notation. Note that the coupling is intensity dependent. Calculate the atomic inversion and discuss its evolution in terms of the various time scales, i.e., Rabi flopping time, the collapse time, and the revival time, for (a) an initial coherent state of the field and (b) an initial thermal state of the field. Note that the infinite series in the expression for inversion can be summed exactly in this case.

- 6.2** Calculate the population inversion for a two-level atom interacting with a single-mode quantized radiation field in the dipole and rotating-wave approximations for arbitrary time  $t$  when, at  $t = 0$ , the field is in a coherent state  $|\alpha\rangle$ , and the atomic state is  $|\psi\rangle_{\text{atom}} = (|a\rangle + e^{-i\phi}|b\rangle)/\sqrt{2}$  ( $|a\rangle$  and  $|b\rangle$  are the upper and lower levels, respectively). Discuss the conditions under which the populations in the two levels remain ‘trapped’.

- 6.3** Consider the atomic system shown in Fig. 6.6 with two closely spaced upper levels  $|a\rangle$  and  $|a'\rangle$  and a lower level  $|b\rangle$ . The selection rules and the energy spacing of levels  $|a\rangle$  and  $|a'\rangle$  is such that they interact with the same vacuum modes. The interaction of this system with a multi-mode vacuum field is

described by the interaction picture Hamiltonian,

$$\begin{aligned}\mathcal{V} = \hbar \sum_{\mathbf{k}} & \left[ g_{\mathbf{k}}^{(ab)} a_{\mathbf{k}}^\dagger |b\rangle \langle a| e^{-i(\omega_{ab} - \nu_{\mathbf{k}})t} \right. \\ & \left. + g_{\mathbf{k}}^{(a'b)} a_{\mathbf{k}}^\dagger |b\rangle \langle a'| e^{-i(\omega_{a'b} - \nu_{\mathbf{k}})t} \right] \\ & + \text{H.c.}\end{aligned}$$

Here  $a_{\mathbf{k}}^\dagger$  is the creation operator for the mode with wave vector  $\mathbf{k}$ , and  $\omega_{ab} = \omega_a - \omega_b$ ,  $\omega_{a'b} = \omega_{a'} - \omega_b$ . Derive the amplitude equations of motion for the three levels and show that quantum interference effects arise due to the sharing of common vacuum modes by the upper two levels.

Hint: see Zhu, Narducci, and Scully, *Phys. Rev. A* **52**, 6 (1995).

- 6.4** If  $C = \frac{1}{2}\Delta\sigma_z + g(\sigma_+a + a^\dagger\sigma_-)$  and  $N = a^\dagger a + \sigma_+\sigma_-$ , show that

$$C^2 = \frac{\Delta^2}{4} + g^2N.$$

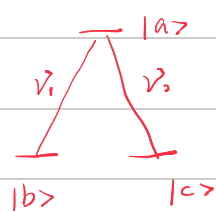
- 6.5** Prove Eq. (6.2.44).

补充:

## 其之一些相互作用现象

### ① 暗态, dark state

半经典



$$\text{Hamiltonian} \quad \hat{H} = \hat{H}_0 + \hat{H}_1$$

$$\hat{H}_0 = \hbar\omega_a |a><a| + \hbar\omega_b |b><b| + \hbar\omega_c |c><c|$$

$$\hat{H}_1 = -\frac{\hbar}{2} (\Delta_{R1} e^{-i\phi_1} e^{-i\omega t} |a><b| + \Delta_{R2} e^{-i\phi_2} e^{-i\omega t} |a><c|) + \text{H.c.}$$

设态的一般形式

$$|\Psi(t)\rangle = C_a(t) e^{-i\omega_a t} |a\rangle + C_b(t) e^{-i\omega_b t} |b\rangle + C_c(t) e^{-i\omega_c t} |c\rangle$$

$$i\hbar \frac{d}{dt} |\Psi(t)\rangle = \hat{H} |\Psi(t)\rangle$$

$$\begin{cases} \dot{C}_a = \frac{i}{2} (\Delta_{R1} e^{i\phi_1} C_b + \Delta_{R2} e^{-i\phi_2} C_c) \\ \dot{C}_b = \frac{i}{2} \Delta_{R1} e^{i\phi_1} C_a \\ \dot{C}_c = \frac{i}{2} \Delta_{R2} e^{i\phi_2} C_a \end{cases}$$

$$\text{若初值条件为 } |\Psi(0)\rangle = C_b(\theta/2) |b\rangle + \sin(\theta/2) e^{-i\frac{\pi}{4}} |c\rangle$$

则可解得:

$$\begin{cases} C_a(t) = \frac{i \sin(\sqrt{\omega_a} t)}{\sqrt{2}} [\Delta_{R1} e^{i\phi_1} \cos(\theta/2) + \Delta_{R2} e^{-i(\phi_2 + \frac{\pi}{4})} \sin(\theta/2)] \\ C_b(t) = \frac{1}{\sqrt{2}} \left[ [\Delta_{R1}^2 + \Delta_{R2}^2 \cos^2(\sqrt{\omega_a} t/2)] \cos(\theta/2) - 2\Delta_{R1}\Delta_{R2} e^{i(\phi_1 - \phi_2 - \frac{\pi}{4})} \sin^2(\sqrt{\omega_a} t/2) \sin(\theta/2) \right] \\ C_c(t) = \frac{1}{\sqrt{2}} \left[ -2\Delta_{R1}\Delta_{R2} e^{-i(\phi_1 - \phi_2)} \sin^2(\sqrt{\omega_a} t/2) \sin(\theta/2) \right] \end{cases}$$

存在暗态,  $C_a(t) = 0 = C_c(t)$ ,  $|a\rangle$  能级无泵浦

条件:  $\hbar\omega_a = \Delta_{R1} = \Delta_{R2}$      $\theta = \frac{\pi}{2}$      $\phi_1 - \phi_2 - \frac{\pi}{4} = \pm\pi$

$$\text{此时 } C_a(t) = 0 \quad C_b(t) = \frac{1}{\sqrt{2}} \quad C_c(t) = \frac{1}{\sqrt{2}} e^{-i\frac{\pi}{4}}$$

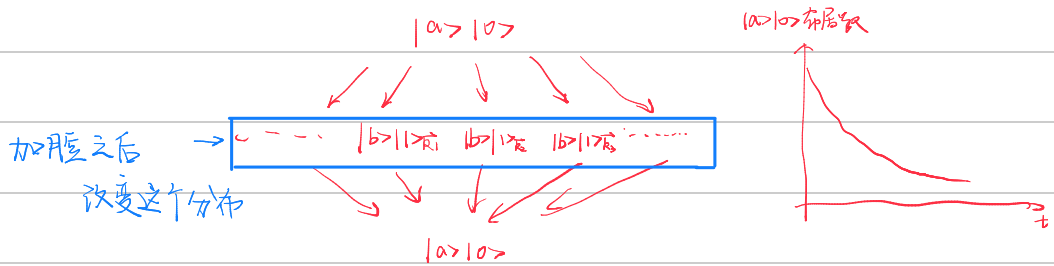
应用: EIT, 无反驰激光 (高能级  $|a\rangle$  不下来, 持续激光)

传统激光需要 上能级 > 下能级

### ② 自发辐射的抑制与增强 —— Purcell 效应

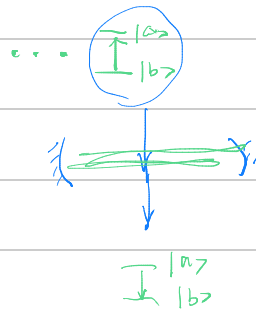
原理: 改变环境模密度分布 (真空模式)

## 正常自发辐射



$$F_p = \frac{B^3}{V}$$

## ③ 单原子激光 受激辐射占主导



## ④ Jaynes-Cummings Model JC模型

$$H_0 = \hbar\omega a^\dagger a + \frac{1}{2}\hbar\omega\sigma_z$$

$$H_1 = \hbar g (\sigma_+ a + \sigma_- a^\dagger)$$

$$\hat{H} = \hat{H}_0 + \hat{H}_1$$

① 原子发光分布表象 ——  $H_0$  本征态

② dressed state 表象 ——  $\hat{H}$  本征态

在  $\{|a,n\rangle, |b,n\rangle\}$  3空间

$$I = |a,n\rangle\langle a,n| + |b,n\rangle\langle b,n|$$

$$\hat{H} = \begin{pmatrix} & I \\ I & \end{pmatrix} \hat{H} \begin{pmatrix} & I \\ I & \end{pmatrix}$$

$$= \begin{pmatrix} \frac{1}{2}\hbar\omega + \hbar\omega n & \hbar g \sqrt{n+1} \\ \hbar g \sqrt{n+1} & -\frac{1}{2}\hbar\omega + \hbar\omega(n+1) \end{pmatrix} \quad \det(\hat{H} - \lambda I) = 0 \Rightarrow \lambda_{\pm} = \frac{\hbar\omega(n \pm \frac{1}{2})}{2} \pm \hbar\sqrt{(n+1)g}$$

$$\begin{aligned} |t,n\rangle &= \cos\theta_n |a,n\rangle - \sin\theta_n |b,n\rangle \\ |t,n\rangle &= \sin\theta_n |a,n\rangle + \cos\theta_n |b,n\rangle \end{aligned}$$

在此表象下，

$$|\psi(t)\rangle = a |t,n\rangle + b |t,-n\rangle$$

$$|\psi(t)\rangle = a e^{-iE_t t/\hbar} |t,n\rangle + b e^{-iE_t t/\hbar} |t,-n\rangle$$

$$\text{其中 } \cos\theta_n = \frac{R_n - \Delta}{\sqrt{(R_n - \Delta)^2 + 4g^2(n+1)}}$$

$$R_n = \sqrt{4\hbar\omega n^2 + \Delta^2} \text{ 实部 Prob. }$$

$$\text{或 } \cos 2\theta_n = -\frac{\Delta}{R_n}$$

### ③ 大失谐 J-C 模

$$\Delta = \omega - \gamma \Rightarrow g \quad \Delta \ll \omega, \gamma$$

此时有效 Hamiltonian

$$\hat{V}_e = \frac{\hbar g^2}{\Delta} \sigma_z a^\dagger a \quad (\text{相移, 但反相数不变})$$

证明: 原本  $\hat{V} = \hbar g (\sigma_x a e^{i\omega t} + H.c.)$

$$U(t) = \hat{I} \exp \left( -\frac{i}{\hbar} \int_0^t \hbar g (\sigma_x^\dagger a e^{i\omega t'} + a^\dagger \sigma_x e^{-i\omega t'}) dt' \right)$$

$$= I + \underbrace{\left( -\frac{i}{\hbar} \int_0^t \hat{V}(t') dt' \right)}_{\text{全 } e^{i\omega t} \text{ 次, 把}} + \underbrace{\left( -\frac{i}{\hbar} \int_0^t dt' \int_0^{t'} dt'' g^2 (\sigma_x^\dagger a e^{i\omega t''} + a^\dagger \sigma_x e^{-i\omega t''}) (\sigma_x^\dagger a e^{i\omega t''} + a^\dagger \sigma_x e^{-i\omega t''}) \right)}_{\text{一次平方后, 发现不含 } e^{i\omega t} \text{ 项, 保 } \Delta}$$

$$= -ig^2 \frac{1}{\Delta} [\sigma_x a^\dagger a + \sigma_x^\dagger \sigma_x] + \quad (\text{用到 } \sigma_x^\dagger \sigma_x - \sigma_x \sigma_x^\dagger = \delta^2)$$

$$\approx \exp \left( -i \frac{g^2}{\Delta} \hbar (\sigma_x a^\dagger a + \sigma_x^\dagger \sigma_x) t / \hbar \right) \quad \text{与相位无关}$$

$$\hat{V}_e = \frac{\hbar g^2}{\Delta} \sigma_z a^\dagger a$$

Rabi 频率 振幅小, 但相移

### ④ 若有额外强光驱动

$$\hat{H} = \frac{1}{2} \hbar \omega \sigma_z + \hbar \gamma a^\dagger a + \hbar g (\sigma_x^\dagger a + a^\dagger \sigma_x) + E_0 e^{-i\Omega t} (\sigma_x^\dagger + \sigma_x)$$

弱光(量光学)      强光(半经典)

### ⑤ Raman 型 J-C 模

表振

$$\hat{H} = \hbar \omega_1 |e><e| + \hbar \omega_2 |g><g| + \hbar \omega_3 |i><i| + \hbar \gamma_1 a^\dagger a_1 + \hbar \gamma_2 a^\dagger a_2 +$$

$$+ \hbar (g_{1,0} |i><e| + g_{2,0} |i><g| + H.c.)$$



$$\hbar \gamma_1 = \hbar (\omega_i - \omega_e) - \hbar \Delta$$

$$\hbar \gamma_2 = \hbar (\omega_i - \omega_g) - \hbar \Delta$$

自由项一样, 相互作用图像中

$$\hbar = 1$$

$$H_e = \underbrace{(g a^\dagger a_1^\dagger |e><e| + H.c.)}_{①} - \underbrace{a^\dagger a_1 \frac{g^2}{\Delta} |e><e|}_{②} - \underbrace{\frac{g^2}{\Delta} |g><g| a_2^\dagger a_2}_{③}$$

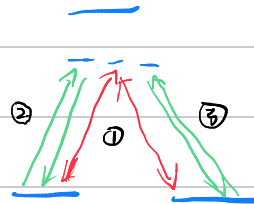
做法: 在相互作用图像中,  $\hat{I}$  展开取二阶

☆ 大尖端 comments:

① 二能级

上不去，只能发生虚过程

② 三能级：虚过程



对应上述公式中的 ①②③

同样，三能级系统中也可引入强光，对应腔衰板量换成半经典即可。

④ 双光子级联 JC 模

① 单振

$$-|e\rangle \rightarrow |i\rangle (g_1 a_1^+ |i\rangle \langle e| + H.c.)$$

$$-|g\rangle \rightarrow |g\rangle (g_2 a_2^+ |g\rangle \langle i| + H.c.)$$

(2) 大尖端

$$\begin{array}{c} \uparrow \\ -|e\rangle \\ \downarrow \\ -|i\rangle \\ \downarrow \\ -|g\rangle \end{array} \quad \text{若 } \gamma_1 = \gamma_2 \quad g(a_1^* \delta^- + a_2^* \delta^+) \quad \text{其中 } \delta^- = |g\rangle \langle e| \quad \delta^+ = |e\rangle \langle g|$$

$$\begin{array}{c} \uparrow \\ -|e\rangle \\ \downarrow \\ -|i\rangle \\ \downarrow \\ -|g\rangle \end{array} \quad \text{若 } \gamma_1 \neq \gamma_2, a^2 \text{ 是 } a_1 a_2.$$

⑤ 量子 Bloch 方程 —— Heisenberg 方程组

单于二能级原子 + 多模场

$$\hat{H} = \frac{1}{2} \hbar \omega \hat{\sigma}_z + \hbar (g \delta^- + g^* \delta^+) A + \frac{\epsilon}{\hbar} \hbar \omega_n a_\lambda^+ a_\lambda \quad A = \frac{\epsilon}{\hbar} (a_\lambda + a_\lambda^*)$$

Heisenberg 方程中

$$\begin{cases} \frac{d\delta^-}{dt} = 2i [g\delta^- - g^*\delta^+] A \\ \frac{d\delta^+}{dt} = i\hbar\omega\delta^+ - igA\delta^- \\ \frac{d\delta^-}{dt} = -i\hbar\omega\delta^- + ig^*A\delta^+ \end{cases}$$

$$\begin{cases} \dot{R}_1 = -\omega R_2 \\ \dot{R}_2 = \omega R_1 + kAR_3 \\ \dot{R}_3 = -kAR_1 \\ R_0 = |g|\hat{\sigma}_z \end{cases}$$

$$\begin{aligned} \text{令 } \vec{R} &= -kA\omega \hat{e}_x + \omega \hat{e}_z \\ \Rightarrow \frac{d\vec{R}}{dt} &= \vec{\Omega} \times \vec{R} \end{aligned}$$

自旋进动模型。

# Quantum theory of damping – density operator and wave function approach

In many problems in quantum optics, damping plays an important role. These include, for example, the decay of an atom in an excited state to a lower state and the decay of the radiation field inside a cavity with partially transparent mirrors. In general, damping of a *system* is described by its interaction with a *reservoir* with a large number of degrees of freedom. We are interested, however, in the evolution of the variables associated with the system only. This requires us to obtain the equations of motion for the system of interest only after tracing over the reservoir variables. There are several different approaches to deal with this problem.

In this chapter, we present a theory of damping based on the density operator in which the reservoir variables are eliminated by using the *reduced density operator* for the system in the Schrödinger (or interaction) picture. We also present a ‘quantum jump’ approach to damping. In the next chapter, the damping of the system will be considered using the noise operator method in the Heisenberg picture.

An insight into the damping mechanism is obtained by considering the decay of an atom in an excited state inside a cavity. The atom may be considered as a single system coupled to the radiation field inside the cavity. Even in the absence of photons in the cavity, there are quantum fluctuations associated with the vacuum state. As discussed in Chapter 1, the field may be visualized as a large number of harmonic oscillators, one for each mode of the cavity. As the size of the cavity increases, the mode density increases, and, in free space, we get a continuum of modes. There is therefore a “cavity mode” which is resonant with the atomic transition.

We can also visualize the atom as an oscillator, with the excited atom corresponding to an oscillator in the excited state. The coupling

of the atom to a large number of oscillators (associated with the large number of field modes) leads to decay. That is energy initially in the atom will distribute itself among damping oscillators, thus causing the decay of the atom to a lower energy state.

The dissipation is accompanied by fluctuations. We shall encounter this aspect of the damping mechanism, more formally put in the form of the so-called fluctuation-dissipation theorem, in the systems studied in this and the following chapters. We now start with a general reservoir theory before considering the atom and field damping by a reservoir of harmonic oscillator (bosonic) modes.

## 8.1 General reservoir theory

We consider in general a system denoted by  $S$  interacting with a reservoir denoted by  $R$ . The combined density operator is denoted by  $\rho_{SR}$ . The reduced density operator for the system  $\rho_S$  is obtained by taking a trace over the reservoir coordinates, i.e.,

$$\rho_S = \text{Tr}_R(\rho_{SR}). \quad (8.1.1)$$

We assume that the system-reservoir interaction energy is given by  $\mathcal{V}(t)$ . The equation of motion for  $\rho_{SR}$  is then given by

$$i\hbar\dot{\rho}_{SR} = [\mathcal{V}(t), \rho_{SR}(t)]. \quad (8.1.2)$$

This equation can be formally integrated, and we obtain

$$\rho_{SR}(t) = \rho_{SR}(t_i) - \frac{i}{\hbar} \int_{t_i}^t [\mathcal{V}(t'), \rho_{SR}(t')] dt'. \quad (8.1.3)$$

Here  $t_i$  is an initial time when the interaction starts. On substituting  $\rho_{SR}(t)$  back into Eq. (8.1.2), we find the equation of motion

$$\dot{\rho}_{SR} = -\frac{i}{\hbar} [\mathcal{V}(t), \rho_{SR}(t_i)] - \frac{1}{\hbar^2} \int_{t_i}^t [\mathcal{V}(t), [\mathcal{V}(t'), \rho_{SR}(t')]] dt'. \quad (8.1.4)$$

If the interaction energy  $\mathcal{V}(t)$  is zero, the system and reservoir are independent and the density operator  $\rho_{SR}$  would factor as a direct product  $\rho_{SR}(t) = \rho_S(t) \otimes \rho_R(t_i)$  where we assume the reservoir at equilibrium. Since  $\mathcal{V}$  is small, we look for a solution of Eq. (8.1.4) of the form

$$\rho_{SR}(t) = \rho_S(t) \otimes \rho_R(t_i) + \rho_c(t), \quad (8.1.5)$$

where  $\rho_c(t)$  is of higher order in  $\mathcal{V}$ . In order to satisfy (8.1.1), we

一直保持初态

= 相互作用

require

$$\text{Tr}_R[\rho_c(t)] = 0. \quad (8.1.6)$$

If we substitute for  $\rho_{SR}(t)$  from Eq. (8.1.5) into the integrand of (8.1.4), and retain terms up to order  $\gamma^2$ , we have

$$\dot{\rho}_S = -\frac{i}{\hbar} \text{Tr}_R[\gamma(t), \rho_S(t_i) \otimes \rho_R(t_i)] - \frac{1}{\hbar^2} \text{Tr}_R \int_{t_i}^t [\gamma(t), [\gamma(t'), \rho_S(t') \otimes \rho_R(t_i)]] dt'. \quad (8.1.7)$$

这一步用到  $\text{Tr}_R[V(t), \rho_{dt}] = \text{Tr}_R(V(t)\rho_{dt} - \rho_{dt}V(t)) \xrightarrow{\text{Tr}(AB) = \text{Tr}(BA)} 0$   
 $\text{Tr}_R(\rho_{dt}) = 0$

The reduced density operator  $\rho_S(t)$ , which determines the statistical properties of the system, depends on its past history from  $t = t_i$  to  $t'$ . This can be seen in Eq. (8.1.7) as  $\rho_S(t')$  occurs in the integrand. However, the reservoir is typically an extended open system having many degrees of freedom. Moreover, as is shown by specific example in the next section, the large number of reservoir degrees of freedom (modes, photons, etc.) leads to a delta function  $\delta(t - t')$ . Hence, the system density matrix  $\rho_S(t')$  can be replaced by  $\rho_S(t)$  and the process is said to be *Markovian*. This is a reasonable assumption since damping destroys memory of the past. Equation (8.1.7) now becomes

$$\dot{\rho}_S = -\frac{i}{\hbar} \text{Tr}_R[\gamma(t), \rho_S(t_i) \otimes \rho_R(t_i)] - \frac{1}{\hbar^2} \text{Tr}_R \int_{t_i}^t [\gamma(t), [\gamma(t'), \rho_S(t) \otimes \rho_R(t_i)]] dt'. \quad (8.1.8)$$

This is a valid equation for a system represented by  $\rho_S$  interacting with a reservoir represented by  $\rho_R$ . In the next sections, we consider several examples of the system-reservoir interaction.

马尔科夫近似  
“环境无记忆性”  
可以迅速消除  $\rho_S$  对  $\rho_R$  的影响

## 8.2 Atomic decay by thermal and squeezed vacuum reservoirs

The decay of an atom in an excited state may be understood from a simple model in which the atom is coupled to a reservoir of simple harmonic oscillators. In a very similar manner, the decay of the radiation field inside a cavity may be described by a model in which the mode of the field of interest is coupled to a whole set of reservoir modes. Such problems are of interest not only in maser and laser physics, but also in the quantum theory of passive interferometers such as those used in the detection of gravitational waves.

We first consider the radiative decay of a two-level atom damped by a reservoir of simple harmonic oscillators described by annihilation (and creation) operators  $b_{\mathbf{k}}$  (and  $b_{\mathbf{k}}^\dagger$ ) and density distributed frequencies  $\nu_k = ck$ . In the interaction picture and the rotating-wave approximation, the Hamiltonian is simply

$$\text{相互作用哈密顿量} \quad \mathcal{V}(t) = \hbar \sum_{\mathbf{k}} g_{\mathbf{k}} \left[ b_{\mathbf{k}}^\dagger \sigma_- e^{-i(\omega - \nu_k)t} + \sigma_+ b_{\mathbf{k}} e^{i(\omega - \nu_k)t} \right], \quad (8.2.1)$$

where  $\sigma_- = |b\rangle\langle a|$  and  $\sigma_+ = |a\rangle\langle b|$  in terms of the excited ( $|a\rangle$ ) and ground ( $|b\rangle$ ) states. The system now corresponds to the two-level atom ( $\rho_S \equiv \rho_{\text{atom}}$ ). On inserting the interaction energy  $\mathcal{V}$  (Eq. (8.2.1)) into the equation of motion (8.1.7) for  $\rho_S \equiv \rho_{\text{atom}}$ , we obtain

$$\begin{aligned} \dot{\rho}_{\text{atom}} = & -i \sum_{\mathbf{k}} g_{\mathbf{k}} \langle b_{\mathbf{k}}^\dagger \rangle [\sigma_-, \rho_{\text{atom}}(t_i)] e^{-i(\omega - \nu_k)t} \\ & - \int_{t_i}^t dt' \sum_{\mathbf{k}, \mathbf{k}'} g_{\mathbf{k}} g_{\mathbf{k}'} \{ [\sigma_- \sigma_- \rho_{\text{atom}}(t') - 2\sigma_- \rho_{\text{atom}}(t') \sigma_- \\ & \quad + \rho_{\text{atom}}(t') \sigma_- \sigma_-] \\ & \times e^{-i(\omega - \nu_k)t - i(\omega - \nu_{k'})t'} \langle b_{\mathbf{k}}^\dagger b_{\mathbf{k}'}^\dagger \rangle + [\sigma_- \sigma_+ \rho_{\text{atom}}(t') - \sigma_+ \rho_{\text{atom}}(t') \sigma_-] \\ & \times e^{-i(\omega - \nu_k)t + i(\omega - \nu_{k'})t'} \langle b_{\mathbf{k}}^\dagger b_{\mathbf{k}'} \rangle + [\sigma_+ \sigma_- \rho_{\text{atom}}(t') - \sigma_- \rho_{\text{atom}}(t') \sigma_+] \\ & \times e^{i(\omega - \nu_k)t - i(\omega - \nu_{k'})t'} \langle b_{\mathbf{k}} b_{\mathbf{k}'}^\dagger \rangle \} + \text{H.c.}, \end{aligned} \quad (8.2.2)$$

where the expectation values refer to the initial state of the reservoir. At this point we choose a particular model for the state of the reservoir.

### 8.2.1 Thermal reservoir (多模谐振子热光场模型占90%用途)

As a first example, we assume that the reservoir variables are distributed in the uncorrelated thermal equilibrium mixture of states. The reservoir reduced density operator is the multi-mode extension of the thermal operator, namely,

注意：这里说的分布，不是交换对称。  
 $\text{Tr}(\hat{A}\hat{B}\hat{C}) = \text{Tr}(\hat{C}\hat{A}\hat{B}) = \text{Tr}(\hat{B}\hat{C}\hat{A})$

$$\rho_R = \prod_{\mathbf{k}} \left[ 1 - \exp \left( -\frac{\hbar \nu_k}{k_B T} \right) \right] \exp \left( -\frac{\hbar \nu_k b_{\mathbf{k}}^\dagger b_{\mathbf{k}}}{k_B T} \right), \quad (8.2.3)$$

where  $k_B$  is the Boltzmann constant and  $T$  is the temperature. It can be shown easily that

$$\text{Tr}_R(p_R b_{\mathbf{k}}) = \langle b_{\mathbf{k}} \rangle = \langle b_{\mathbf{k}}^\dagger \rangle = 0, \quad (8.2.4a)$$

$$\langle b_{\mathbf{k}}^\dagger b_{\mathbf{k}'} \rangle = \bar{n}_{\mathbf{k}} \delta_{\mathbf{k}\mathbf{k}'}, \quad (8.2.4b)$$

$$\langle b_{\mathbf{k}} b_{\mathbf{k}'}^\dagger \rangle = (\bar{n}_{\mathbf{k}} + 1) \delta_{\mathbf{k}\mathbf{k}'}, \quad (8.2.4c)$$

$$\langle b_{\mathbf{k}} b_{\mathbf{k}'}^\dagger \rangle = \langle b_{\mathbf{k}}^\dagger b_{\mathbf{k}'}^\dagger \rangle = 0, \quad (8.2.4d)$$

where the thermal average boson number

$$\bar{n}_k = \frac{1}{\exp\left(\frac{\hbar\nu_k}{k_B T}\right) - 1}. \quad (8.2.5)$$

On substituting for the various expectation values from Eqs. (8.2.4) into Eq. (8.2.2), we obtain

$$\begin{aligned} \dot{\rho}_{\text{atom}} &= - \int_{t_i}^t dt' \sum_k g_k^2 \{ [\sigma_- \sigma_+ \rho_{\text{atom}}(t') - \sigma_+ \rho_{\text{atom}}(t') \sigma_-] \\ &\quad \bar{n}_k e^{-i(\omega - \nu_k)(t-t')} \\ &\quad + [\sigma_+ \sigma_- \rho_{\text{atom}}(t') - \sigma_- \rho_{\text{atom}}(t') \sigma_+] (\bar{n}_k + 1) e^{i(\omega - \nu_k)(t-t')} \} + \text{H.c.} \end{aligned} \quad (8.2.6)$$

We now carry out the same procedure as was used in the Weisskopf–Wigner theory of spontaneous emission.

The sum over  $\mathbf{k}$  may be replaced by an integral through the standard prescription (Eq. (6.3.9))

$$\sum_k \rightarrow 2 \frac{V}{(2\pi)^3} \int_0^{2\pi} d\phi \int_0^\pi d\theta \sin\theta \int_0^\infty dk k^2, \quad \xleftarrow{(8.2.7)} \text{这一步马尔科夫近似出现.}$$

where  $V$  is the quantization volume. The integrations in Eq. (8.2.6) can be carried out in the Weisskopf–Wigner approximation as discussed in Section 6.3. In this way, we encounter integrals of the form (6.3.12). We thus find for the reduced density operator  $\rho_{\text{atom}}$

$$\begin{aligned} \dot{\rho}_{\text{atom}}(t) &= -\bar{n}_{\text{th}} \frac{\Gamma}{2} [\sigma_- \sigma_+ \rho_{\text{atom}}(t) - \sigma_+ \rho_{\text{atom}}(t) \sigma_-] \\ &\quad - (\bar{n}_{\text{th}} + 1) \frac{\Gamma}{2} [\sigma_+ \sigma_- \rho_{\text{atom}}(t) - \sigma_- \rho_{\text{atom}}(t) \sigma_+] + \text{H.c.}, \end{aligned} \quad (8.2.8)$$

★ 注意:  $\int_0^t \delta(t-t') \rho(t') dt' = \frac{1}{2} \rho(t)$   
因为  $\int_0^t \delta(t-t') dt' = \frac{1}{2}$

where  $\bar{n}_{\text{th}} \equiv \bar{n}_{k_0}$  ( $k_0 = \omega/c$ ) and

$$\Gamma = \frac{1}{4\pi\epsilon_0} \frac{4\omega^3 \varphi_{ab}^2}{3\hbar c^3} \quad (8.2.9)$$

is the atomic decay rate which is identical to the decay constant (Eq. (6.3.14)) derived in the Weisskopf–Wigner theory of spontaneous emission. In deriving Eq. (8.2.8) we substituted the value of  $g_k$  from Eq. (6.1.8).

The equations of motion for the atomic density matrix elements can now be obtained from Eq. (8.2.8):

$$\begin{aligned}\dot{\rho}_{aa} &= \langle a | \dot{\rho}_{\text{atom}} | a \rangle \\ &= -(\bar{n}_{\text{th}} + 1)\Gamma\rho_{aa} + \bar{n}_{\text{th}}\Gamma\rho_{bb},\end{aligned}\quad (8.2.10\text{a})$$

$$\dot{\rho}_{ab} = \dot{\rho}_{ba}^* = -\left(\bar{n}_{\text{th}} + \frac{1}{2}\right)\Gamma\rho_{ab}, \quad (8.2.10\text{b})$$

$$\dot{\rho}_{bb} = -\bar{n}_{\text{th}}\Gamma\rho_{bb} + (\bar{n}_{\text{th}} + 1)\Gamma\rho_{aa}. \quad (8.2.10\text{c})$$

It may be noted that  $\dot{\rho}_{aa} + \dot{\rho}_{bb} = 0$ . This is due to the fact that we are considering the decay from the upper level  $|a\rangle$  to the lower level  $|b\rangle$  only. The conservation of probability therefore implies  $\rho_{aa} + \rho_{bb} = 1$ . This situation is different from that discussed in Section 5.3, where atomic levels  $|a\rangle$  and  $|b\rangle$  decayed to some other levels via nonradiating transitions. For zero temperature ( $\bar{n}_{\text{th}} = 0$ ), these equations simplify to

真這樣

这说明这种方程是

Weisskopf-Wigner 方程的结果

$$\dot{\rho}_{aa} = -\Gamma\rho_{aa}, \quad (8.2.11\text{a})$$

$$\dot{\rho}_{ab} = -\frac{\Gamma}{2}\rho_{ab}, \quad (8.2.11\text{b})$$

$$\dot{\rho}_{bb} = \Gamma\rho_{aa}. \quad (8.2.11\text{c})$$

Equation (8.2.11a) is just the Weisskopf–Wigner result (6.3.15).

## 8.2.2 Squeezed vacuum reservoir

For our second example, we consider the situation where the atom is coupled to a squeezed vacuum field reservoir. The reservoir reduced density operator is given by

$$\begin{aligned}\rho_R &= |\xi\rangle\langle\xi| \\ &= \prod_{\mathbf{k}} S_{\mathbf{k}}(\xi)|0_{\mathbf{k}}\rangle\langle 0_{\mathbf{k}}|S_{\mathbf{k}}^\dagger(\xi),\end{aligned}\quad (8.2.12)$$

where the squeeze operator (see Eq. (2.8.9) with  $b_{\mathbf{k}} \equiv b(ck)$ , etc.) is

$$S_{\mathbf{k}}(\xi) = \exp\left(\xi^* b_{\mathbf{k}_0+\mathbf{k}} b_{\mathbf{k}_0-\mathbf{k}} - \xi b_{\mathbf{k}_0+\mathbf{k}}^\dagger b_{\mathbf{k}_0-\mathbf{k}}^\dagger\right), \quad (8.2.13)$$

with  $\xi = r \exp(i\theta)$ ,  $r$  being the squeeze parameter and  $\theta$  being the reference phase for the squeezed field. A multi-mode squeezed field is not just a product of independently squeezed modes, rather there are correlations between modes symmetrically placed about the central,

resonant frequency  $\nu = ck_0$  of the squeezing device. Following the method used to derive Eqs. (2.7.6) and (2.7.7), we obtain

$$S_{\mathbf{k}-\mathbf{k}_0}^\dagger b_{\mathbf{k}} S_{\mathbf{k}-\mathbf{k}_0} = b_{\mathbf{k}} \cosh(r) - b_{2\mathbf{k}_0-\mathbf{k}}^\dagger e^{i\theta} \sinh(r), \quad (8.2.14a)$$

$$S_{\mathbf{k}-\mathbf{k}_0}^\dagger b_{\mathbf{k}}^\dagger S_{\mathbf{k}-\mathbf{k}_0} = b_{\mathbf{k}}^\dagger \cosh(r) - b_{2\mathbf{k}_0-\mathbf{k}} e^{-i\theta} \sinh(r). \quad (8.2.14b)$$

Similar expressions exist for  $S_{\mathbf{k}_0-\mathbf{k}}^\dagger b_{\mathbf{k}} S_{\mathbf{k}_0-\mathbf{k}}$  and  $S_{\mathbf{k}_0-\mathbf{k}}^\dagger b_{\mathbf{k}}^\dagger S_{\mathbf{k}_0-\mathbf{k}}$ . The calculation of the expectation values, such as  $\langle b_{\mathbf{k}}^\dagger b_{\mathbf{k}'} \rangle$ , may therefore be simplified by writing

$$\langle b_{\mathbf{k}}^\dagger b_{\mathbf{k}'} \rangle = \prod_{\mathbf{q}} \langle 0_{\mathbf{q}} | S_{\mathbf{q}}^\dagger b_{\mathbf{k}}^\dagger S_{\mathbf{q}} S_{\mathbf{q}}^\dagger b_{\mathbf{k}'} S_{\mathbf{q}} | 0_{\mathbf{q}} \rangle. \quad (8.2.15)$$

It follows that

$$\langle b_{\mathbf{k}} \rangle = \langle b_{\mathbf{k}}^\dagger \rangle = 0, \quad (8.2.16a)$$

$$\langle b_{\mathbf{k}}^\dagger b_{\mathbf{k}'} \rangle = \sinh^2(r) \delta_{\mathbf{k}\mathbf{k}'}, \quad (8.2.16b)$$

$$\langle b_{\mathbf{k}} b_{\mathbf{k}'}^\dagger \rangle = \cosh^2(r) \delta_{\mathbf{k}\mathbf{k}'}, \quad (8.2.16c)$$

$$\langle b_{\mathbf{k}} b_{\mathbf{k}'} \rangle = -e^{i\theta} \sinh(r) \cosh(r) \delta_{\mathbf{k}',2\mathbf{k}_0-\mathbf{k}}, \quad (8.2.16d)$$

$$\langle b_{\mathbf{k}}^\dagger b_{\mathbf{k}'}^\dagger \rangle = -e^{-i\theta} \sinh(r) \cosh(r) \delta_{\mathbf{k}',2\mathbf{k}_0-\mathbf{k}}. \quad (8.2.16e)$$

On substituting Eqs. (8.2.16a-8.2.16e) into Eq. (8.2.2) and proceeding as in the derivation of Eq. (8.2.8), we obtain

$$\begin{aligned} \dot{\rho}_{\text{atom}} &= -\frac{\Gamma}{2} \underbrace{\cosh^2(r)}_{(N+1)} (\sigma_+ \sigma_- - 2\sigma_- \rho_{\text{atom}} \sigma_+ + \rho_{\text{atom}} \sigma_+ \sigma_-) \\ &\quad - \frac{\Gamma}{2} \underbrace{\sinh^2(r)}_N (\sigma_- \sigma_+ + \rho_{\text{atom}} - 2\sigma_+ \rho_{\text{atom}} \sigma_- + \rho_{\text{atom}} \sigma_- \sigma_+) \\ &\xrightarrow{\text{对称消去 } b^\dagger b^\dagger} -\Gamma e^{-i\theta} \sinh(r) \cosh(r) \sigma_- \rho_{\text{atom}} \sigma_- \\ &\xrightarrow{\text{对称消去 } b b} -\Gamma e^{i\theta} \sinh(r) \cosh(r) \sigma_+ \rho_{\text{atom}} \sigma_+. \end{aligned} \quad (8.2.17)$$

In deriving Eq. (8.2.17) we used  $\sigma_- \sigma_- = \sigma_+ \sigma_+ = 0$ .

From Eq. (8.2.17), equations of motion for the expectation value of the operators  $\sigma_x = (\sigma_- + \sigma_+)/2$ ,  $\sigma_y = (\sigma_- - \sigma_+)/2i$ , and  $\sigma_z = (2\sigma_+ \sigma_- - 1)/2$  are

(S<sub>2</sub>中):

$$\langle \dot{\sigma}_z \rangle = \text{Tr}_p (\dot{\sigma}_z \rho_{\text{atom}}) \quad (8.2.18a)$$

原因:  $\langle \dot{\sigma}_z \rangle = \sum P_n \langle n | \dot{\sigma}_z | n \rangle$

$$\langle \dot{\sigma}_z \rangle = \sum P_n (\langle n | \sigma_z | n \rangle + \langle n | \sigma_z | n \rangle) = \text{Tr}(\sigma_z \dot{\rho})$$

这个技巧: 拆模对称

$$\text{Tr}(\sigma_z \dot{\rho})$$

$$=\text{Tr}(\sigma_z \sigma_z \dot{\rho})$$

全换成  $\rho$  后再加

$$\text{Tr}((\ ) \rho)$$

$S_{\text{总}} = \langle \dot{\sigma}_x \rangle$

$$\xrightarrow{\text{对称消去 } b^\dagger b^\dagger} \langle \dot{\sigma}_x \rangle = -\frac{\Gamma}{2} e^{2r} \langle \sigma_x \rangle,$$

$$\langle \dot{\sigma}_y \rangle = -\frac{\Gamma}{2} e^{-2r} \langle \sigma_y \rangle,$$

$$\langle \dot{\sigma}_z \rangle = -\Gamma [2 \sinh^2(r) + 1] \langle \sigma_z \rangle - \Gamma = -\Gamma_z \langle \sigma_z \rangle - \Gamma, \quad (8.2.18c)$$

where  $\Gamma_z = \Gamma [2 \sinh^2(r) + 1]$  and we have chosen the phase  $\theta = 0$ .

It is therefore clear that a squeezed vacuum reservoir leads to a phase sensitive decay of the atom. The in-phase and in-quadrature components,  $\langle \sigma_x \rangle$  and  $\langle \sigma_y \rangle$ , of the atomic dipole moment decay at different rates depending on its initial phase relative to the phase  $\theta$  of the squeezed vacuum.

$\langle \dot{\sigma}_z \rangle = \frac{d\langle \sigma_z \rangle}{dt}$  为经典量

$$\frac{d\langle \sigma_z \rangle}{dt} = \text{Tr}(\sigma_z \dot{\rho}) \leftarrow \text{Schrodinger 国家}$$

本章是 S 国家

### 8.3 Field damping

We may apply the method developed in the last section to the decay of a mode of the electromagnetic field of frequency  $\nu$  inside a cavity. Instead of Eq. (8.2.1), we now use an interaction Hamiltonian of the form

$$\mathcal{H} = \hbar \sum_{\mathbf{k}} g_{\mathbf{k}} [b_{\mathbf{k}}^\dagger a e^{-i(\nu - \nu_k)t} + a^\dagger b_{\mathbf{k}} e^{i(\nu - \nu_k)t}], \quad (8.3.1)$$

$b_{\mathbf{k}}$  场强  
 $a$  源  
 $b_{\mathbf{k}}^\dagger$  系综  
 $a^\dagger$  反演速率

where  $a$  (and  $a^\dagger$ ) are the destruction (and creation) operators of the mode of interest. The operators  $b_{\mathbf{k}}$  and  $b_{\mathbf{k}}^\dagger$  represent modes of the reservoir which damp the field. For transmission losses they actually represent the field outside the cavity.

The equation of motion for the reduced density operator for the field can now easily be obtained, since the calculation exactly parallels the one for the atomic system discussed in the last section. This is done by replacing  $\sigma_-$  and  $\sigma_+$  by the field operators  $a$  and  $a^\dagger$ , respectively.

When the modes  $b_{\mathbf{k}}$  are initially in the thermal equilibrium mixture of states (8.2.3), the result is

$$\dot{\rho} = -\frac{\mathcal{C}}{2} \bar{n}_{\text{th}} (aa^\dagger \rho - 2a^\dagger \rho a + \rho a a^\dagger) - \frac{\mathcal{C}}{2} (\bar{n}_{\text{th}} + 1) (a^\dagger a \rho - 2a \rho a^\dagger + \rho a^\dagger a), \quad (8.3.2)$$

$\mathcal{C}$  损耗散速率

where, as before,  $\mathcal{C}$  is the decay constant and  $\bar{n}_{\text{th}} = \bar{n}_{\mathbf{k}_0}$  is the mean number of quanta (at frequency  $\nu$ ) in the thermal reservoir. Here  $\rho$  denotes the reduced density operator for the field. In particular, at zero temperature ( $\bar{n}_{\text{th}} = 0$ ),

$$\dot{\rho} = -\frac{\mathcal{C}}{2} (a^\dagger a \rho - 2a \rho a^\dagger + \rho a^\dagger a). \quad (8.3.3)$$

例题:  $\langle \dot{a} \rangle = \frac{d \langle a \rangle}{dt} = \frac{d \text{Tr}(a\rho)}{dt} = \text{Tr}(a\dot{\rho})$  带衰减 Tr(a\rho) = 0  
 (假设)  $= -\frac{\mathcal{C}}{2} \text{Tr}[aa^\dagger a - a^\dagger a a + \rho a^\dagger a]$  取 t=0, 带入初值  
 $= -\frac{\mathcal{C}}{2} \text{Tr}[a(a^\dagger a - a^\dagger a + \rho a^\dagger a)]$   
 $= -\frac{\mathcal{C}}{2} \text{Tr}[\rho a^\dagger a] = -\frac{\mathcal{C}}{2} \langle a \rangle$   
 $\Rightarrow \langle \dot{a} \rangle = e^{-\frac{\mathcal{C}}{2}t} \langle a \rangle$

If all the losses are transmission losses,  $\mathcal{C}$  may be related to the quality factor  $Q$  of the cavity by  $\mathcal{C} = \nu/Q$ .

When the modes  $b_{\mathbf{k}}$  are initially in a squeezed vacuum (Eq. (8.2.12)), the resulting equation of motion for the reduced density matrix  $\rho$  is

$$\begin{aligned} \dot{\rho} = & -\frac{\mathcal{C}}{2} (N + 1) (a^\dagger a \rho - 2a \rho a^\dagger + \rho a^\dagger a) \\ & - \frac{\mathcal{C}}{2} N (aa^\dagger \rho - 2a^\dagger \rho a + \rho a a^\dagger) \\ & + \frac{\mathcal{C}}{2} M (a a \rho - 2a \rho a + \rho a a) \\ & + \frac{\mathcal{C}}{2} M^* (a^\dagger a^\dagger \rho - 2a^\dagger \rho a^\dagger + \rho a^\dagger a^\dagger), \end{aligned} \quad (8.3.4)$$

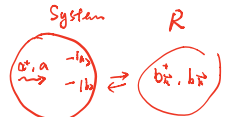
上节 原理  $\leftrightarrow$  理论  
原理  $\leftrightarrow$  实验

直接用上节的运动学中

$\sigma^+, \sigma^- \rightarrow a^+, a$   
 $\bar{n}_{\text{th}}$   $\bar{n}_{\text{th}}$

0°C 换光路

where  $N = \sinh^2(r)$  and  $M = \cosh(r) \sinh(r) \exp(-i\theta)$ . This equation describes, for instance, the evolution of the field in a cavity coupled through a partially transmitting mirror to an outside field which is in a squeezed vacuum state. The equation of motion for the thermal reservoir (Eq. (8.3.2)) can be recovered from Eq. (8.3.4) by the substitutions  $N \rightarrow \bar{n}_{\text{th}}$ ,  $M \rightarrow 0$ . The parameters  $N$  and  $M$  are however related to each other via the equation  $|M| = [N(N + 1)]^{1/2}$  for a squeezed vacuum reservoir.



若更复杂体系：

$$\dot{\rho}_S = \frac{1}{i\hbar} [\hat{H}_S, \rho_S] + L(\beta)$$

## 8.4 Fokker–Planck equation

经典概率分布

P → P表示(本态)/反表示

A particularly interesting representation into which the density operator equation of motion can be transformed is the coherent state representation or  $P$ -representation discussed in Chapter 3. In this section, we derive an equation of motion for the  $P$ -representation corresponding to Eq. (8.3.2) for the density operator for a harmonic oscillator mode damped by a thermal bath full of harmonic oscillators. The resulting equation will have the form of a Fokker–Planck equation. The solution of this equation will reveal some interesting features about the temporal evolution of the field distribution.

We substitute the  $P$ -representation, see Eq. (3.1.16),

$$\rho = \int P(\alpha, \alpha^*, t) |\alpha\rangle\langle\alpha| d^2\alpha \quad (8.4.1)$$

into Eq. (8.3.2) and the resulting equation is

$$\begin{aligned} \int \dot{P}(\alpha, \alpha^*, t) |\alpha\rangle\langle\alpha| d^2\alpha &= -\frac{\mathcal{C}}{2} \bar{n}_{\text{th}} \int P(\alpha, \alpha^*, t) (aa^\dagger |\alpha\rangle\langle\alpha| \\ &\quad - 2a^\dagger |\alpha\rangle\langle\alpha| a + |\alpha\rangle\langle\alpha| aa^\dagger) d^2\alpha \\ &\quad - \frac{\mathcal{C}}{2} (\bar{n}_{\text{th}} + 1) \int P(\alpha, \alpha^*, t) (a^\dagger a |\alpha\rangle\langle\alpha| \\ &\quad - 2a |\alpha\rangle\langle\alpha| a^\dagger + |\alpha\rangle\langle\alpha| a^\dagger a) d^2\alpha. \end{aligned} \quad (8.4.2)$$

It follows from

$$a^\dagger |\alpha\rangle\langle\alpha| = \left( \frac{\partial}{\partial\alpha} + \alpha^* \right) |\alpha\rangle\langle\alpha|, \quad (8.4.3a)$$

$$a |\alpha\rangle\langle\alpha| = \alpha |\alpha\rangle\langle\alpha|, \quad (8.4.3b)$$

$$|\alpha\rangle\langle\alpha| a^\dagger = \alpha^* |\alpha\rangle\langle\alpha|, \quad (8.4.3c)$$

$$|\alpha\rangle\langle\alpha| a = \left( \frac{\partial}{\partial\alpha^*} + \alpha \right) |\alpha\rangle\langle\alpha|, \quad (8.4.3d)$$

that

$$\begin{aligned}
 & aa^\dagger |\alpha\rangle\langle\alpha| - 2a^\dagger|\alpha\rangle\langle\alpha|a + |\alpha\rangle\langle\alpha|aa^\dagger \\
 &= \left[ \left( \frac{\partial}{\partial\alpha} + \alpha^* \right) \alpha - 2 \left( \frac{\partial}{\partial\alpha} + \alpha^* \right) \left( \frac{\partial}{\partial\alpha^*} + \alpha \right) \right. \\
 &\quad \left. + \left( \frac{\partial}{\partial\alpha^*} + \alpha \right) \alpha^* \right] |\alpha\rangle\langle\alpha| \\
 &= - \left( \alpha \frac{\partial}{\partial\alpha} + \alpha^* \frac{\partial}{\partial\alpha^*} + 2 \frac{\partial^2}{\partial\alpha\partial\alpha^*} \right) |\alpha\rangle\langle\alpha|,
 \end{aligned} \tag{8.4.4}$$

and

$$\begin{aligned}
 & a^\dagger a |\alpha\rangle\langle\alpha| - 2a|\alpha\rangle\langle\alpha|a^\dagger + |\alpha\rangle\langle\alpha|a^\dagger a \\
 &= \left[ \alpha \left( \frac{\partial}{\partial\alpha} + \alpha^* \right) - 2|\alpha|^2 + \alpha^* \left( \frac{\partial}{\partial\alpha^*} + \alpha \right) \right] |\alpha\rangle\langle\alpha| \\
 &= \left( \alpha \frac{\partial}{\partial\alpha} + \alpha^* \frac{\partial}{\partial\alpha^*} \right) |\alpha\rangle\langle\alpha|.
 \end{aligned} \tag{8.4.5}$$

We now substitute Eqs. (8.4.4) and (8.4.5) into Eq. (8.4.2) and integrate the result by parts. In doing so we encounter the integral

$$\begin{aligned}
 & \int P(\alpha, \alpha^*, t) \left( \alpha \frac{\partial}{\partial\alpha} |\alpha\rangle\langle\alpha| \right) d^2\alpha \\
 &= \alpha P(\alpha, \alpha^*, t) |\alpha\rangle\langle\alpha| \Big|_{-\infty}^{\infty} - \int \left[ \frac{\partial}{\partial\alpha} \alpha P(\alpha, \alpha^*, t) \right] |\alpha\rangle\langle\alpha| d^2\alpha.
 \end{aligned} \tag{8.4.6}$$

Since the distribution vanishes at the infinite limits, Eq. (8.4.6) becomes

$$\int P(\alpha, \alpha^*, t) \left( \alpha \frac{\partial}{\partial\alpha} |\alpha\rangle\langle\alpha| \right) d^2\alpha = - \int \left[ \frac{\partial}{\partial\alpha} \alpha P(\alpha, \alpha^*, t) \right] |\alpha\rangle\langle\alpha| d^2\alpha. \tag{8.4.7}$$

Similarly

$$\int P(\alpha, \alpha^*, t) \left( \frac{\partial^2}{\partial\alpha\partial\alpha^*} |\alpha\rangle\langle\alpha| \right) d^2\alpha = \int \left[ \frac{\partial^2}{\partial\alpha\partial\alpha^*} P(\alpha, \alpha^*, t) \right] |\alpha\rangle\langle\alpha| d^2\alpha. \tag{8.4.8}$$

Then we have from Eq. (8.4.2)

$$\begin{aligned}
 \int \dot{P}(\alpha, \alpha^*, t) |\alpha\rangle\langle\alpha| d^2\alpha &= \frac{\mathcal{C}}{2} \int \left[ \left( \frac{\partial}{\partial\alpha} \alpha + \frac{\partial}{\partial\alpha^*} \alpha^* + 2\bar{n}_{\text{th}} \frac{\partial^2}{\partial\alpha\partial\alpha^*} \right) \right. \\
 &\quad \left. \times P(\alpha, \alpha^*, t) \right] |\alpha\rangle\langle\alpha| d^2\alpha.
 \end{aligned} \tag{8.4.9}$$

It follows on identifying the coefficients of  $|\alpha\rangle\langle\alpha|$  in the integrands that the equation of motion for  $P(\alpha, \alpha^*, t)$  is

$$\dot{P} = \frac{\mathcal{C}}{2} \left( \frac{\partial}{\partial \alpha} \alpha + \frac{\partial}{\partial \alpha^*} \alpha^* \right) P + \mathcal{C} \bar{n}_{\text{th}} \frac{\partial^2 P}{\partial \alpha \partial \alpha^*}. \quad (8.4.10)$$

This is the Fokker–Planck equation for the  $P$ -representation.

Next we find a solution of the Fokker–Planck equation. We assume that the field is initially in a coherent state  $|\alpha_0\rangle$ , i.e.,

$$P(\alpha, \alpha^*, 0) = \delta^{(2)}(\alpha - \alpha_0). \quad (8.4.11)$$

In the Gaussian representation of the  $\delta$ -function,

$$P(\alpha, \alpha^*, 0) = \lim_{\epsilon \rightarrow 0} \frac{1}{\pi \epsilon} \exp \left( \frac{-|\alpha - \alpha_0|^2}{\epsilon} \right). \quad (8.4.12)$$

We therefore seek a solution of Eq. (8.4.10) in the form

$$P(\alpha, \alpha^*, t) = \exp[-a(t) + b(t)\alpha + c(t)\alpha^* - d(t)\alpha\alpha^*], \quad (8.4.13)$$

subject to the initial conditions

$$a(0) = \frac{|\alpha_0|^2}{\epsilon} + \ln(\pi\epsilon), \quad (8.4.14a)$$

$$b(0) = \frac{\alpha_0^*}{\epsilon}, \quad (8.4.14b)$$

$$c(0) = \frac{\alpha_0}{\epsilon}, \quad (8.4.14c)$$

$$d(0) = \frac{1}{\epsilon}. \quad (8.4.14d)$$

On substituting expression (8.4.13) for  $P(\alpha, \alpha^*, t)$  into Eq. (8.4.10) and carrying out the necessary  $t$  and  $\alpha$  differentiations, we obtain

$$\begin{aligned} -\dot{a} + \dot{b}\alpha + \dot{c}\alpha^* - \dot{d}|\alpha|^2 &= \mathcal{C} \left[ 1 + \bar{n}_{\text{th}}(bc - d) + \left( \frac{b}{2} - \bar{n}_{\text{th}}bd \right) \alpha \right. \\ &\quad \left. + \left( \frac{c}{2} - \bar{n}_{\text{th}}cd \right) \alpha^* - (d - \bar{n}_{\text{th}}d^2)|\alpha|^2 \right]. \end{aligned} \quad (8.4.15)$$

A comparison of the terms proportional to  $|\alpha|^2$ ,  $\alpha^*$ ,  $\alpha$ , and unity lead to the following set of differential equations:

$$\dot{d} = \mathcal{C}(d - \bar{n}_{\text{th}}d^2), \quad (8.4.16a)$$

$$\dot{c} = \mathcal{C} \left( \frac{c}{2} - \bar{n}_{\text{th}}cd \right), \quad (8.4.16b)$$

$$\dot{b} = \mathcal{C} \left( \frac{b}{2} - \bar{n}_{\text{th}}bd \right), \quad (8.4.16c)$$

$$\dot{a} = -\mathcal{C}[1 + \bar{n}_{\text{th}}(bc - d)]. \quad (8.4.16d)$$

The solution of these equations subject to the initial conditions (8.4.14a)–(8.4.14d) is given by

$$d(t) = \frac{1}{\bar{n}_{\text{th}}(1 - e^{-\mathcal{C}t}) + \epsilon e^{-\mathcal{C}t}}, \quad (8.4.17a)$$

$$c(t) = \frac{\alpha_0 e^{-\mathcal{C}t/2}}{\bar{n}_{\text{th}}(1 - e^{-\mathcal{C}t}) + \epsilon e^{-\mathcal{C}t}}, \quad (8.4.17b)$$

$$b(t) = \frac{\alpha_0^* e^{-\mathcal{C}t/2}}{\bar{n}_{\text{th}}(1 - e^{-\mathcal{C}t}) + \epsilon e^{-\mathcal{C}t}}, \quad (8.4.17c)$$

$$a(t) = \frac{|\alpha_0|^2 e^{-\mathcal{C}t}}{\bar{n}_{\text{th}}(1 - e^{-\mathcal{C}t}) + \epsilon e^{-\mathcal{C}t}} + \ln \left\{ \pi \left[ \bar{n}_{\text{th}} (1 - e^{-\mathcal{C}t}) + \epsilon e^{-\mathcal{C}t} \right] \right\}. \quad (8.4.17d)$$

A substitution of these solutions into Eq. (8.4.13) results in the Gaussian form for  $P(\alpha, \alpha^*, t)$ :

$$P(\alpha, \alpha^*, t) = \frac{1}{\pi D(t)} \exp \left[ -\frac{|\alpha - \alpha_0 U(t)|^2}{D(t)} \right], \quad (8.4.18)$$

where

$$D(t) = \bar{n}_{\text{th}}(1 - e^{-\mathcal{C}t}) \quad (8.4.19)$$

is the dispersion of the Gaussian function about its mean value

$$\alpha_0 U(t) = \alpha_0 e^{-\mathcal{C}t/2 - ivt}. \quad (8.4.20)$$

In Eq. (8.4.20), we have included the factor  $\exp(-ivt)$  by going back from the interaction picture to the Schrödinger picture.

The dispersion  $D(t)$  increases from the initial value zero, while the center of the Gaussian distribution circles about on the exponential spiral given by Eq. (8.4.20). This is shown in Fig. 8.1 where the  $P$ -representation is plotted as a function of complex amplitude  $\alpha$ . When the time  $t$  is much greater than the damping time,  $\mathcal{C}^{-1}$ , the field distribution comes to equilibrium with the heat bath oscillators. In the steady state, the dispersion has its limiting value  $\bar{n}_{\text{th}}$  and the Gaussian distribution is centered about the origin. Thus the field loses its initial excitation to the heat bath oscillators but acquires noise in the process of damping. This is a manifestation of the fluctuation–dissipation theorem, i.e., the dissipation via heat bath oscillators is accompanied by fluctuations. We will discuss it in the next chapter.

It is interesting to note that if we take the heat bath to be at zero temperature ( $\bar{n}_{\text{th}} = 0$ ), the dispersion  $D(t)$  remains zero at all times and  $P(\alpha, \alpha^*, t)$  always remains a  $\delta$ -function, i.e.,

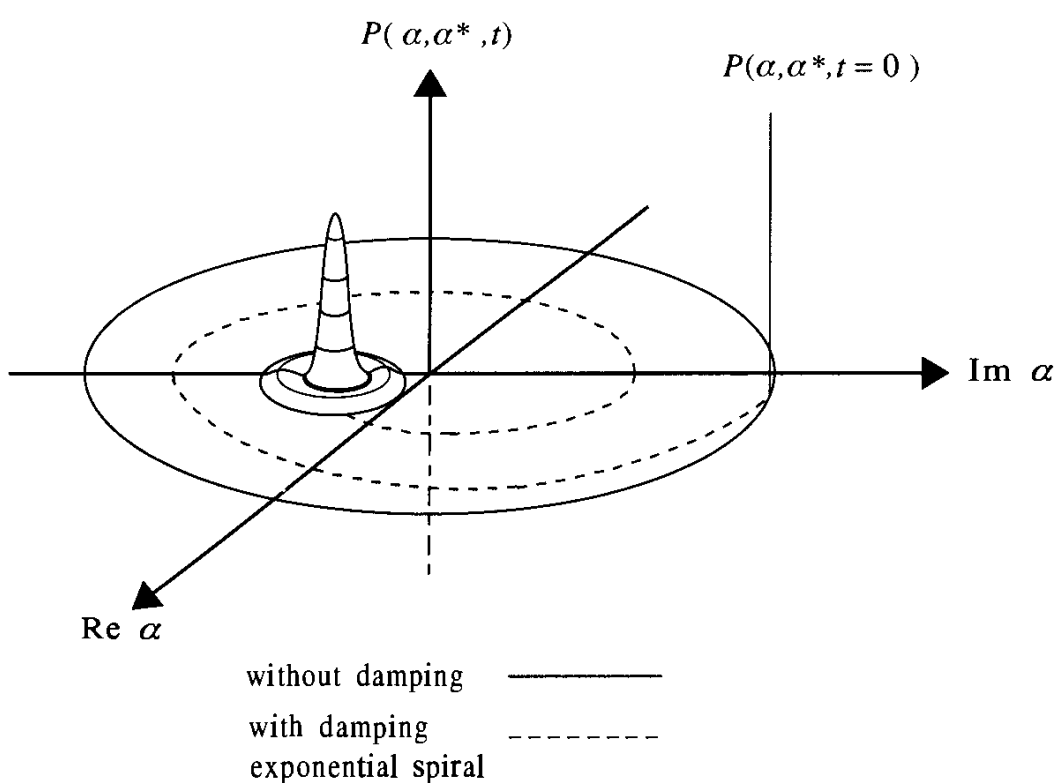


Fig. 8.1  
The  $P$ -representation for the complex amplitude of a harmonic oscillator mode damped by a thermal bath. The harmonic oscillator mode starts at  $t = 0$  in a pure coherent state  $|\alpha\rangle$  and the mean value of the amplitude moves on an exponential spiral decreasing steadily in modulus, while its dispersion increases.

$$P(\alpha, \alpha^*, t) = \delta^{(2)}[\alpha - \alpha_0 U(t)]. \quad (8.4.21)$$

The state of the field remains at all times in a pure coherent state. This form of dissipation is completely noise free.

## 8.5 The ‘quantum jump’ approach to damping

*Monte Carlo.*

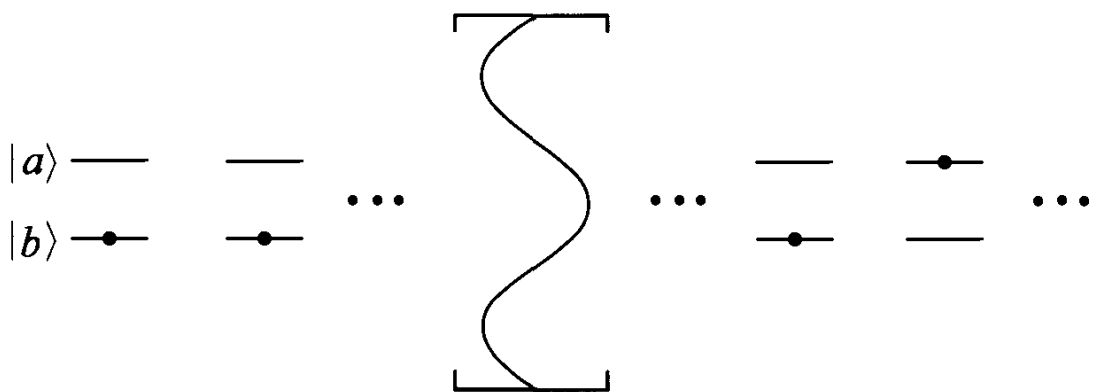
Historically, the notions of quantum jumps and instantaneous collapse of the wave function go back to the early days in which Einstein worried about outgoing spherical waves ‘collapsing’ when a photoelectron is detected; and the notion of Bohr concerning the emission of light when an atom ‘jumped’ between Bohr orbits.

However, with the coming of wave mechanics the whole question of quantum jumps took on a new perspective. Atomic transitions were ‘induced’ and one often encountered statements that ‘there were no such a thing as quantum jumps’.

Recently, the work of Dehmelt and others clearly shows that sudden jumps are evident in many aspects of quantum optics, e.g., the spectacular work involving single ions in a Paul trap.

More recently a new ‘quantum jump’ approach to dissipation has developed, one can find names and concepts like: Monte Carlo simulation, quantum trajectories, collapse or reduction of the state vector,

Fig. 8.2  
Two-level atoms in their ground state  $|b\rangle$  passing through a resonant cavity.



no count or ‘null’ measurement, and conditional density matrices. We will here give a short account of this interesting idea as it applies to damping or dissipation in quantum optics.

### 8.5.1 Conditional density matrices and the null measurement

In the previous sections of this chapter we have developed the theory of damping or dissipation in quantum mechanics from a density matrix perspective. The result is typically an expression of the form of (8.3.3) which describes the decay of a single mode of a resonant cavity at temperature  $T = 0$ . There we took the model of a large number of bath oscillators, e.g., phonons coupling energy out of the cavity mode. However the result, Eq. (8.3.3), is not specific to the model and we will here investigate the problem again using another model which will lead us naturally to a different point of view concerning dissipation processes.

Consider the model of Fig. 8.2 in which we are passing ground state atoms through a cavity which is resonant with the atoms, i.e., the Hamiltonian in the interaction picture is

$$\mathcal{V} = \hbar g(a^\dagger|b\rangle\langle a| + |a\rangle\langle b|a). \quad (8.5.1)$$

Consider the density matrix for the field at time  $t + \tau$ ,  $\rho(t + \tau)$ , resulting from a ground state atom injected at time  $t$ , i.e.,

$$\begin{aligned} \rho(t + \tau) &= \text{Tr}_{\text{atom}} \left[ e^{-i\mathcal{V}\tau/\hbar} \rho(t) \otimes |b\rangle\langle b| e^{i\mathcal{V}\tau/\hbar} \right] \\ &= \langle a|\rho_{\text{atom-field}}(t + \tau)|a\rangle + \langle b|\rho_{\text{atom-field}}(t + \tau)|b\rangle. \end{aligned} \quad (8.5.2)$$

It is natural to identify the two terms in (8.5.2) as ‘conditional’ density matrices, i.e.,

$$\begin{aligned} \rho_a(t + \tau) &= \text{conditional density matrix for field, atom excited} \\ &= \langle a|e^{-i\mathcal{V}\tau/\hbar} \rho(t) \otimes |b\rangle\langle b| e^{i\mathcal{V}\tau/\hbar}|a\rangle, \end{aligned} \quad (8.5.3a)$$

$$\begin{aligned}
\rho_b(t + \tau) &= \text{conditional density matrix for field, atom not excited} \\
&= \langle b | e^{-i\gamma\tau/\hbar} \rho(t) \otimes |b\rangle \langle b | e^{i\gamma\tau/\hbar} |b\rangle. \tag{8.5.3b}
\end{aligned}$$

We may regard  $\rho_a$  and  $\rho_b$  as conditional density matrices corresponding to our having observed a count (excited atom) or no count (ground state atom) in our atomic beam. That is, the atomic beam serves two functions: it is a dissipation mechanism and it is also a kind of probe, or photodetector, of the field.

We proceed by noting that for small times  $\tau$ , we may expand the  $\exp(\pm i\gamma\tau/\hbar)$  factors and find

$$\rho_a(t + \tau) \cong g^2 \tau^2 a \rho(t) a^\dagger, \tag{8.5.4a}$$

$$\begin{aligned}
\rho_b(t + \tau) &\cong \rho(t) - \frac{1}{2} g^2 \tau^2 [a^\dagger a \rho(t) + \rho(t) a^\dagger a] \\
&\cong e^{-R\tau a^\dagger a} \rho(t) e^{-R\tau a^\dagger a}, \tag{8.5.4b}
\end{aligned}$$

where  $R = g^2 \tau / 2$ .

Now we make the key step. We let the time  $\tau \rightarrow 0$  and make the ansatz that Eq. (8.5.4a) is to be associated with a ‘quantum jump’ of photoabsorption at time  $t$ . Then if we consider a process in which  $n$  counts are observed at times  $t_1, t_2, \dots, t_n$  with no counts in between these times, we have the conditional density matrix

$$\begin{aligned}
\rho^{(n)} &= [e^{-S(t-t_n)} a e^{-S(t_n-t_{n-1})} \dots a e^{-S(t_2-t_1)} a e^{-S t_1} \\
&\quad \times \rho(0) e^{-S t_1} a^\dagger e^{-S(t_2-t_1)} a^\dagger e^{-S(t_n-t_{n-1})} a^\dagger e^{-S(t-t_n)}] \\
&/\text{Tr}, \tag{8.5.5}
\end{aligned}$$

where  $S = Ra^\dagger a$  and the trace factor in the denominator is the normalization factor. This may be simplified by taking account of the fact that, e.g.,

$$\begin{aligned}
e^{-S(t_2-t_1)} a e^{-S t_1} &= e^{-Ra^\dagger a(t_2-t_1)} a e^{-Ra^\dagger a t_1} \\
&= e^{-Ra^\dagger a(t_2-t_1)} e^{-Ra^\dagger a t_1} e^{Ra^\dagger a t_1} a e^{-Ra^\dagger a t_1} \\
&= e^{-Ra^\dagger a t_2} e^{-R t_1} a, \tag{8.5.6}
\end{aligned}$$

which may be used repeatedly to reduce Eq. (8.5.5) to the simple form

$$\rho^{(n)}(t) = \frac{e^{-Ra^\dagger a t} a^n \rho(0) a^{\dagger n} e^{-Ra^\dagger a t}}{\text{Tr}[\rho(0) a^{\dagger n} e^{-2Ra^\dagger a t} a^n]}, \tag{8.5.7}$$

where the various factors of  $\exp(-R t_1)$  are canceled by the normalization. Equation (8.5.7) (and its generalizations) is the main result of

this section. In particular, if we consider  $\rho(0)$  to be a pure case density matrix  $\rho(0) = |\psi(0)\rangle\langle\psi(0)|$ , then Eq. (8.5.7) may be written as

$$\rho^{(n)}(t) = \frac{e^{-Ra^\dagger at} a^n |\psi(0)\rangle}{\sqrt{\langle\psi(0)|a^{\dagger n} e^{-2Ra^\dagger at} a^n |\psi(0)\rangle}} \\ \frac{\langle\psi(0)|a^{\dagger n} e^{-Ra^\dagger at}}{\sqrt{\langle\psi(0)|a^{\dagger n} e^{-2Ra^\dagger at} a^n |\psi(0)\rangle}}. \quad (8.5.8)$$

Equation (8.5.8) provides a natural introduction to the wave function approach to dissipative processes.

### 8.5.2 The wave function Monte Carlo approach to damping

Motivated by the result of the previous section, i.e., Eq. (8.5.8), we present here a short account of damping via a wave function approach. In order to present the ideas we will continue to consider the simple problem of a damped single-mode field, but we will have a more general reservoir, such as that in Section 8.3, in mind. Thus, the decay rate  $R$  is no longer governed by the time  $\tau$  but by the much shorter reservoir correlation times. From Eq. (8.5.8) we are led to write the ‘conditional state vector’

$$|\psi^{(n)}(t + \delta t)\rangle = \frac{e^{-Ra^\dagger a\delta t} a^n |\psi(t)\rangle}{\sqrt{\langle\psi(t)|a^{\dagger n} e^{-2Ra^\dagger a\delta t} a^n |\psi(t)\rangle}}, \quad (8.5.9)$$

which represents the state of the field under the condition of  $n$  photons absorbed in time  $\delta t$  starting from  $|\psi(t)\rangle$ . In particular, the state involving only zero or one such event is of special interest. That is, the state at time  $t + \delta t$  for  $n = 0$  (a null measurement) is

$$|\psi^{(0)}(t + \delta t)\rangle = \frac{e^{-Ra^\dagger a\delta t} |\psi(t)\rangle}{\sqrt{\langle\psi(t)|e^{-2Ra^\dagger a\delta t} |\psi(t)\rangle}} \\ \cong \frac{(1 - Ra^\dagger a\delta t)}{\sqrt{1 - 2R\langle a^\dagger a\rangle\delta t}} |\psi(t)\rangle, \quad (8.5.10a)$$

where  $\langle a^\dagger a\rangle = \langle\psi(t)|a^\dagger a|\psi(t)\rangle$ ; and the state corresponding to  $n = 1$  (quantum jump) is

$$|\psi^{(1)}(t + \delta t)\rangle = \frac{e^{-Ra^\dagger a\delta t} a |\psi(t)\rangle}{\sqrt{\langle\psi(t)|a^\dagger e^{-2Ra^\dagger a\delta t} a |\psi(t)\rangle}} \\ \cong \frac{a}{\sqrt{\langle a^\dagger a\rangle}} |\psi(t)\rangle. \quad (8.5.10b)$$

For example, if the initial quantum state for the field mode is

$$|\psi(t)\rangle = c_0(t)|0\rangle + c_1(t)|1\rangle, \quad (8.5.11)$$

then (8.5.10a) and (8.5.10b) imply the conditional state vectors

$$|\psi^{(0)}(t + \delta t)\rangle = \frac{c_0|0\rangle + c_1(1 - R\delta t)|1\rangle}{\sqrt{1 - 2c_1^*c_1R\delta t}}, \quad (8.5.12a)$$

and

$$|\psi^{(1)}(t + \delta t)\rangle = \frac{c_1}{\sqrt{|c_1|^2}}|0\rangle. \quad (8.5.12b)$$

However, we want to describe the evolution from  $|\psi(t)\rangle$  as given by Eq. (8.5.11) to a general state at later times which must become  $|0\rangle$  eventually. During the time  $\delta t$  the unnormalized ‘no count’ or ‘null measurement’  $|\tilde{\psi}\rangle$  is seen from Eq. (8.5.10a) to obey the equation of motion

$$\frac{|\tilde{\psi}^{(0)}(t + \delta t)\rangle - |\tilde{\psi}^{(0)}(t)\rangle}{\delta t} = -Ra^\dagger a|\tilde{\psi}^{(0)}(t)\rangle, \quad (8.5.13a)$$

that is

$$\frac{d}{dt}|\tilde{\psi}^{(0)}(t)\rangle = -\frac{i}{\hbar}(-i\hbar Ra^\dagger a)|\tilde{\psi}^{(0)}(t)\rangle. \quad (8.5.13b)$$

Thus we are motivated to describe the time evolution of the unnormalized state vector for the case of no absorption by a nonunitary Schrödinger equation

$$\frac{d}{dt}|\tilde{\psi}^{(0)}(t)\rangle = -\frac{i}{\hbar}\mathcal{V}_1|\tilde{\psi}^{(0)}(t)\rangle \quad (8.5.14)$$

governed by the non-Hermitian Hamiltonian

$$\mathcal{V}_1 = -i\hbar Ra^\dagger a. \quad (8.5.15)$$

The temporal development implied by Eq. (8.5.14) is, of course, interrupted by quantum jumps or collapses of the wave function at random times. When such a collapse occurs, the state is given by  $|0\rangle$ . This happens only once, from that time on the field is in the vacuum state. Continuing with our simple example, according to Eq. (8.5.14) the unnormalized state vector

$$|\tilde{\psi}(t)\rangle = \tilde{c}_0(t)|0\rangle + \tilde{c}_1(t)|1\rangle \quad (8.5.16)$$

obeys the simple equations of motion

$$\dot{\tilde{c}}_0(t) = 0, \quad (8.5.17a)$$

$$\dot{\tilde{c}}_1(t) = -R\tilde{c}_1(t), \quad (8.5.17b)$$

which imply

$$\tilde{c}_0(t) = \tilde{c}_0(0), \quad (8.5.18a)$$

$$\tilde{c}_1(t) = \tilde{c}_1(0)e^{-Rt}, \quad (8.5.18b)$$

and the corresponding normalized probability amplitudes

$$c_0(t) = \frac{c_0(0)}{\sqrt{|c_0(0)|^2 + |c_1(0)|^2 e^{-2Rt}}}, \quad (8.5.19a)$$

and

$$c_1(t) = \frac{c_1(0)e^{-Rt}}{\sqrt{|c_0(0)|^2 + |c_1(0)|^2 e^{-2Rt}}}. \quad (8.5.19b)$$

Thus we have the complete coherent evolution for the conditional state vector up to the point of collapse,

$$|\psi^{(0)}(t)\rangle = \frac{c_0(0)|0\rangle + c_1(0)e^{-Rt}|1\rangle}{\sqrt{|c_0(0)|^2 + |c_1(0)|^2 e^{-2Rt}}}. \quad (8.5.20)$$

Note that as  $t \rightarrow \infty$  the state  $|\psi^{(0)}(t)\rangle \rightarrow |0\rangle$ . This is as it should be since the conditional state  $|\psi^{(0)}(t)\rangle$  is that state which is conditioned on the premise that no photons are absorbed. Hence if after a long time we never see a ‘count’, then the conclusion is that we must have been in the vacuum state,  $|0\rangle$ , all along. To summarize: the field develops from  $t = 0$  up to some time  $t$  according to Eq. (8.5.14), and between  $t$  and  $t + \delta t$  a jump occurs, that is

$$|\psi(0)\rangle = c_0(0)|0\rangle + c_1(0)|1\rangle \quad (8.5.21a)$$

$$\begin{array}{c} \downarrow \\ \text{‘no counts’ from } 0 \rightarrow t \end{array}$$

$$|\psi(t)\rangle = c_0(t)|0\rangle + c_1(t)|1\rangle \quad (8.5.21b)$$

$$\begin{array}{c} \downarrow \\ \text{collapse } t \rightarrow t + \delta t \end{array}$$

$$\begin{aligned} |\psi(t + \delta t)\rangle &= \frac{a}{\sqrt{\langle \psi(t) | a^\dagger a | \psi(t) \rangle}} |\psi(t)\rangle \\ &= |0\rangle, \end{aligned} \quad (8.5.21c)$$

where  $c_0(t)$  and  $c_1(t)$  in (8.5.21b) are given by Eqs. (8.5.19a) and (8.5.19b) and Eq. (8.5.21c) follows from Eq. (8.5.10b). Now we recall that the probability of a collapse or jump at time  $t$  is governed by the density matrix conditional upon a single photon absorption, i.e., a ‘count’. With that in mind, we write Eq. (8.3.3) for  $R = \mathcal{C}/2$  as

$$\begin{aligned} \dot{\rho} &= -R(a^\dagger a \rho + \rho a^\dagger a) + 2Ra\rho a^\dagger \\ &= \underbrace{-\frac{i}{\hbar}(\mathcal{V}_1 \rho - \rho \mathcal{V}_1^\dagger)}_{\dot{\rho}(\text{no count})} + \underbrace{2Ra\rho a^\dagger}_{\dot{\rho}(\text{count})}. \end{aligned} \quad (8.5.22)$$

Hence the probability for a collapse between  $t$  and  $t + \delta t$  is given by

$$\begin{aligned}\text{Tr}[\dot{\rho}(\text{count})]\delta t &= 2R\delta t\text{Tr}[\rho(t)a^\dagger a] \\ &= 2R\delta t\langle\psi(t)|a^\dagger a|\psi(t)\rangle \\ &= 2R\delta t\frac{\langle\tilde{\psi}(t)|a^\dagger a|\tilde{\psi}(t)\rangle}{\langle\tilde{\psi}(t)|\tilde{\psi}(t)\rangle}.\end{aligned}\quad (8.5.23)$$

Therefore, from Eqs. (8.5.16)–(8.5.19b) and (8.5.23), we have the jump probability for our present problem

$$P_{\text{jump}}(t) = 2R\delta t\frac{|c_1(0)|^2 e^{-2Rt}}{|c_0(0)|^2 + |c_1(0)|^2 e^{-2Rt}}. \quad (8.5.24)$$

Finally we turn the above into a plot of the probability of finding a photon in the cavity after a time  $t$  given that  $c_0(0) = 0$  and  $c_1(0) = 1$ . Then  $P_{\text{jump}}(t) = 2R\delta t$ . This we do via a Monte Carlo procedure as follows. First, we start the field in state  $|1\rangle$  with  $c_1(0) = 1$  and we choose a number between 0 and 1 using a computer random number generator. If the number is smaller than  $P_{\text{jump}}(0)$ , then a jump or collapse is taken to have occurred, and the photon number is set to zero. Most likely, however, the number will be larger than  $P_{\text{jump}}$  and we reevaluate  $|\psi(t)\rangle$  from (8.5.20) and start again. We repeat this  $n$  times until a random number turns up which is smaller than  $P_{\text{jump}}(t)$  given by (8.5.24). At that point we make an entry in our table as follows:

$$\begin{array}{ll} t = 0 & |\psi(0)\rangle = c_0(0)|0\rangle + c_1(0)|1\rangle \\ & \downarrow \text{evolve} \\ t = \delta t & |\psi(\delta t)\rangle = c_0(\delta t)|0\rangle + c_1(\delta t)|1\rangle \\ & \downarrow \text{evolve} \\ t = 2\delta t & |\psi(2\delta t)\rangle = c_0(2\delta t)|0\rangle + c_1(2\delta t)|1\rangle \\ & \vdots \\ & \downarrow \text{evolve} \\ t = n\delta t & |\psi(n\delta t)\rangle = c_0(n\delta t)|0\rangle + c_1(n\delta t)|1\rangle \\ & \downarrow \text{collapse} \\ t = (n+1)\delta t & |\psi[(n+1)\delta t]\rangle = |0\rangle.\end{array}\quad (8.5.25)$$

Needless to say, the preceding simple example was chosen for pedagogical purposes. Many more involved problems can be and have been solved by the quantum jump–Monte Carlo approach. These include spontaneous emission, resonance fluorescence, Doppler cooling, population trapping, and the dark line resonance, to name a few.

In conclusion we note that the approach of the present section is often referred to as the ‘quantum trajectory method’. We also point to the interesting work of Willis Lamb in which the trajectories of Gaussian wave packets are calculated in order to treat the quantum theory of certain problems dealing with the measurement process. This work also uses a computer analysis to characterize the (random) outcomes of the experiment.

## Problems

- 8.1** Derive Eqs. (8.2.14a) and (8.2.14b) and use these results to evaluate the correlation functions (8.2.16a)–(8.2.16e).
- 8.2** The equation of motion for the reduced density operator for a single-mode cavity field coupled to a vacuum reservoir through a partially transmitting mirror is

$$\dot{\rho} = -\frac{\mathcal{C}}{2}(a^\dagger a \rho - 2a\rho a^\dagger + \rho a^\dagger a).$$

Here  $\mathcal{C}$  is the loss rate related to the  $Q$ -factor of the cavity by  $\mathcal{C} = v/Q$ . Derive the equations of motion for the relevant quantities, and then solve them to show that the variances  $(\Delta X_1)_t^2$  and  $(\Delta X_2)_t^2$  (with  $X_1 = (a+a^\dagger)/2$  and  $X_2 = (a-a^\dagger)/2i$ ) increase due to dissipation (fluctuation–dissipation theorem!). This situation can be viewed as a bosonic mode, uncorrelated to the cavity field, entering the cavity through the partially transmitting mirror, and hence adding the uncorrelated noise.

- 8.3** If the reservoir in the above problem is in a multi-mode squeezed vacuum state, the resulting equation of motion for the reduced density matrix is given by Eq. (8.3.4). As before, calculate the variances  $(\Delta X_1)_t^2$  and  $(\Delta X_2)_t^2$ . Is it possible to suppress the added noise in this situation?

**8.4** For a thermal reservoir

$$\dot{\rho} = -\frac{\mathcal{C}}{2}(\bar{n}_{\text{th}} + 1)(a^\dagger a \rho - 2a\rho a^\dagger + \rho a^\dagger a)$$

$$-\frac{\mathcal{C}}{2}\bar{n}_{\text{th}}(aa^\dagger \rho - 2a^\dagger \rho a + \rho aa^\dagger),$$

where  $\bar{n}_{\text{th}}$  is the mean number of photons in the reservoir.  
Derive the corresponding equation for the  $Q$ -representation  
and solve it.

**8.5** Derive Eqs. (8.2.18a)–(8.2.18c).

# Intro to Chapter 9

经典力学方程

① 分子无规则运动 → 随机微分(积分)方程  
 ② 撞击独立

随机 ⇔ 独立

$$T_1 = T_2 \text{ 直平衡状态} \quad \langle \frac{1}{2}mv^2 \rangle = \frac{1}{2}m\langle v^2 \rangle = \frac{1}{2}kT \quad (\text{单-维度})$$

力: 固定外力  $F=0$

$$\text{阻力} \quad -b\gamma v a \frac{dx}{dt} = -\gamma v$$

$$\text{涨落力} \quad F(t) = \begin{cases} \langle F(t) \rangle = 0 & \text{对所有颗粒平均} \\ \langle F(t)F(t') \rangle = Q\delta(t-t') \end{cases}$$

$$m \frac{d\dot{x}}{dt} = -\gamma \frac{dx}{dt} + F(t)$$

$$m=1 \text{ kg}, \quad \Rightarrow V(t) = \int_0^t e^{-\gamma(t-\tau)} F(\tau) d\tau + V(0) e^{-\gamma t}$$

$$\text{假设 } V(0)=0: \quad \langle V(t) \rangle = \int_0^t e^{-\gamma(t-\tau)} \underbrace{\langle F(\tau) \rangle}_{=0} d\tau + \underbrace{\langle V(0) e^{-\gamma t} \rangle}_{=0} = 0$$

$$\begin{aligned} \langle V(t)V(t') \rangle &= \left\langle \int_0^t e^{-\gamma(t-\tau)} F(\tau) d\tau \int_0^{t'} e^{-\gamma(t'-\tau')} F(\tau') d\tau' \right\rangle \\ &= \int_0^t \int_{\tau'}^{t'} \langle F(\tau) F(\tau') \rangle e^{-\gamma(t-\tau)} d\tau d\tau' \\ &= \frac{Q}{2P} \exp(-\gamma |t-t'|) \end{aligned}$$

$$\Rightarrow \frac{1}{2}m\langle v^2 \rangle = \frac{1}{2}m \frac{Q}{2P} = \frac{1}{2}kT$$

$$\Rightarrow Q = \frac{2P k T}{m}$$

$Q$ : 涨落  $\gamma$ : 粘度

\*. 涨落和粘度

# Quantum theory of damping – Heisenberg–Langevin approach

---

In the previous chapter, we developed the equation of motion for a system as it evolved under the influence of an unobserved (reservoir) system. We used the density matrix approach and worked in the interaction picture. In this chapter, we consider the same problem of the system–reservoir interaction using a quantum operator approach. We again eliminate the reservoir variables. The resulting equations for the system operators include, in addition to the damping terms, the *noise* operators which produce fluctuations. These equations have the form of classical Langevin equations, which describe, for example, the Brownian motion of a particle suspended in a liquid. The Heisenberg–Langevin approach discussed in this chapter is particularly suitable for the calculation of two-time correlation functions of the system operator as is, for example, required for the determination of the natural linewidth of a laser.

We first consider the damping of the harmonic oscillator by an interaction with a reservoir consisting of many other simple harmonic oscillators. This system describes, for example, the damping of a single-mode field inside a cavity with lossy mirrors. The reservoir, in this case, consists of a large number of phonon-like modes in the mirrors. We also consider the decay of the field due to its interaction with an atomic reservoir. An interesting application of the theory of the system–reservoir interaction is the evolution of an atom inside a damped cavity. It is shown that the spontaneous transition rate of the atom can be substantially enhanced if it is placed in a resonant cavity.

## 9.1 Simple treatment of damping via oscillator reservoir: Markovian white noise

We consider a system consisting of a single-mode field of frequency  $\nu$  and annihilation operator  $a(t)$  interacting with a reservoir. The reservoir may be taken as any large collection of systems with many degrees of freedom. We assume that the reservoir consists of many oscillators (e.g., phonons, other photon modes, etc) with closely spaced frequencies  $\nu_k$  and annihilation (and creation) operators  $b_{\mathbf{k}}$  (and  $b_{\mathbf{k}}^\dagger$ ). This system therefore describes the damping of a harmonic oscillator by an interaction with a reservoir consisting of many other simple harmonic oscillators. The field-reservoir system evolves in time under the influence of the total Hamiltonian

$$\mathcal{H} = \mathcal{H}_0 + \mathcal{H}_1, \quad (9.1.1)$$

*Handwritten notes:*  $\mathcal{H}_0 = \hbar\nu a^\dagger a + \sum_{\mathbf{k}} \hbar\nu_k b_{\mathbf{k}}^\dagger b_{\mathbf{k}}$

$$\mathcal{H}_0 = \hbar\nu a^\dagger a + \sum_{\mathbf{k}} \hbar\nu_k b_{\mathbf{k}}^\dagger b_{\mathbf{k}}, \quad (9.1.2)$$

$$\mathcal{H}_1 = \hbar \sum_{\mathbf{k}} g_{\mathbf{k}} (b_{\mathbf{k}}^\dagger a + a^\dagger b_{\mathbf{k}}). \quad (9.1.3)$$

As before,  $\mathcal{H}_0$  consists of the energy of the free field and the reservoir modes, and  $\mathcal{H}_1$  is the interaction energy. The field operators commute with the reservoir operators at a given time. We note that in Eq. (9.1.3) we have here made the usual rotating wave approximation.

The Heisenberg equations of motion for the operators are

$$\dot{a} = \frac{i}{\hbar} [\mathcal{H}, a] = -i\nu a(t) - i \sum_{\mathbf{k}} g_{\mathbf{k}} b_{\mathbf{k}}(t), \quad (9.1.4)$$

$$\dot{b}_{\mathbf{k}} = -i\nu_k b_{\mathbf{k}}(t) - ig_{\mathbf{k}} a(t). \quad (9.1.5)$$

We are interested in a closed equation for the harmonic oscillator operator  $a(t)$ . The equation for the reservoir operator  $b_{\mathbf{k}}(t)$  can be formally integrated to yield

$$b_{\mathbf{k}}(t) = b_{\mathbf{k}}(0)e^{-i\nu_k t} - ig_{\mathbf{k}} \int_0^t dt' a(t') e^{-i\nu_k(t-t')}. \quad (9.1.6)$$

Here the first term represents the free evolution of the reservoir modes, whereas the second term arises from their interaction with the harmonic oscillator. The reservoir operators  $b_{\mathbf{k}}(t)$  can be eliminated by substituting the formal solution of  $b_{\mathbf{k}}(t)$  into Eq. (9.1.4). We find

$$\dot{a} = -i\nu a - \sum_{\mathbf{k}} g_{\mathbf{k}}^2 \int_0^t dt' a(t') e^{-i\nu_k(t-t')} + f_a(t), \quad (9.1.7)$$

$$f_a(t) = -i \sum_{\mathbf{k}} g_{\mathbf{k}} b_{\mathbf{k}}(0) e^{-i\nu_k t}. \quad (9.1.8)$$

In Eq. (9.1.7),  $f_a(t)$  is a noise operator because it depends upon the reservoir operators  $b_k(0)$ . The evolution of the expectation values involving the harmonic oscillator operator will therefore depend upon the fluctuations in the reservoir. The noise operator varies rapidly due to the presence of all the reservoir frequencies. The fast frequency dependence of  $a(t)$  can be removed by transforming to the slowly varying annihilation operator

$$\tilde{a}(t) = a(t)e^{ivt}. \quad (9.1.9)$$

We see that

$$[\tilde{a}(t), \tilde{a}^\dagger(t)] = 1, \quad (9.1.10)$$

and Eq. (9.1.7) reduces to

$$\dot{\tilde{a}} = -\sum_{\mathbf{k}} g_{\mathbf{k}}^2 \int_0^t dt' \tilde{a}(t') e^{-i(v_k - v)(t-t')} + F_{\tilde{a}}(t), \quad (9.1.11)$$

$$F_{\tilde{a}}(t) = e^{ivt} f_a(t) = -i \sum_{\mathbf{k}} g_{\mathbf{k}} b_{\mathbf{k}}(0) e^{-i(v_k - v)t}. \quad (9.1.12)$$

The time integration in Eq. (9.1.11) is similar to that encountered in the Weisskopf–Wigner theory discussed in Section 6.3. As in the Weisskopf–Wigner approximation, the summation in Eq. (9.1.11) yields a  $\delta(t - t')$  function and the integration can then be carried out. We obtain

$$\sum_{\mathbf{k}} g_{\mathbf{k}}^2 \int_0^t dt' \tilde{a}(t') e^{-i(v_k - v)(t-t')} \simeq \frac{1}{2} \mathcal{C} \tilde{a}(t), \quad \text{马尔科夫近似, } \delta(t-t') \downarrow \quad (9.1.13)$$

where the damping constant

$$\mathcal{C} = 2\pi [g(v)]^2 D(v). \quad (9.1.14)$$

Here,  $g(v) \equiv g_{v/c}$  is the coupling constant evaluated at  $k = v/c$  and  $D(v) = Vv^2/\pi^2c^3$  (with  $V$  being the quantization volume) is the density of states (see Eq. (1.1.26)). We can therefore replace Eq. (9.1.11) by the Langevin equation

$$\dot{\tilde{a}} = -\frac{1}{2} \mathcal{C} \tilde{a} + F_{\tilde{a}}(t), \quad \text{该方程 (以快有, 否则 A 为慢分量) } \quad (9.1.15)$$

where  $F_{\tilde{a}}(t)$  is the noise operator which depends on the reservoir variables.

It is interesting to note that the presence of the noise operator in Eq. (9.1.15) is necessary to preserve the commutation relation (9.1.10) at all times. In the absence of the noise term ( $F_{\tilde{a}}(t) = 0$ ), Eq. (9.1.15) can be solved and we get

$$\tilde{a}(t) = \tilde{a}(0)e^{-\mathcal{C}t/2}. \quad (9.1.16)$$

If the operator  $\tilde{a}$  satisfies the commutation relation (9.1.10) at  $t = 0$ , then

$$[\tilde{a}(t), \tilde{a}^\dagger(t)] = e^{-\mathcal{C}t}, \quad (9.1.17)$$

representing a violation of the commutation relation. The noise operator with appropriate correlation properties helps to maintain the commutation relation (9.1.10) at all times. The presence of the noise term along with the damping term in Eq. (9.1.15) is a manifestation of the fluctuation-dissipation theorem of statistical mechanics, i.e., dissipation is always accompanied by fluctuations.

We suppose that the reservoir is in thermal equilibrium, so that

$$\langle b_{\mathbf{k}}(0) \rangle_R = \langle b_{\mathbf{k}}^\dagger(0) \rangle_R = 0, \quad (9.1.18)$$

$$\text{热平衡} \rightarrow \langle b_{\mathbf{k}}^\dagger(0)b_{\mathbf{k}'}(0) \rangle_R = \delta_{\mathbf{kk}'}\bar{n}_{\mathbf{k}}, \quad (9.1.19)$$

$$\text{弱相关} \quad \langle b_{\mathbf{k}}(0)b_{\mathbf{k}'}^\dagger(0) \rangle_R = (\bar{n}_{\mathbf{k}} + 1)\delta_{\mathbf{kk}'}, \quad (9.1.20)$$

$$\langle b_{\mathbf{k}}(0)b_{\mathbf{k}'}(0) \rangle_R = \langle b_{\mathbf{k}}^\dagger(0)b_{\mathbf{k}'}^\dagger(0) \rangle_R = 0. \quad (9.1.21)$$

Using these relations with the noise operator value (9.1.12), we can evaluate various first- and second-order correlation functions involving  $F_{\tilde{a}}(t)$  as follows:

(a) It follows trivially from Eq. (9.1.18) that the reservoir averages of  $F_{\tilde{a}}(t)$  and its adjoint  $F_{\tilde{a}}^\dagger(t)$  vanish, i.e.,

$$\langle F_{\tilde{a}}(t) \rangle_R = \langle F_{\tilde{a}}^\dagger(t) \rangle_R = 0. \quad (9.1.22)$$

(b) On using Eq. (9.1.19) we obtain  $\langle F_{\tilde{a}}^\dagger(t)F_{\tilde{a}}(t') \rangle_R = \langle F_{\tilde{a}}^\dagger(t)F_{\tilde{a}}^\dagger(t') \rangle_R = 0$

$$\begin{aligned} \langle F_{\tilde{a}}^\dagger(t)F_{\tilde{a}}(t') \rangle_R &= \sum_{\mathbf{k}} \sum_{\mathbf{k}'} g_{\mathbf{k}} g_{\mathbf{k}'} \langle b_{\mathbf{k}}^\dagger b_{\mathbf{k}'} \rangle_R \exp[i(v_k - v)t - i(v_{k'} - v)t'] \\ &= \sum_{\mathbf{k}} g_{\mathbf{k}}^2 \bar{n}_{\mathbf{k}} \exp[i(v_k - v)(t - t')] \\ &= \int_0^\infty D(v_k) [g(v_k)]^2 \bar{n}(v_k) e^{i(v_k - v)(t - t')} dv_k. \quad (9.1.23) \end{aligned}$$

$$D(v_k) = \frac{\sqrt{V} V^3}{\pi^2 C^3}$$

In the last line, we have gone from a discrete representation to a continuous representation in the usual way. We can now pull out the slowly varying terms  $D(v_k)$ ,  $g(v_k)$ , and  $\bar{n}(v_k)$  at  $v_k = v$  and replace the integral by a  $\delta$ -function. This gives

$$\langle F_{\tilde{a}}^\dagger(t)F_{\tilde{a}}(t') \rangle_R = \mathcal{C}\bar{n}_{\text{th}}\delta(t - t'), \quad (9.1.24)$$

where  $\mathcal{C}$  is given by Eq. (9.1.14) and  $\bar{n}_{\text{th}} = \bar{n}(v_k)$ . In analogy with the

随机场的统计性质：知道“过去”即可



运动速度是经典力学

classical Langevin theory, we define the diffusion coefficient  $D_{\tilde{a}^\dagger \tilde{a}}$  for  $\tilde{a}^\dagger \tilde{a}$  through the equation

$$\langle F_{\tilde{a}}^\dagger(t) F_{\tilde{a}}(t') \rangle_R = 2 \langle D_{\tilde{a}^\dagger \tilde{a}} \rangle_R \delta(t - t'). \quad (9.1.25)$$

Hence, from Eq. (9.1.24), the diffusion coefficient is given by

$$2 \langle D_{\tilde{a}^\dagger \tilde{a}} \rangle_R = C \bar{n}_{\text{th}}. \quad (9.1.26)$$

In a similar manner, we can show that

$$\langle F_{\tilde{a}}(t) F_{\tilde{a}}^\dagger(t') \rangle_R = C(\bar{n}_{\text{th}} + 1) \delta(t - t'), \quad (9.1.27)$$

$$\langle F_{\tilde{a}}(t) F_{\tilde{a}}(t') \rangle_R = \langle F_{\tilde{a}}^\dagger(t) F_{\tilde{a}}^\dagger(t') \rangle_R = 0, \quad (9.1.28)$$

so that

$$2 \langle D_{\tilde{a} \tilde{a}^\dagger} \rangle_R = C(\bar{n}_{\text{th}} + 1), \quad (9.1.29)$$

$$\langle D_{\tilde{a} \tilde{a}} \rangle_R = \langle D_{\tilde{a}^\dagger \tilde{a}^\dagger} \rangle_R = 0. \quad \text{热平衡假设} \quad (9.1.30)$$

(c) We now determine  $\langle F_{\tilde{a}}^\dagger(t) \tilde{a}(t) \rangle_R$ . This quantity will be needed below in the derivation of the equation of motion for  $\langle \tilde{a}^\dagger \tilde{a} \rangle_R$ . It follows, on solving Eq. (9.1.15), that

$$\tilde{a}(t) = \tilde{a}(0) \exp\left(-\frac{C}{2}t\right) + \int_0^t dt' \exp\left[-\frac{C}{2}(t-t')\right] F_{\tilde{a}}(t') \quad (9.1.31)$$

We then obtain

$$\begin{aligned} \langle F_{\tilde{a}}^\dagger(t) \tilde{a}(t) \rangle_R &= \langle F_{\tilde{a}}^\dagger(t) \rangle_R \tilde{a}(0) \exp\left(-\frac{C}{2}t\right) \\ &\quad + \int_0^t dt' \exp\left[-\frac{C}{2}(t-t')\right] \langle F_{\tilde{a}}^\dagger(t) F_{\tilde{a}}(t') \rangle_R. \end{aligned} \quad (9.1.32)$$

Here, we assumed that  $F_{\tilde{a}}(t)$  and  $\tilde{a}(0)$  are statistically independent. From Eqs. (9.1.22) and (9.1.24), it follows that

$$\langle F_{\tilde{a}}^\dagger(t) \tilde{a}(t) \rangle_R = \frac{C}{2} \bar{n}_{\text{th}} = \langle D_{\tilde{a}^\dagger \tilde{a}} \rangle_R. \quad (9.1.33)$$

Similarly, we can show that

$$\langle \tilde{a}^\dagger(t) F_{\tilde{a}}(t) \rangle_R = \frac{C}{2} \bar{n}_{\text{th}}. \quad (9.1.34)$$

These correlation functions will be employed to derive equations of motion for the field correlation functions in Section 9.3. We next consider the damping of a single-mode field via an atomic reservoir and also extend and strengthen the present oscillator reservoir treatment. The main result of these consideration is a correlation function for the noise operator which is not a delta function, thus corresponding to ‘colored’ noise as opposed to the white noise presented in this section.

将在第9.3节中讨论。

## 9.2 Extended treatment of damping via atom and oscillator reservoirs: non-Markovian colored noise

In this section we extend our approach to the problem of damping, this time involving finite (i.e., not delta function) correlation times. We first assume a field damping mechanism via two-level atoms in thermal distribution, passing through the cavity. The atoms are assumed to be long lived and monoenergetic so that they interact with the field inside the cavity for a fixed duration  $\tau$ . We then return to the oscillator reservoir model extending the treatment of the oscillator reservoir problem beyond the Markovian limit.

马尔科夫: 热源很大  $\delta(t-t')$   
 $\delta(t-t')$  指缓作用 关联时间 0

非马尔科夫: 热源有限 或不指缓作用

trapped atom 不在工作线上 关联时间  $\tau$

### 9.2.1 An atomic reservoir approach\*

We here consider the damping of a single-mode field by an ensemble of atoms. The Hamiltonian for the present problem is given by

$$\mathcal{H} = \mathcal{H}_0 + \mathcal{H}_1, \quad (9.2.1)$$

$$\mathcal{H}_0 = \hbar v a^\dagger a + \frac{1}{2} \hbar v \sum_i \sigma_z^i, \quad \begin{array}{l} \text{退源} \\ \text{不随时间变化} \end{array} \quad (9.2.2)$$

$$\mathcal{H}_1 = \hbar g \sum_i [f(t_i, t, \tau) a^\dagger \sigma_-^i + \text{H.c.}], \quad \begin{array}{l} \text{有效工作时间} \end{array} \quad (9.2.3)$$

where  $\sigma_z^i$  and  $\sigma_-^i$  are the operators for the  $i$ th atom and  $f(t_i, t, \tau)$  is a function which represents the injection of an atom at time  $t_i$  and its removal at a later time  $t_i + \tau$ . In this sense,  $f(t_i, t, \tau)$  is a notch function which has the value

$$f(t_i, t, \tau) = \begin{cases} 1 & \text{for } t_i \leq t < t_i + \tau, \\ 0 & \text{otherwise.} \end{cases} \quad \begin{array}{l} \text{第 } i \text{ 个原子} \end{array} \quad (9.2.4)$$

For the sake of simplicity, we have assumed that the injected atoms are resonant with the field. Using this Hamiltonian, we write the equations for the field and atom operators in the interaction picture

$$\dot{a}(t) = -ig \sum_i f(t_i, t, \tau) \sigma_-^i(t), \quad (9.2.5)$$

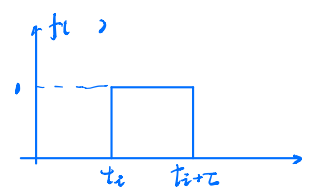
$$\dot{\sigma}_-^i(t) = ig f(t_i, t, \tau) \sigma_z^i a(t). \quad (9.2.6)$$

As before, we are interested in a closed equation for the operator  $a(t)$ . Integration of the atomic operator equation (9.2.6) yields

$$\sigma_-^i(t) = \sigma_-^i(t_i) + ig \int_{t_i}^t dt' f(t_i, t', \tau) \sigma_z^i(t') a(t'). \quad (9.2.7)$$

On substituting this expression for  $\sigma_-^i(t)$  into the field operator

\* The reader should consult Chapter 12 and Scully, Süssmann, and Benkert [1988] for further reading on the material of this section.



equation, we obtain

类似獨立

$$\dot{a} = g^2 \sum_i \int_{t_i}^t dt' f(t_i, t, \tau) f(t_i, t', \tau) \sigma_z^i(t') a(t') - ig \sum_i f(t_i, t, \tau) \sigma_-^i(t_i). \quad (9.2.8)$$

Transition time  $\sim ns$  很短

$a(t)$  在这段时间内相位在  $\omega$  中运动  
变化不大,  $a(t) \rightarrow a(t)$

If the field does not change appreciably during the transit time of the atoms,  $a(t')$  in Eq. (9.2.8) can be replaced by  $a(t)$ . In a linear analysis,  $\sigma_z^i(t')$  is also replaced by its value at the time of injection  $\sigma_z^i(t_i)$ . The resulting equation is

$$\dot{a} = -\frac{1}{2} \mathcal{C} a + F_a(t), \quad (9.2.9)$$

where

$$\mathcal{C} = -2g^2 \sum_i \int_{t_i}^t dt' f(t_i, t, \tau) f(t_i, t', \tau) \sigma_z^i(t_i), \quad (9.2.10)$$

$$F_a(t) = -ig \sum_i f(t_i, t, \tau) \sigma_-^i(t_i). \quad (9.2.11)$$

Here the decay constant  $\mathcal{C}$  is positive as the initial inversion  $\sigma_z^i(t_i)$  is negative in thermal equilibrium.

The noise operator  $F_a(t)$  may be seen to have the moments

$$\langle F_a(t) \rangle = 0, \quad (9.2.12)$$

接下来研究噪声功率  $F_a^\dagger(t) F_a(t')$

$$\begin{aligned} \langle F_a^\dagger(t) F_a(t') \rangle &= g^2 \sum_{i,j} f(t_i, t, \tau) f(t_j, t', \tau) \langle \sigma_+^i(t_i) \sigma_-^j(t_j) \rangle \\ &= g^2 [1 + \exp(\hbar v/k_B T)]^{-1} \sum_i f(t_i, t, \tau) f(t_i, t', \tau), \end{aligned} \quad (9.2.13)$$

where we have used, with the atoms in a thermal equilibrium state at temperature  $T$ , (by solving Eqs. (8.2.10a) and (8.2.10c) in the steady state and using Eq. (8.2.5))

$$\langle \sigma_+^i(t_i) \sigma_-^j(t_j) \rangle = \delta_{ij} [1 + \exp(\hbar v/k_B T)]^{-1}. \quad (9.2.14)$$

After replacing the sum over  $i$  in Eq. (9.2.13) by an integral over the injection time,

$$\sum_i \rightarrow r_a \int_{-\infty}^t dt_i, \quad \begin{array}{l} \text{假设腔中不停添加原子} \\ \text{在时刻加入的原子相关时间是 } (t_i, t_{i+1}) \text{ 之间} \\ \text{则对不同 } t_i \text{ 的原子的和就变成了对时间的积分} \end{array} \quad (9.2.15)$$

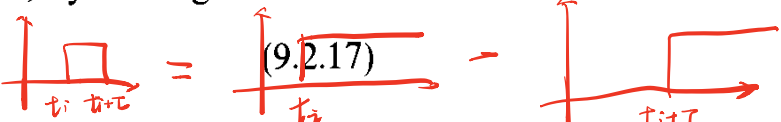
正负相位抵消

where  $r_a$  is the rate of injection of atoms into the cavity, we find

$$\langle F_a^\dagger(t)F_a(t') \rangle = r_a g^2 \left[ 1 + \exp\left(\frac{\hbar v}{k_B T}\right) \right]^{-1} \int_{-\infty}^t dt_i f(t_i, t, \tau) f(t_i, t', \tau). \quad (9.2.16)$$

The integration can be carried out, for example, by writing

$$f(t_i, t, \tau) = \Theta(t - t_i) - \Theta(t - \tau - t_i),$$



where  $\Theta$  is the unit step function and using

$$\int_{-\infty}^{\infty} dt_i \Theta(t_1 - t_i) \Theta(t_2 - t_i) = \Theta(t_1 - t_2) \int_{-\infty}^{t_2} dt_i + \Theta(t_2 - t_1) \int_{-\infty}^{t_1} dt_i. \quad (9.2.18)$$

$t_1 < t_2$   $t_1 < t_2$   $t_1 > t_2$   $t_2 > t_1$

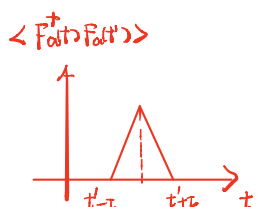
We then obtain

$$\begin{aligned} \int_{-\infty}^t dt_i f(t_i, t, \tau) f(t_i, t', \tau) &= [\Theta(t - t') - \Theta(t - t' - \tau)] \int_{-\infty}^{t'} dt_i \\ &\quad + [\Theta(t - t') - \Theta(t - t' + \tau)] \int_{-\infty}^{t' - \tau} dt_i \\ &\quad + [\Theta(t' - t) - \Theta(t' - t - \tau)] \int_{-\infty}^t dt_i \\ &\quad + [\Theta(t' - t) - \Theta(t' - t + \tau)] \int_{-\infty}^{t - \tau} dt_i. \end{aligned} \quad (9.2.19)$$

A careful examination shows that the right hand-side of Eq. (9.2.19) is zero unless  $\tau \geq |t - t'|$  in which case it is equal to  $\tau - |t - t'|$ . The correlation function (9.2.16) is therefore given by

$$\langle F_a^\dagger(t)F_a(t') \rangle = \begin{cases} \alpha_F(\tau - |t - t'|)/\tau^2 & \text{for } |t - t'| \leq \tau, \\ 0 & \text{otherwise,} \end{cases} \quad (9.2.20)$$

where  $\alpha_F = r_a g^2 \tau^2 [1 + \exp(\hbar v / k_B T)]^{-1}$ . The correlation function is triangularly shaped as depicted in Fig. 9.1. This is one of the simplest examples of a ‘colored’ noise problem.



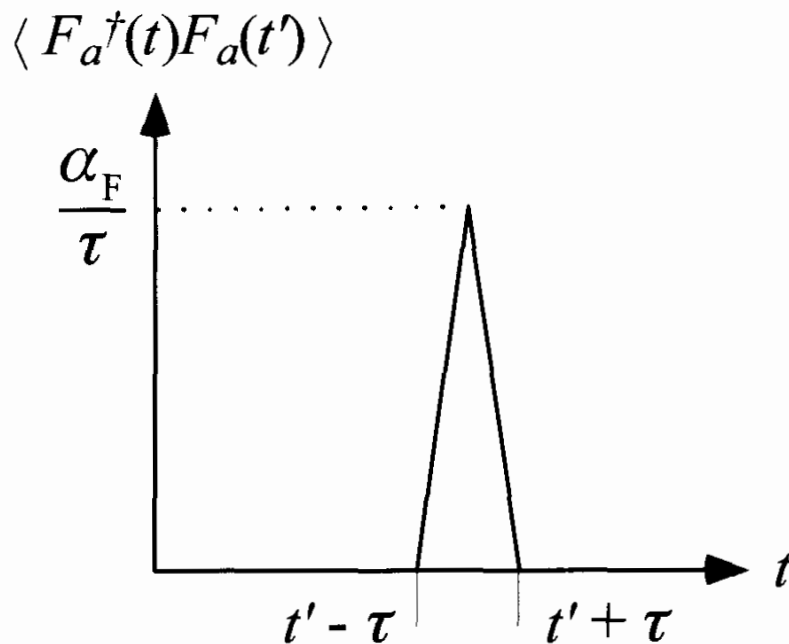
## 9.2.2 A generalized treatment of the oscillator reservoir problem\*

固体物理有用，PRA

We now present a treatment of the multi-oscillator heat bath problem. For an oscillator of momentum  $p$  and coordinate  $x$  coupled to a bath of

\* This section follows the paper by Ford, Lewis, and O’Connell [1988].

Fig. 9.1  
Noise correlation  
function  $\langle F_a^\dagger(t)F_a(t') \rangle$   
as given in  
Eq. (9.2.20).



oscillators having momentum  $p_j$  and position  $q_j$ , the system-reservoir Hamiltonian can be written as

$$\mathcal{H} = \frac{p^2}{2m} + \frac{1}{2}mv^2x^2 + \sum_j \frac{p_j^2}{2m_j} + \frac{1}{2}m_j\omega_j^2(q_j - x)^2. \quad (9.2.21)$$

Note that in this form the Hamiltonian (9.2.21) does not make the rotating-wave approximation. Including the normal commutation rules  $[x, p] = i\hbar$  and  $[q_j, p_k] = i\hbar\delta_{jk}$ , we find

$$\dot{x} = \frac{1}{i\hbar} [x, \mathcal{H}] = \frac{p}{m}, \quad (9.2.22a)$$

$$\dot{p} = \frac{1}{i\hbar} [p, \mathcal{H}] = -mv^2x + \sum_j m_j\omega_j^2(q_j - x), \quad (9.2.22b)$$

$$\dot{q}_j = \frac{1}{i\hbar} [q_j, \mathcal{H}] = \frac{p_j}{m_j}, \quad (9.2.22c)$$

$$\dot{p}_j = \frac{1}{i\hbar} [p_j, \mathcal{H}] = -m_j\omega_j^2(q_j - x). \quad (9.2.22d)$$

Differentiating Eqs. (9.2.22a) and (9.2.22c) and using Eqs. (9.2.22b) and (9.2.22d), we find

$$\ddot{x}(t) = -v^2x(t) + \sum_j \frac{m_j}{m}\omega_j^2[q_j(t) - x(t)], \quad (9.2.23a)$$

$$\ddot{q}_j(t) = -\omega_j^2[q_j(t) - x(t)]. \quad (9.2.23b)$$

As may be verified by direct substitution, the solution for  $q_j(t)$  may be written in the form

$$q_j(t) - x(t) = q_j^0(t) - \int_{-\infty}^t dt' \cos [\omega_j(t-t')] \dot{x}(t'), \quad (9.2.24)$$

where  $q_j^0(t)$  is the solution to the problem in the absence of coupling  $x = 0$

$$q_j^0(t) = q_j \cos \omega_j t + p_j \frac{\sin \omega_j t}{m_j \omega_j}, \quad (9.2.25)$$

in which  $q_j$  and  $p_j$  are the usual time-independent position and momentum operators.

Substituting (9.2.24) into (9.2.23a) we find

$$m\ddot{x}(t) + \int_{-\infty}^t dt' \mu(t-t') \dot{x}(t') + mv^2 x(t) = F(t), \quad (9.2.26)$$

where the damping function is given by

$$\mu(t-t') = \sum_j m_j \omega_j^2 \cos [\omega_j(t-t')], \quad (9.2.27a)$$

and the noise operator takes the form

$$F(t) = \sum_j m_j \omega_j^2 q_j^0(t). \quad (9.2.27b)$$

As it stands, Eq. (9.2.26) is closely related to Eq. (9.1.11). However, the problem can be extended to include memory effects by writing the following general expression for a damped oscillator

$$m\ddot{x}(t) + \int_{-\infty}^t dt' \mu(t-t') \dot{x}(t') + mv^2 x = F(t), \quad (9.2.28)$$

where

$$\begin{aligned} & \frac{1}{2} \langle F(t)F(t') + F(t')F(t) \rangle \\ &= \frac{1}{\pi} \int_0^\infty d\omega \operatorname{Re} [\tilde{\mu}(\omega + i0^+)] \hbar\omega \coth \left( \frac{\hbar\omega}{2k_B T} \right) \cos [\omega(t-t')], \end{aligned} \quad (9.2.29)$$

with  $\tilde{\mu}$  being the Fourier transform of  $\mu(t)$ .

Now for the case of constant damping, which is the one of most interest to us,  $\operatorname{Re} [\tilde{\mu}(\omega + i0^+)] = \Gamma$  and the correlation function takes the form

$$\begin{aligned} & \frac{1}{2} \langle F(t)F(t') + F(t')F(t) \rangle \\ &= \frac{\Gamma}{\pi} \int_0^\infty d\omega \hbar\omega \coth \left( \frac{\hbar\omega}{2k_B T} \right) \cos [\omega(t-t')] \\ &= \Gamma k_B T \frac{d}{dt} \coth \left[ \frac{\pi k_B T(t-t')}{\hbar} \right]. \end{aligned} \quad (9.2.30)$$

We note that Eq. (9.2.30), while going to  $\delta(t-t')$  in the limit, in general goes beyond the Markovian approximation, i.e., it implies colored noise.

### 9.3 Equations of motion for the field correlation functions

We can now derive the mean motion of  $\tilde{a}(t)$  and of the number operator  $\tilde{a}^\dagger \tilde{a}$ . Since  $\langle F_{\tilde{a}}(t) \rangle_R = 0$ , it follows from Eq. (9.1.15), that

*Setzt 9.1*

$$\frac{d}{dt} \langle \tilde{a}(t) \rangle_R = -\frac{1}{2} \mathcal{C} \langle \tilde{a}(t) \rangle_R. \quad (9.3.1)$$

Here, we see that the mean value of the system operator goes to zero in time. Note that Eq. (9.3.1) is only averaged over the reservoir coordinates. It remains an operator in the field coordinates.

The mean time development of the field number operator is

$$\begin{aligned} \frac{d}{dt} \langle \tilde{a}^\dagger(t) \tilde{a}(t) \rangle_R &= \left\langle \frac{d\tilde{a}^\dagger(t)}{dt} \tilde{a}(t) \right\rangle_R + \left\langle \tilde{a}^\dagger(t) \frac{d\tilde{a}(t)}{dt} \right\rangle_R \\ &= -\mathcal{C} \langle \tilde{a}^\dagger(t) \tilde{a}(t) \rangle_R + \langle F_{\tilde{a}}^\dagger(t) \tilde{a}(t) \rangle_R + \langle \tilde{a}^\dagger(t) F_{\tilde{a}}(t) \rangle_R \\ &= -\mathcal{C} \langle \tilde{a}^\dagger(t) \tilde{a}(t) \rangle_R + \mathcal{C} \bar{n}_{\text{th}}. \end{aligned} \quad (9.3.2)$$

$\frac{d}{dt}(\cdot) = 0 \Rightarrow \text{steady state}$

Thus, the steady-state value of the number operator  $\langle \tilde{a}^\dagger(t) \tilde{a}(t) \rangle_R$  is  $\bar{n}_{\text{th}}$  (times the field identity operator); this is nonzero in contrast to  $\langle \tilde{a}^\dagger(t) \rangle_R$  and  $\langle \tilde{a}(t) \rangle_R$ , which decay to zero in time according to Eq. (9.3.1).

In a similar manner, it can be shown that

$$\frac{d}{dt} \langle \tilde{a}(t) \tilde{a}^\dagger(t) \rangle_R = -\mathcal{C} \langle \tilde{a}(t) \tilde{a}^\dagger(t) \rangle_R + \mathcal{C} (\bar{n}_{\text{th}} + 1). \quad (9.3.3)$$

On combining Eqs. (9.3.2) and (9.3.3), we see that the commutator  $[\tilde{a}(t), \tilde{a}^\dagger(t)]$  retains its unity reservoir average in time instead of decaying to zero.

Using the same arguments as given for the derivation for the equations of motion for  $\langle \tilde{a}(t) \rangle_R$  and  $\langle \tilde{a}^\dagger(t) \tilde{a}(t) \rangle_R$ , Eqs. (9.3.1) and (9.3.2), we can show that for arbitrary products of the creation and annihilation operators,

$$\Rightarrow \frac{d}{dt} \langle (\tilde{a}^\dagger)^m \tilde{a}^n \rangle_R = -\frac{\mathcal{C}}{2} (m+n) \langle (\tilde{a}^\dagger)^m \tilde{a}^n \rangle_R + \mathcal{C} m n \bar{n}_{\text{th}} \langle (\tilde{a}^\dagger)^{m-1} \tilde{a}^{n-1} \rangle_R. \quad (9.3.4)$$

*逐项求和*

In terms of the operators  $a$  and  $a^\dagger$  (Eq. (9.1.9)) this equation reads

$$\begin{aligned} \frac{d}{dt} \langle (a^\dagger)^m (a)^n \rangle_R &= \left[ iv(m-n) - \frac{\mathcal{C}}{2} (m+n) \right] \langle (a^\dagger)^m a^n \rangle_R \\ &\quad + \mathcal{C} m n \bar{n}_{\text{th}} \langle (a^\dagger)^{m-1} a^{n-1} \rangle_R. \end{aligned} \quad (9.3.5)$$

This equation, in a general way, describes the effect of the reservoir.

*不取平均也能算*

$$\begin{aligned} \text{估上近似值, 由 Sec 9.1 得} \\ \frac{d}{dt} [\tilde{a}(t), \tilde{a}^\dagger(t)] &= -\mathcal{C} [(\tilde{a}^\dagger t - \tilde{a} t^\dagger) +] \\ \text{且 } \tilde{a}(t) = [\tilde{a}(t), \tilde{a}^\dagger(t)] \\ \text{有 } \frac{d\tilde{a}}{dt} = -\mathcal{C} (X^{-1}) \\ \rightarrow X^{-1} - 1 &= (X-1)^{-1} \\ \rightarrow X^{-1} = 1 & \text{相当高, 因为 } X \end{aligned}$$

*若算一下力学量*

*直接*  $(\tilde{a}^\dagger m \tilde{a}^n) = \tilde{a}^m \tilde{a}^n$

$$\frac{d \langle \tilde{a}^\dagger m \tilde{a}^n \rangle}{dt} = \dots = \text{已算过}$$

As mentioned earlier, the present Heisenberg–Langevin approach to the quantum theory of damping is particularly suited for the calculation of multi-time correlation functions. This can be appreciated by considering the simple example of the damping of the field of frequency  $\nu$  inside the cavity at the rate  $\mathcal{C} = \nu/Q$ . Here  $Q$  is the quality factor of the cavity.

The field operator  $\tilde{a}(t) = a(t) \exp(i\omega t)$  obeys the equation

$$\dot{\tilde{a}} = -\frac{\nu}{2Q}\tilde{a} + F_{\tilde{a}}(t), \quad (9.3.6)$$

which can be solved to yield (with  $\tau > 0$ )

$$\begin{aligned} \tilde{a}(t_i + \tau) &= \tilde{a}(t_i) \exp\left(-\frac{\nu}{2Q}\tau\right) \\ &\quad + \int_{t_i}^{t_i + \tau} dt' \exp\left[-\frac{\nu}{2Q}(t_i + \tau - t')\right] F_{\tilde{a}}(t'). \end{aligned} \quad (9.3.7)$$

It follows, on using  $\langle \tilde{a}^\dagger(t_i) F_{\tilde{a}}(t') \rangle_R = \langle \tilde{a}^\dagger(t_i) \rangle_R \langle F_{\tilde{a}}(t') \rangle_R = 0$ , that

$$\langle \tilde{a}^\dagger(t_i) \tilde{a}(t_i + \tau) \rangle_R = \langle \tilde{a}^\dagger(t_i) \tilde{a}(t_i) \rangle_R \exp\left(-\frac{\nu}{2Q}\tau\right), \quad (9.3.8)$$

See q. 1 in add

i.e., the field correlation function decays exponentially with time. The field spectrum can be obtained by taking the Fourier transform of the correlation function

$$\begin{aligned} \langle a^\dagger(t_i) a(t_i + \tau) \rangle_R &= \langle \tilde{a}^\dagger(t_i) \tilde{a}(t_i + \tau) \rangle_R e^{-i\nu\tau} \\ &= \langle n \rangle \exp\left(-i\nu\tau - \frac{\nu}{2Q}\tau\right), \end{aligned} \quad (9.3.9)$$

(9.3.10)

where  $\langle n \rangle$  is the mean number of photons at the initial time  $t_i$ . We then obtain (see Eq. (4.3.14))

$$\begin{aligned} S(\omega) &= \frac{1}{\pi} \operatorname{Re} \int_0^\infty \langle a^\dagger(t) a(t + \tau) \rangle_R e^{i\omega\tau} d\tau \quad \text{功率谱密度 } S = \text{FT}(\text{相关函数}) \\ &= \frac{\langle n \rangle}{\pi} \frac{\nu/2Q}{(\omega - \nu)^2 + (\nu/2Q)^2}. \end{aligned} \quad (9.3.11)$$

This is a Lorentzian distribution centered at  $\omega = \nu$  with half-width  $\nu/2Q$ .

An approximate expression of the mode density of the empty cavity,  $D_c(\omega)$ , is obtained by dividing  $S(\omega)$  by  $\langle n \rangle$ , i.e.,  $D_c(\omega) = \frac{S(\omega)}{\langle n \rangle}$  膜密度

$$D_c(\omega) = \frac{1}{\pi} \frac{\nu/2Q}{(\omega - \nu)^2 + (\nu/2Q)^2}. \quad (9.3.12)$$

The density of states inside the cavity is therefore significantly different from its value in free space (see Eq. (1.1.26)).

由  $\omega = \frac{v}{2Q}$  得  $D_c(\omega) = \frac{V_0 v^2}{\pi^2 c^3} d\omega$   
与  $V_0$  有关，但  $D_c(\omega)$  无关

## 9.4 Fluctuation-dissipation theorem and the Einstein relation

We now make a connection between the present quantum Langevin approach and the classical approach. In Section 9.1 we derived the second-order correlation function of the Langevin noise  $F_{\tilde{a}}(t)$

$$\langle F_{\tilde{a}}^\dagger(t) F_{\tilde{a}}(t') \rangle_R = \mathcal{C} \bar{n}_{\text{th}} \delta(t - t'). \quad (9.4.1)$$

On integrating both sides, we obtain

$$\mathcal{C} = \frac{1}{\bar{n}_{\text{th}}} \int_{-\infty}^{\infty} \langle F_{\tilde{a}}^\dagger(t) F_{\tilde{a}}(t') \rangle_R dt'. \quad (9.4.2)$$

This states that the system damping  $\mathcal{C}$  is determined from the fluctuating forces of the reservoir. Thus the fluctuations induced by the reservoir give rise to dissipation in the system. This is one formulation of the fluctuation-dissipation theorem.

Next we make use of Eqs. (9.1.15) and (9.1.26) to rewrite Eq. (9.3.2) as follows

$$\begin{aligned} 2\langle D_{\tilde{a}\dagger\tilde{a}} \rangle_R &= \frac{d}{dt} \langle \tilde{a}^\dagger(t) \tilde{a}(t) \rangle_R - \left\langle \left[ \frac{d\tilde{a}^\dagger}{dt} - F_{\tilde{a}}^\dagger(t) \right] \tilde{a}(t) \right\rangle_R \\ &\quad - \left\langle \tilde{a}^\dagger(t) \left[ \frac{d\tilde{a}}{dt} - F_{\tilde{a}}(t) \right] \right\rangle_R. \end{aligned} \quad (9.4.3)$$

This is the Einstein relation to determine the diffusion constant. We have derived this relation for the damped harmonic oscillator problem. It can, however, be shown that this relation is valid for many general system-reservoir problems. It can be similarly shown that

$$\begin{aligned} 2\langle D_{\tilde{a}\tilde{a}\dagger} \rangle_R &= \frac{d}{dt} \langle \tilde{a}(t) \tilde{a}^\dagger(t) \rangle_R - \left\langle \tilde{a}(t) \left[ \frac{d\tilde{a}^\dagger}{dt} - F_{\tilde{a}}^\dagger(t) \right] \right\rangle_R \\ &\quad - \left\langle \left[ \frac{d\tilde{a}}{dt} - F_{\tilde{a}}(t) \right] \tilde{a}^\dagger(t) \right\rangle_R. \end{aligned} \quad (9.4.4)$$

The Einstein relation relates the *drift* terms  $[d\tilde{a}/dt - F_{\tilde{a}}(t)]$  and  $[d\tilde{a}^\dagger/dt - F_{\tilde{a}}^\dagger(t)]$  to the diffusion coefficients. In many problems of interest, this relation provides an extremely simple way to calculate the diffusion constant.

The Einstein relation can be employed to determine the diffusion coefficients from the density matrix equations in a straightforward manner. In order to indicate the procedure, we consider the simple

example of Eq. (8.3.2) which governs the damping of the field by an interaction with a thermal reservoir. It follows from this equation that

$$\left\langle \frac{da}{dt} \right\rangle = \text{Tr}(a\dot{\rho}) = -\frac{\mathcal{C}}{2} \langle a \rangle, \quad (9.4.5)$$

$$\left\langle \frac{da^\dagger}{dt} \right\rangle = -\frac{\mathcal{C}}{2} \langle a^\dagger \rangle, \quad (9.4.6)$$

$$\frac{d}{dt} \langle a^\dagger a \rangle = -\mathcal{C}(\langle a^\dagger a \rangle - \bar{n}_{\text{th}}), \quad (9.4.7)$$

where, in deriving these equations, we used the cyclic property of the trace (i.e.,  $\text{Tr}(ABC) = \text{Tr}(CAB)$ , etc) and the commutation relation  $[a, a^\dagger] = 1$ . Now the quantities  $[da/dt - F_a(t)]$  and  $[da^\dagger/dt - F_a^\dagger(t)]$  can be obtained from Eqs. (9.4.5) and (9.4.6), respectively, by removing the expectation value sign on the right-hand side. We then obtain

$$\left[ \frac{da}{dt} - F_a(t) \right] = -\frac{\mathcal{C}}{2} a, \quad (9.4.8)$$

$$\left[ \frac{da^\dagger}{dt} - F_a^\dagger(t) \right] = -\frac{\mathcal{C}}{2} a^\dagger. \quad (9.4.9)$$

On substituting Eqs. (9.4.7)–(9.4.9) into Eq. (9.4.3), we get

$$2\langle D_{a^\dagger a} \rangle = \mathcal{C}\bar{n}_{\text{th}}, \quad (9.4.10)$$

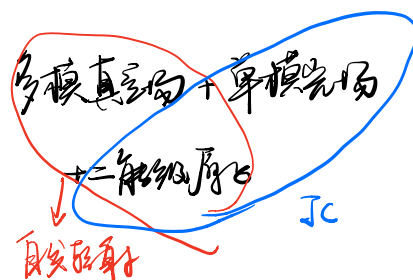
in agreement with Eq. (9.1.26).

## 9.5 Atom in a damped cavity

*共振腔中的单原子* *Purcell 效应*

A very simple application of the mathematical framework developed in this chapter is the study of the evolution of a single two-level atom initially prepared in the upper level  $|a\rangle$  of the transition resonant with the cavity mode. In particular, it is seen that the spontaneous emission rate of the atom inside a resonant cavity is substantially enhanced over its free-space value. The enhancement factor can be derived rigorously from a quantum mechanical analysis where the cavity damping is considered via interaction of the single-mode field with a reservoir consisting of a large number of simple harmonic oscillators. First, we present an heuristic argument to understand this interesting phenomenon.

We recall that, in Section 6.3, we considered the spontaneous emission of an atom in free space, so that the atom interacts with a continuum of modes of the electromagnetic field. The decay rate  $\Gamma$ , as given by Eq. (6.3.14) can be rewritten as



$$\Gamma = 2\pi \langle |g(\omega)|^2 \rangle D(\omega), \quad (9.5.1)$$

where angle brackets represent an angular average,  $g(\omega)$  is the vacuum Rabi frequency, and  $D(\omega) = V\omega^2/\pi^2c^3$  is the density of states at the atomic transition frequency  $\omega$ . The spontaneous decay rate is therefore proportional to the density of states. The mode structure of the vacuum field is dramatically altered in a cavity whose size is comparable to the wavelength. In a cavity of quality factor  $Q$ , the mode density  $D_c(\omega)$  can be approximated by the Lorentzian (Eq. (9.3.12))

$$D_c(\omega) = \frac{1}{\pi} \frac{\nu/2Q}{(\omega - \nu)^2 + (\nu/2Q)^2}. \quad (9.5.2)$$

The spontaneous decay rate of the atom inside the cavity is therefore obtained by replacing  $D(\omega)$  by  $D_c(\omega)$  in Eq. (9.5.1)

$$\Gamma_c = 2\pi \langle |g(\omega)|^2 \rangle D_c(\omega). \quad (9.5.3)$$

For a cavity tuned near the atomic resonance frequency, we have  $D_c(\omega) \simeq 2Q/\pi\omega$  and

$$\Gamma_c = \frac{2\pi}{3} \left( \frac{\omega \wp_{ab}^2}{2\hbar\epsilon_0 V} \right) \left( \frac{2Q}{\pi\omega} \right) = \Gamma Q \left( \frac{2\pi c^3}{V\omega^3} \right). \quad (9.5.4)$$

Thus, apart from the geometrical factor of order unity (for the lowest cavity mode  $\omega = \pi c/L$ , where  $L$  is the length of the side of the cavity, this factor is equal to  $2/\pi^2$ ), the spontaneous decay rate inside the cavity is enhanced by a factor  $Q$  over its free-space value.

Another simple interpretation of the spontaneous emission enhancement can be given in terms of the image charges. We can simulate the effect of the cavity mirrors on the evolution of the atom by replacing them by the  $Q$  images of the atoms in these mirrors. As the cavity is resonant with the atomic transition, all the dipoles of these images are in phase with the atomic dipole. They therefore act as  $Q$  aligned antenna in phase. A given antenna in this array radiates  $Q$  times faster than an isolated antenna. The atomic energy is therefore dissipated  $Q$  times faster than in free space.

We now turn to a rigorous derivation of the atomic decay in a damped cavity. We consider a system of a two-level atom interacting with a single-mode electromagnetic field inside a cavity. The cavity is

coupled to a thermal reservoir through the walls of the cavity. The atom–field reservoir Hamiltonian is therefore

$$\mathcal{H} = \mathcal{H}_F + \mathcal{H}_A + \mathcal{H}_{AF} + \mathcal{H}_R + \mathcal{H}_{FR}, \quad (9.5.5)$$

$$\mathcal{H}_F = \hbar v a^\dagger a, \quad (9.5.6)$$

$$\mathcal{H}_A = \frac{1}{2} \hbar v \sigma_z, \quad (9.5.7)$$

$$\mathcal{H}_{AF} = \hbar g (\sigma_+ a + a^\dagger \sigma_-), \quad (9.5.8)$$

$$\mathcal{H}_R = \sum_{\mathbf{k}} \hbar v_k b_{\mathbf{k}}^\dagger b_{\mathbf{k}}, \quad (9.5.9)$$

$$\mathcal{H}_{FR} = \hbar \sum_{\mathbf{k}} g_{\mathbf{k}} (b_{\mathbf{k}}^\dagger a + a^\dagger b_{\mathbf{k}}). \quad (9.5.10)$$

Here  $\mathcal{H}_F$  and  $\mathcal{H}_A$  are the free field and atom Hamiltonians, respectively,  $\mathcal{H}_{AF}$  represents the interaction of the single-mode cavity field with the atom,  $\mathcal{H}_R$  is the energy of the reservoir modes and  $\mathcal{H}_{FR}$  represents the interaction of the field with the reservoir. For transmission losses, the reservoir modes correspond to the vacuum modes that enter the cavity through partially transmitting mirrors. We shall assume the reservoir modes to be in thermal equilibrium at temperature  $T$ .

The quantities of interest in the system are the energy of the field  $\langle a^\dagger a \rangle$  and the atomic inversion  $\langle \sigma_z \rangle$ . The equation of motion for any operator of the form  $(a^\dagger)^m a^n O_A$ , (where  $O_A$  is an atomic operator, e.g.,  $\sigma_+, \sigma_-, \sigma_z$ ) is given by

$$\begin{aligned} \frac{d}{dt} [(a^\dagger)^m a^n O_A] &= -\frac{i}{\hbar} [(a^\dagger)^m a^n O_A, \mathcal{H}_F + \mathcal{H}_A + \mathcal{H}_{AF}] \\ &\quad + \left\langle \frac{d}{dt} [(a^\dagger)^m a^n] \right\rangle_R O_A, \end{aligned} \quad (9.5.11)$$

where  $\langle d[(a^\dagger)^m a^n]/dt \rangle_R$  is given by Eq. (9.3.5). Using this equation, we can derive the following equations of motion for  $\langle a^\dagger a \rangle$  and  $\langle \sigma_z \rangle$ :

$$\frac{d\langle a^\dagger a \rangle}{dt} = ig \langle \sigma_+ a - a^\dagger \sigma_- \rangle - \mathcal{C} \langle a^\dagger a \rangle + \mathcal{C} \bar{n}_{th}, \quad (9.5.12)$$

腔和外部  
热力学平衡  
R (9.5.12)

$$\frac{d\langle \sigma_z \rangle}{dt} = -2ig \langle \sigma_+ a - a^\dagger \sigma_- \rangle. \quad (9.5.13)$$

系统, 可以忽略  
R (9.5.13)

The angle brackets denote the reservoir as well as the quantum mechanical average. These equations involve the average of the Hermitian operator  $\langle \sigma_+ a - \sigma_- a^\dagger \rangle$  whose equation of motion in turn involves the quantity  $\langle a^\dagger \sigma_z a \rangle$  and so on. In general, we get an infinite set of equations which may not be analytically solvable. However, the situation is considerably simpler if initially the atom is in the excited state  $|a\rangle$ , the field inside the cavity is in the vacuum state  $|0\rangle$ , and the cavity is

at zero temperature ( $\bar{n}_{\text{th}} = 0$ ). There can be at most one photon in the field and the state of the field inside the cavity at any time  $t$  will be a linear superposition of the vacuum state  $|0\rangle$  and the one-photon state  $|1\rangle$ . The expectation value of the operators involving quadratic or higher powers in the field operators  $a$  and  $a^\dagger$ , e.g.,  $\langle(a^\dagger)^2 \sigma_z a^2\rangle$ , are therefore zero at all times. Under these conditions, we obtain the following closed set of equations

$$\frac{d\langle a^\dagger a \rangle}{dt} = gA_1 - \mathcal{C}\langle a^\dagger a \rangle, \quad (9.5.14)$$

$$\frac{d\langle \sigma_z \rangle}{dt} = -2gA_1, \quad (9.5.15)$$

$$\frac{dA_1}{dt} = g\langle \sigma_z \rangle + 2gA_2 + g - \frac{\mathcal{C}}{2}A_1, \quad (9.5.16)$$

$$\frac{dA_2}{dt} = -gA_1 - \mathcal{C}A_2, \quad (9.5.17)$$

where

$$A_1 = i\langle \sigma_+ a - a^\dagger \sigma_- \rangle, \quad (9.5.18)$$

$$A_2 = \langle a^\dagger \sigma_z a \rangle. \quad (9.5.19)$$

### Laplace 变换解方程

It may be noted that, in Eq. (9.5.17), we neglected the term proportional to  $\langle \sigma_+ a^\dagger a^2 - (a^\dagger)^2 \sigma_- \rangle$  in light of the above argument. The four equations (9.5.14)–(9.5.17) can be solved using, for example, the Laplace transform method. The resulting solutions for  $\langle a^\dagger a \rangle_t$  and  $\langle \sigma_z \rangle_t$ , subject to the initial conditions  $\langle a^\dagger a \rangle_0 = A_1(0) = A_2(0) = 0$  and  $\langle \sigma_z \rangle_0 = 1$  are

$$\langle a^\dagger a \rangle_t = -\frac{8g^2 e^{-\mathcal{C}t/2}}{\mathcal{C}^2 - 16g^2} \left\{ 1 - \cosh [(\mathcal{C}^2 - 16g^2)^{1/2} t/2] \right\}, \quad (9.5.20)$$

$$\begin{aligned} \langle \sigma_z \rangle_t = & -1 + \frac{4e^{-\mathcal{C}t/2}}{(\mathcal{C}^2 - 16g^2)} \left\{ -4g^2 \right. \\ & + \left[ \frac{\mathcal{C}^2}{4} - 2g^2 + \frac{\mathcal{C}}{4}(\mathcal{C}^2 - 16g^2)^{1/2} \right] \times e^{(\mathcal{C}^2 - 16g^2)^{1/2} t/2} \\ & \left. + \left[ \frac{\mathcal{C}^2}{4} - 2g^2 - \frac{\mathcal{C}}{4}(\mathcal{C}^2 - 16g^2)^{1/2} \right] \times e^{-(\mathcal{C}^2 - 16g^2)^{1/2} t/2} \right\}. \end{aligned} \quad (9.5.21)$$

(正常)

正常时，腔与环境耦合大于耗散  
反常时，环境耦合大于耗散

腔耗散速率

原子频率

In Fig. 9.2, the probability of the atom being in the upper level  $P_a = (1 + \langle \sigma_z \rangle)/2$  is plotted for different values of  $\mathcal{C}/4g$ . Here we see a transition from damped Rabi oscillations to an overdamped situation.

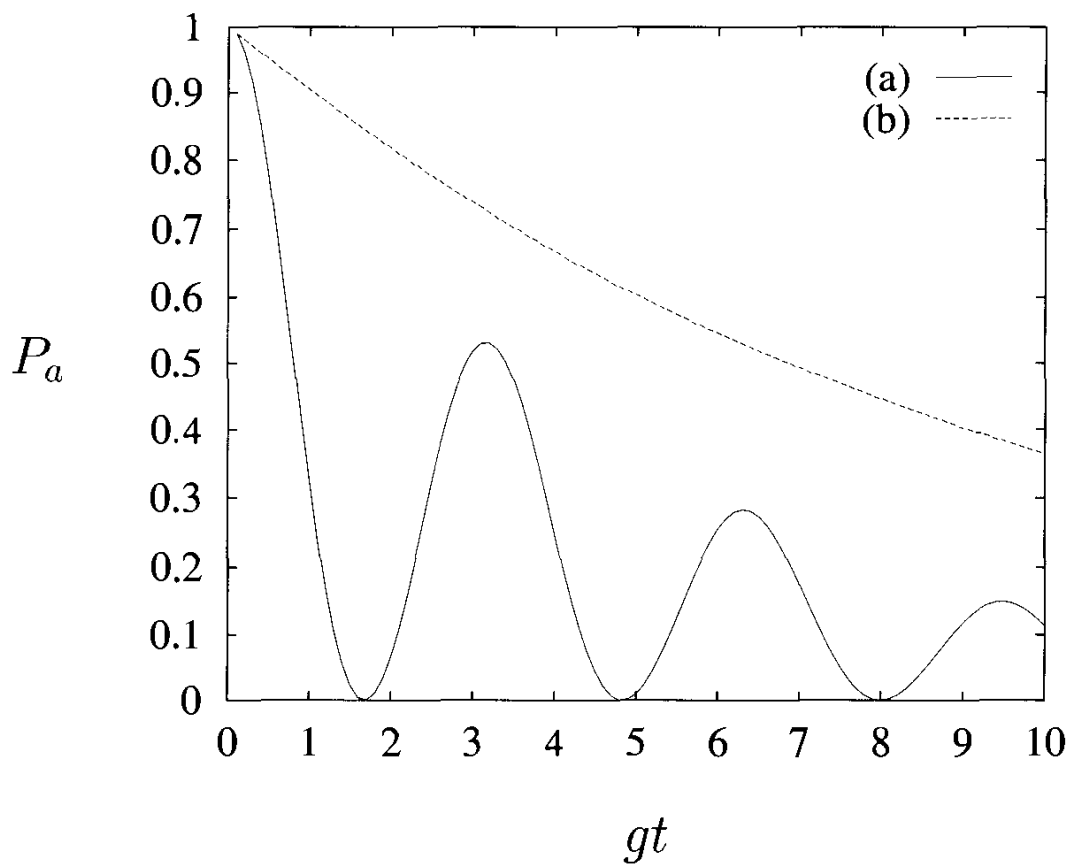


Fig. 9.2  
A plot of  $P_a$  versus dimensionless time  $gt$  for (a)  $\mathcal{C}/4g = 0.1$  and (b)  $\mathcal{C}/4g = 10$ .

This different behavior can be seen easily by considering two limiting cases of Eq. (9.5.21). When  $\mathcal{C} \ll 4g$ , the atomic inversion  $\langle \sigma_z(t) \rangle$  and the probability  $P_a$  take the simple forms

$$\langle \sigma_z(t) \rangle = -1 + e^{-\mathcal{C}t/2} [1 + \cos(2gt)], \quad (9.5.22)$$

$$P_a(t) = \frac{e^{-\mathcal{C}t/2}}{2} [1 + \cos(2gt)]. \quad (9.5.23)$$

These damped Rabi oscillations are at the frequency  $2g$ . In the opposite limit  $\mathcal{C} \gg 4g$ , we obtain

$$\langle \sigma_z(t) \rangle = -1 + 2e^{-(4g^2 t/\mathcal{C})}, \quad (9.5.24)$$

and

$$P_a(t) = e^{-(4g^2 t/\mathcal{C})}, \quad (9.5.25)$$

i.e., the atom decays exponentially with a damping constant

$$\Gamma_c = \frac{4g^2}{\mathcal{C}} = \left( \frac{1}{4\pi\epsilon_0} \frac{4\pi^3 \delta_{ab}^2}{3\hbar c^3} \right) \left( \frac{v}{\mathcal{C}} \right) \left( \frac{6\pi c^3}{V v^3} \right) = 3\Gamma Q \left( \frac{2\pi c^3}{V v^3} \right) \quad (9.5.26)$$

Apart from a trivial factor of 3, this expression is identical to Eq. (9.5.4), which was obtained using a heuristic argument based on the density of states. The factor of 3 disappears if, in Eq. (9.5.26), we replace  $g^2$  by its average value over different orientations.

和取向有关  
Q很大 Rabi振荡  
Q一般 增强吸收辐射  
Q很小 吸收辐射

## Problems

- 9.1** A single mode of frequency  $\nu$  interacts with a thermal reservoir. The evolution of the field-reservoir system is described by the Langevin equation

$$\dot{\tilde{a}} = -\frac{1}{2}\mathcal{C}\tilde{a} + F_{\tilde{a}}(t),$$

where  $\tilde{a}(t) = a(t)e^{i\nu t}$ ;  $a$  is the destruction operator for the field mode. Calculate the variance  $(\Delta X_1)^2$  (with  $X_1 = (\tilde{a} + \tilde{a}^\dagger)/2$ ) at a time  $t$  in terms of the variance at the initial time  $t = 0$ .

- 9.2** Find the correlation function  $\langle F_a^\dagger(t)F_a(t') \rangle$  in Eq. (9.2.13) for

$$f(t_i, t, \tau) = \begin{cases} e^{-\Gamma(t-t_i)} & \text{for } t_i \leq t < t_i + \tau, \\ 0 & \text{otherwise.} \end{cases}$$

- 9.3** Calculate the second-order correlation functions

$$\begin{aligned} &\langle F_{\tilde{a}}^\dagger(t)F_{\tilde{a}}(t') \rangle_R, \quad \langle F_{\tilde{a}}(t)F_{\tilde{a}}^\dagger(t') \rangle_R, \\ &\langle F_{\tilde{a}}(t)F_{\tilde{a}}(t') \rangle_R, \text{ and } \langle F_{\tilde{a}}^\dagger(t)F_{\tilde{a}}^\dagger(t') \rangle_R \end{aligned}$$

of the Langevin operator for a multi-mode squeezed vacuum reservoir.

- 9.4** Derive the equation of motion for arbitrary products of creation and destruction operators  $\langle (a^\dagger)^m a^n \rangle$  for (a) a thermal reservoir and (b) a squeezed reservoir.

- 9.5** Consider the reservoir in a squeezed vacuum state. Use the equation of motion for the density matrix for the field mode and the Einstein relation to calculate the diffusion coefficient  $D_{\tilde{a}\tilde{a}^\dagger}$ . Verify your results from Langevin theory.

---

# Atom optics

---

Matter-wave interferometry dates from the inception of quantum mechanics, i.e., the early electron diffraction experiments. More recent neutron interferometry experiments have yielded new insights into many fundamental aspects of quantum mechanics. Presently, atom interferometry has been demonstrated and holds promise as a new field of optics – matter-wave optics. This field is particularly interesting since the potential sensitivity of matter-wave interferometers far exceeds that of their light-wave or ‘photon’ antecedents.

In this chapter we consider the physics of light-induced forces on the center-of-mass motion of atoms and their application to atom optics (Fig. 17.1). The most obvious being the recoil associated with the emission and absorption of light. This ‘radiation pressure’ is the basis for laser induced cooling.\*

Another very important mechanical effect is the gradient force due to, e.g., transverse variation in the laser beam. These, essentially semiclassical, forces are useful in guiding and trapping neutral atoms.

After considering the basic forces which allow us to cool, guide, and trap atoms, we turn to the optics of atomic center-of-mass de Broglie waves, i.e., atom optics. In keeping with the spirit of the present text, we will focus on the quantum limits to matter-wave interferometry. An analysis of a matter-wave gyro in an obvious extension of the laser gyro and the similarity and relative merits of the two will be compared and contrasted.

Finally we derive the “recoil limit” to laser cooling; and show that it is possible to supersede this limit via atomic coherence effects.

\* For further reading, see the proceedings of the CXIII Enrico Fermi School, edited by Arimondo, Phillips, and Strumia (1992).

## 17.1 Mechanical effects of light

As a consequence of the conservation of energy and momentum, atoms can experience light-induced forces during their interaction with a radiation field. In this section, we discuss the application of these forces in causing the deflection, cooling, and diffraction of the atomic beams. We also discuss the gradient force due to transverse variation of the laser field.

### 17.1.1 Atomic deflection

When an atom absorbs or emits a photon of frequency  $\nu$  from a light beam, a transfer of recoil momentum  $\Delta p = \hbar k = \hbar\nu/c$  takes place between the atom and the field. If absorption is followed by stimulated emission, no net momentum is transferred to the atom as the momentum transferred in the process of absorption is canceled by an equal but opposite transfer of momentum in the process of stimulated emission. If, however, absorption is followed by spontaneous emission, there is a net momentum transfer to the atom as the spontaneous emission in arbitrary directions gives no average contribution to the momentum. If this process (absorption followed by spontaneous emission) takes place a large number of times, a substantial transfer of momentum can occur, from the light beam to the atom, leading to atomic deflection. In the following, we derive an expression for the deflection or recoil force on the atoms.

受激吸收+自发辐射  
有结果  
受激吸收+受激辐射  
结果是0。  
但受激辐射和Rabi频率有关，由空间几乎为0.可忽略。

As discussed above, an atom experiences a momentum recoil of  $\Delta p = \hbar k$  upon each radiative event. Hence the absorptive force of the atom  $F_a$  is given by

$$F_a = r\hbar k, \quad (17.1.1)$$

where  $r$  is the rate of radiation decay or the net fluorescence rate. For a two-level atom at rest, with a transition frequency  $\omega$ , the rate  $r$  is proportional to the upper level occupancy  $\rho_{aa}$  of the atom, i.e.,

$$r = \Gamma\rho_{aa}, \quad (17.1.2)$$

where  $\Gamma$  is the spontaneous emission rate from the excited state  $|a\rangle$  to the ground state  $|b\rangle$ .

The interaction of a two-level atom with a radiation field of frequency  $\nu$  is described by the following set of equations for the density matrix elements:

$$\dot{\rho}_{ab} = - \left( i\Delta + \frac{\Gamma}{2} \right) \rho_{ab} + i\Omega_R \rho_{aa} - \frac{i}{2} \Omega_R, \quad (17.1.3)$$

$$\dot{\rho}_{aa} = -\Gamma \rho_{aa} + \frac{i\Omega_R}{2} (\rho_{ab} - \rho_{ba}). \quad (17.1.4)$$

$$\dot{\rho}_{ba} = \left( i\Delta - \frac{\Gamma}{2} \right) \rho_{ba} - i\Omega_R \rho_{aa} + \frac{i}{2} \Omega_R. \quad (17.1.5)$$

These equations are obtained by generalizing Eqs. (10.C.1)–(10.C.4) to include the detuning  $\Delta = \omega - v$ . Here  $\Omega_R$  is the Rabi frequency associated with the light beam. A steady-state solution of Eqs. (17.1.3)–(17.1.5) yields

$$\rho_{aa} = \frac{\Omega_R^2}{4\Delta^2 + \Gamma^2 + 2\Omega_R^2}. \quad (17.1.6)$$

The absorptive force is thus given by

$$F_r = \hbar k \Gamma \frac{\Omega_R^2}{4\Delta^2 + \Gamma^2 + 2\Omega_R^2}, \quad (17.1.7)$$

and is in the same direction as the light beam.

### 17.1.2 Laser cooling\*

So far we have considered the force of a light beam on an atom at rest. If the atom is moving with a velocity  $v$  along the light beam, it sees a Doppler shifted frequency,  $v \pm kv$ , of the light beam. Here the  $+$  (or  $-$ ) sign corresponds to a situation when the atom is moving in the opposite (or same) direction to the light beam. The expression for the absorptive force  $F_a$  then becomes

$$F_a = \hbar k \Gamma \frac{\Omega_R^2}{4(\Delta \mp kv)^2 + \Gamma^2 + 2\Omega_R^2}. \quad (17.1.8)$$

In the limit of no saturation ( $\Omega_R = 0$  in the denominator) and a small velocity, we can expand the denominator. The resulting expression for  $F_a$  is

$$F_a = F_o \pm \beta m v, \quad (17.1.9)$$

\* The laser cooling concept was first proposed by Hänsch and Schawlow [1975] for free atoms and by Wineland and Dehmelt [1975] for trapped ions.

where

$$F_o = \hbar k \Gamma \frac{\Omega_R^2}{4\Delta^2 + \Gamma^2}, \quad (17.1.10)$$

$$\beta = 8\hbar k^2 \Gamma \frac{\Omega_R^2 \Delta}{m(4\Delta^2 + \Gamma^2)^2}. \quad (17.1.11)$$

The first term in Eq. (17.1.9) is a constant deflecting force, whereas the second term, proportional to atomic velocity, acts like a friction term.

If the atom is located in a standing wave, it sees two oppositely moving light waves, one in the same direction as the velocity of the atom and other in the opposite direction. We assume that the forces due to the two beams can be superimposed. Hence the total force on the atom in a standing wave is

$$\begin{aligned} F_{\text{standing wave}} &= (F_o - \beta mv) - (F_o + \beta mv) \\ &= -2\beta mv, \end{aligned} \quad (17.1.12)$$

i.e., the deflection forces  $F_o$  cancel and the friction forces from the two beams remain. The friction force is responsible for the slowing down of the atom leading to *laser cooling*.

Physically, we can understand the process of laser cooling as follows. If  $\Delta > 0$ , i.e.,  $\omega > v$ , the field moving in the opposite direction to the atom will be Doppler up-shifted, thus compensating the detuning. The atom will therefore be decelerated. By this mechanism the atoms can be slowed down to the pace of extremely sluggish atomic molasses.

### 17.1.3 Atomic diffraction

When a beam of atoms interacts with the periodic structure of a standing wave, a diffractive scattering takes place. This sends the atomic beam in many directions as shown in Fig. 17.1(a). This phenomenon is analogous to the scattering of a light wave from an optical grating. Under suitable conditions, the atomic beam can be diffracted into two directions only, resulting in an atomic beam-splitter. Such a beam-splitter can be used in atomic interferometers.

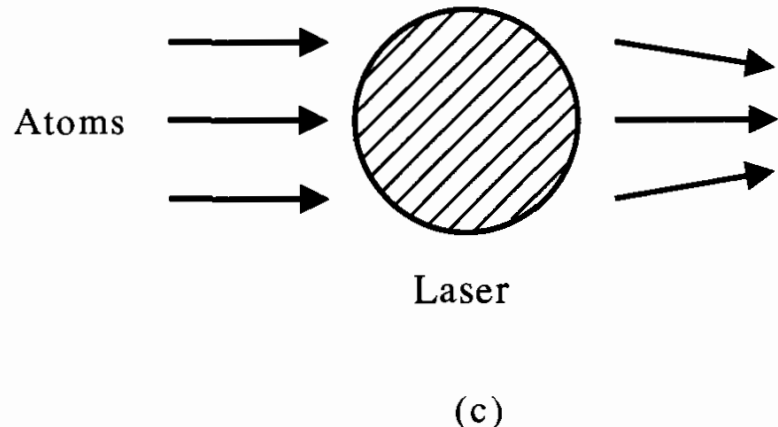
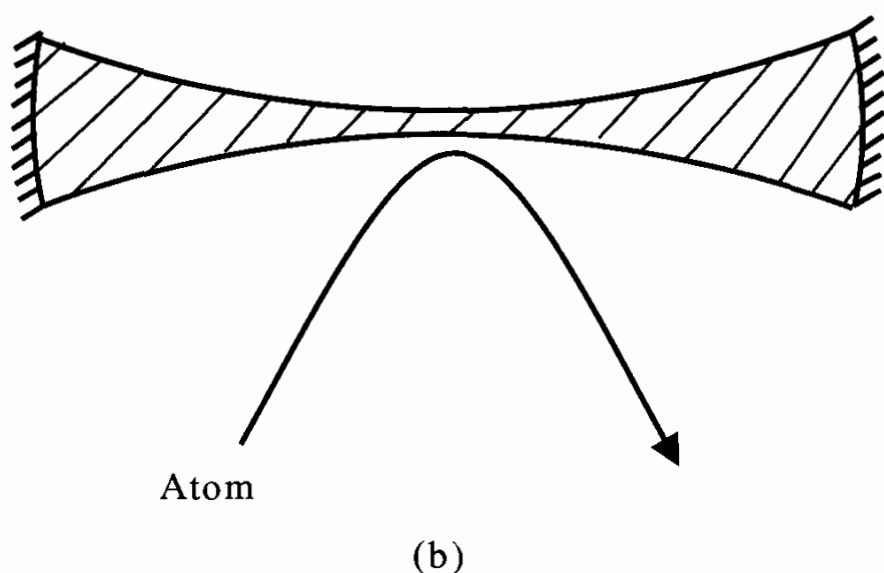
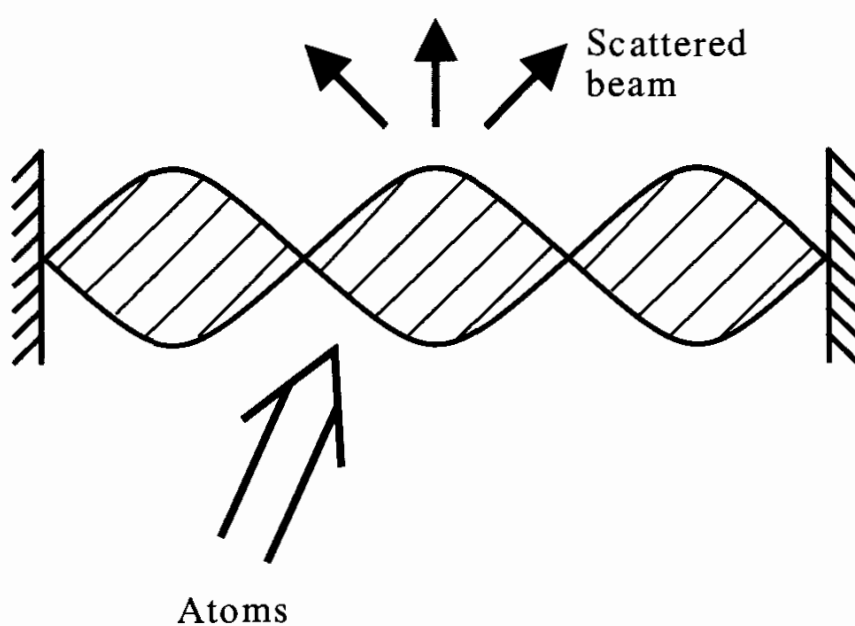
Here we give a simple derivation of this effect, which neglects the internal two-level structure of the atom.

The dipole interaction of an atom interacting resonantly with a standing-wave field in the  $z$ -direction is given by

$$\mathcal{H}_1 = \phi \mathcal{E}_0 \sin kz, \quad (17.1.13)$$

Fig. 17.1

(a) Interaction of the atomic beam with a standing wave can result in atomic diffraction. (b) Field gradient force can make atoms rebound like a light beam reflected from a mirror. (c) Atomic beam may be focussed by the gradient force of the electromagnetic field.



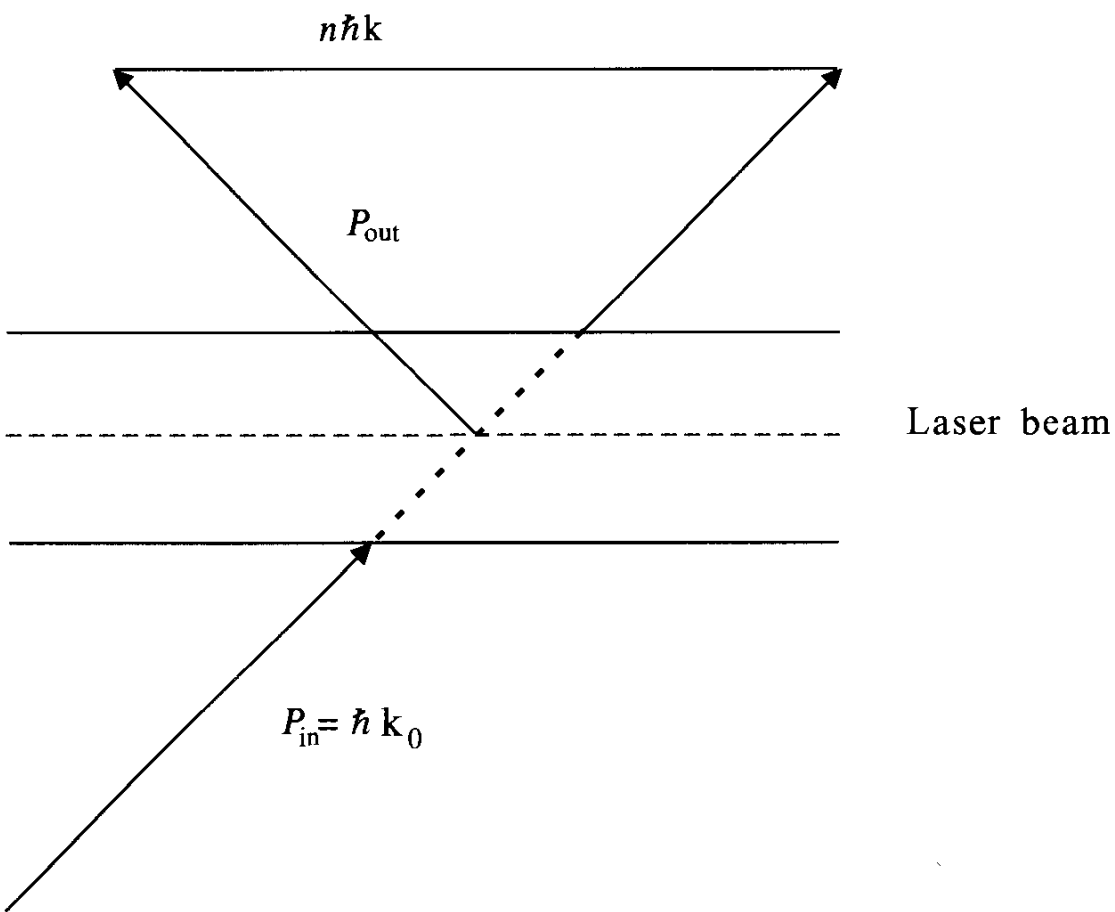


Fig. 17.2  
An atomic beam of wave vector  $\mathbf{k}_0$  can acquire a momentum  $n\hbar\mathbf{k}$  during passage through a standing wave resulting in atomic diffraction.

where  $\varphi$  is the atomic dipole moment. If the atom is initially in a momentum eigenstate with momentum  $\hbar k_0$ , i.e.,  $\psi(z, 0) = \exp(i k_0 z)$ , we find the time-dependent wave function

$$\begin{aligned}\psi(z, t) &= \exp\left(-\frac{i}{\hbar} \mathcal{H}_1 t\right) \psi(z, 0) \\ &= \exp(-i\Omega_R t \sin kz) \exp(ik_0 z) \\ &= \sum_{n=-\infty}^{\infty} J_n(\Omega_R t) \exp[i(k_0 + nk)z],\end{aligned}\quad (17.1.14)$$

where  $\Omega_R = \varphi \mathcal{E}_0 / \hbar$  is the Rabi frequency and  $J_n$  is the  $n$ th order Bessel function. The momentum representation of  $\psi(z, t)$ , i.e.,  $\tilde{\psi}(p, t)$ , is obtained by taking the Fourier transformation of Eq. (17.1.14):

$$\tilde{\psi}(p, t) = \hbar \sum_{n=-\infty}^{\infty} J_n(\Omega_R t) \delta[p - \hbar(k_0 + nk)]. \quad (17.1.15)$$

This represents the diffractive scattering into many momentum components spaced by the photon momenta  $\hbar k$ . This diffractive scattering is due to the fact that the atom, during its passage through the standing wave, can exchange an integral number of photons of momenta  $\hbar k$  in the  $+/-z$ -direction (see Fig. 17.2).

### 17.1.4 Semiclassical gradient force

We now consider the force of an atom which enters the cavity in a field region having a strong transverse variation. This is, for example, the situation in a highly focussed Gaussian laser beam. We calculate the magnitude of this gradient force.

The interaction Hamiltonian for an atom interacting with the field can be written in the dipole approximation as

$$\mathcal{H}_1 = -\hat{\phi}E(\mathbf{r}, t), \quad (17.1.16)$$

where, for a light beam propagating in the  $z$ -direction,

$$E(\mathbf{r}, t) = \frac{1}{2}\mathcal{E}_0(x, y)e^{-i(vt-kz)} + \text{c.c.} \quad (17.1.17)$$

In the semiclassical approximation, we can replace the dipole moment operator  $\hat{\phi}$  in Eq. (17.1.16) by its expectation value

$$\langle \hat{\phi} \rangle = \phi_{ab}\rho_{ab}e^{i(vt-kz)} + \text{c.c.} \quad (17.1.18)$$

In the rotating-wave approximation, the interaction energy is thus equal to

$$W_1 = \frac{-\hbar\Omega_R}{2}(\rho_{ba} + \rho_{ab}), \quad (17.1.19)$$

where  $\Omega_R = \phi_{ab}\mathcal{E}_0/\hbar$  is the Rabi frequency, which we assume to be real.

A steady-state solution of Eqs. (17.1.3)–(17.1.5) yields

$$\rho_{ab} = \frac{-2\Omega_R(\Delta + i\Gamma/2)}{4\Delta^2 + \Gamma^2 + 2\Omega_R^2}, \quad (17.1.20)$$

which gives

$$W_1 = \frac{2\hbar\Delta\Omega_R^2(x, y)}{4\Delta^2 + \Gamma^2 + 2\Omega_R^2}. \quad (17.1.21)$$

Now the atom entering the field region will experience a force (for  $\Omega_R \ll \Gamma$ )

$$\begin{aligned} \mathbf{F} &= -\nabla_{\perp} W_1 \\ &= -\frac{2\hbar\Delta}{4\Delta^2 + \Gamma^2} \nabla_{\perp} \Omega_R^2(x, y), \end{aligned} \quad (17.1.22)$$

where  $\nabla_{\perp}$  is the transverse gradient. For a plane wave,  $\Omega_R$  is independent of transverse coordinates, and this force vanishes. However for a focussed beam of width  $a$

$$|\nabla_{\perp} \Omega_R^2| \simeq \frac{\Omega_R^2}{a}, \quad (17.1.23)$$

the force (17.1.22) then becomes

$$F = \frac{2\hbar\Delta\Omega_R^2}{a(4\Delta^2 + \Gamma^2)}. \quad (17.1.24)$$

The semiclassical gradient force is thus proportional to the detuning and its direction depends on the sign of  $\Delta$ . For positive detuning the force is in the direction of the field gradient. This force may thus make the atoms rebound like a light beam reflected from a mirror (Fig. 17.1(b)). Alternatively, an atomic beam may experience focussing and the situation corresponds to that of a cylindrical lens (Fig. 17.1(c)).

## 17.2 Atomic interferometry

In this section, we develop the theory of atomic interferometers cast in an operator formalism. This formalism will be employed to study the quantum limit on the overall sensitivity of the device in the next section. We also consider the use of an atom interferometer as a rotation detector or a gyroscope.

### 17.2.1 Atomic Mach–Zehnder interferometer

As depicted in Fig. 17.3, we consider a scheme whereby a stream of  $N$  atoms are sent through a Mach–Zehnder interferometer during a measurement time  $t_m$ . The atoms are split at beam-splitter 1, follow paths  $\alpha$  or  $\beta$ , are reflected off mirrors, and are then recombined at beam-splitter 2. The recombined atoms are detected at upper detector  $a$  or lower detector  $b$  where interference fringes are recorded.

We assume that, upon reflection from a beam-splitter surface, the particles undergo an unimportant phase shift that we take to be  $\pi/2$ , but that, in reality, depends upon the structure of the beam-splitter. Upon passage *through* a beam-splitter, however, the atom undergoes a phase shift of  $\varphi_i$  ( $i = 1, 2$  for the first and second beam-splitter, respectively). The cumulative effect in the interferometer of these various processes on the atomic wave function  $\psi$  is depicted in Fig. 17.3(b), and leads to a wave function  $\psi_a$  corresponding to the upper detector, namely

$$\psi_a = \frac{\psi}{2} e^{i\theta_a} [1 - e^{-ik(l_\alpha - l_\beta)}], \quad (17.2.1)$$

and

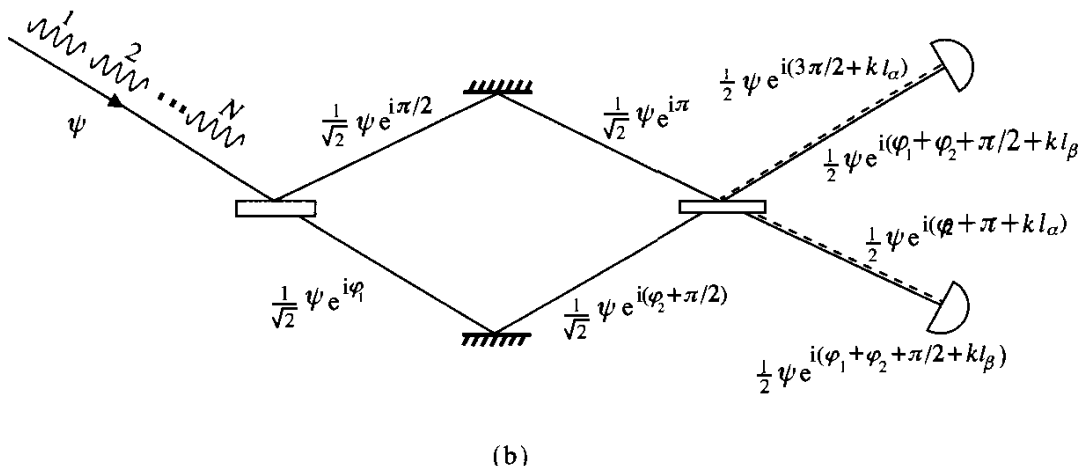
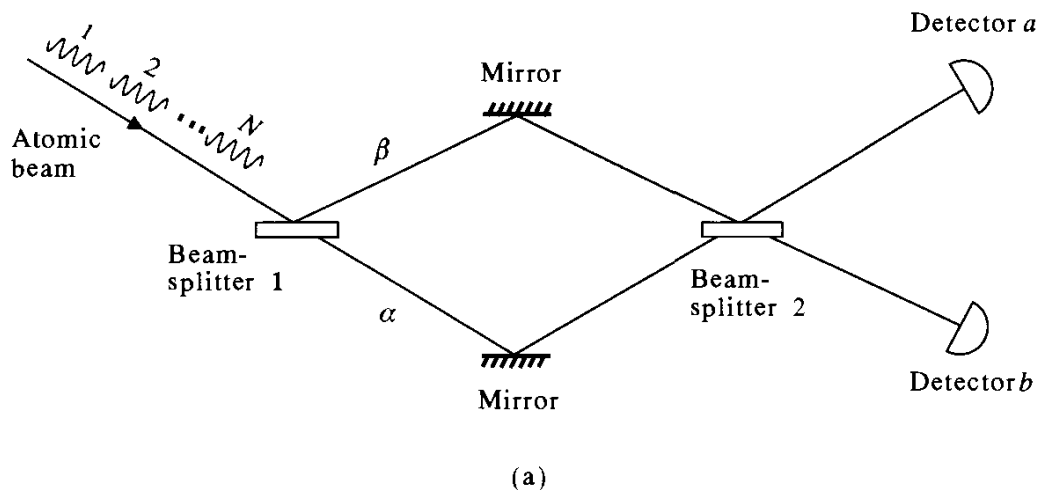
$$\psi_b = \frac{\psi}{2} e^{i\theta_b} [1 + e^{-ik(l_\alpha - l_\beta)}], \quad (17.2.2)$$

where  $\theta_a \equiv \pi/2 + kl_\alpha + \varphi_2$ , and  $\theta_b \equiv kl_\alpha + \varphi_1 + \varphi_2$ , and where, without

Fig. 17.3

(a) Schematic of the atomic Mach-Zehnder interferometer.

(b) Phase changes by the beam-splitters and mirrors account for accumulated phase shifts in the upper or lower branches. (From M. O. Scully and J. P. Dowling, *Phys. Rev. A* **48**, 3186 (1993).)



loss of generality, we let  $\varphi_1 = \varphi_2 = \pi$ . Here,  $k$  is the atomic wave number and  $l_\alpha$  and  $l_\beta$  are the path lengths through the upper and the lower branches, respectively. We imagine now that the beam is recombined by the second beam-splitter and the detectors  $a$  and  $b$  shown in Fig. 17.3(a) count the number of atoms as they arrive in the recombined upper beam or lower beam, respectively. If we label  $N$  atoms with the index  $i = 1, \dots, N$ , as those sent through the interferometer during the measurement time  $t_m$ , then the appropriate state vector  $|\varphi\rangle_i$  for the  $i$ th atom in the interferometer, after recombination, is given by

$$|\varphi\rangle_i = \frac{e^{i\theta_a}}{2} (1 - e^{-i\varphi_{ab}}) |1_a, 0_b\rangle_i + \frac{e^{i\theta_b}}{2} (1 + e^{-i\varphi_{ab}}) |0_a, 1_b\rangle_i, \quad (17.2.3)$$

where here  $\varphi_{ab} \equiv k(l_\alpha - l_\beta)$ . We see that this state is an appropriate superposition of the number states  $|1_a, 0_b\rangle$  and  $|0_a, 1_b\rangle$  corresponding to an atom incident on the upper or lower detector, respectively. The state vector  $|\Phi\rangle_N$  for the  $N$ -atom state is then constructed via a direct product of the individual atomic states, namely

$$|\Phi\rangle_N \equiv \prod_{i=1}^N |\varphi\rangle_i. \quad (17.2.4)$$

Let  $c_{\sigma,i}^\dagger$  and  $c_{\sigma,i}$ , where  $\sigma = a, b$ , be the creation and annihilation operators, respectively, for the number states  $|n_a, n_b\rangle_i$ , where, corresponding to number operators  $n_{\sigma,i} \equiv c_{\sigma,i}^\dagger c_{\sigma,i}$ , the eigenvalues  $n_a$  and  $n_b$  are 0 or 1. Then the number operator  $N_\sigma$  for the number of upper or lower atoms is determined by

$$N_\sigma = \sum_{i=1}^N n_{\sigma,i} \quad (\sigma = a, b), \quad (17.2.5)$$

and the operator  $c$  obeys the commutation relations

$$\left[ c_{\sigma,i} c_{\sigma,j}^\dagger \pm c_{\sigma,j}^\dagger c_{\sigma,i} \right] = \delta_{ij}, \quad (17.2.6)$$

where the plus or minus sign indicates Bose or Fermi statistics, respectively. The statistical nature of the atoms will be important in circumstances where the density of particles in the interferometer is so large that there is more than one atom at a time within a single coherence length, or if the atoms are injected in a correlated manner into the input port. The expectation values  $\langle N_\sigma \rangle_N$  of these number operators, Eq. (17.2.5), are given by

$$N \langle \Phi | N_a | \Phi \rangle_N = \sum_{i=1}^N \left| \frac{1 - e^{-i\varphi_{\alpha\beta}}}{2} \right|^2 i \langle 1_a, 0_b | n_{a,i} | 1_a, 0_b \rangle_i, \quad (17.2.7)$$

$$N \langle \Phi | N_b | \Phi \rangle_N = \sum_{i=1}^N \left| \frac{1 + e^{-i\varphi_{\alpha\beta}}}{2} \right|^2 i \langle 0_a, 1_b | n_{b,i} | 0_a, 1_b \rangle_i. \quad (17.2.8)$$

This yields the expressions for the mean number of atoms in the  $\alpha$  and  $\beta$  branches as

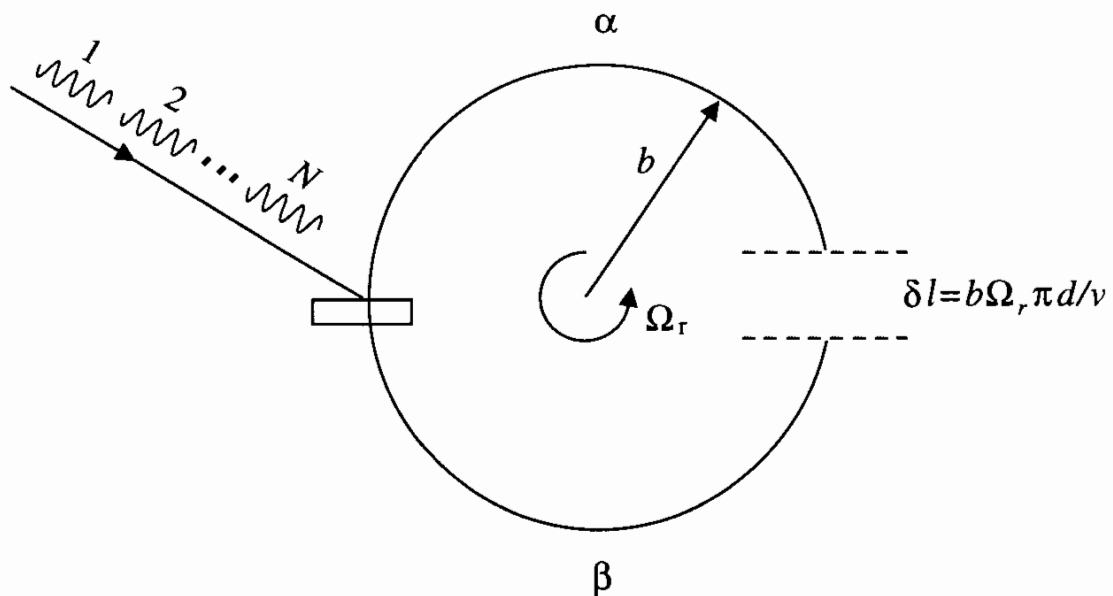
$$\langle N_a \rangle_N = N \sin^2 \varphi_{\alpha\beta} / 2, \quad \langle N_b \rangle_N = N \cos^2 \varphi_{\alpha\beta} / 2. \quad (17.2.9)$$

These expectations constitute the signal.

### 17.2.2 Atomic gyroscope (原子陀螺仪)

We now consider an idealized atomic interferometer used as a rotation sensor or gyroscope. The atom interferometer consists of semicircular arms as depicted in Fig. 17.4. If the loop rotates with an angular

Fig. 17.4  
Schematic of an atomic interferometer with semicircular arms to be used as a rotation sensor or gyroscope.



frequency  $\Omega_r$ , about an axis through its center and normal to the loop plane, the path difference between counter-propagating and co-propagating beams can be seen to be (see Eq. (4.1.12))

$$\Delta L = \frac{2\pi b^2 \Omega_r}{v}, \quad (17.2.10)$$

where  $b$  is the radius of the beam path and  $v$  is the atomic velocity. This path difference translates into a Sagnac phase difference of

$$\Delta\theta = \frac{2\pi b^2 \Omega_r}{v\bar{\lambda}} = \frac{2A\Omega_r}{v\bar{\lambda}}, \quad (17.2.11)$$

where  $A$  is the area enclosed by the arms and

$$\bar{\lambda} = \frac{\hbar}{mv} \quad (17.2.12)$$

is the atomic de Broglie wavelength. The phase difference is then given by

$$\Delta\theta = \frac{2Am\Omega_r}{\hbar}. \quad (17.2.13)$$

This expression holds for both atom and light interferometers, if, in the photon case, we define an effective photon mass  $m_\gamma$  implicitly by

$$m_\gamma c^2 = \hbar v. \quad (17.2.14)$$

Now, since the ‘mass’ of a photon is governed by optical energies of a few electron volts whereas atomic masses are of the order  $10^3$  Mev, we see that the matter-wave gyroscopes potentially have a signal that is enhanced by many orders of magnitude, compared to the laser gyroscopes. However, in order to determine the minimum rotation rate, we have to consider the noise in an atom interferometer, to which we turn in the next section.

### 17.3 Quantum noise in an atomic interferometer

We compute the quantum noise fluctuations using the second quantized formalism developed earlier. Recalling the definitions for the number operator  $N_\sigma$ , Eq. (17.2.5), and the state vector  $|\Phi\rangle_N$ , Eq. (17.2.4), and using the commutation relations, Eq. (17.2.6), we may write,

$$\begin{aligned}
 \langle\Delta N_\sigma^2\rangle &= {}_N\langle\Phi|N_\sigma^2|\Phi\rangle_N - \left({}_N\langle\Phi|N_\sigma|\Phi\rangle_N\right)^2 \\
 &= {}_N\langle\Phi|\sum_{i=1}^N n_{\sigma,i}\sum_{j=1}^N n_{\sigma,j}|\Phi\rangle_N - \left({}_N\langle\Phi|\sum_{i=1}^N n_{\sigma,i}|\Phi\rangle_N\right)^2 \\
 &= \sum_{i=1}^N {}_i\langle\varphi|n_{\sigma,i}|\varphi\rangle_i \sum_{\substack{j=1 \\ j\neq i}}^N {}_j\langle\varphi|n_{\sigma,j}|\varphi\rangle_j \\
 &\quad + \sum_{i=1}^N {}_i\langle\varphi|c_{\sigma,i}^\dagger(1 \pm n_{\sigma,i})c_{\sigma,i}|\varphi\rangle_i - \left(\sum_{i=1}^N {}_i\langle\varphi|n_{\sigma,i}|\varphi\rangle_i\right)^2 \\
 &= \frac{N}{4} \sin^2 \varphi_{\alpha\beta} \pm \sum_{i=1}^N {}_i\langle\varphi|c_{\sigma,i}^\dagger c_{\sigma,i}^\dagger c_{\sigma,i} c_{\sigma,i}|\varphi\rangle_i \quad (\sigma = a, b),
 \end{aligned} \tag{17.3.1}$$

where, as before, the upper and lower terms correspond to  $\sigma = a$  or  $b$ , respectively, and the  $\pm$  sign refers to the statistics of the particles: a plus sign for bosons and a minus sign for fermions. We note that the last, statistics-dependent term of Eq. (17.3.1) is the sum of nonnegative matrix elements and so itself is nonnegative or nonpositive, according to the plus sign or negative sign, respectively. A quantitative analysis of the contribution of this statistics-dependent term requires a specific model of the coherences between atoms in a dense beam. However, one can qualitatively state that for sufficiently high densities the use of fermionic atoms will tend to *lower* the quantum noise limit. This is because the last term will be negative. Bosons will have the opposite effect. In many experiments of interest, the beam intensity is so low that there is only one atom at a time within a single coherence length. In this case, the statistics-dependent term in the last line of Eq. (17.3.1) is zero, and we are left with the result

$$\langle\Delta N_\sigma\rangle = \frac{\sqrt{N}}{2} \sin \varphi_{\alpha\beta}. \tag{17.3.2}$$

We notice that this result depends on the total number of atoms  $N$ . Now, the signal in either branch  $N_\sigma$  is given by Eq. (17.2.9).

The quantum fluctuations in phase  $\Delta\varphi_{\alpha\beta}$  in the measured phase difference  $\varphi_{\alpha\beta}$  may be determined by (see Eq. (4.4.51))

$$\begin{aligned} |\Delta\varphi_{\alpha\beta}| &\equiv \frac{\langle\Delta N_\sigma\rangle}{|\partial\langle N_\sigma\rangle/\partial\varphi_{\alpha\beta}|} \\ &= \frac{1}{\sqrt{N}}, \end{aligned} \quad (17.3.3)$$

a result that is *independent* of  $\varphi_{\alpha\beta}$ . This independence might appear surprising at first, but it is a direct result of the fact that the quantum number state noise  $\langle\Delta N_\sigma\rangle$  is proportional to the slope of the signal  $\langle N_\sigma\rangle$  for the upper and lower number states considered here.

We conclude by applying this result to the gyroscope problem. Let us note that the atom number  $N$  is given by  $jt_m$ , where  $j$  is the atom flux (in atoms per second) hitting the detector. We have from Eq. (17.3.3) the minimum detectable phase shift,  $\varphi_{\min} = 1/\sqrt{jt_m}$ , and equating this to the signal derived earlier,  $\varphi^{\text{signal}} = 4Am\Omega_r/\hbar$ , we find the minimum detectable rotation rate  $\Omega_r^{\min}$  is given by

$$\Omega_r^{\min} \cong \frac{\hbar}{2Am} \frac{1}{\sqrt{jt_m}} \quad (\text{matter}). \quad (17.3.4)$$

This should be compared to the same result obtained using an optical interferometer in which the flux  $j$  is given by the power  $P$  divided by the photon energy  $\hbar\nu$ , in other words

$$\Omega_r^{\min} \cong \frac{\hbar}{Am_\gamma} \sqrt{\frac{\hbar\nu}{Pt_m}} \quad (\text{light}), \quad (17.3.5)$$

where  $m_\gamma$  is the effective photon mass, defined by  $m_\gamma \equiv \hbar\nu/c^2$ . As mentioned before, we note that the typical photon effective mass gives an increase in sensitivity of  $10^{10}$ . This mass factor, however, is offset by the low particle flux available for atoms. This fact increases the laser gyroscope sensitivity over that of matter-wave devices by a factor of around  $10^2$ . In addition, the atoms make about one ‘round trip’ through an interferometer, whereas in a ring laser gyroscope the photons make many ( $\approx 10^4$ ) circuits around the ring and yield an additional sensitivity factor of  $10^4$  in favor of the laser system. This still leaves the matter-wave device  $10^4$  times more sensitive.

## 17.4 Limits to laser cooling

### 17.4.1 Recoil limit

We turn now to the question of velocity spread i.e., fluctuations in the momentum distribution associated with laser cooling. The  $z$  compo-

ment of the atomic momentum after absorption of  $n$  photons is given by

$$p = p_0 + n\hbar k + \sum_{j=1}^n \hbar k \cos \theta_j \quad (17.4.1)$$

where  $\hbar k \cos \theta_j$  is the projection, onto the  $z$  axis, of the  $j$ th spontaneously emitted photon.

Note that both the number of absorption events,  $n$ , and the emission directions of the emitted photons are random variables. We next give a heuristic derivation of the fluctuations in radiation pressure due to these two random processes.

Considering the fluctuations due to spontaneous emission (SE), we note that the number of SE events per second is given by

$$\frac{dN}{dt} = \Gamma P_{\text{ex}} \quad (17.4.2)$$

where  $\Gamma$  is the spontaneous emission rate and  $P_{\text{ex}}$  is the probability that the laser-driven atom is in the excited state. The diffusion in momentum in a time  $\Delta t$  is then characterized by

$$\Delta p^2 = \langle p^2 \rangle - \langle p \rangle^2 \quad (17.4.3)$$

and since  $\langle p \rangle$  vanishes due to a large number of SE events we have

$$\begin{aligned} \Delta p^2 &= (\hbar k)^2 \frac{dN}{dt} \Delta t \\ &= \hbar^2 k^2 \frac{\Gamma}{2} \Delta t \end{aligned} \quad (17.4.4)$$

where in the last line we have noted that  $dN/dt = \Gamma/2$  since  $P_{\text{ex}} \Rightarrow 1/2$  for a damped, driven, two-level atom.

Recalling that the diffusion coefficient is  $2D_{\text{SE}} = \Delta p^2/\Delta t$  we have

$$D_{\text{SE}} = \frac{1}{4} \hbar^2 k^2 \Gamma, \quad (17.4.5)$$

which is the momentum diffusion coefficient due to spontaneous emission.

Likewise, there are fluctuations in radiation pressure due to fluctuations in the number of absorption events leading to atomic excitation. It turns out that this source of noise is essentially equal to that due to SE fluctuations. Hence the fluctuations due to emission and absorption are characterized by a diffusion in velocity given by

$$D = \hbar^2 k^2 \Gamma / m^2. \quad (17.4.6)$$

Thus may we write the Fokker–Planck equation for the velocity space probability density  $P(v, t)$  :

$$\frac{\partial P}{\partial t} = \frac{\partial}{\partial v} \left[ d(v) + D(v) \frac{\partial}{\partial v} \right] P , \quad (17.4.7)$$

where the drift (damping) coefficient  $d$  governs the cooling process and the diffusion (fluctuation) coefficient  $D$  governs the effective temperature of the cold gas.

From Eq (17.4.7) we see that, at steady state,

$$P(v) = P(0) \exp \left[ - \int_0^v d(v') / D(v') dv' \right] , \quad (17.4.8)$$

and using the fact that maximum damping occurs when  $\Delta$  and  $\Omega_R$  in Eq. (17.1.11) are of order  $\Gamma$ , we have  $d \approx \hbar k^2 v / mg$ , and taking  $D(v)$  from Eq. (17.4.6), the velocity distribution (17.4.8) becomes

$$P(v) = P(0) \exp(-mv^2 / \hbar \Gamma) . \quad (17.4.9)$$

Comparing (17.4.9) to the usual Boltzmann distribution

$$f(v) = f(0) \exp(-mv^2 / 2k_B T) , \quad (17.4.10)$$

we have the effective temperature for a laser cooled gas

$$T_{\text{eff}} \cong \hbar \Gamma / 2k_B . \quad (17.4.11)$$

Eq. (17.4.11) is called the multi-photon recoil (“Doppler”) limit to laser cooling, and is in the ballpark of a few hundred micro-Kelvin. Such low temperatures are interesting in many applications, but things get even better when we add the physics of atomic coherence, i.e., population trapping, to the laser cooling problem, as we see in the next section.

### 17.4.2 Velocity selective coherent population trapping\*

In the previous section we found that for two-level atoms the recoil limit to laser cooling is given by Eq. 17.4.11. But if we extend our considerations to multi-level atoms, and in particular atoms having two lower levels, then it is possible to cool beyond the single photon recoil limit,  $k_B T \cong \hbar^2 k^2 / 2m$ .

In order to see this, consider the situation as depicted in Fig. 17.5. There we see an atom of momentum  $p_z \equiv p$  driven by two fields of polarization  $\sigma^+$  and  $\sigma^-$ . Now velocity selective coherent population

\* For a good account of this ingenious idea see A. Aspect, E. Arimondo, R. Kaiser, N. Vantseenkiste, and C. Cohen-Tannoudji, *J. Opt. Soc. Am.* **B6**, 2112 (1989); for another clever ‘subrecoil cooling’ scheme see M. Kasevich and S. Chu, *Phys. Rev. Lett.* **69**, 1741 (1992). Please note that by “subrecoil” we mean below the single photon limit; which is, naturally, below the multi-photon recoil limit.

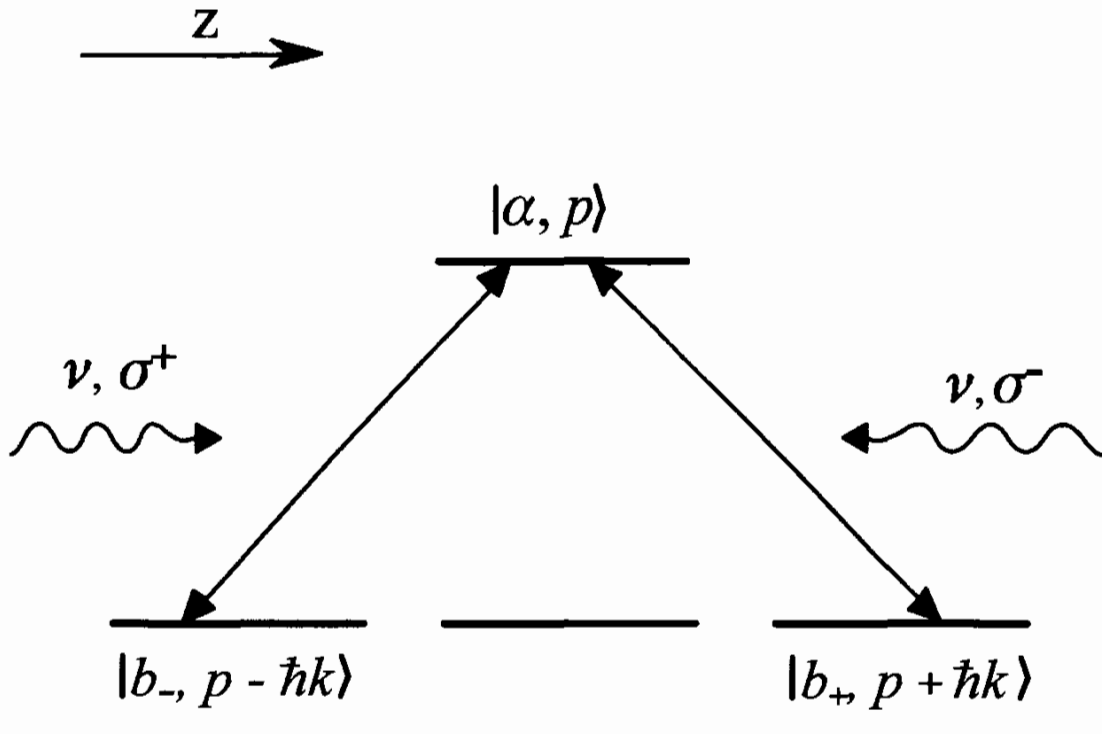


Fig. 17.5  
 Atom moving in  $z$ -direction with momentum  $p$  while driven from lower level ( $J = 1, m = -1$ ) state  $|b_- \rangle$  to upper level ( $J = 1, m = 0$ ) state  $|a \rangle$  via  $\sigma^+$  radiation, and ( $J = 1, m = +1$ ) state  $|b \rangle$  to  $|a \rangle$  state via  $\sigma^-$  radiation.  
 Momentum of atom in states  $b_{\pm}$  coupling to excited state having momentum  $p$ , is  $p \pm \hbar k$ .

trapping (VSCPT) occurs when the atom, after being excited, falls into the state

$$|\Psi_{NC}\rangle(p) = \frac{1}{\sqrt{2}} [ |b_+, p + \hbar k\rangle + |b_-, p - \hbar k\rangle ]. \quad (17.4.12)$$

We take the interaction with the laser field to be

$$V = \frac{\Omega_R}{2} \left[ -|a\rangle\langle b_-|e^{-i(vt-kz+\phi)} + |a\rangle\langle b_+|e^{-i(vt+kz+\phi)} \right] + \text{h.c.} \quad (17.4.13)$$

where we have chosen the matrix elements such that  $\phi_{a,b_-}$  and  $\phi_{a,b_+}$  differ by a sign. From (17.4.12) and (17.4.13) we see that

$$\langle a, p | V | \Psi_{NC}(P) \rangle = 0. \quad (17.4.14)$$

When an atom is excited to state  $|a, p\rangle$ , it can spontaneously emit a photon in any direction, and the atomic momentum can change by any amount,  $q$ , from  $\hbar k$  to  $-\hbar k$ . But when it happens to fall into a noncoupled state it will cease to absorb laser photons.

In order to see clearly what is happening in VSCPT consider the situations wherein a spontaneously emitted photon has left the atom in a superposition of the two states

$$|\Psi_{NC}(q)\rangle = \frac{1}{\sqrt{2}} \left( |b_+, q + \hbar k\rangle + |b_-, q - \hbar k\rangle \right) \quad (17.4.15a)$$

$$|\Psi_C(q)\rangle = \frac{1}{\sqrt{2}} \left( |b_+, q + \hbar k\rangle - |b_-, q - \hbar k\rangle \right) \quad (17.4.15b)$$

However, these states are, in general, coupled by the kinetic energy operator, that is

$$\langle \Psi_C(q) | \frac{p_z^2}{2m} | \Psi_{NC}(q) \rangle = \frac{\hbar k q}{m}. \quad (17.4.16)$$

Hence an atom which falls into the state  $|\Psi_{NC}(q)\rangle$  will evolve into a superposition of  $|\Psi_{NC}(q)\rangle$  and  $|\Psi_C(q)\rangle$  due to the nonvanishing matrix element (17.4.16) of the kinetic energy operator coupling these states. However, in the case of  $q = 0$ , these states are uncoupled, and  $|\Psi_{NC}(0)\rangle$  is seen to be a ‘perfect’ trapping state.

To summarize: a multi-level atom, of the type shown in Fig. 17.5, can be cooled below the single photon limit of some micro-Kelvin via VSCPT. Atoms are trapped in the zero-velocity non-coupled state  $|\Psi_{NC}(0)\rangle$ . At present, VSCPT has been used to yield temperatures in the nano-Kelvin domain.

## Problems

- 17.1** As seen in Eq. (17.1.15), an atom experiences a diffractive scattering in a standing wave with momentum components spaced by the photon momenta  $\hbar k$ . Show that the momentum width is given by

$$\langle \Delta p^2 \rangle = \frac{1}{2} \hbar^2 k^2 \Omega_R^2 t^2.$$

# Quantum Optics

Notes